

96 1212 502

AD-A286 914



96-02515



Investigation Into Hybrid Rockets and Other Cost-Effective Propulsion System Options for Small Satellites

*Thesis submitted to The University of Surrey
for the degree of Doctor of Philosophy*

DISTRIBUTION STATEMENT A

Approved for public release
Distribution Unlimited

by

Major

Jerry Jon Sellers
United States Air Force

Centre for Satellite Engineering Research,
University of Surrey
Guildford, Surrey, UK.

May 1996

REPORT DOCUMENTATION PAGE

*Form Approved
OMB No. 0704-0188*

Public reporting burden for this collection of information is estimated to average 1 hour per response, including the time for reviewing instructions, searching existing data sources, gathering and maintaining the data needed, and completing and reviewing the collection of information. Send comments regarding this burden estimate or any other aspect of this collection of information, including suggestions for reducing this burden, to Washington Headquarters Services, Directorate for Information Operations and Reports, 1215 Jefferson Davis Highway, Suite 1204, Arlington, VA 22202-4302, and to the Office of Management and Budget: Paperwork Reduction Project (0704-0188), Washington, DC 20503.

1. AGENCY USE ONLY (Leave blank)	2. REPORT DATE	3. REPORT TYPE AND DATES COVERED	
	May 1996		
4. TITLE AND SUBTITLE		5. FUNDING NUMBERS	
Investigation Into Hybrid Rockets and Other Cost-Effective Propulsion System Options for Small Satellites			
6. AUTHOR(S)			
Jerry Jon Sellers			
7. PERFORMING ORGANIZATION NAME(S) AND ADDRESS(ES)		8. PERFORMING ORGANIZATION REPORT NUMBER	
University of Surrey, UK		96-022D	
9. SPONSORING/MONITORING AGENCY NAME(S) AND ADDRESS(ES)		10. SPONSORING/MONITORING AGENCY REPORT NUMBER	
DEPARTMENT OF THE AIR FORCE AFIT/CI 2950 P STREET, BLDG 125 WRIGHT-PATTERSON AFB OH 45433-7765			
11. SUPPLEMENTARY NOTES			
Unlimited			
12a. DISTRIBUTION/AVAILABILITY STATEMENT		12b. DISTRIBUTION CODE	
DISTRIBUTION STATEMENT A Approved for public release Declassify/Unrestrict			
13. ABSTRACT (Maximum 200 words)			
14. SUBJECT TERMS		15. NUMBER OF PAGES	
		8-7+	
		16. PRICE CODE	
17. SECURITY CLASSIFICATION OF REPORT	18. SECURITY CLASSIFICATION OF THIS PAGE	19. SECURITY CLASSIFICATION OF ABSTRACT	20. LIMITATION OF ABSTRACT

GENERAL INSTRUCTIONS FOR COMPLETING SF 298

The Report Documentation Page (RDP) is used in announcing and cataloging reports. It is important that this information be consistent with the rest of the report, particularly the cover and title page. Instructions for filling in each block of the form follow. It is important to stay *within the lines* to meet optical scanning requirements.

Block 1. Agency Use Only (Leave blank).

Block 2. Report Date. Full publication date including day, month, and year, if available (e.g. 1 Jan 88). Must cite at least the year.

Block 3. Type of Report and Dates Covered.

State whether report is interim, final, etc. If applicable, enter inclusive report dates (e.g. 10 Jun 87 - 30 Jun 88).

Block 4. Title and Subtitle. A title is taken from the part of the report that provides the most meaningful and complete information. When a report is prepared in more than one volume, repeat the primary title, add volume number, and include subtitle for the specific volume. On classified documents enter the title classification in parentheses.

Block 5. Funding Numbers. To include contract and grant numbers; may include program element number(s), project number(s), task number(s), and work unit number(s). Use the following labels:

C - Contract	PR - Project
G - Grant	TA - Task
PE - Program	WU - Work Unit
Element	Accession No.

Block 6. Author(s). Name(s) of person(s) responsible for writing the report, performing the research, or credited with the content of the report. If editor or compiler, this should follow the name(s).

Block 7. Performing Organization Name(s) and Address(es). Self-explanatory.

Block 8. Performing Organization Report Number. Enter the unique alphanumeric report number(s) assigned by the organization performing the report.

Block 9. Sponsoring/Monitoring Agency Name(s) and Address(es). Self-explanatory.

Block 10. Sponsoring/Monitoring Agency Report Number. (If known)

Block 11. Supplementary Notes. Enter information not included elsewhere such as: Prepared in cooperation with; Trans. of...; To be published in.... When a report is revised, include a statement whether the new report supersedes or supplements the older report.

Block 12a. Distribution/Availability Statement.

Denotes public availability or limitations. Cite any availability to the public. Enter additional limitations or special markings in all capitals (e.g. NOFORN, REL, ITAR)

DOD - See DoDD 5230.24, "Distribution Statements on Technical Documents."

DOE - See authorities.

NASA - See Handbook NHB 2200.2.

NTIS - Leave blank.

Block 12b. Distribution Code.

DOD - Leave blank.

DOE - Enter DOE distribution categories from the Standard Distribution for Unclassified Scientific and Technical Reports.

NASA - Leave blank.

NTIS - Leave blank.

Block 13. Abstract. Include a brief (Maximum 200 words) factual summary of the most significant information contained in the report.

Block 14. Subject Terms. Keywords or phrases identifying major subjects in the report.

Block 15. Number of Pages. Enter the total number of pages.

Block 16. Price Code. Enter appropriate price code (NTIS only).

Blocks 17.-19. Security Classifications. Self-explanatory. Enter U.S. Security Classification in accordance with U.S. Security Regulations (i.e., UNCLASSIFIED). If form contains classified information, stamp classification on the top and bottom of the page.

Block 20. Limitation of Abstract. This block must be completed to assign a limitation to the abstract. Enter either UL (unlimited) or SAR (same as report). An entry in this block is necessary if the abstract is to be limited. If blank, the abstract is assumed to be unlimited.

Abstract

Affordable small satellites need affordable propulsion systems. The primary objective of this research was to investigate cost-effective propulsion system options for small satellites. The research comprised four interrelated goals:

- Identify key cost drivers for spacecraft hardware.
- Characterise propulsion technology costs.
- Characterise propulsion system costs.
- Evaluate and compare the cost-effectiveness of system options.

Each of these goals was attained. Important results and conclusions emerged. To begin with, *key spacecraft hardware cost drivers were shown to occur during each phase of a mission—definition, design and acquisition—and a process for resolving them was advanced*. Furthermore, propulsion system costs were shown to include far more than performance and price. *A new paradigm for understanding the total cost of propulsion systems was defined that encompasses nine dimensions—mass, volume, time, power, system price, integration, logistics, safety and technical risk*.

This paradigm was used to characterise propulsion technology options. From this effort, hybrid rockets emerged as a promising but underdeveloped technology with great potential for cost-effective application. To evaluate this potential, a dedicated research program was completed during which a hybrid motor was designed, built and tested using 85% hydrogen peroxide as oxidiser and polythene as fuel. The basic concept for a hybrid upper stage was proven. Excellent combustion performance was measured and characterised. Real total costs for future small satellite applications were assessed. This research demonstrated that *hybrid rockets offer a safe, reliable upper stage option that is a versatile, cost-effective alternative to solid rocket motors*. In addition, despite negative industry bias, hydrogen peroxide proved itself as a safe, effective oxidiser for hybrid and mono-propellant applications.

The characterisation of propulsion system costs led to a complete design case study for a minisatellite aimed at the most cost-effective solution. It was shown that *by focusing on the key cost drivers and trading among the cost dimensions, a truly versatile, cost-effective system design can be achieved*.

Finally, an innovative technique was derived to parametrically combine the diverse cost dimensions into a useful, quantifiable figure of merit for mission and research planning. Overall, it was shown that *the most cost-effective solution is found by weighing all options along the nine dimensions of the cost paradigm within the context of a specific mission*.

Overall, the research advances the state of the art of hybrid rocket technology specifically, and satellite engineering in general.

Acknowledgments

"I have accomplished so much only because I have stood on the shoulders of Giants."

Isaac Newton

"To borrow from one person is plagiarism. To borrow from many people is research." Anon.

Few PhDs are accomplished completely without outside assistance. In my case, I often felt in writing this thesis that I spent more time reporting what other people had done to help me than actually documenting my own contributions. In every facet of my research, I have been helped and supported by the UoSAT/SSTL team as well as many outside contributors. I would like to identify several outstanding individuals and organisations without whom I wouldn't have been able to write up what I did:

- Max—for knowing everything about everything.
 - Malcolm Paul—for knowing everything about building and testing rockets.
 - Dr. Ward—for his ready advice and suggestions.
 - Richard Brown of Project Machinery—for his enthusiastic support.
 - Richard Williams & Andy Currie—for all the great minisatellite mechanical drawings
 - David Montgomery—for production support.
 - The SSTL purchasing dept. and stores—for getting things for me “yesterday.”
 - Ron Humble & Mike Lydon at USAFA—for technical advice.
 - Ed Milton—for the endless iterations of the Wertz chapter.
 - Surrey Satellite Technology Ltd. (SSTL)—for research support.
 - British Aerospace, Royal Ordnance Rocket Motors Division, Westcott—for facilities and other support.
- and, most important,
- Prof. Sweeting—for his guidance, support and vision (and he actually believed me when I said I could build a rocket).

"Better"

is the Enemy

of

"Good"

Table of Contents

1.1. BACKGROUND.....	1-2
1.1.1. UoSAT Microsatellites.....	1-2
1.1.2. Future mission opportunities.....	1-3
1.1.3. The UoSAT Minisatellite.....	1-5
1.2. RESEARCH PLAN	1-7
1.2.1. Requirements and Constraints.....	1-7
1.2.2. Approach.....	1-7
1.3. PUBLICATIONS.....	1-11
2.1. OVERVIEW.....	2-2
2.2. MISSION DEFINITION PHASE.....	2-3
2.2.1. Launch & Space Environment.....	2-5
2.2.2. The Political Environment.....	2-5
2.3. MISSION DESIGN PHASE	2-6
2.3.1. Performance Requirements with Margins.....	2-7
2.3.2. Quality Level.....	2-8
2.3.3. System Architecture Design.....	2-9
2.4. HARDWARE ACQUISITION PHASE.....	2-10
2.4.1. Hardware Source.....	2-10
2.4.2. Procurement Process.....	2-12
2.4.3. Space Qualifying.....	2-14
2.5. PROPULSION SYSTEM COSTS	2-14
2.5.1. Design Justification.....	2-15
2.5.2. Cost Dimensions.....	2-16
2.5.3. Approach.....	2-19
2.6. CONCLUSIONS	2-20
2.7. REFERENCES	2-21
3.1. BACKGROUND.....	3-2
3.2. OVERVIEW OF TECHNOLOGY OPTIONS.....	3-2
3.3. COLD-GAS THRUSTERS.....	3-5
3.3.1. Background.....	3-5
3.3.2. Performance Cost.....	3-6
3.3.3. Price and Mission Costs.....	3-7
3.4. SOLID MOTORS	3-8
3.4.1. Background.....	3-9
3.4.2. Performance Costs.....	3-10
3.4.3. Price and Mission Costs.....	3-11

3.5. LIQUID ENGINES	3-13
3.5.1. Bi-Propellant Option	3-15
3.5.2. Mono-Propellants	3-20
3.5.3. Mono-Propellants vs. Bi-Propellants	3-22
3.5.4. Mission Costs	3-22
3.6. HYBRID MOTORS	3-24
3.6.1. Costs	3-27
3.7. ELECTRIC ENGINES	3-30
3.7.1. Resistojet	3-30
3.7.2. Pulsed Plasma Thrusters	3-34
3.8. CONCLUSIONS	3-37
3.9. REFERENCES	3-38

4.1. HISTORICAL DEVELOPMENT.....	4-2
4.2. RESEARCH PROPOSAL	4-4
4.3. HYBRID DESIGN PROCESS	4-5
4.4. SYSTEM REQUIREMENTS.....	4-6
4.5. BASIC DESIGN DECISIONS	4-7
4.5.1. Oxidiser Selection	4-7
4.5.2. Fuel Selection	4-13
4.5.3. O/F Ratio	4-13
4.5.4. Operating Pressure	4-14
4.5.5. Port Design	4-15
4.5.6. Oxidiser Flow Rate	4-16
4.6. PERFORMANCE ESTIMATION	4-16
4.6.1. Theoretical Results	4-16
4.6.2. Previous Empirical Results	4-17
4.7. COMPONENT DESIGN	4-22
4.7.1. Fuel Grain	4-22
4.7.2. Nozzle	4-24
4.7.3. Combustion Chamber	4-26
4.7.4. Oxidiser Delivery System	4-27
4.7.5. Support Structure	4-27
4.8. SYSTEM DESCRIPTION	4-28
4.8.1. Test Site	4-28
4.8.2. Motor	4-29
4.8.3. Test Stand	4-32
4.8.4. Oxidiser Delivery System ("Plumbing")	4-33
4.8.5. Data Collection and Control	4-35
4.9. CONCLUSIONS	4-37
4.10. REFERENCES	4-38

5.1. PROOF-OF-CONCEPT	5-2
5.2. CATALYST PACK DEVELOPMENT & TESTING	5-4
5.2.1. Catalyst Pack Design	5-4
5.2.2. Program Overview	5-6
5.2.3. Phase 1 Discussion	5-6
5.2.4. Phase 2 Discussion	5-15
5.2.5. Catalyst Testing Conclusions	5-19
5.3. HYBRID PERFORMANCE CHARACTERISATION	5-20
5.3.1. Discussion	5-21
5.3.2. Remarks	5-25
5.3.3. Upper Stage Motor Design	5-32
5.4. HYBRID COST ANALYSIS	5-36
5.4.1. Motor Price	5-36
5.4.2. Mission Costs	5-37
5.4.3. HTP Mono-Propellant Option	5-40
5.5. CONCLUSIONS	5-41
5.6. REFERENCES	5-41
<hr/>	
6.1. BACKGROUND.....	6-2
6.1.1. Mission Cost Drivers	6-2
6.1.2. Baseline Architecture	6-3
6.1.3. Cost Estimating Relationships	6-4
6.1.4. Market Analysis	6-6
6.2. SYSTEM DEVELOPMENT	6-8
6.2.1. Design Requirements	6-9
6.2.2. Previous Examples	6-11
6.2.3. Trade-offs	6-17
6.2.4. Acquisition Process	6-23
6.2.5. Results	6-25
6.3. TOTAL SYSTEM COST	6-27
6.3.1. Performance	6-27
6.3.2. System Price	6-30
6.3.3. Integration Cost	6-31
6.4. CONCLUSIONS	6-39
6.5. REFERENCES	6-41

7.1. OVERVIEW.....	7-2
7.2. DESCRIBING TOTAL COST.....	7-5
7.2.1. Design Justification Process.....	7-5
7.2.2. Total Cost Figures of Merit.....	7-6
7.3. COMPARING TOTAL COST.....	7-8
7.3.1. Approach.....	7-8
7.3.2. Mission Scenarios.....	7-9
7.3.3. Propulsion System Options.....	7-11
7.4. RESULTS.....	7-16
7.4.1. Commercial Missions.....	7-16
7.4.2. Experimental and Lunar Missions.....	7-19
7.5. CONCLUSIONS.....	7-21
7.6. REFERENCES.....	7-22
<hr/>	
8.1. RESULTS.....	8-2
8.2. CONCLUSIONS.....	8-3
8.2.1. Spacecraft Hardware Costs.....	8-3
8.2.2. Cost-Effective Propulsion Systems.....	8-3
8.2.3. Propulsion Technology.....	8-4
8.3. ACCOMPLISHMENTS	8-7
<hr/>	
<hr/>	
<hr/>	

COMPLETE TEXT OF THESIS

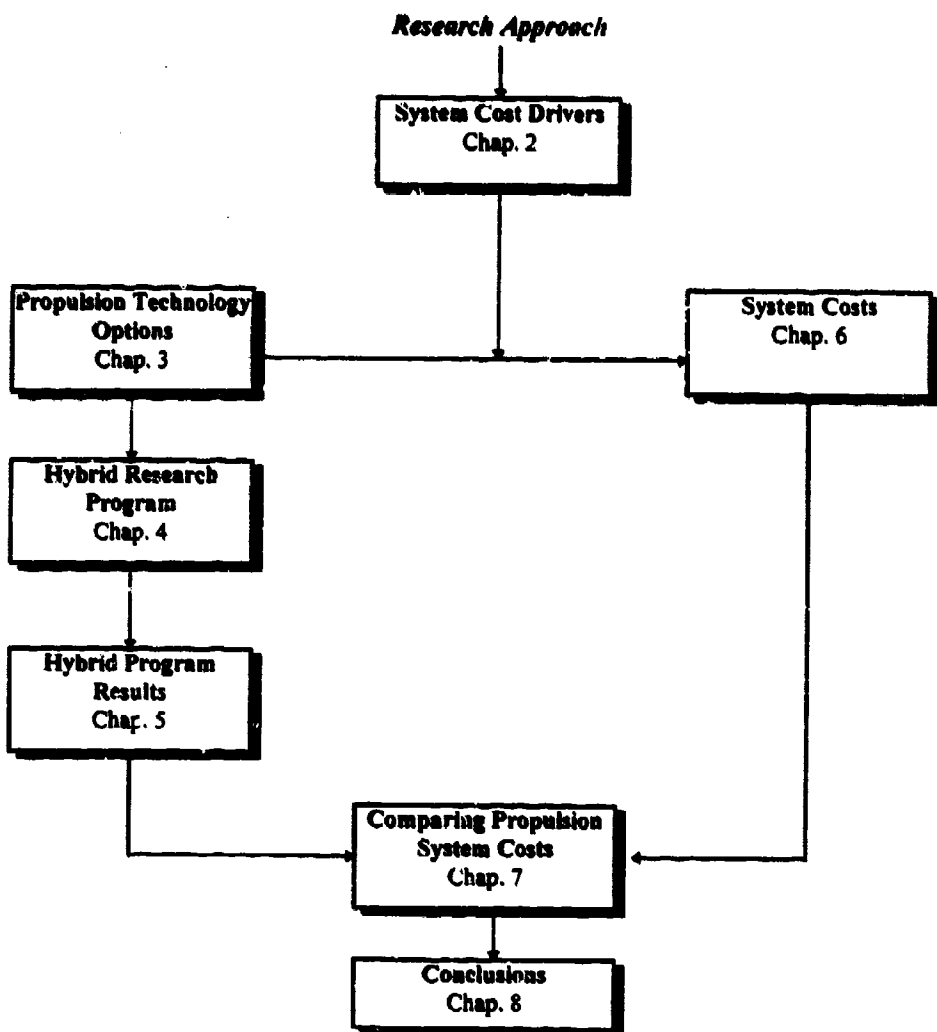
ROCKET PROPULSION FUNDAMENTALS

EXPERIMENTAL DATA (MICROSOFT EXCEL FILES)

ANALYSIS WORKSHEETS (MATHSOFT MATHCAD FILES)

HYBRID & CATALYST PACK FIRING VIDEO CLIPS

ORGANISATION OF THESIS AND RESEARCH



List of Symbols & Abbreviations

\dot{r}	Hybrid fuel regression rate (mm/sec)
\dot{m}_{ox}	Oxidiser mass flow rate (kg/sec)
\dot{m}	Propellant mass flow rate (kg/sec)
\dot{V}_{fuel}	Volume flow rate of fuel (m ³ /sec)
a	Burn rate coefficient (appropriate units)
A	Cross-sectional area of catalyst pack (m ²)
$accel$	Acceleration (m/sec ²)
ADCS	Attitude determination and control system
A_e	Nozzle exit area (m ²)
AMSAT	Amateur satellite organisation (responsible for OSCAR missions)
A_{port}	Hybrid port cross-sectional area (m ²)
A_t	Nozzle throat area (m ²)
C^*	Characteristic exhaust velocity (m/sec)
CER	Cost estimating relationship
C_p	Propellant heat capacity (cal/gmK)
CVPR	Cavitating venturi pressure recovery = 72.5%
$dIsp$	Density specific impulse (s.g. sec)
DoD	U.S. Department of Defence
Δr	Required average fuel regression rate (mm/sec)
ΔT	Temperature change from standard conditions (K)
ΔV	Change in velocity for a manoeuvre
ESA	European Space Agency
FN	Cavitating Venturi Flow Number
γ	Ratio of specific heats
G	Total propellant (fuel plus oxidiser) mass flux (kg/m ² sec)
GEO	Geostationary orbit
g_0	Standard gravitational acceleration at sea level = 9.81 m/sec ²
G_{ox}	Oxidiser mass flux (kg/m ² sec)
GTO	Geosynchronous transfer orbit
HTP	High test peroxide, hydrogen peroxide in concentrations for rocket applications (> 80%)
HTPB	Hydroxyl-terminated polybutadiene
I_{PR}	Injector pressure recovery = 80%
I_{sp}	Specific impulse (sec)

<i>J</i>	Discharge current (A)
<i>L</i>	Port length (m)
<i>L/D</i>	Length to diameter ratio for hybrid port
LEO	Low-Earth orbit
<i>LF</i>	Catalyst pack loading factor (kg/sec/m ²)
LOX	Liquid oxygen
<i>M</i>	Molecular weight of propellant (kg/kmole)
μ	Permeability of free space ($4\pi \times 10^{-7}$ henries/m)
<i>m_{deployed}</i>	Deployed mass of spacecraft (kg)
MMH	Monomethyl hydrazine
MON	Mixed oxides of nitrogen, generally nitrogen tetroxide with 1 - 25% added NO
MPD	Magneto-plasma dynamic (a type of electrostatic thruster)
<i>m_{prop}</i>	Mass of propellant (kg)
<i>n</i>	Burn rate exponent
NASA	National Aeronautics and Space Administration
NTO	Nitrogen tetroxide
<i>O/F</i>	Oxidiser to fuel ratio
<i>P</i>	Power (W)
<i>P_{ambient}</i>	Ambient pressure (bar)
<i>P_{atmosphere}</i>	Atmospheric pressure = 1 bar
<i>P_c</i>	Chamber pressure
<i>PE</i>	Polythene
<i>P_{exit}</i>	Nozzle exit pressure (bar)
PPT	Pulsed plasma thruster
<i>P_{Tank}</i>	Oxidiser tank pressure (bar)
<i>P_{ave}</i>	Average specific gravity of propellants (non-dimensional)
<i>r_b</i>	Solid propellant burning rate (mm/sec)
RFQ	Request for Quotation
<i>p_{fuel}</i>	Fuel density (kg/m ³)
ROM	Rough order of magnitude
<i>p_{ox}</i>	Oxidiser density
SCAPE	Self-contained aspirated protection ensemble
<i>σ_p</i>	Burning rate temperature sensitivity parameter (at constant pressure) (appropriate units)
SSTL	Surrey Satellite Technology Ltd.
<i>T_c</i>	Chamber temperature (K)

<i>TGO</i>	Time to Go, duration of manoeuvre
<i>time</i>	Total burn time (sec)
<i>Tinitial</i>	Initial propellant temperature (K)
UoSAT	University of Surrey Satellite or University of Surrey Satellite Engineering Unit
<i>Volfuel</i>	Volume of fuel (litre)
<i>Volox</i>	Volume of oxidiser (litre)
<i>Vratio</i>	Velocity ratio, used in TGO calculation.
<i>x</i>	Distance along hybrid port (m)
PMD	Propellant management device

Hybrid Rocket Testing Photographs



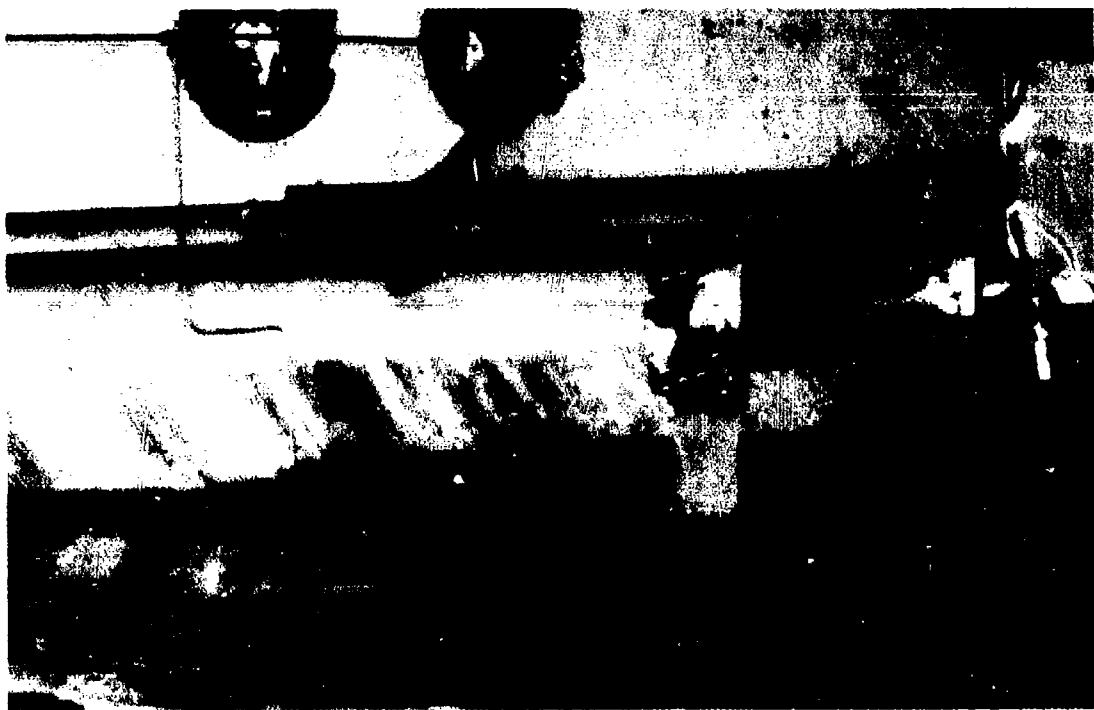
Hybrid Rocket Motor Test Apparatus



The Author standing next to the hybrid test rig at Royal Ordnance, Westcott.



Hybrid motor at initial start-up prior to ignition.



Hybrid motor firing.

Chapter 1

Introduction

- 1.1. BACKGROUND**
- 1.2. RESEARCH PLAN**
- 1.3. THESIS SUMMARY**
- 1.4. LITERATURE REVIEW**
- 1.5. PUBLICATIONS**
- 1.6. REFERENCES**

My primary research objective was to investigate cost-effective propulsion system options for small satellite missions. This chapter serves as an introduction to the thesis and provides an overview of this research. To explain the context for my work the chapter begins with a brief background on the satellite engineering group at the University of Surrey (UoSAT). From there, future mission opportunities for small satellites are described from which the motivation for this research topic derives. Concurrent with this research, the University was designing a multi-mission minisatellite bus. The design objectives for this project are summarised to indicate the near-term application for my results. The minisatellite project provided a well-defined set of requirement and constraints enabling me to narrow the scope of my research and develop a detailed set of research goals. With these goals in mind, specific tasks were derived to guide the program. These goals are reviewed and an overview of the research plan is presented. Each goal and its corresponding tasks are summarised. A list of my own publications during the research concludes the chapter.

1. Introduction

1.1. *Background*

This section presents a brief background on the University of Surrey satellite engineering group, or UoSAT, within which my research was conducted. Future mission opportunities for UoSAT-class satellites are then examined. From this discussion, the need for cost-effective propulsion systems emerges as a key enabling technology to allow truly low-cost satellites to take on more challenging missions. Finally, the section describes the UoSAT minisatellite. This multi-mission 250-kg-class satellite was being developed concurrent with my own research and served as an important focal point for the near-term applications of the results.

1.1.1. *UoSAT Microsatellites*

The current catch-phrase of the aerospace industry—"faster, better, cheaper"—represents political and economic necessity as much as good engineering practice. While industry as a whole struggles to fully define this "new" strategy in the wake of the post-cold war draw down, the University of Surrey and its commercial arm Surrey Satellite Technology Ltd. (SSTL), as well as others in the so-called "amateur" satellite community, have been quietly implementing this philosophy all along. Since 1981, University of Surrey satellites (UoSATs) have shown that small, reliable satellites can be built and operated at costs far less than one would find in the mainstream aerospace industry. The basic UoSAT design, evolved over more than ten missions, has proven itself as a reliable cost-effective platform for quick access to low Earth orbit. Since the launch of UoSAT-1 in 1981, the role for microsatellites in low Earth orbit has evolved from a useful education, technology demonstration and radio amateur project to play a small but significant role in commercial electronic communications, remote sensing, technology transfer and military research. As of this writing, the SSTL/UoSAT team have logged nearly 50 orbit-years of operational experience.

Part of the reason for UoSAT's success is the remarkably short project time scale and comparatively low project cost that has been achieved. A UoSAT microsatellite mission can be completed within 12 months from contract kick-off to in-orbit delivery enabling a rapid response to the customer's requirements. Time scales are kept short and costs low by the adoption of small-team techniques, a high degree of modularization within the microsatellite bus and experiments, as well as a variety of other cost-effective engineering practices.

So far, all UoSAT spacecraft have been in the microsatellite range (~ 50 kg), designed to operate in the relatively benign environment of low-Earth orbit (LEO). These spacecraft have all been gravity gradient stabilised, augmented with magnetorquers. A diagram of the latest configuration represented by FASat-Alfa, built for the Chilean Air Force, is shown in Figure 1-1 with the gravity gradient boom extended (6 meter boom not to scale).

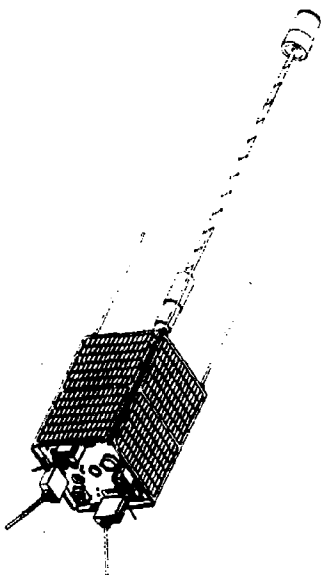


Figure 1-1: FASat-Alfa with gravity gradient boom deployed (6 meter boom not to scale).

1.1.2. Future mission opportunities

Deployed directly into stable, operational orbits as “piggy-back” secondary payloads, UoSAT-class microsatellites have proven to be capable platforms for store-and-forward communications, space science and remote sensing. As currently configured, these microsatellites fill a specialised niche. However, the primary motivation for my research was a desire to expand the role of these low-cost, small satellites beyond this niche to take on a variety of more ambitious missions.

Obviously, small satellite missions depend on launch opportunities. So far, the majority of UoSAT missions have been on *Ariane* launchers attached to the *Ariane* Structure for Secondary Payloads (ASAP) ring and deployed into LEO. However, a review of *Ariane* launch manifests into the foreseeable future at the outset of my research revealed the majority of opportunities for secondary payloads would be into geosynchronous transfer orbit (GTO). This is a highly elliptical orbit 200 x 36,000 km altitude with an inclination of 7°. GTO offers a variety of mission opportunities. OSCAR Phase-3 missions, for example, have used GTO as starting point for Molniya communications missions. Other mission opportunities that could exploit low-cost launches into GTO include:

- *Small geosynchronous (GEO) communications*—Currently, developing countries must lease transponders on large, expensive commercial satellites. The possibility exists for them to purchase their own small, dedicated satellite at a competitive price.
- *Meteorological monitoring*—Microsatellites have demonstrated their utility for localised weather monitoring from LEO. Small satellites beginning in GTO could be used as low-cost weather monitoring platforms with the higher altitude providing more global access.
- *Geomagnetic data collection*—Because spacecraft in GTO travel through the entire depth of the Van Allen radiation belts twice daily, they offer an ideal vantage point from which to monitor important phenomena in the space environment such as solar wind and magnetic field interactions, galactic cosmic rays and solar flares.

- *Ground-based astronomy calibration*—Ground-based optical astronomy is handicapped by the dynamic nature of Earth's atmosphere which attenuates faint signals. A satellite in very high Earth orbit with a low-power laser of known wavelength could provide the feedback necessary to perform real-time calibration and correction of these signals, greatly enhancing their resolution.
- *Lunar and planetary exploration*—From GTO, the total velocity change (ΔV) necessary to go to lunar orbit, Earth approaching asteroids or even other planets is roughly equivalent to that needed to go into GEO. Spacecraft such as the U.S. *Clementine* mission have demonstrated how very good planetary science can be conducted from small, relatively low-cost (~\$70M) platforms. The opportunity exists to use GTO as a springboard to explore the solar system with even smaller, and far cheaper (~\$10M) satellites.

In addition to these missions specifically related to GTO, other exciting opportunities are emerging for LEO small satellites:

- *Micro-LEO constellations*—Constellations of two or more store-and-forward communication satellites to support world-wide paging, data collection from geographically remote scientific or industrial facilities, disaster relief and other services.
- *"Personal" Remote Sensing*—Developing countries currently depend on large, expensive remote sensing platforms such as SPOT or LANDSAT. A dedicated small satellite with nearly the same resolution that also offers on-demand coverage and the ability for the user to exercise far greater control over imaging times, targets, lighting and area re-visits appears feasible at a competitive cost.
- *SAR missions*—Synthetic aperture radar (SAR) offers the ability to pierce through cloud cover to collect images day or night. So far, this technology has been limited to very large, expensive platforms, however, it now appears feasible to deploy a limited but useful SAR capability on a small LEO satellite.
- *Equatorial belt missions*—All of the LEO missions listed above would provide global coverage from a polar orbit. However, developing countries, especially in the Pacific Rim such as Indonesia, Malaysia, Singapore and the Philippines are increasingly interested in dedicated regional coverage. This could best be provided by satellites operating in very low inclination orbits.

Unfortunately, at the outset of my work, UoSAT spacecraft (as well as similar satellites built by other Universities and companies) lacked one critical system that would allow them to exploit fully the mission opportunities outlined above: a propulsion system. Propulsion systems are a common feature on virtually all larger satellites. However, until now there has been no need for very small, low-cost satellites to have these potentially costly systems. As secondary payloads, they were deployed into stable, useful orbits and natural orbit perturbations (drag, J2, etc.) were acceptable within the context of the relatively modest mission objectives. Over the years, these pioneering small satellite missions have proven that effective communication, remote sensing and space science can be done from a cost-effective platform. As these missions have evolved, various technical challenges in on-board data handling, low-power communication, autonomous operations and low-cost engineering have been met and solved. Now, as mission planners look beyond passive missions in LEO to the new missions described above, all of which require active orbit and attitude control, a new challenge is faced—cost-effective propulsion.

Propulsion systems are needed to perform a variety of tasks essential to active missions in LEO and beyond. These include:

- *Orbit Manoeuvring*—the ability to move from an initial parking orbit to an escape trajectory or insert into a final mission orbit, e.g. changing from GTO to GEO.
- *Orbit Maintenance*—the ability to maintain a specific orbit against drag and other perturbations, or phase the orbit to maintain proper angular separation of a constellation.
- *Attitude Control*—The ability to rotate the spacecraft to reorient sensors or dump momentum, especially beyond LEO where magnetorquing and gravity gradient stabilisation are not viable options.

Obviously, all these capabilities can be found in off-the-shelf systems used throughout the aerospace community. However, as this thesis will show, current off-the-shelf technology may not be appropriate for cost-effective applications within the context of small satellite missions. Furthermore, the cost of these systems, when procured using standard aerospace practices can be prohibitive. Thus, small satellite mission planners face a dilemma—future missions demand a propulsion capability but the cost of this single system may be prohibitive, keeping the entire mission grounded.

By the nature of the small satellite industry, technology development costs must often be funded “in-house.” This is certainly the case at UoSAT/SSTL. There is no external customer to pass on these costs to, and no easy way to amortise these costs over several missions. As a result, there is a very sensitive “threshold cost” level for new spacecraft subsystems, meaning that below this threshold level the mission can proceed. Above this level, the mission is not feasible. A cost-effective propulsion system could be the one piece of enabling technology that acts as a key to unlock the future for small satellites and allow them to economically evolve beyond LEO and reach out to the planets. I recognised this as a unique research opportunity at the outset of my work with immediate and significant applications.

1.1.3. The UoSAT Minisatellite

Concurrent with my research, engineers in SSTL/UoSAT were designing a flexible, multi-mission minisatellite to position themselves to exploit the emerging opportunities discussed above. With an approximate mass of 250 kg, the minisatellite structural design builds on the modular approach used in the UoSAT microsatellites in a way that allows maximum re-use of subsystems between the two platforms. The minisatellite structure starts with a honeycomb attach frame on which three stacks of module boxes are arranged in a triangle. Solar panels of the same width as those used on the microsatellites are arranged around the sides to get a total of nine sides. By extending the height of the panels, an equipment or payload bay is formed at the top of the module box stack. A diagram of the minisatellite is shown in

Figure 1-2. As this is written, the first flight of this new satellite bus, dubbed UoSAT-12, is in critical design for a launch in Mid-1997.

The technical objectives for the minisatellite mission strike a compromise between all the features a flexible minisatellite bus would have and what can be achieved within the available budget and time scale. The following technical objectives have been defined for the UoSAT-12 mission:

- Demonstrate a commercially viable minisatellite bus with industry-standard support systems
 - 28 VDC power bus
 - 1 MBPS S-band down-link
- Demonstrate that enhanced core microsatellite technologies can be used in a minisatellite:
 - Intel 386-based on board computers (OBC)
 - Low-rate VHF/UHF data links
 - Distributed TT&C via control area network (CAN)
- Demonstrate major new subsystems:
 - Enhanced attitude determination and control capability
 - Propulsion system capability with orbit maintenance and attitude control
- Enhance existing UoSAT payloads using resources of the minisatellite to provide operational demonstration of:
 - High-resolution (<30 m) multi-spectral visible imaging
 - Store-and-forward communications to small terminals

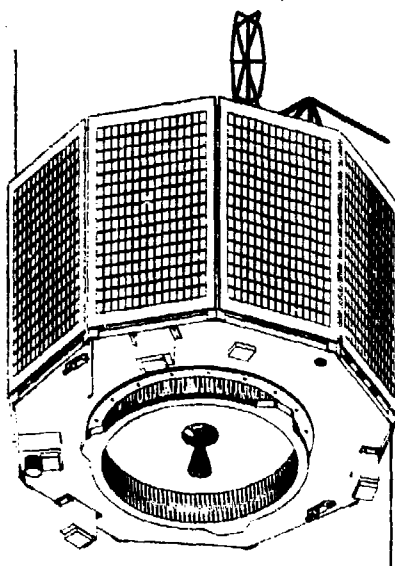


Figure 1-2: Diagram of University of Surrey Minisatellite

Of these objectives, my research had direct application to the desire for propulsion capability. This created a specific context for my research and provided me an opportunity to narrow the scope of my efforts by working within a well-defined set of engineering requirements and constraints. Furthermore, because I carried out my research as an integral member of the minisatellite development team, I had continuous feedback on the utility of my results.

1.2. Research Plan

The formulation of my research plan drew upon the vast resources and expertise available within SSTL/UoSAT as well as my own ten year's experience working in the industry. This section will show how I devised a methodical approach for the research by first identifying relevant requirements and constraints. From there, a specific set of research goals were defined, with corresponding tasks, to form the basis for the overall plan.

1.2.1. Requirements and Constraints

Because the first application for the results of this research would be on the UoSAT minisatellite, it was important to define the specific integration requirements and constraints imposed by this spacecraft on any propulsion system technology options developed. Working with the UoSAT team, the following set of system requirements and constraints were identified which served as guidelines for the research:

1. System compatible with minisatellite envelope, mass and power
 - Total propulsion system loaded mass < 50 kg
 - Total system envelope as defined in Chapter 6
 - Power system requirements—total orbit average power available ~100 W, 28 VDC bus, maximum battery capacity 6 A-hr, maximum short-term power 560 W (20 amps at 28 V for 10 minutes takes the batteries to 40% depth of discharge).
2. System in compliance with U.S. Air Force specifications for pressure systems and acceptable to Vandenberg Air Force Base range safety requirements (actual launch site was initially not known so this was chosen as the most conservative).
3. Propulsion system research and development constrained by available facilities, resources, man-power and budget.

1.2.2. Approach

As stated above, the primary objective of this research was to investigate cost-effective propulsion system options for small satellite applications. The relatively wide scope of this objective required that the research encompass not only rocket technology but systems engineering as well. Years of experience, at UoSAT and elsewhere, have repeatedly emphasised the importance of this two-phased approach to effective small satellite engineering. It is not sufficient to concentrate only on technology. In fact, the "best" technology is often not the "best" solution, especially for small satellites. Rather, a truly cost-effective design is an innovative blend of sufficient technology with thorough systems engineering.

Recognising this necessity, the research encompassed both the purely theoretical and technological issues of rocket science in depth as well as the broader, systems engineering issues of adapting this technology to the philosophy of small satellites. Using the requirements and constraints described in the last section, the scope of the research was narrowed by developing the specific set of research goals listed below:

1. Determine key cost drivers for spacecraft systems to identify useful cost-effective engineering practices and develop a paradigm for evaluating the total cost of propulsion system options.
2. Characterise propulsion technology costs by identifying viable options and investigating each to evaluate their performance, price, and overall potential for small satellite application.
3. Characterise propulsion system costs by completing a design case study for a representative minisatellite mission.
4. Evaluate and compare the cost-effectiveness of system options by developing a useful process for quantifying total cost and demonstrating its utility as a mission planning and research tool.

With these goals in mind, an overall research strategy was devised to encompass them. This strategy is best illustrated using a "road map" as shown in Figure 1-3. Each phase of the strategy is shown along with the specific chapter of the thesis where it is discussed. As you can see, the research begins by fully exploring cost-effective engineering practices to identify specific cost drivers for spacecraft hardware important throughout the life of a mission. Based on this investigation into spacecraft systems engineering, I developed a nine-dimensional cost paradigm for propulsion systems that recognised that their costs can be tackled on two fronts: propulsion technology (what type of rocket is used) and system architecture (how the rocket is used). This revelation pointed the way to two parallel lines of research, one looking at rockets, the other looking at complete systems.

Focusing first on rocket options, my research began by considering all realistic near-term technologies. Cold-gas thrusters, solid rocket motors, storable liquid systems, hybrid rockets and electric propulsion options were all examined in detail. Each was fully characterised using the nine dimensions of the total cost paradigm. From this analysis, hybrid rockets emerged as having various inherent features that make them attractive for cost-effective upper stage applications. Unfortunately, because hybrid technology does not exist off-the-shelf, an in-depth basic research effort was called for to develop this technology to a sufficient level to realistically evaluate its true potential. This effort resulted in a comprehensive hybrid research program looking at all aspects of this little-used technology to prove its feasibility, characterise its performance and fully assess its total cost.

With all the technology options fully characterised, the research proceeded down the second path to examine complete systems. It was determined that the best technique for fully quantifying the systems engineering effects on total cost was to actually design a complete system for a well-defined minisatellite mission. Using conventional off-the-shelf technology, this design exercise took a complete system through to Critical Design Review in order to develop a real system that could be flown on the UoSAT minisatellite, evaluate the influence of mission cost drivers on total system cost, and establish a realistic system cost model useful for future mission planning. The success of this effort was assessed by comparing derived system cost with that predicted by standard cost estimating relationships.

The final goal of the research was to evaluate total system costs by developing a simple method for synthesising my results and applying them to preliminary mission planning. This would enable important conclusions about cost-effective propulsion systems to be drawn. The effort involved the development of a parametric technique to combine each of the nine dimensions of the total cost paradigm to produce a single figure of merit for each system option within the context of a given mission. These figures of merit serve to combine and quantify diverse data and proved to be a total quality planning tool with immediate application.

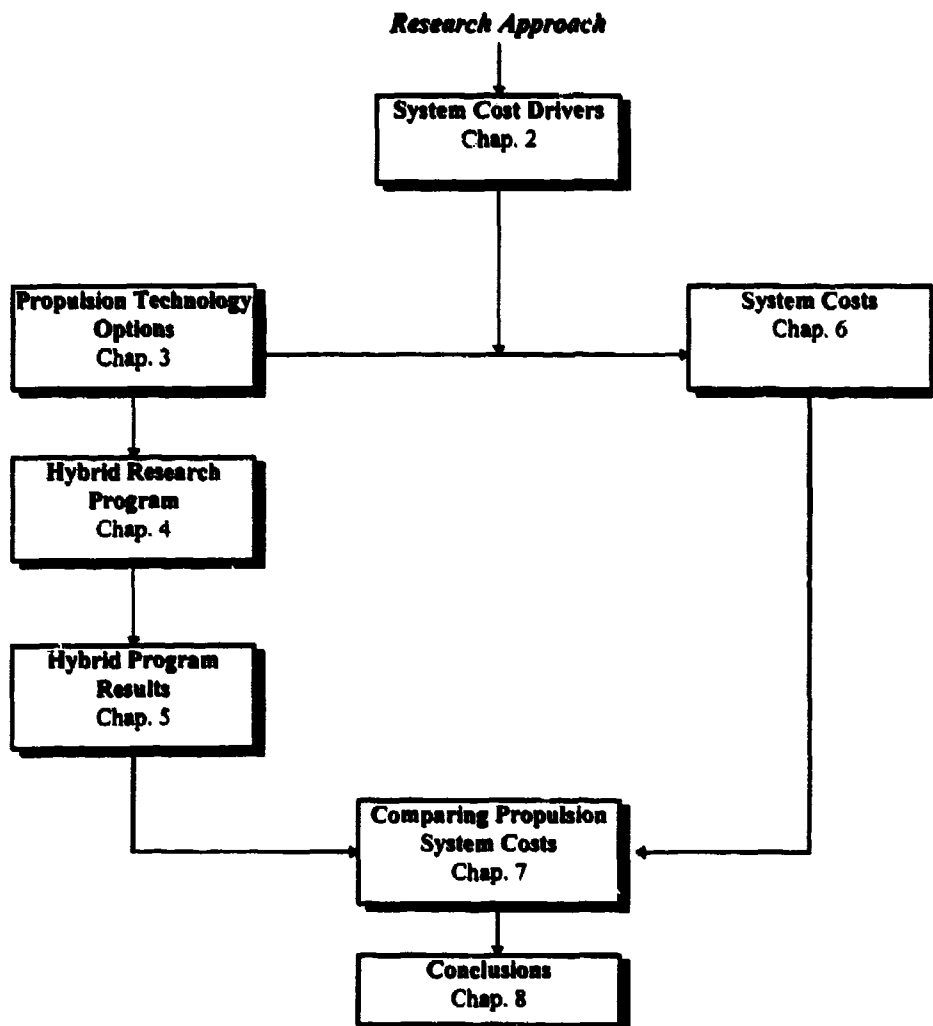


Figure 1-3: "Road Map" of research strategy.

Working from these basic research goals, with the overall strategy in mind, a specific set of tasks was defined to guide my work. Table 1-1 summarises the tasks undertaken to accomplish each research goal and indicates the chapter of the thesis where each is discussed.

Research Goal	Tasks	Chapter
1. Determine key cost drivers for spacecraft systems to identify useful cost-effective engineering practices and develop a paradigm for evaluating the total cost of propulsion system options.	1.1 Review low-cost satellite engineering practices at UoSAT and elsewhere. 1.2 Identify cost drivers at each phase of spacecraft hardware development and cost-effective engineering methods to address them. 1.3 Develop a total cost paradigm for propulsion systems.	2
2. Identify candidate propulsion technology options and investigate them to a sufficient level to characterise their total cost, performance, and overall potential for small satellite application.	2.1 Identify candidate propulsion technology options. 3.2 Fully characterise each option with respect to the total cost paradigm—Hybrid rockets emerge as a promising technology in need of further research. 2.1 Define goals of a hybrid research program and set about attaining them: <ul style="list-style-type: none">• Prove the Concept—demonstrate the basic accessibility of hybrid technology, address and solve significant engineering problems• Characterise Performance—experimentally determine hybrid combustion relationships.• Assess total cost—analyse and assess the total cost of hybrid for satellite applications.	3, 4, 5
3. Design and analyse a representative propulsion system architecture for the minisatellite in order to identify and evaluate useful cost-effective engineering practices and fully characterise total system costs.	3.2 Review and apply existing propulsion system cost models to derive system cost estimates. 3.3 Perform a market survey of propulsion system component costs. 3.4 Evaluate cost-effective propulsion system engineering practices on other low-cost missions. 3.5 Perform a detailed design of a minisatellite propulsion system based on off-the-shelf technology—bi-propellant and cold-gas—to use the design justification process for evaluating overall costs. 3.6 Apply cost-effective engineering practices to iterate the system architecture in order to simplify operations and lower cost. 3.7 Select a potential supplier for propulsion system components (tanks, valves, etc.) to determine system configuration, size, mass, and cost. 3.8 Define a realistic system price model.	6
4. Develop a metric for evaluating cost-effectiveness of system options by using the results from the previous objectives to derive a total cost figure of merit and demonstrate its utility for future mission planning.	4.1. Use the propulsion system cost paradigm and the design justification process to develop a total system cost figure of merit. 4.2. Apply the cost figure of merit to various system options to evaluate them for different mission scenarios. 4.3. Evaluate all results to draw useful conclusions.	7

Table 1-1: Summary of research goals, their specific corresponding tasks and the chapter of the thesis where they are addressed.

1.3. Publications

Below is a list of publications during the first two years of the research. Additional publications are envisioned after completion of this thesis:

Sellers, J.J., Sweeting, M., Hodgart, S., "UoSAT and Other European Activities in Small Satellite Attitude Control," AAS 94-042, Presented at the 17th Annual AAS Guidance and Control Conference, Keystone, Colorado, 2-6 February, 1994.

Allery, M.N., Sellers, J.J., Sweeting, M., "Results of University of Surrey On Orbit Microsatellite Experiments," Presented at the 2nd International Symposium on Small Satellite Systems and Services, Biarritz, France, 27 June - 1 July, 1994.

Sellers, J.J., Meerman, M., Paul, M., Sweeting, M., "A Low-Cost Propulsion System Option for Small Satellites," Journal of the British Interplanetary Society, Vol. 48., pp. 129-138, March, 1995.

Sellers, J.J., Hashida, Y., Williams, R. Sweeting, M., "The Attitude and Orbit Control System for the University of Surrey Minisatellite," Presented at the International Symposium on Space Dynamics, Toulouse, France, 19-23 June, 1995.

Sellers, J.J., Paul, M., Meerman, M., Wood, R., "Investigation into Low-Cost Propulsion System Options for Small Satellites" Presented at the 9th Annual AIAA/USU Small Satellite Conference, Logan, Utah, September 1995.

Sellers, J.J., Milton, E., "Cost-Effective Spacecraft Hardware & Technology," Chapter in *Reducing Space Mission Costs*, Dr. James Wertz, editor, to be published, early 1996.

Chapter 2

System Cost Drivers

- 2.1. OVERVIEW**
- 2.2. MISSION DEFINITION PHASE**
- 2.3. MISSION DESIGN PHASE**
- 2.4. HARDWARE ACQUISITION PHASE**
- 2.5. PROPULSION SYSTEM COSTS**
- 2.6. CONCLUSIONS**
- 2.7. REFERENCES**

Before one can begin to design cost-effective propulsion systems it is essential to understand the basic cost environment of spacecraft hardware in general. This chapter begins by identifying the fundamental cost drivers affecting space hardware. The purpose of this exercise was to establish a useful context for understanding the expensive process of selecting and flying space hardware. Based on this analysis, the critical cost dimensions for propulsion systems could then be isolated. A new paradigm for understanding and evaluating these costs is described and a preview of its application in subsequent chapters is given.

2. System Cost Drivers

2.1. Overview

As I began research into the factors affecting the cost of propulsion systems, it immediately became obvious that I must first address the broader issues of spacecraft hardware costs in general. Only by first isolating and explaining the fundamental cost drivers of these traditionally expensive components could I formulate a credible strategy for reducing the costs of propulsion hardware specifically. Furthermore, the most useful application for this research would be on commercially viable small satellites which demand systems with predictable, repeatable total costs. Therefore, it was important to understand both near-term non-recurring and longer term recurring costs.

To that end, the research began by identifying specific hardware cost drivers which occur during each phase of a mission. The purpose was to provide a useful context for understanding the process of selecting and flying space hardware in general which could then be applied to propulsion systems. Taken separately, the specific cost drivers identified here, and the recommendations offered for overcoming them, could well be viewed as simply common sense. However, it is important to emphasise that for the first time this research combines these diverse cost drivers into a coherent strategy firmly rooted within the context of mission development. In so doing, the complex interrelationships between the various trade-off decisions made during the course of a mission can be better understood and dealt with. The discussion in this chapter summarises a more detailed chapter on the subject which I wrote during the research. The unique nature of this approach is underscored by its selection for publication in a new industry-standard reference, *Reducing Space Mission Costs*, edited by Dr. Jim Wertz [Wertz 96].

The first question to ask when trying to reduce spacecraft system costs is “why is space hardware so expensive?” Some, like space economist Chris Elliot [Sellers 94a] argue that space missions (and their associated hardware) are so expensive simply because we expect them to be. That is, when it is assumed that space missions will be expensive, programmatic decisions are often made which turn this into a self-fulfilling prophecy, as Figure 2-1 illustrates. High-cost missions mean there will be fewer missions. Fewer missions dictates higher reliability for those that do fly. Demand for high reliability leads to high cost, and so on, a vicious circle. To break out of this vicious circle, organisations must first accept that missions can be inexpensive. Only then can decisions be made which allow this to happen.

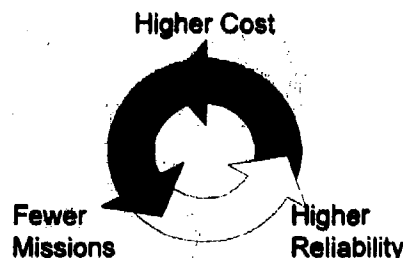


Figure 2-1: Vicious circle of high cost mission. Assuming space is expensive means fewer missions are planned which demand greater reliability. This becomes a self-fulfilling prophecy.

So, assuming one can make this leap of faith and accept that low-cost spacecraft are an achievable goal, how does one go about obtaining the necessary low-cost hardware? To simplify the discussion of this complex process, I will divide the life-cycle of a mission, as it pertains to specific hardware cost, into three phases:

- Mission Definition Phase
- Mission Design Phase
- Hardware Acquisition Phase

During each of these mission phases, decisions and actions are carried out that directly influence the bottom line price paid for hardware. The first part of the chapter will examine these mission phases in detail to identify specific hardware cost drivers. By understanding the cost sensitivity of these decisions and actions, one can be in a better position to capitalise on specific low-cost hardware technology options. As this chapter will show, cost-effective hardware is most often achieved by an innovative definition of requirements tempered by a sound understanding of mission drivers.

A “road map” summarising the approach explained in this chapter is presented in Table 2-1. Understand that while this is presented in a linear fashion, by its nature the process is one requiring feedback, iteration and imagination. The purpose is to develop a comprehensive but flexible approach that encompasses the critical aspects of cost-effective hardware selection and qualification. The following three sections will go through cost drivers in each of the mission phases. The final sections will tie these back together to formulate a coherent cost analysis paradigm for propulsion systems.

2.2. Mission Definition Phase

Despite the best cost-cutting attention of any engineer or program manager, there are certain harsh realities of planning and operating space missions that cannot be simply budgeted away. During the Mission Definition Phase, the “who, what, where, why & when” of a mission are defined. The answers to these questions determine the entire mission environment.

There are two aspects of this environment that are among the biggest cost drivers for space hardware:

- The physical launch & space environments
- The political environment

Mission Phase	Cost Drivers	Technical Impact	Cost Implications
1. Mission Definition	1.1 Launch & Space Environment—what the hardware will be subjected to.	<ul style="list-style-type: none"> Specific hardware performance requirements e.g. radiation hardness Materials and practices to use or avoid. 	<ul style="list-style-type: none"> Missions to very high radiation orbits e.g. inside the Van Allen belts, may not be able to use terrestrial semiconductors. Space environment requirements may preclude cheap, terrestrial material options
	1.2 Political Environment—what hardware decisions are possible.	<ul style="list-style-type: none"> Specified quality level of components Acceptable risk vs. allowable risk of a given technical approach e.g. what you can technically accept vs. what you can politically allow. 	<ul style="list-style-type: none"> If the customer or political force requires Space Qualified components costs will increase. Use of specific low-cost but higher risk technology options may be precluded.
2. Mission Design	2.1 Performance requirements and margins—what the hardware must do.	<ul style="list-style-type: none"> Subsystem performance specifications Engineering margins to be followed during component manufacturing & testing. 	<ul style="list-style-type: none"> Higher performance leads to higher cost. Specified performance may preclude the use of some technology solutions. Overly-constraining margins increase manufacturing, analysis and testing costs.
	2.2 Quality Level—how you will manage performance uncertainty.	<ul style="list-style-type: none"> Specific components, materials and processes that must be met. Acceptance tests requirements. 	<ul style="list-style-type: none"> "Space Qualified" components cost more than their industrial-grade counterparts. Quality verification during acceptance testing increases manpower and documentation costs.
	2.3 System Architecture Design—how the hardware will be put together.	<ul style="list-style-type: none"> Type, number and deployment of components Redundancy philosophy 	<ul style="list-style-type: none"> Some system architectures may lead to a simpler, lower cost design with little or no performance degradation. True functional redundancy is expensive.
3. Hardware Acquisition	3.1 Hardware Source—the decision to buy, build or "borrow" specific hardware.	<ul style="list-style-type: none"> Component manufacturing process. Insight into technical aspects of hardware. 	<ul style="list-style-type: none"> Type and level of in-house expertise and facilities.
	3.2 Procurement Process—how you will work with suppliers	<ul style="list-style-type: none"> Risk sharing Acceptance testing requirements and procedures. 	<ul style="list-style-type: none"> Level of supplier oversight—risk sharing, documentation & meetings.
	3.3 Space Qualifying—how do you ensure it will work in space.	<ul style="list-style-type: none"> Qualification requirements and procedures. Number of dedicated components needed for qualification. 	<ul style="list-style-type: none"> Type and level of in-house expertise and facilities. In-house hardware and expertise.

Table 2-1: Space hardware cost drivers during each phase of the mission life-cycle.

2.2.1. Launch & Space Environment

During mission definition, the launcher is identified along with the mission orbit. Of course, the price of the launch is a significant portion of the total mission cost. However, the actual launcher and orbit also have a direct impact on available hardware options and their associated cost. Any potential hardware options must be screened and tested to ensure they will survive the punishing ride into space and function in the harsh space environment. Because of this inflexible constraint, some promising low-cost terrestrial hardware must be rejected due to materials or other aspects that are incompatible with launch requirements or space itself. In this way, the launch and space environment serves as an important driver of the technical approach that must be used.

Launch vehicle requirements are strictly defined by launcher agencies. For the Ariane launch vehicle, for example, these procedures and requirements are contained in the *Interface Control Document* (ICD) [DCI] which identifies the temperature, vibration, acceleration and other aspects of the launch environment. Along with the purely technical mechanical requirements spelled out in the ICD, there are also a variety of other requirements specified. These are summarised in my chapter of [Wertz 96].

Compliance with these requirements is especially important when low-cost satellites fly in “piggy-back” mode along with the primary spacecraft customer who bears most of the launch cost. In these situations especially, the launch agency will not tolerate low-cost, corner-cutting options which could endanger the primary payload. Any designer of spacecraft systems must factor these launch agency requirements into the design from the very beginning of the program to avoid costly changes later on. For example, propulsion systems to be used with launch operations out of Vandenberg AFB in California are governed by WRR 127-1 *Range Safety Requirements* [WRR 93]. In addition to this regulation, Military Standards dictate requirements for specific components, for example MIL-STD-1522A [MS 1522A] covers “Standard General Requirements for Safe Design and Operation of Pressurised Missile and Space Systems.” Propulsion systems intended to fly on spacecraft out of Vandenberg, no matter how innovative they may be, must comply with these regulations.

Once your hardware has survived the launch, it next faces the unpleasant environment of space. For a more complete discussion of the physics of the space environment, see [Sellers 1994a] for a basic introduction to the topic, [Jersa 85] for a much more detailed discussion, and [Larson 1992] for specific spacecraft design requirements. Key aspects that affect hardware selection including specific practices to use or avoid are discussed in my Chapter of [Wertz 96].

2.2.2. The Political Environment

In addition to the well-defined launch and space environment, there is an equally constraining, if less well-defined, political environment which is just as hard to ignore. Whatever cost-cutting techniques

are applied to a given space mission, whether its the use of some particular terrestrial hardware or the elimination of a specific documentation requirement, the overriding concern, at least for commercial endeavours, is “will it be politically acceptable?”

It is an unfortunate but true fact of life that the optimum engineering solution is often irrelevant in the face of political demands. Any discussion of options for buying or producing low-cost system hardware can only be effective once this basic context is understood. While the purely technical side of this political environment determines the “acceptable risk” of a given engineering solution, the political dimension determines “allowable risk.” That is, a given technical approach, e.g. use of commercial-grade computer hardware, may be deemed by engineers to constitute an acceptable risk to the program, however, mission managers, with their own agendas and superiors to answer to, may override this decision saying it is not an allowable risk.

Regardless of how cleverly you can manage to cut corners on a particular engineering solution and how confident you are it will actually work, if your customer or the launch authority cannot be convinced the risk is acceptable then it will not be allowed. Fortunately, within the context of small missions, especially those undertaken by University researchers, the customer and the designer are sometimes one and the same. When you are your own customer, you are more likely to fully appreciate all the mission trade-offs and therefore more willing to raise the threshold of both acceptable and allowable risk.

In addition to internal issues, there are external agencies which also drive hardware costs. Parts bought in from abroad often require government export licenses to be obtained by the supplier which can be a very time consuming process, especially where new technologies are involved. The cost of this administration will be passed on in the price of the goods. It is also worth remembering that it may take many months to obtain a license. This is not acceptable in projects using short time scales to contain costs, not forgetting the risk that a license may not be granted at all.

2.3. Mission Design Phase

Once the mission definition phase is completed, the basic mission context is established. At that point, the Mission Design Phase can begin. During this phase, many key designs and technical philosophies are established which serve as important cost drivers for spacecraft hardware. Among the most critical of these are fundamental performance requirements, with corresponding margins, the required component quality level and the basic system architecture definition. It is during this phase that there is the greatest leverage for designing cost effectively.

This process of designing for cost falls under the topic of *cost engineering*. Dean and Unal [Dean 91] provide an excellent overview of this topic as applied to the aerospace industry. As they point out, too often satellite designers focus on reducing mass in order to reduce cost. Unfortunately, this is a

misdirected approach. Parametric analysis consistently reveals that the best leverage for cost reduction is through *complexity reduction*. Reducing mass alone may actually drive up costs because of the associated increase in production complexity. In other words, the best advise is “keep it simple.” For mechanical components, this involves efforts to simplify specifications and reduce parts count as well as assembly and finish tolerances. This section will examine two aspects of system complexity as it relates to cost—performance requirements and system architecture—as well as a third, related issue—component quality level.

2.3.1. Performance Requirements with Margins

Mission performance requirements have one of the biggest impacts on what specific hardware can be considered for a mission. For example, mission ΔV requirements, coupled with mass constraints, can limit you to consider only propulsion options above a certain performance level. Unfortunately, these requirements can be expensive. Furthermore, for most systems there is an exponential relationship between performance (whether measured in reliability, specific impulse or bits/sec) and cost. By carefully considering the impact of each requirement on the total system, it may mean, in some cases, that by simply relaxing a single requirement by 10%, the overall savings could be many times that.

Another point to consider is the performance margin. *Margin* is the engineering tolerance given to a particular specifications. For example, specifications for an engine inlet pressure may be 25 bar with a margin of ± 0.07 bar. The smaller the allowable gap between a system's actual performance and its specification, the more it will cost to ensure compliance. Over-specifying the margin can needlessly drive up the cost. This simple fact has been verified both in practice and through parametric study [Dean 91]. Low cost spacecraft engineering focuses on increasing such margins by controlling requirements. This can lead to a wider range of possible solutions as well as less testing and analysis. By increasing the margin for inlet pressure specification in the above example by a factor of 10 to 40 bar, less than 1% would be lost in engine performance but the overall savings to the program could be many times that. To begin with, the relaxed margin would be much easier and cheaper to ensure compliance. Furthermore, by designing in a wider operating range, overall performance becomes less sensitive to small changes in configuration or performance of related support systems such as tanks, valves and regulators.

There are two important points to keep in mind when specifying the margin for a given performance requirement:

- 1) How difficult is this margin to achieve?
- 2) How will you verify the margin has been met?

Typically, a design is thoroughly tested before committing it to flight model manufacture. However, in systems dependent on precision items, operating with very small margins, the breadboards and demonstrator models become more expensive, tending towards the cost and complexity of the flight

unit. For this reason, modelling and analysis tools are used to simulate the precise components that would be too costly to fabricate for a demonstrator model. Tools and models can also lead to proof of concept in shorter time scales than breadboards which may involve complex machining or long lead time components. A further advantage of modelling is that it is possible to simulate conditions over a much wider range than is possible with physical units.

Unfortunately, sometimes as much effort is required to validate the model as was required to create it in the first place. This drives the models to be more complex which in turn increases costs. Unless the risks and limitations of analysis are properly understood, it can easily become more expensive than building flight representative hardware. The lowest cost is achieved in a design that has sufficient margins to make modelling or demonstrators unnecessary.

Unfortunately, by the nature of small, fast missions, engineers can sometimes not be completely certain of how wide their design margins are until there is a failure. This problem is primarily due to rapid mission turnover, in some cases less than one year from blank paper to launch, which can be both good and bad. On one hand, the short time scale dictates that only the most crucial tests are performed which saves both time and money on expensive tests. On the other hand, this means engineers and operators can not “live” with their hardware for long enough to fully explore all possible failure modes and characterise system performance over a variety of off-nominal conditions. Once again, there is a classic cost vs. risk trade-off that must be faced.

2.3.2. Quality Level

Another important cost driver is inherent in the quality level demanded of components. You obviously pay more for components certified to be “space qualified” than you do for ordinary industrial grade components. Unfortunately, there is no universally accepted definition of what makes a particular component “space qualified.” The most obvious argument, of course, would be if a component had actually been used in space for some considerable length of time under similar operating conditions without failure. However, in some cases, even this argument does not hold.

As any engineer knows, no amount of testing or analysis can completely guarantee that a particular component will never fail. Attempting to manage this uncertainty is the purpose of the entire space-qualifying process.

To deal with the process of managing the uncertainty of specific pieces of hardware, industry has evolved a quality spectrum for components. This *quality spectrum* can be defined in terms of increasing confidence or reliability as you start at one end with commercial/industrial grade components and then moves up to MiLSPEC then High REL and finally Space Qualified at the top end. Each of these quality grades are defined in detail in my chapter of [Wertz 96].

2.3.3. System Architecture Design

System architecture is a broad term used to describe the selection, deployment and interaction of components within a system. It is another cost driver established during the Mission Design Phase. For propulsion systems, this process determines the “plumbing” lay-out of the tanks, valves and engines and their concept for operations. This is fundamentally a design exercise that determines the number and type of components used. During this process, cost vs. performance trade-offs are identified. The decisions made will directly correspond to the final system cost.

Dean and Unal [Dean 91] describe system architecture as the first step in a robust design process. Following this step, *parameter design* begins during which the engineer selects near optimum levels for controllable design parameters such that the “system is functional, exhibits a high level of performance under a wide range of conditions, and is robust to noise factors.” *Noise factors* are those design variables that can not or are too expensive to control. Ideally, an engineer would define all the design variables, identifying those that are controllable and those that are noise. From there, the robust design approach would apply Taguchi Methods [ITT 88] to systematically reduce the total number of configurations to consider. This technique allows the designer to develop statistical measures of “signal/noise” for each design option to highlight the optimum configuration.

While this robust design approach is appealing in its mathematical precision, it implies that the designer can clearly define all design variables at the outset of the process. While this can usually be done for straightforward component design trades, it is not necessarily feasible when trying to trade off cost/benefit between competing system technologies (e.g. choosing between a hybrid or bi-propellant engine) when important control parameters are qualitative rather than quantitative in nature.

Noble and Tanchoco [Noble 89] offer an alternate approach to robust design for assessing and comparing competing options by focusing on cost. Their concept, called *design justification*, calls for the simultaneous development of the product design and its cost model. This method will be discussed in greater detail in the final section of this chapter as it applies to my own research.

Another fallout of the system architecting process which directly drives cost is the redundancy philosophy used. In the realm of low-cost, small satellites, true 1:1 hardware redundancy is virtually impossible. The additional mass, power and volume requirements of flying complete back-up systems, in addition to the additional overhead required to manage this redundancy, are prohibitive. Yet, even on low-cost missions, single-point failures, while inevitable, must be dealt with.

The philosophical approach to redundancy taken for UoSAT spacecraft traditionally begins at the circuit board level and is reflected in the overall mission design. This approach is one of *degraded*

functional redundancy. The aim is to minimise the impact of single point failures by allowing continued, if somewhat degraded, performance of spacecraft systems and even the entire mission.

With the UoSAT approach, it is understood that low-power circuits are inherently reliable. Paths are identified which allow hardware to be reconfigured by software command to isolate potential failure modes. In many cases, "sacrificial circuits" are identified which can be turned off to protect other, more vital areas on the same board. To implement this approach, board designs allow for a minimum state control mode whereby bypass circuits can be commanded when only rudimentary spacecraft command capability is available.

At higher levels, this degraded functional redundancy can be found in the selection of chips for RAM and microprocessors. RAM chips are selected from several different suppliers so a generic failure of one design leaves an acceptable amount of memory. New missions are usually built around the newest generation of microprocessor chips, with interfaces designed to take maximum advantage of the latest capability. However, underlying this primary control level, back-up microprocessors employing older, flight-proven hardware allow for degraded command and control of bus and payload functions. Additionally, the use of special-purpose microcontrollers to independently command and control payload and other functions allows greater flexibility in case of failure. Normally, payload and other commands are sent through the primary CPU, but this can be by-passed, allowing commands directly to subsystem or payload in the event of failure. Thus, the ability for operational reconfiguration of hardware and software gives the entire system a greater degree of reliability without resort to individual HighREL parts or redundant components. In Chapter 6, these system architecture cost drivers will be revisited to explore their application in a design exercise for a minisatellite propulsion system.

2.4. Hardware Acquisition Phase

The final phase of a mission that directly drives system cost is hardware acquisition. During this phase, the design is brought to life through a process of purchasing, manufacturing, assembly and testing. As this section will show, the primary drivers of cost during this phase come about through the source of the hardware, how it is procured and the testing procedures.

2.4.1. Hardware Source

There are different routes to procuring spacecraft hardware. The route you chose is another important cost driver. On the one hand, you can design, manufacture and test hardware yourself, or you can buy complete assemblies from subcontractors or other manufacturers. Each of these routes can offer the spacecraft designer opportunities for low cost. But before looking at these options, it is worthwhile to look briefly at a third option—"free" hardware.

By "free" hardware I refer to hardware that already exists due to production overruns, flight spares, program cancellations or even salvaged from museums (as was the actual case with gravity gradient booms used in early UoSAT missions!). However, a particular mission can only take advantage of these opportunities if

- 1) The program is aware of them
- 2) The mission design can adapt to accommodate them.

For example, it would be frustrating to find out that you could have used a donated hydrazine/MON rocket engine after the structural design has already been committed to accommodate an MMH/MON configuration.

This idea of "free" components is not without precedent. Many missions in the world of low-cost spacecraft engineering, at least in the "amateur" and University research environment, have depended on seeking out and using these spare components. The OSCAR series spacecraft are a good example (see Chapter 6 or the AMSAT example in [Wertz 96]). Many of their critical components over the years were either donated or provided at a much reduced cost.

Another option for "free" hardware is to form a co-operative research and development agreement with a component supplier who wishes to flight test new technology. In this way, you benefit from a very low-cost or even free component and the supplier gains potentially valuable flight experience. The FASat-Alfa spacecraft built for the Chilean Air Force by SSTL contained an advanced data recorder provided by Sanders, a Lockheed/Martin Company, as part of a co-operative R&D agreement.

If "free" hardware is not available, then you are left to either buy it or built it yourself. Here it is understood that parts or components are bought (applying the criteria used in the next section) and then components, assemblies or an entire subsystem is the item to be built. So, no matter how much of the spacecraft you can build from scratch, you are going to have to buy some basic components. However, for specific hardware options, such as a magnetorquer or flight batteries, the build vs. buy debate is quite important. The following discussion includes the option of buying equivalent terrestrial/commercial grade hardware and doing a separate qualification program.

Table 2-2 includes a summary of the advantages and disadvantages of building vs. buying flight hardware. As you can see, the primary advantages gained in building hardware in-house are in an increased span of control over a particular component. This of course creates the potential for cost savings, but by no means guarantees it. The other primary advantage stems from the opportunity to introduce new or untried hardware. Small satellites have been in the forefront of space technology, trying and perfecting new technologies or "old" technologies which have never before been used in space.

The disadvantages of building your own hardware come from the inconvenience caused by having to do it all yourself. Realise that while building vs. buying is presented here as a black and white issue, in many cases you are more likely to face a grey situation in which you buy significant parts or even components and put in some degree of engineering effort to adapt it for your own specific needs. For example, you may choose to use a terrestrial grade component such as a GPS receiver to gain low-cost and high reliability and then add significant modifications to adapt it for space use.

Option	Advantages	Disadvantages
<i>Building Hardware In-House</i>	<p>YOU...</p> <ul style="list-style-type: none"> • Control the specifications and performance • Control the design and interfaces • Control the schedule • Control the cost • Can introduce new or untried technology • Spend over-head costs within your organisation • Gain expertise that should make it even cheaper next time 	<p>YOU...</p> <ul style="list-style-type: none"> • Carry all the risk • Need the in-house expertise to design the entire component and manufacture it • Need to space qualify it • Need to acceptance test it
<i>Buying Hardware</i>	<p>YOU...</p> <ul style="list-style-type: none"> • Share risk with supplier • Use tried and tested hardware • May reduce or avoid development costs • Learn from subcontractors 	<p>YOU...</p> <ul style="list-style-type: none"> • Have less control over specifications • Have less control over schedule and cost • Spend overhead outside your organisation • Do not learn how to do it yourself next time

Table 2-2: Advantages and disadvantages of building vs. buying your flight hardware.

Once the programmatic decision has been made to build hardware in-house, the basic steps in the manufacturing, integration and testing processes differ very little from those used throughout industry. These processes are summarised in [Wertz 96].

2.4.2. Procurement Process

Whether you are buying entire components or just individual parts, another important cost driver is the procurement process itself. During this process there are several opportunities to reduce (or increase) the cost of identical quality items. Table 2-3 outlines the important steps to follow when buying components to ensure the desired quality and the lowest cost.

Cost drivers for hardware procurement begin with the definition of procurement specifications. Here the decisions made during the Mission Design Phase get translated into precise language that must be communicated to potential suppliers. While every effort should be made during the Mission Design Phase to define flexible requirements, it is during the Hardware Acquisition Phase that the actual hardware options come to light. To take advantage of these hardware options, designers must be prepared to revisit their earlier decisions and possibly modify the system architecture or compromise

on performance. The iterative nature of this process is highlighted in Chapter 6 in the discussion of the system architecture design and acquisition of an actual minisatellite propulsion system.

To achieve the lowest cost, the emphasis must be on flexibility and co-operation. This is especially true when buying major spacecraft subsystem such as batteries, solar panels or rocket engines. It is important to realise that for small, low-cost missions, the subsystem supplier may have as much, if not more, to lose from a mission failure as you do. By tapping into that motivation for success, customer and supplier can work together to lower cost while maintaining high quality. This means you must be prepared to view your supplier as a *de facto* partner in the mission. Furthermore, you must be prepared to consider their suggestions for alternate technology, hardware or architecture to lower your final cost. The request for quotation (RFQ) should focus on tangible results, not philosophies on how the supplier should run their company. An adversarial or dictatorial approach may get you good hardware in the end, but it may not be cheaper. The system design case study presented in Chapter 6 will demonstrate the importance of focusing on these cost drivers.

Step	Cost Driver	Guidelines
1. Define procurement specifications	1.1 Specified performance	<ul style="list-style-type: none"> • Do not over-specify • Maintain large margins
	1.2 Specified quality level	<ul style="list-style-type: none"> • Recognise you can often get the "same" part with less "assured quality"
2. Select a Supplier	2.1 Number of potential suppliers	<ul style="list-style-type: none"> • Several data bases list suppliers of space hardware • Final customer may specify your supplier
	2.2 Request for quotation (RFQ)	<ul style="list-style-type: none"> • Many commercial parts can be bought off-the-shelf thus no RFQ is needed. Skip to step 2.3. • Do not over define your requirements and margins • Specify requirements only, do not design the internals or tell them how to run their company
	2.3 Review of bids and selection of a supplier	<ul style="list-style-type: none"> • Look for proven track record • Look at previous projects to get a feel for the company's scope and approach to projects i.e. don't ask a company to do more (or less) than they can
3. Establish supplier relationship	3.1 Supplier/customer risk sharing	<ul style="list-style-type: none"> • Get involved with suppliers • Penalty and performance clauses can sometimes cost more than they are worth and don't share the risk
	3.2 Acceptance test requirements	<ul style="list-style-type: none"> • Work hands-on when possible • Paper work doesn't substitute for direct knowledge • Avoid redundant tests
	3.3 Contract management	<ul style="list-style-type: none"> • Define milestones and documentation requirements • Limit formal meetings—use frequent informal meetings • Define change procedures
4. Receive Goods	4.1 In-house screening and burn-in procedures	<ul style="list-style-type: none"> • As required

Table 2-3: Steps and cost drivers in the low-cost procurement process. This process applies to components or individual parts.

2.4.3. Space Qualifying

With the component assembled, assuming all parts have been screened to ensure they are not disqualified for use in space, true space qualification testing can begin. My chapter in [Wertz 96] outlines the basic steps in space qualification testing process assuming the component (or part) has already been subjected to acceptance testing to verify compliance with performance specifications. Following each step in this process, the component is tested to ensure it still functions.

Assuming the technology passes the qualification tests, then it will be regarded as "space qualified" for these particular conditions providing exactly the same parts, materials and processes are used. This highlights the importance of repeatability between qualification and flight models.

The space qualification testing procedures can be applied to either dedicated qualification hardware or the first set of flight hardware. In other cases, qualification testing may be skipped altogether if you can prove to your (and the customer's and launch authority's) satisfaction that the component is "qualified by similarity." Each of these options is described in Table 2-4.

Obviously, you would like to avoid this expensive process as much as possible. Therefore, for low-cost missions, you want to qualify as much hardware as possible by similarity. When that is not possible (as is often the case) then the *proto-flight* approach which reserves full-blown space qualification testing for the assembled spacecraft is generally the lowest cost approach. However, while the proto-flight approach can be much more cost effective than individually qualifying each component and then separately qualifying the entire spacecraft, it runs the risk of only uncovering disqualified components very late in the program, possibly too late to fix before flight.

Approach	Characteristic
Dedicated qualification hardware	A separate set of components for qualification are constructed and tested at qualification levels. This set of components or a second set of qualification components is assembled into the spacecraft and tested together at qualification levels.
Qualify the first set of flight hardware	The first set of flight components are tested at qualification levels, then assembled into the spacecraft which is also tested at qualification levels. The spacecraft is then launched. This is the <i>proto-flight</i> approach.
Qualify by similarity	Demonstrate that the component and the environment are identical to previously qualified hardware.

Table 2-4: Space qualification testing approaches (adapted from E. Reeves, Chapter 12, SMAD [Larson 92])

2.5. Propulsion System Costs

We can now apply the general spacecraft hardware cost drivers identified in the previous sections to the problem of propulsion systems specifically. The objective is to develop a total cost paradigm to guide the remainder of the research and supply a framework for understanding subsequent results. This section describes the concept of design justification in greater detail and outlines an approach for analysing propulsion system costs by focusing on its key dimensions. This approach will serve as a

basis from which to examine both propulsion technology and complete systems. It will also be used compare competing options for different mission scenarios.

2.5.1. Design Justification

As mentioned in Section 2.3.3, Noble and Tanchoco [Noble 89] describe an approach for simultaneous development of product design and cost modelling called *design justification*. This approach implies the design is both economically and functionally justified as it develops. The authors note that the basic concept of design justification is that there is a “need to have meaningful interaction between design and economic justification at all major points of design trade-off. This will result in greater attention focused on the design factors which will enhance product performance with respect to best cost efficiency.” [Noble 89] The importance of this approach is noted by Fad and Summers, “too many developers fail to recognise that cost has historically been treated as an inevitable result caused by a required design rather than a variable that can be planned for strategically and used to control design.” [Fad 88]

The purpose for taking the design justification approach was to develop a tool which would allow a realistic comparison of propulsion system costs between widely varying technology options—options where many of the cost dimensions may be qualitative rather than quantitative in nature. Design justification sets out to track the benefits and costs of a given product. According to [Noble 89] benefits can be measured in one of several ways:

1. *The dollar value of a product sales or production*—This is possible when the result of the design is an easily determined product or system.
2. *Arbitrary measure of performance (i.e. system flexibility)*—This is used when the direct benefit of the product is hard to determine.
3. *Neglect of all benefit*—This can be used when comparing several alternative designs that have equal benefit.

The goal for my research was to compare the real cost of competing propulsion system options designed to deliver the same benefit, i.e. ΔV , the third approach was taken, meaning that cost modelling alone could be focused on. These costs can be modelled in one of several ways according to [Noble 89]:

1. *Budget constraint analysis*—This entails using the budget from each design function to develop the cost model.
2. *Bill of Materials analysis*—This method requires the cost model to be developed by working down the bill of materials for the product or system.
3. *Parametric modelling*—This consists of developing the empirical relationships between certain cost parameters and selected physical and performance parameters.

My approach relied on the third option for modelling cost; however, where appropriate, I used realistic prices for actual component. The next section will isolate the specific cost dimensions as they apply to propulsion systems.

2.5.2. Cost Dimensions

As this Chapter has shown, the cost of hardware is driven by a variety of decisions that occur during every phase of a mission. Therefore, to evaluate total propulsion system cost, we must somehow encompass all of the cost drivers discussed. Traditionally, the approach taken to describe propulsion cost has been to isolate a single descriptive parameter of the technology, one that determines what was perceived to be the most important premium on a satellite—mass. The propellant mass used by a given system is determined by its *specific impulse*, *Isp*. Specific impulse is similar in concept to the “miles per gallon” rating used to compare automobile fuel efficiency. However, while mass is certainly one important descriptive dimension of system cost it is not the only one. In fact, the evidence presented from [Dean 91] clearly indicates that by focusing solely on mass, true cost reduction may not be achieved. It is even possible that the overall cost is increased due to the increased system complexity needed to achieve the higher mass efficiency.

Yet, propulsion research has traditionally focused on this single goal. A recent paper sponsored by NASA entitled “Small Satellite Propulsion System Options,” Myers, et al, [Myers 94] argues that the “recent emphasis on cost reduction and spacecraft downsizing has forced a re-evaluation of technologies with critical mass impact.” The paper goes on to point out the potential offered by advanced chemical rockets and electric propulsion options in drastically reducing propellant mass requirements. Follow-on research [Dudzinski 95] continues to advocate the advantages of these technologies for a future class of NASA planetary missions. Certainly, some of these new propulsion systems may offer critical enabling technologies allowing smaller satellites to conduct the same missions as once flown by larger, more expensive platforms. However, while the mission as a whole may be “smaller and faster” the propulsion system may not be cheaper.

If mass is not the only dimension, what else is there to consider? The most obvious that springs to mind is the price paid for the hardware. In some situations, price can be the most important dimension, especially for low-budget missions such as those flown by small, University-sponsored satellites. For these missions, if the price exceeds a certain threshold limit, the mission simply will cannot proceed.

However, focusing too closely on the price may also cause you to miss important implications. All decisions come with associated opportunity costs. Thus, while a given system option may appear to be a bargain in terms of price, the ensuing logistics or operating costs may far exceed other, seemingly more expensive options.

Therefore, as part of my research, I set out to define all the dimensions that encompass total propulsion system cost. Beginning with the easiest to quantify, performance, I will posit that system performance can be fully characterised along four basic dimensions: These are:

1. Propellant mass
2. Propellant volume
3. Total elapse thrust time (to complete all ΔV)
4. Power consumed

Each of these performance dimensions represents a different aspect of mission cost. Obviously, mass is always at a premium on space missions, however, for small satellites volume can often be even more valuable than mass. Furthermore, it is often said that "time is money." For missions beginning in the harsh environment of GTO, this is especially true. In these orbits, there is a finite spacecraft lifetime due to total dose effects of ionising radiation on electronics hardware. Thus, there is an extra cost to be paid for low-thrust systems due to this added exposure. Finally, the power consumed by the system must also be considered. While there is no obvious difference in power requirements for chemical options such as hybrid or bi-propellant, or when the energy is stored in the form of high pressure as with cold-gas systems, this dimension is included to allow us to consider the additional cost to the system for electrical propulsion options such as resistojets or pulse plasma thrusters. Calculations for these dimensional values depend on the actual mission ΔV , deployed spacecraft mass and the various technical specification of the propulsion technology used.

Along with performance dimensions, there is the easily understood price for the system that will be defined as the fifth total cost dimension. Here it must be emphasised that the total system price must be considered. As results in Chapter 6 will indicate, the cost of the engine is actually only a small percentage of the overall system price. This implies that a cheap engine may not necessarily result in a cheap system.

In addition to the obvious performance and price dimensions of cost, there are other less obvious opportunity costs to consider as well. Collectively, I will refer to these as *mission costs* as they depend on the technology used and the mission environment. The first of these mission cost dimensions is *technical risk*. For example, while a certain technology option, e.g. hybrid rockets, may appear promising for certain applications, the inherent technical risk to the overall mission from this untried technology must be traded against other options, e.g. bi-propellant, which are safer from a technical standpoint due to their proven flight heritage.

Another important dimension with overall mission cost implications is *integration*. Integration cost is assumed to encompass all aspects of installing and operating the propulsion system on the spacecraft. This can include any number of issues such as mechanical and electrical interface, thermal control, the operational requirements placed on the attitude determination and control system (ADCS), along with the corresponding impact on payload operations.

There are also inherent dangers involved with handling high energy rocket propellants, especially hypergolic propellants such as MMH and MON. Even cold-gas systems which use benign propellants such as nitrogen have an inherent danger associated with handling tanks and other components that

are at very high pressure. Therefore, the direct and indirect costs associated with ensuring the personal safety of engineers working on a given propulsion system must be factored into the total cost accounting. This *safety cost* is another dimension to add to the paradigm.

In defining safety cost it must be emphasised that personal safety is of primary importance regardless of the propellant used. Programmatically, all reasonable steps must be taken to minimise personal risk. The necessary personal safety equipment (such as SCAPE suits, etc.) as well as basic safety infrastructure (propellant leak detectors, water deluge devices, easy building egress, etc.) must be either available as part of normal launch site services or provided by the spacecraft builder along with other support systems such as ground support equipment (GSE). Safety costs account for the added recurring costs for insuring a minimum safety level for a given propellant option at a given launch site.

Unfortunately, providing a safe working environment for propellant loading can be expensive. At well-established launch sites, i.e. Kourou, this safety infrastructure is already in place along with detailed procedures for their use by spacecraft servicing personnel. At these sites, the necessary safety infrastructure is already in-place. Thus the additional recurring cost for using it would be minimal (but not zero). However, at other launch sites being considered for low-cost spacecraft this is not necessarily the case. For example, detailed site surveys of Baikonur Cosmodrome in Kazakhstan conducted for Motorola/Iridium [Valentine 94] and for British Aerospace Royal Ordnance Rocket Motors Division [RMD 94] reveals a very different approach with respect to propellant loading safety. There, they take a "success oriented" approach, that is, it assumed that major accidents (e.g. propellant spills) will not happen. Therefore, the basic safety infrastructure is not nearly up to the same standard as a Western site such as Kourou. Other sites being considered, such as Svobodny, appear to have even less safety infrastructure in place. This is further complicated by the communication difficulties associated with these sites. Some equipment may actually be available but ensuring it is there and serviceable on launch day may not be possible. As a result, prudent mission planning would dictate that virtually all safety equipment be shipped in along with the spacecraft. As a result, while these sites may offer "free" launches, the added safety cost for operating at these sites is significantly higher than at Western sites and must be factored into the final system cost equation. Hughes, for example, spent on the order of \$400,000 to install safety equipment at a Chinese launch site [AstroTech 96]

All launch campaigns depend on good logistical support. For propulsion systems, the most important aspect of this support is related to propellant availability and handling during launch preparation. With the exception of cold-gas systems, a spacecraft rarely sees the actual propellant until it reaches the launch site. At the launch site the propellant tanks are loaded or the solid motor installed prior to mating with the launch vehicle. Somehow, the propellant or solid motor and all necessary handling

equipment must be delivered to the launch site. This can add significantly to launch campaign costs when the additional requirements for safely transporting hazardous propellants are included. This *logistics cost* is the final dimension in the cost paradigm I will consider.

By their nature, the assessment of these mission costs is qualitative and subjective, based on engineering judgement. Being qualitative, they require a relative comparison on an arbitrary scale to allow them to be quantified for comparison with other cost dimensions. This task will be undertaken in Chapters 3 and put into practice in Chapter 7.

We can now summarise the nine dimensions of the propulsion system cost paradigm:

1. Propellant mass
2. Propellant volume
3. Total elapsed thrust time (to complete desired ΔV)
4. Power required
5. System price
6. Technical risk (to the program)
7. Safety (to deal with inherent personal risk)
8. Integration
9. Logistics

Returning to the cost driver discussion presented earlier, we can now determine how each of these dimensions flows from the drivers identified during each mission phase. This is shown in Figure 2-2. Starting at the top of the figure and focusing on the Mission Definition Phase, you can see, as noted earlier, that during this phase inflexible mission constraints are established. These are similar to the noise variables described by Dean and Unal [Dean 91] in their robust design approach in that they are impossible or very expensive to change. Chapter 7 will re-examine these constraints as they serve to establish the weightings applied to the other cost dimensions. The majority of the remainder of this thesis will focus on the cost dimensions during the Mission Design and Hardware Acquisition Phases. The next subsection will outline this approach.

2.5.3. Approach

The next three chapters of the thesis will address those aspects of the cost dimensions that are driven by the technology option chosen. Chapter 3 will look at the technology options available for propulsion systems. Chapters 4 and 5 will continue that analysis looking more closely at hybrid rocket technology. Chapter 6 will return to the other side of the Mission Design Phase diagram to address the influence of system design on total cost. Finally, in Chapter 7, the system technology options will be brought together with the system architectures to analyse total system cost. The weightings imposed by the Mission Definition will then be included to develop a useful means for parametrically comparing system options.

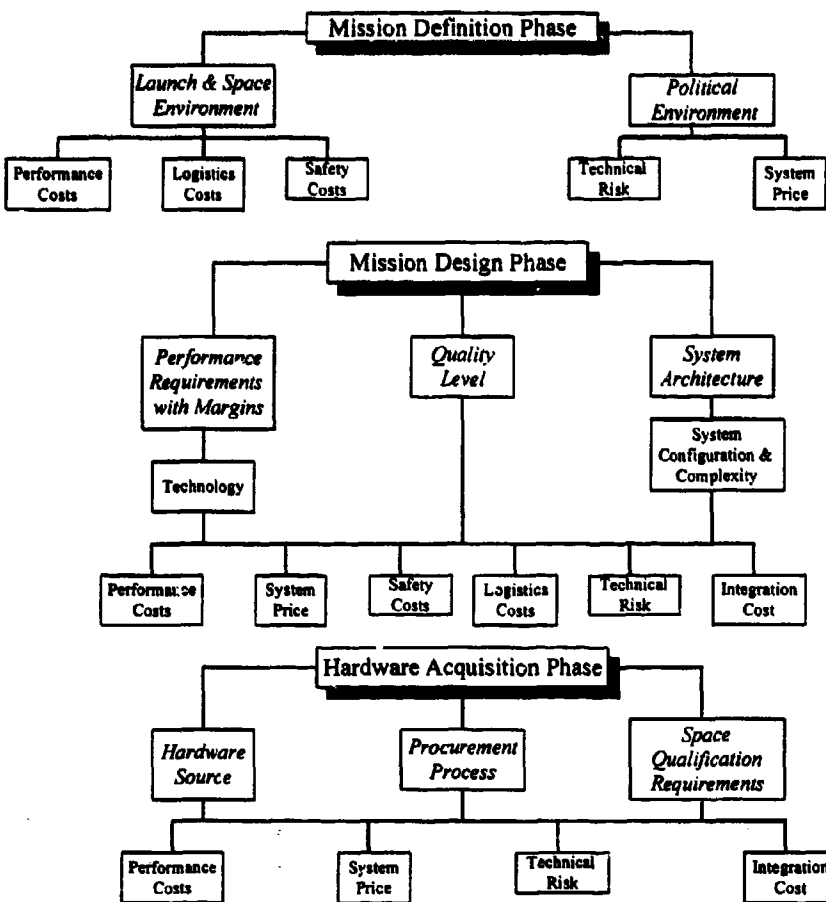


Figure 2-2: This diagram illustrates how the various cost drivers discussed in this chapter can be followed to understand how they determine relevant dimensions of propulsion system cost.

2.6. Conclusions

This chapter has presented a complete analysis of spacecraft hardware cost drivers and developed a coherent context for understanding and dealing with them. Three mission phases were identified—Definition, Design and Hardware Acquisition. During each phase, specific actions and decisions which effect the final cost of hardware were identified. Engineering practices to take or avoid in order to reduce overall hardware costs were discussed.

An important result of this analysis was a new paradigm for understanding propulsion system costs. Previous analysis has focused only on the engine performance as measured by specific impulse. This paradigm shift causes us to consider other performance dimensions as well—volume, time, power—along with system price and mission costs. These mission costs include follow-on effects that result from the selection of a particular technology option such as technical risk, integration, safety and logistics. Another innovative feature of this new paradigm is the widening of perspective to consider both technology and systems issues. This paradigm will be applied to give fresh insight into

technology options in Chapter 3. Chapter 6 will return to consider system issues as part of total system design case study for the minisatellite.

2.7. References

- [AstroTech 96] AstroTech, Inc., Cape Canaveral Florida, personal communication, Mr. Dwight Light, 8 January 96;
- [DCI] Arianespace, *Dossier de Contrôle des Interfaces (Interface Control Document)*, UoSAT-F, DCI 10/392 01, Issue 2, Rev. 0, March 1991.
- [Dean 91] Dean, E., Unal, R., "Designing for Cost," *Transactions of the American Association of Cost Engineers*, pp. D.4.1 - D.4.6, Seattle, Washington, 23- 26 June, 1991.
- [Dudzinski 95] Dudzinski, L.A., Myers, R.M., "Advanced Propulsion Benefits to New Millennium Class Missions," Presented at the 9th Annual AIAA/Utah State Conference on Small Satellites, 1995.
- [Fad 88] Fad, B.E., Summers, R.M., "Parametric Estimating for New Business Ventures," *Engineering Cost and Production Economics*, vol. 14(2), 1988.
- [ITT 88] ITT Statistical Programs Group, *Taguchi Methods—SPC Case Studies*, 1988.
- [Jersa 85] Jersa, A.S. (editor), *Handbook of Geophysics and the Space Environment*, Air Force Geophysics Laboratory, Air Force Systems Command, United States Air Force, 1985.
- [Larson 92] Larson, W.J., Wertz, J.R. (ed), *Space Mission Analysis and Design*, 2nd edition, Microcosm, Inc. Torrance, California and Kluwer Academic Publishers, Dordrecht, The Netherlands, 1992.
- [MS 1522A] MIL-STD-1522A Standard General Requirements for Safe Design and Operation of Pressurized Missile and Space Systems.
- [Myers 94] Myers, R.M., Oleson, S.R., "Small Satellite Propulsion Options," AIAA 94-2997, 30th Joint Propulsion Conference, Indianapolis, Indiana, June 27-29, 1994.
- [Noble 89] Noble, J.S., Tanchoco, J.M.A., "Cost Modeling for Design Justification," Cost Analysis Applications of Economics and Operations Research, Gulledge, T.R., jr, Littoral, L.A. (eds). Proceedings, Washington, DC, Springer-Verlag, New York, NY, 1989.
- [RMD 94] British Aerospace Rocket Motors Division, "Baikonur Launch Site Visit," Internal Report 200 972-TR/1/E000, August 1994.
- [Sellers 94a] Sellers, J.J., Astore, W.J., Crumpton, K.S., Elliot, C., Giffen, R.B., Larson, W.J. (ed), *Understanding Space: An Introduction to Astronautics*, McGraw-Hill, New York, N.Y., 1994.
- [Valentine 94] Valentine, A., "Kazakhstan: Radiation and Chemical Hazard Conditions/Precautions General Health Precautions," Prepared by The Delphi Groupe, Inc., Austin, Texas, for Motorola, Inc., Phoenix, Arizona, August 1994.
- [Wertz 96] Wertz, J. (editor), *Reducing Space Mission Costs*, Kluwer Publishing, to be published 1996.
- [WRR] WRR 127-1, *Range Safety Requirements*, 30th Space Wing, United States Air Force, 30 June 1993.

Chapter 3

Propulsion Technology Options

- 3.1. BACKGROUND**
- 3.2. OVERVIEW OF TECHNOLOGY OPTIONS**
- 3.3. COLD-GAS THRUSTERS**
- 3.4. SOLID MOTORS**
- 3.5. LIQUID ENGINES**
- 3.6. HYBRID MOTORS**
- 3.7. ELECTRIC ENGINES**
- 3.8. CONCLUSIONS**
- 3.9. REFERENCES**

The analysis of spacecraft hardware cost drivers presented in Chapter 2 resulted in a new paradigm for viewing propulsion system costs. This paradigm looks at the two sides of the problem—technology and systems. This chapter will begin the evaluation of the total cost of propulsion technologies. The research goal addressed in this chapter was to identify candidate technology options and investigate them to a sufficient level to fully characterise their total cost, performance, and overall potential for small satellite application. The chapter begins with a very brief background summarising important definitions and relationships used in the research. Following this introduction, the chapter undertakes a realistic assessment of candidate technologies. Viable options are identified and the potential costs for each in terms of the various dimensions of the cost paradigm are reviewed. Cold-gas, solid, storable liquid, hybrid and electric systems are analysed in this manner. Several important conclusions from this analysis which served to guide further research include:

- Hybrid rocket systems offer great potential for low-cost application, however, additional research is needed to fully characterise this technology. This will be the basis of additional research discussed in Chapters 4 and 5.
- The LEROS-20 bi-propellant engine, along with cold-gas thrusters, offers a low-cost off-the-shelf technology option with a variety of applications. These technologies will form the basis for the system design study in Chapter 6.

Other promising technology options—mono-propellant, solid and electric—will be assessed together with the bi-propellant, cold-gas and hybrid options in Chapter 7 to determine the most cost-effective option for a given application.

3. Propulsion Technology Options

3.1. Background

The research goal addressed in this chapter was to identify candidate propulsion technology options and investigate them to a sufficient level to fully characterise their total cost, performance, and overall potential for small satellite application. This process required a detailed understanding of rocket science including thermodynamics, thermochemistry and spacecraft dynamics. A complete discussion of these background subjects is beyond the scope of this thesis. It is assumed that the reader has a general background in propulsion theory and terminology. The Appendix includes a brief overview of these topics, summarising the most important concepts used in the research. A complete glossary of variables used can be found at the beginning of the thesis. Table 3-1 summarises the most relevant equations used in this and subsequent chapters to assess system performance costs. More detailed background including complete derivations of fundamental equations can be found in [Sellers 94a], [Humble 95], [Sutton 92], [Chang 89a] and [Chang 89b].

Dimension	Relationships
Propellant mass, m_{prop}	$m_{prop} = m_{deployed} - m_{deployed} e^{\left(\frac{-\Delta V}{I_{sp} g_0}\right)}$
Propellant volume, Vol_{ox} and Vol_{fuel}	$m_{ox} = \frac{O/F}{O/F + 1} m_{prop}$ $m_{fuel} = \frac{1}{O/F + 1} m_{prop}$ $Vol_{ox} = \frac{m_{ox}}{\rho_{ox}}$ $Vol_{fuel} = \frac{m_{fuel}}{\rho_{fuel}}$
Total Manoeuvre Time, TGO	$TGO = \frac{\Delta V}{accel(1 + 3Vratio + 3Vratio^2)}$ $Vratio = \frac{\Delta V}{6I_{sp}g_0}$

Table 3-1: Summary of equations used to compute mass, volume and time performance costs.

3.2. Overview of Technology Options

Propulsion system technology can be divided roughly into four categories based on the method used to accelerate the reaction mass. These four methods are employed in either cold-gas, chemical, nuclear or electric systems. (The methods included here focus only on current or near-term technology. For a list of more far-out ideas—fusion, anti-matter, negative matter, etc.—the reader is referred to [Humble 95]).

- *Cold-gas system*—uses the energy of a gas stored at high pressure which is accelerated to high velocity through a nozzle.

- **Chemical system**—uses the energy inherent in chemical bonds released through catalytic action or combustion to produce high temperature exhaust products which are then expanded out a nozzle to high velocity.
- **Nuclear system**—uses the intense heat generated by nuclear fission (or fusion) to heat an inert reaction mass to high temperature. The mass is then expanded out a nozzle to high velocity.
- **Electric system**—uses electrical energy to accelerate a reaction mass, through electrothermal, electromagnetic or electrostatic means, to high velocity.

Table 3-2 summarises these basic categories and gives specific examples of systems within each along with their thrust and *Isp* range.

System Type	Typical Propellants	Isp Range (sec)	Thrust Range (N)
<i>Cold-Gas</i>	N ₂ , He, H ₂	60 - 250	0.01 - 50
<i>Chemical</i>			
<i>Liquid (bi-propellant or mono-propellant)</i>	<ul style="list-style-type: none"> • LOX with RP-1 or LH₂ • N₂H₄ or MMH with N₂O₄ • N₂H₄ or H₂O₂ with a catalyst 	140 - 450	0.1 - 1.2 x 10 ⁷
<i>Solid</i>	Al/NH ₄ ClO ₄	260 - 300	10 - 1.2 x 10 ⁷
<i>Hybrid</i>	LOX, H ₂ O ₂ or N ₂ O with PE or HTPB	290 - 350	10 - 1.2 x 10 ⁷
<i>Nuclear</i>	<ul style="list-style-type: none"> • H₂, He 	800 - 6000	Up to 1.2 x 10 ⁷
<i>Electric</i>			
<i>Electrothermal (e.g. resistojets, arcjets)</i>	N ₂ H ₄ , NH ₃ or H ₂ O	150 - 1500	10 ⁻² - 10
<i>Electromagnetic (e.g. pulse plasma thrusters)</i>	PTFE (Teflon), H ₂ , He, Xe	1000 - 10,000	10 ⁻⁶ - 10 ⁻¹
<i>Electrostatic (e.g. ion, MPD)</i>	Hg, Xe or Cs	2000 - 100,000	10 ⁻⁴ - 10 ⁻¹

Table 3-2: Comparisons of available propulsion system technology (adapted from [Humble 95] and [Sellers 94a])

Given these options, we can briefly review them to determine which ones offer potential for applications on low-cost small satellites. We can begin by eliminating nuclear systems because of practical political, economic and technical issues. Also note that of the chemical systems that can be used we are restricted to propellants that can be stored for reasonably long periods of time on board a spacecraft. Therefore, cryogenic liquid options must be eliminated.

Similarly, we can briefly examine the electric options to see which are truly viable for a small satellite. It is important to note that all types of electrical systems differ markedly from chemical options in that they rely completely on the spacecraft's electrical power system to provide the necessary energy to accelerate the propellant mass. Thus, while chemical systems are energy limited (there is a finite limit to the total energy available in propellant chemical bonds) electrical systems are power limited (for a given spacecraft there is a finite amount of power available from solar arrays and batteries).

Figure 3-1 illustrates the basic trade-off between power and specific impulse for the various electrical options. As the figure indicates, arcjet, ion and MPD systems require power in excess of 1000 W. Pioneering work by Dr. Zube at the University of Stuttgart has pushed the envelope for an ammonia arcjet down to the 750 W level. This experimental thruster operating at 0.115 N thrust with an *Isp* of 430 seconds will see its first use in space on the OSCAR Phase-3 D mission in late 1996 [Zube 95]. [NASA 93] indicates the practical lower power limit for an arcjet may be around 500 W due to frozen flow losses. However, such a low power arcjet thruster has yet to be built. Unfortunately, as defined in Chapter 1, the baseline minisatellite system has ~100 W orbit average power available. Assuming that the batteries could be partly drained each orbit to power a propulsions system, there is a maximum of ~500 W maximum available (20 Amp maximum discharge current at 28 ±4 VDC) for only about 10 minutes at a time (taking the batteries to ~40% DOD requiring at least one orbit to recharge). Therefore, resistojet and PPT appear to offer the most accessible electrical options for the minisatellite application.

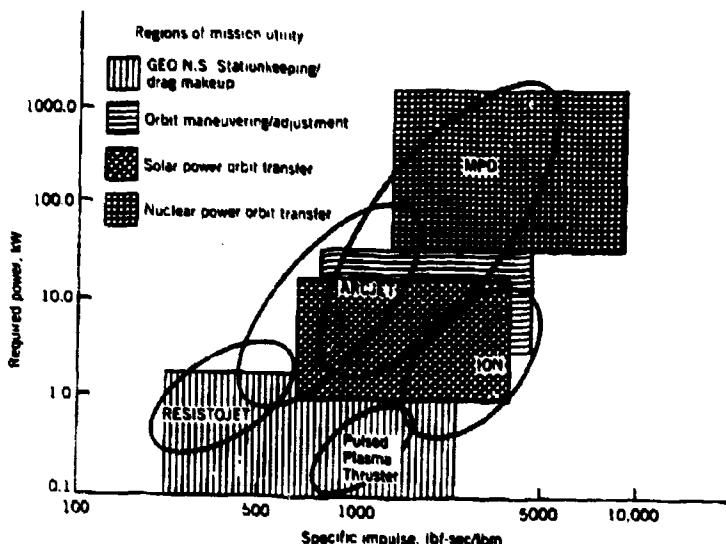


Figure 3-1: Comparison of power requirements vs. delivered specific impulse for various electrical propulsion options [Sutton 92].

Thus, the list of system options to consider comes down to:

- Cold-gas
- Chemical:
 - Storable liquid
 - Solid
 - Hybrid
- Electric
 - Resistojet
 - PPT

To examine this list, we return to the nine dimensions of system cost established in Chapter 2:

1. Propellant mass
2. Propellant volume
3. Total elapse manoeuvre time (to complete desired ΔV)
4. Power
5. System price
6. Technical risk
7. Safety cost
8. Integration cost
9. Logistics cost

To determine which option is "best" for small satellite application, we must evaluate each one against these dimensions. That is the research challenge confronted in the remainder of the thesis. Only by resorting to this total cost approach can mission planners realistically compare system options. In the following sections, each of these options will be reviewed with respect to these dimensions to fully characterise their total costs for small satellite application.

It is important to point out that, to my knowledge, such a comprehensive characterisation of all these propulsion options with respect to these nine dimensions has never been done. Fortunately, performance data was relatively easy to obtain. Price information could be obtained from vendors for specific engines and, in some cases, represents rough order of magnitude (ROM). However, there were no references specifically addressing the other mission costs for each option. Therefore, these evaluations were determined by examining the fundamental requirements of the technology in light of my own engineering judgement and based on experience gained from this research.

3.3. Cold-gas Thrusters

This section explores cold-gas thruster technology to evaluate its potential application on low-cost, small satellites. A brief background is first offered, describing the fundamental principles of this technology and estimates of its performance. Operational requirements are then evaluated followed by a preliminary evaluation of costs along the nine dimensions of the cost paradigm.

3.3.1. Background

Conceptually, cold-gas thrusters are perhaps the simplest of all rockets. A balloon represents a simple cold-gas thruster. A gas (air, in this example) is stored under pressure and released through a nozzle (the neck of the balloon). The energy for a cold-gas thruster comes from energy of the high pressure gas. Onboard a spacecraft, the operating principle is not much more complex. A working fluid, e.g. compressed nitrogen, is stored at high pressure (normally >200 bar). It is then regulated down to some operating pressure (around 10 bar). The nozzle is normally integral to the control valve. Opening the valve releases the gas to expand out of the nozzle producing thrust.

Cold-gas thrusters have seen a variety of spacecraft applications going back to the early 1960s. TRW used them on more than 40 different missions [Greco 72]. Their inherent safety is underscored by their use on Space Shuttle astronaut's Manned Manoeuvring Unit (MMU). However, because of their

very low mass efficiency, and perhaps more important, very low volume efficiency at high ΔV levels, cold-gas thrusters are almost exclusively used for attitude control rather than orbit correction.

3.3.2. Performance Costs

From basic rocket principles, a relationship between specific impulse, temperature and the molecular weight of propellants can be derived.

$$I_{sp} \propto \sqrt{\frac{T_c}{M}}$$

Eqn. 3-1

where

T_c = Chamber temperature (K)

M = Molecular weight of propellant (kg/kmole)

As this equation indicates, the lower the molecular weight of the gas, the higher the efficiency. Table 3-3 lists the theoretical specific impulse, I_{sp} , for various cold-gas propellant options.

Gas	Molecular Weight	Specific Impulse (sec)
Air	28.9	74
Argon	39.9	57
Carbon Dioxide	44.0	67
Helium	4.0	179
Hydrogen	2.0	296
Nitrogen	28.0	80
Methane	16.0	114

Table 3-3: Theoretical specific impulse values for cold-gas thruster propellant options [Sutton 92].

However, I_{sp} tells only part of the story. Consider two extreme options for a cold-gas propellant: nitrogen vs. helium. It is important to note that from a system design standpoint, I_{sp} represents mass specific impulse. However, for many applications, volume can actually be more important than mass. Thus, it is important to consider density specific impulse as well. *Density specific impulse* is defined as

$$dI_{sp} = \rho_{ave} I_{sp}$$

Eqn. 3-2

where dI_{sp} = Density specific impulse (s.g.sec)

ρ_{ave} = average specific gravity of propellants (non-dimensional)

I_{sp} = specific impulse (sec)

Table 3-4 summarises the performance characteristics for the nitrogen and helium options and compares them in terms of density specific impulse and total impulse for a given tank and storage pressure. Note that even though helium has over twice the mass specific impulse as nitrogen, once a real system is considered with a specific tank and storage pressure over twice the total impulse is obtained from the nitrogen system. Of course, a penalty paid in terms of over 4 times the propellant mass. However, while the mass difference is large in terms of propellant (+400%), it is small in terms of the final spacecraft mass (+0.6% for a 250 kg spacecraft). Thus, for cold-gas thruster

applications on volume-limited missions, nitrogen will deliver more total impulse than helium for a given volume. Furthermore, for a given propellant mass, this analysis does not take into account the additional tank mass needed to store the larger volume of the less dense helium. When this is considered, the nitrogen system is even more advantageous overall. Therefore, all cold-gas thruster applications analysed subsequently will assume nitrogen as the propellant.

Parameter	Nitrogen	Helium
Molecular Weight	28.014 kg/kmole	4.003 kg/kmole
Ratio of specific heat, γ	1.397	1.66
Tank Volume	6.57 litre	6.57 litre
Tank Pressure	240 bar	240 bar
Temperature	293 K	293 K
Density	276 kg/m ³	60 kg/m ³
Total initial mass	1.81 kg	0.394 kg
Characteristic Exhaust Velocity, C^*	431 m/sec	1076 m/sec
Throat radius	0.5 mm	0.5 mm
Optimum expansion ratio	100	30
Nozzle exit radius	5 mm	3 mm
Thrust	3.25 N	3 N
I_{sp}	75.6 sec	172.6 sec
Mass flow rate	4.4 gm/sec	1.7 gm/sec
Total impulse available	1344 N-sec	667.8 N-sec
Density I_{sp}	2.09×10^4 kg-sec/m ³	1.04×10^4 kg-sec/m ³

Table 3-4: Performance parameters for nitrogen vs. helium cold-gas thruster options.

Thrust levels for cold-gas systems are practically limited by the maximum operating pressure of the control valves. Typical thrusters operate at < 1 N. Thus, from the standpoint of the time dimension of system cost, cold-gas systems rate relatively high because of the correspondingly long transit times for significant manoeuvres. Finally, their power usage is relatively low as it takes little power to hold open a single, small valve (~ 1W).

3.3.3. Price and Mission Costs

The other dimensions of the total cost paradigm for cold-gas technology will be addressed in this section beginning with thruster price. Because cold-gas thrusters are a well-established technology with a long flight heritage, they are available from a wide selection of vendors. Chapter 6 will describe the costing exercise undertaken as part of an overall system design using cold-gas thrusters. The results that will be described there indicate that a single 0.1 N cold-gas thruster can be purchased for around \$4000 [Arde 96]. This makes the monetary cost of cold-gas technology quite accessible. The cost of an individual thruster, as further discussions will show, is roughly the cost of a single valve needed for other technology options.

Cold-gas thruster costs are also low when the other cost dimensions are considered. Again, because of their long, flight-proven heritage, cold-gas thrusters offer very little technical risk to a program. Not only are they highly reliable, but a failure is unlikely to be catastrophic to the rest of the spacecraft. This implies their safety costs would be relatively low as well. The propellant, nitrogen

as described above, is completely harmless. The primary safety issues are associated with the high storage pressure. However, assuming tank and other component design conforms to Military Standard 1522 *Standard General Requirements for Safe Design and Operation of Pressurised Missile and Space Systems* [MS 1522A] or equivalent industry standards for high pressure vessels and components, these costs can be easily managed.

Logistics costs for cold-gas technology should also be quite manageable. Again, the propellant itself is inert. Dry nitrogen is readily available at all Western launch sites. If it were not available at more remote launch sites, transport of high pressure supply bottles would add somewhat to shipping costs but would not present significant logistical problems.

Finally, integration costs for cold-gas technology would be similarly low. The low thrust implies ease of integration with respect to ADCS and payload operations. Thermal control is also not a problem because it is literally a cold gas being expelled. There are no sensor contamination problems to consider either.

The potential costs of cold-gas technology are summarised in Table 3-5. All of these costs will be examined in greater detail in Chapter 6 as part of the total system design and integration exercise. As the table indicates, cold-gas thrusters are inexpensive and easy to integrate and fly. The primary disadvantage is their extremely poor performance making mass and volume costs high for even moderate ΔV applications. However, for attitude control applications where the actual ΔV is quite low, these costs would be less pronounced. This fact will be made more evident in Chapter 7 when cold-gas is compared to other technology options for specific mission scenarios.

Cost Dimension	Cold-gas
Mass Cost	Very high
Volume Cost	Very high
Time Cost	High
Power Cost	Very low
Thruster Price	~\$4000
Technical Risk	Very low
Safety Cost	Very low
Integration Cost	Low
Logistics Cost	Low

Table 3-5: Summary of potential cold-gas thruster technology costs.

3.4. Solid Motors

This section discusses the solid rocket motor option for small satellite application. A brief background on solids is first offered followed by an analysis of their performance costs. Following this, the other potential costs of solid motor technology are reviewed.

3.4.1. Background

Solid rocket motors are one of the most widely used propulsion technologies in the aerospace industry. They are used for first-stage boosters, on tactical missile systems, gas generators and as upper stages for satellites. Conceptually, a solid motor is relatively simple. A solid fuel and solid oxidiser are mixed together in the correct proportions along with some binding material, then packed into a combustion chamber. In operation, an electrical or pyrotechnic ignition system is used to start combustion. Figure 3-2 shows a cut-away view of a typical solid used for upper stage applications.

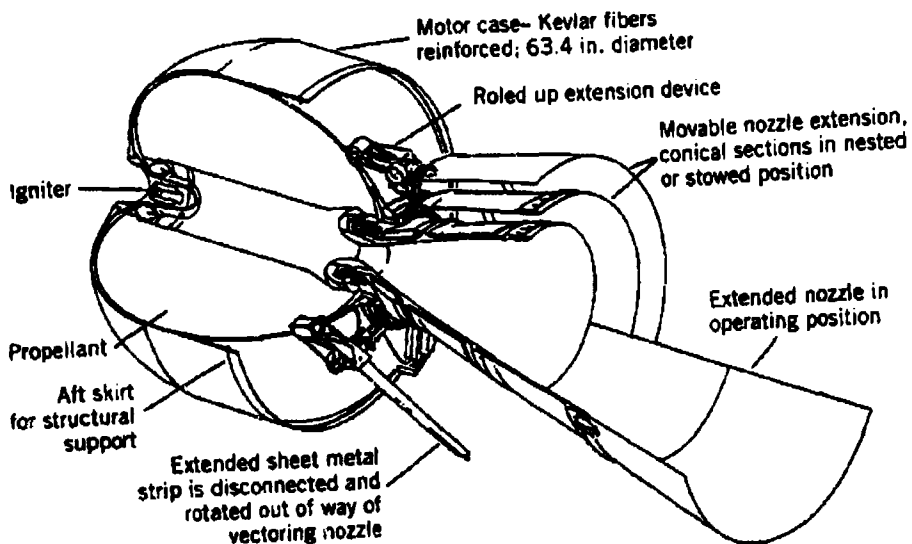


Figure 3-2: Cut-away view of the inertial upper stage (IUS) solid rocket motor [Sutton 92]

Both [Humble 95] and [Sutton 92] offer very good introductions to solid rocket motor technology. [Chang 89a] and [Chang 89b] offer more detailed explanations of internal ballistics with equation derivations.

Typically, solid motors use aluminium, magnesium or beryllium as fuel (2-21% by mass) with oxidisers such as ammonium perchlorate (or AP) (NH_4ClO_4), ammonium nitrate (NH_4NO_3) or sodium nitrate (NaNO_3). Of these options, aluminium with ammonium perchlorate is the most widely used [Humble 95]. While beryllium is more energetic than aluminium, it is also more toxic. AP offers low cost, moderate performance and good processability. Its primary disadvantage is the production of hydrochloric acid (HCl) in the exhaust leading to "acid rain" near launch sites. In addition to the fuel and oxidiser, inert binder material is also needed to provide overall structure to the propellant grain to enable it to withstand the thermal and mechanical environment as well as the high pressures of combustion. Binders normally consist of "long-chain polymers that can keep the propellant's powders and crystals in place by forming a continuous matrix through polymerising and cross-linking. Cross-linking takes place by mixing a curative into the propellant just before casting (pouring) the mixture into the motor." [Humble 95] Typical binder materials include hydroxy-

terminated polybutadiene (HTPB). Solid motor designers strive for high solids loading fractions (the ratio of propellant to binders). In a well-designed motor, binders would make up only 10-16% of motor mass. The next section will begin with an overview of solid combustion ballistics as they influence actual motor performance.

3.4.2. Performance Costs

Solid motor performance is dependant on the propellants used, their oxidiser-to-fuel ratio, *O/F*, port geometry, temperature, pressure and rate of propellant burning within the combustion chamber. One of the most important relationships to describe this process is the solid motor burning rate equation [Humble 95] and [Chang 89b]

$$r_b = e^{(\sigma_p \Delta T)} a p_c^n \quad \text{Eqn. 3-3}$$

where

r_b = Propellant burning rate (mm/s)

σ_p = Burning rate temperature sensitivity parameter (at constant pressure) (appropriate units)

ΔT = Temperature change from standard conditions (K)

a = Burn rate coefficient (appropriate units)

p_c = Chamber pressure (bar)

n = Burn rate exponent (appropriate units)

Note that the burning rate relationship highlights the dependence on both temperature and pressure. These parameters correspondingly depend on the burning rate. Knowing the burning rate and the port geometry, mass flow rate can be determined. The combustion thermochemistry determines the ratio of specific heats, γ , and other important performance parameters. Therefore, any attempt to model solid motor combustion requires an iterative approach. Unfortunately, because of the number of variables involved, solid propellant combustion is very difficult to model even with modern computational fluid dynamics codes. As a result, the coefficients in this relationship are most reliably determined empirically. Thus, solid motor performance prediction is heavily dependant on experimental data. Fortunately, performance values for solids in general vary very little and data is readily available for many off-the-shelf motors. Analysis in this section is based on data for Thiokol motors as shown in [Thiokol 93]. Table 3-6 lists important performance data for their STAR-17A motor.

Parameter	Value
Specific impulse (sec)	287
Density specific impulse (s.g.sec)	498.8
Characteristic exhaust velocity, C* (m/sec)	1532
Adiabatic flame temperature (K)	3400
Propellants	<ul style="list-style-type: none"> • ammonium perchlorate - 70% • aluminium - 16% • carboxy-terminated polybutadiene (CTPB) binder - 14%
Propellant specific gravity	1.738
Propellant mass (kg)	112.3
Propellant volume (litres)	64.6
Total motor mass (kg)	125.6
Propellant mass fraction	0.89
Burn time (sec)	19.4 sec
Burn time average chamber pressure (bar)	46.2
Total Impulse (Nsec)	3.2×10^5
Burn time average thrust (N)	1.6×10^4
Spin capability (RPM)	40 - 100
Average nozzle expansion ratio, ϵ	50.4

Table 3-6: Performance characteristics for the Thiokol STAR-17A solid motor, typical of those used for satellite applications [Thiokol 93].

Based on their specific impulse and density specific impulse, it is apparent that solids offer much lower mass and volume costs than cold-gas systems. As the next sections will show, solids compare quite favourably in both these dimensions with other chemical options such as bi-propellant and hybrid. With their very high thrust (very much higher than cold-gas systems and higher than typical liquid systems), solids offer rapid manoeuvre times making this cost dimension low as well. Finally, the power required for solids is also quite low. Only an initial input is needed to start the pyrotechnic ignition system. Thus, on every performance cost dimension solid rocket technology appears to be low cost. However, the next subsection will reveal other aspects of solid costs which make them somewhat less appealing for many small satellite applications.

3.4.3. Price and Mission Costs

This subsection will address the other cost dimensions related to use of solid rocket motor technology beginning with system price. As addressed in Chapter 2, the first option to consider would be building your own solid. It is not inconceivable that a small satellite organisation could build and fly its own solid motor—amateur rocket enthusiasts have routinely made their own “cheap and dirty” solids for hobby rocket applications for many years. Unfortunately, to scale up these “garage rockets” and qualify them for applications on much more expensive satellites would require resorting to many of the same rigorous, and expensive, procedures used by industry. Because each motor is essentially hand-made, you can only test prototypes, you can never fully test the flight article before committing it to the mission. This implies two expensive consequences with respect to setting up an in-house solid production capability: (1) highly controlled and precise design and production procedures and

(2) many, many tests. Furthermore, the propellants used, most notably ammonium perchlorate (a strong oxidiser) are potentially dangerous to work with and produce environmentally harmful exhaust products such as hydrochloric acid, implying more expense to establish a safe testing facility.

For these reasons, the build-your-own solid option was discarded from further consideration. This leaves buying an off-the-shelf motor. There are only a relatively small number of commercial solid motor suppliers. One of the biggest is Thiokol Corp. in the U.S. They produce a catalogue of their standard motors [Thiokol 93] which gives technical specifications for each. The satellite designer need only specify the total impulse needed for a given mission and then select the motor from the catalogue that most closely matches the requirement. In reality, these motors are not kept in inventory and shipped on order. They are built individually to order based on a proven design. This further restricts the flexibility of the solid option as mission planners must try to adapt the mission to a given motor design. To request a non-standard, specialised design significantly drives up the cost. ROM costs for three representative motors were supplied by Thiokol [Thiokol 96] and are summarised in Table 3-7. Motor prices assumes an order of five motors (not including non-recurring cost for any additional modifications and qualification testing/analyses that may be required for specific applications). "Additional equipment and expenses" includes initiation ordnance, shipping container, ground support equipment, and technical support during the launch campaign. Of course, the inherent simplicity of the solid means no other support components (tanks, valves, etc.) must be purchased beyond these basic prices. Chapter 7 will review how this cost figure compares with those of other system options.

Motor	Total Impulse (Ns)	Motor Price	Additional Equipment and Expenses
STAR-5A	5734	\$40,000	\$85,000
STAR-12G	46,040	\$325,000	\$130,000
STAR-17	197,900	\$525,000	\$185,000

Table 3-7: ROM costs for example solid motors [Thiokol 96].

The mission costs for solids can now be considered. For an off-the-shelf motor with a proven design, the technical risk would be relatively low. The primary safety issues for a solid involves the installation and use of the pyrotechnic ignition device. With a proven design, the safety costs should be moderate to low as compared to handling hypergolic propellants (addressed in the next section).

Unfortunately, integration costs for a solid are not so easily dealt with. As discussed above, solid motors produce relatively high thrust. This requires the spacecraft be in a very stable pointing mode during manoeuvres in order to deal with engine disturbance torques which may interfere with payload operations. Furthermore, where and how the solid motor is mechanically integrated into the spacecraft structure has implications for thermal control as well. Solid combustion takes place at temperatures in excess of 3000° C. While this high temperature is largely contained by the insulating

properties of the propellant itself, there is the potential for excessive heat to soak into the spacecraft which must be addressed as part of the overall spacecraft thermal control design.

The final, and perhaps greatest, integration cost related to solid motor application comes from their inherent inflexibility. To begin with, as stated earlier, mission designers are slaved to a specific off-the-shelf motor configuration unless they are willing to spend significantly greater amounts on one that is tailored to mission requirements. Furthermore, by their very nature, solids cannot be considered practical for station keeping or other applications which require multiple impulses of varying duration. Solid motors are only suited to mission applications that call for a single or at most two manoeuvres (requiring two separate motors).

There are also potentially high logistics costs associated with transporting a live solid motor and providing the necessary infrastructure to install it on the spacecraft prior to mating with the launch vehicle. By their nature, solids are delicate and extremely sensitive to shock or other violent handling which could cause cracks in the grain. Along with transportation issues, there are the practical issues of importing/exporting a live solid motor across international boundaries. Finally, as mentioned above, the necessary logistics infrastructure must be in-place at the launch site to do the final integration into the spacecraft.

The relative costs of solid motors are summarised in Table 3-8, system price reflects information from the discussion above. All these cost issues of solid motors will be revisited in Chapter 7 to allow for one-to-one comparison with other technology options.

Cost Dimension	Solid
Mass Cost	Moderate
Volume Cost	Low
Time Cost	Very low
Power Cost	Very Low
System Price	\$125,000 - \$710,000
Technical Risk	Low
Safety Cost	Moderate
Integration Cost	Very high
Logistics Cost	Moderate

Table 3-8: Summary of Solid motor costs.

3.5. Liquid Engines

German work on the V-2 during the 1940s greatly advanced liquid rocket research. Powered by LOX/alcohol engines, the V-2 required a dedicated propellant handling team with the volatile liquid oxygen loaded shortly before launch. Following the War, rocket development both in the US and the USSR followed similar lines in the pursuit of rocket propellants which would be more "storable" for both tactical and strategic missiles. Military planners were looking for a "fill and forget" propellant combination that would allow missiles to be loaded once and stored indefinitely, ready for use.

Ideally, this combination would be hypergolic, eliminating the need for complex ignition systems. These same attributes later made these combinations ideal for spacecraft use.

In his book *Ignition*, John D. Clark [Clark 72] chronicles the twisting paths and numerous dead ends that researchers followed after the War and into the late 1950s in search of the ideal hypergolic propellant combinations. Today, there are only a handful of hypergolic oxidisers and fuels in common use on spacecraft (additional options can be found for tactical applications). These are listed in Table 3-9.

Fuels	Oxidisers
Hydrazine, N_2H_4	Nitrogen tetroxide (NTO), N_2O_4 . (With varying percentages of NO added this often called mixed oxides of nitrogen or MON).
Monomethyl hydrazine (MMH), CH_3NNH_2	Inhibited Red Fuming Nitric Acid (IRFNA), HNO_3 , (with 6 to 20% NTO) ("Inhibited" implies the addition HF)
Unsymmetrical dimethyl hydrazine (UDMH), $(CH_3)_2NNH_2$	White Fuming Nitric Acid (WFNA), HNO_3
"Aerozine-50" = 50/50 hydrazine + UDMH	

Table 3-9: Commonly used hypergolic propellants

For in-space applications, the only oxidiser in common use is NTO. This is often combined with small concentrations (1 to 3%) of NO to reduce stress corrosion over long periods of storage and scavenge dissolved oxygen. This combination is then referred to as mixed oxides of nitrogen, or MON. From the standpoint of thermochemistry and combustion, MON behaves like NTO. Another oxidiser not listed in Table 3-9 but which was widely used until the late 1960s is hydrogen peroxide. The advantages of this oxidiser, especially for hybrid applications, will receive considerable attention in Chapter 4.

It should be noted that a new mono-propellant option is receiving considerable research attention in the U.S. A combination of hydroxyl Ammonium Nitrate (HAN) and tri-ethanol ammonium nitrate (TEAN) is being investigated for small engine applications with the potential for specific impulses in the range of 245 - 280 sec. The primary advantage of this new propellant option is that it is non-toxic. As later discussion will bring out, the most widely used propellants currently used, hydrazine and nitrogen tetroxide, are extremely toxic leading to considerable safety and logistics costs. HAN/TEAN is a water-based solution that could, in theory, be loaded into the spacecraft prior to shipment. [Allied 95] Unfortunately, as this new technology is still in its infancy, I was not able to consider it as part of the technology assessment.

The most commonly used fuels for liquid propellant applications on Western spacecraft include hydrazine and MMH (with Aerozine 50 seen in some applications e.g. OSCAR P3C). UDMH is widely used for Russian and Chinese applications. Hydrazine is often used in a "dual-mode" system

on spacecraft which uses hydrazine/MON in a large bi-propellant engine for orbit insertion with extra hydrazine loaded to be used as a mono-propellant in other, much smaller thrusters for attitude control.

For purposes of discussion, I will focus on monomethylhydrazine (MMH) and nitrogen tetroxide (NTO or MON) for bi-propellant applications and hydrazine as a mono-propellant. Some of the physical properties for hydrazine, MMH and NTO are shown in Table 3-10.

Parameter	Hydrazine	Monomethylhydrazine (MMH)	Nitrogen Tetroxide (NTO or MON)
Chemical formula	N_2H_4	CH_3NHNH_2	N_2O_4
Molecular mass	32.05	46.08	92.016
Melting/freezing point (K)	274.7	220.7	261.5
Boiling point (K)	386.7	360.6	294.3
Heat of vaporisation (kJ/kg)	1256	790	413
Specific heat (cal/kgK)	0.736	0.688 (293 K)	0.367 (290 K)
Specific gravity	1.023	0.8788 (293 K)	1.447 (293 K)
Viscosity (centipoise)	0.97	0.855 (293 K)	0.423 (293 K)
Vapour pressure (MPa)	0.0014 (293 K)	0.0069 (300 K)	0.0958 (293 K)

Table 3-10: Physical properties of hydrazine, MMH and NTO (adapted from [Sutton 92])

The following sections will address bi-propellant and mono-propellant options separately. Their basic operating principles will first be reviewed, candidate engines for small satellite application chosen and performance estimates presented. The advantages and disadvantages of each option will then be evaluated. The final subsection will review price and mission costs associated with both options.

3.5.1. Bi-Propellant Option

The oxidiser/fuel combinations listed in the previous section are all *hypergolic*. That is, the chemical reactivity is so high that ignition takes place on contact (unlike a combination of pure hydrogen and oxygen which requires a spark to initiate combustion). This combustion process within a bi-propellant engine can best be understood by dividing the combustion chamber into four zones as described below and illustrated in Figure 3-3.

1. *Injection/atomisation zone*—Entering the combustion chamber, the two propellants pass through an injector plate or “shower head” where they are atomised to aid in rapid and complete mixing. Injector patterns are carefully designed to provide sufficient pressure drop to de-couple chamber pressure from feed pressure and cause impingement of fuel and oxidiser. The injector may also direct a thin spray of fuel along the chamber walls to provide film cooling. Within this zone, chemical reactions begin to occur but temperatures are relatively low due to the presence of both liquid and gaseous propellants.
2. *Rapid combustion zone*—Within this zone, intense and rapid chemical reactions occur. Any remaining liquid propellant is vaporised. Mixing is aided by local turbulence. The combustion gases begin to heat up, expand and increase in velocity. By some analysis, this process is not steady-state but rather a series of localised explosions leading to a series of shock waves. At any one location within the chamber there are rapid changes in pressure, temperature, density and mixture ratio.

3. **Streamtube combustion zone**—Here chemical reactions continue but at a lower rate as the mixture drives toward equilibrium. Velocities are higher in this zone (200 to 600 m/s) so residence time is comparatively shorter.
4. **Supersonic expansion zone**—Past sonic conditions in the throat, continued expansion in the nozzle increased gas velocity to supersonic. The streamtube reactions continue on out the nozzle and beyond.

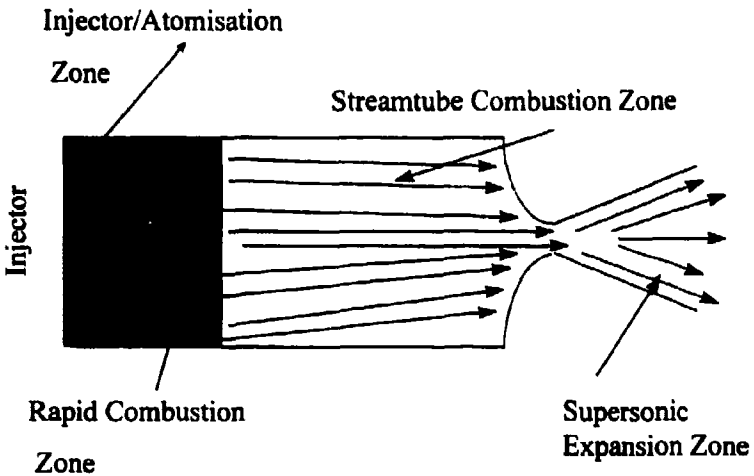


Figure 3-3: Combustion zones within a bi-propellant engine. Adapted from [Sutton 92].

As this discussion indicates, the combustion process is extremely dynamic and therefore difficult to model completely. Fortunately, basic thermodynamic and thermochemical theory provides accurate approximations within 1% - 5%. More detailed information on thermochemistry variables is obtainable from computer codes such as the USAF *Isp* program [Selph 92]. The actual performance estimates for bi-propellant applications depends on the engine used. The selection of a potentially cost-effective engine for further analysis will be the subject of the next subsection

3.5.1.1. Engine Selection—Price & Performance

Before proceeding to an analysis of bi-propellant total cost, it is important first to select a candidate engine to consider. Bi-propellant engines come in a variety of sizes from tiny 10-N thrusters used for attitude control to mighty booster rockets at 10,000+ N. The selection of an actual engine that would lend itself to practical integration on a small satellite is the first big step toward realistically quantifying their total cost.

Conventional spacecraft typically use large bi-propellant engines (400+N) for major orbit correction. This is the same approach taken by the OSCAR (the Orbiting Satellite Carrying Amateur Radio) series of spacecraft. Since the first OSCAR spacecraft in 1961, the OSCAR series has grown in size and sophistication. OSCAR 21 (or P3C), launched in 1988 used a 500 N Aerozine-50/NTO engine to take it from geosynchronous transfer orbit to a Molniya orbit. The latest and most ambitious OSCAR design, Phase III-D (P3D), will use the same basic engine with an MMH/NTO combination. These relatively large engines are very expensive, >\$200,000 each [Wood 95]. Fortunately for the OSCAR designers, their engine and supporting components were donated to the program by the manufacturer

(the OSCAR approach to propulsion system acquisition will be covered in greater detail in Chapter 6).

However, as the purpose of this research is to characterise realistic recurring cost, such charity cannot be considered as a long-term option. Therefore, a less expensive engine was needed. One was found by focusing on the cost-drivers identified in chapter 2 and taking the non-conventional approach of adapting mission requirements to fit the least expensive engine. As my hybrid research put me in close contact with British Aerospace, Royal Ordnance Rocket Motors Division (RO), their line of bi-propellant engines was a logical place to start the search. RO has a long history in developing, testing and manufacturing bi-propellant engines in thrust ranges 10 to 400-N. However, my discussion with them on engine costs led me to consider one engine in particular, an industry-standard 20-N engine burning MMH/MON—the LEROS-20. These engines are used on large, conventional satellite platforms for attitude control. Using one a small spacecraft in the primary orbit control role would represent an innovative application.

By using one of these small engines which are produced in relatively large numbers, the system could take advantage of existing economies of scale. Furthermore, because this is the same engine repeatedly tested for very large-scale programs, direct evidence of component quality would be available without resorting to expensive, and in this case redundant, acceptance testing. Thus, we were lead to ask the question—could one of these small, low-thrust engines serve as the *primary* propulsion system on a small satellite?

A diagram of the LEROS-20 engine is shown in Figure 3-4. The thruster design is based on years of research and development at RO aimed at reliability and performance while slashing the production cost. By focusing on design and manufacturing techniques (the complete engine has a total of five parts), the Royal Ordnance team has been able to develop a production engine at very low cost. RO engineer Robert Wood describes the development and design philosophy behind the LEROS-20 in [Wood 90].

In addition, because the LEROS-20 was primarily designed for the attitude control role on large, very expensive satellites, it has to incorporate high reliability and pulse-to-pulse repeatability. The three primary requirements in the LEROS-20 design were, according to Wood:

- Long life
- High reliability
- Low cost

The LEROS-20 design incorporates many advanced (and simple) features to meet these requirements. Most of these represent an evolution from the larger, 470-N LEROS-1 engines which have a previous long history of success at RO.

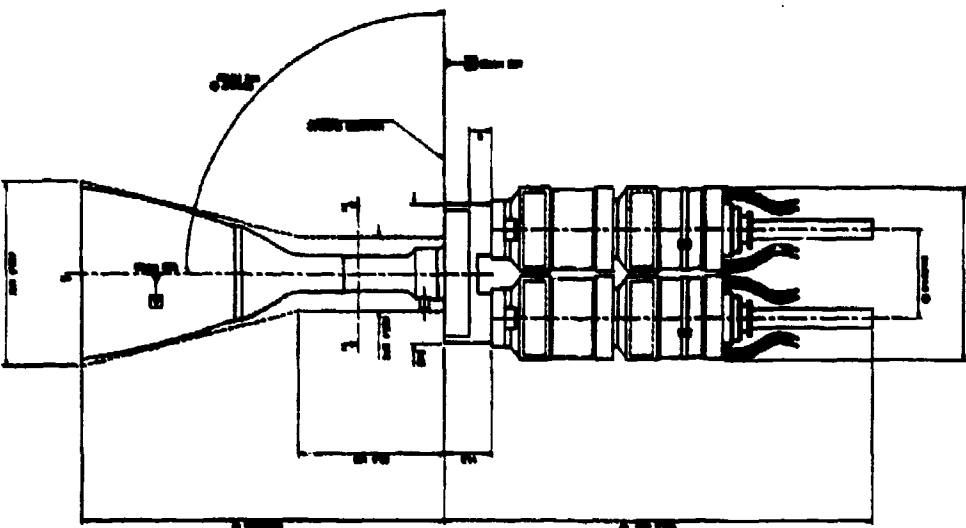


Figure 3-4: Diagram of LEROS-20 engine. The entire engine is less than 30 cm in length with a mass of less than 1 kg.

The LEROS-20 option offers several unique advantages for small satellite application:

- Proven, off-the-shelf technology means very low risk.
- Industry standard configuration means no equipment and launch interface surprises.
- “Teaming” with RO gives instant credibility.
- A ready-built engine frees up UoSAT/SSTL resources to concentrate on the design, integration and testing of the entire propulsion system as well as programmatic and logistics issues.
- A low-thrust engine is inherently easier to control on a small satellite than a higher thrust engine.
- A low-thrust engine offers the opportunity of many, short manoeuvres with wider margin for error which is more compatible with the UoSAT operations concept.
- The low-thrust engine offers a very flexible system with a range of finely controlled ΔV ($1 - 1000 \text{ m/s} \pm 1 \text{ m/s}$).

The LEROS-20, when procured to “normal industry standards,” at first appears quite expensive. In a reply to a Request for Quotation (RFQ), RO responded that a “programme to meet typical spacecraft requirement would consist of Design Verification Testing, Qualification and Production.” ROM costs for these phases would be [RO 94]

- Design Verification Testing using “bolt-up” thruster—£101,000 (\$161,000)
- Qualification—£360,000 (\$576,000)
- One-off engineering model—£60,000 (\$96,000)
- Flight model (at two-off)—£60,000 (\$96,000) each
- 14 months for delivery of engineering model and 16 months for flight models.

Given the nature of the small satellite business, “production runs” of spacecraft are unheard of. Furthermore, the nature of the SSTL/UoSAT funded missions means that development cost for new technology cannot be effectively amortised over several missions. This means that the first

minisatellite mission would have to absorb all of this cost, putting the total cost of the engine alone for its first use at over £580,000 (\$928,000).

However, as part of my research, I worked with RO engineers on determining rational ways of reducing this cost by accepting slightly lower performance and moderately greater programmatic risk. Applying the approaches described in Chapter 2, we came up with several key areas for reducing the unit cost of the engine:

- Take maximum advantage of qualification by similarity—the LEROS-20 already has a strong development heritage. This also goes for the engine valves (supplied by EG & G Wright) which also have a proven flight heritage.
- Reduce acceptance tests—thruster and valve acceptance tests would include leakage and functional tests only [RO 94].
- Reduce performance requirements—accept an *Isp* of 290 sec vs. 293 sec. (about 1%)

Taking these steps, the unit price of the engine can be reduced dramatically. The RO quotation for the LEROS-20 with series redundant EG & G/Wright valves [RO 94] using this approach is:

- Non-recurring/qualification—£46,800
- One-off engineering model—£24,500
- Two-off flight models—£24,500
- Delivery—6 month for engineering model, 8 months for flight model

This reduced the total cost for the first mission engine to under £100,000 (\$160,000), a reduction of over 5:1. Unfortunately, even at this price, the LEROS-20 option was still quite expensive to consider for a very low-cost minisatellite mission, especially an experimental mission such as UoSAT-12 with flexible propulsion system requirements.

However, subsequent discussions and negotiation with RO engineers determined that the engine cost for a technology demonstration mission could be reduced still further by agreeing to fly an engineering model which RO had used for development work. This engine would have a proven test background and have more than sufficient lifetime left to fulfil the minisatellite's mission requirements. The cost for this engine would be £24,500 (\$39,200). By reducing the engine cost below the threshold level, the LEROS-20 becomes a very attractive option. For an experimental mission, UoSAT/SSTL could accept the additional risk associated with this cost saving approach. Of course, this is essentially a one-off approach. However, once an entire propulsion system based around the LEROS-20 were proven on the Minisatellite platform, future missions with more clearly defined propulsion requirements could revisit the engine qualification scheme outlined above to work out a reasonably low recurring cost approach for a series of production engines. For these reasons, and the added advantage of having logistical support from RO, the LEROS-20 was chosen as the baseline engine for the minisatellite propulsion design exercise described in Chapter 6. The next subsection will examine the performance of the LEROS-20 option.

Engine specifications for the LEROS-20 are listed in Table 3-11. With this performance, the mass cost of using this option is nearly the same as the solid propellant option. Density I_{sp} , however, is considerably lower requiring higher propellant volume. The much lower thrust levels implies longer manoeuvres times than with solids but much less than for cold-gas. Power requirements are restricted to that needed to open the dual redundant valves (four valves total) or about 4 W. A much more detailed analysis of LEROS-20 performance is presented in Chapter 6 as part of the system design case study. The other dimensions of the total cost paradigm for the LEROS-20 bi-propellant option will be discussed together with the mono-propellant option at the end of the section.

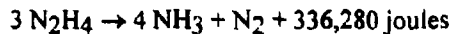
Parameter	Value
Fuel	MMH
Oxidiser	MON3
Nominal Thrust (N)	22
Nominal mass flow rate (kg/sec)	0.0075
O/F	1.65
Inlet pressure (bar)	10 to 20
Chamber pressure (bar)	8.88
Nozzle expansion ratio	180
Maximum chamber temperature ($^{\circ}\text{C}$)	1250
Steady state I_{sp} (sec)	293
Mass (kg)	0.45
Average propellant specific gravity	1.16
Density I_{sp} (s.g. sec)	339.9

Table 3-11: LEROS-20 engine performance parameters (adapted from [Wood 90]).

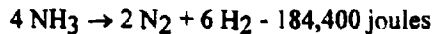
3.5.2. Mono-Propellant

As their name implies, mono-propellant rockets rely on a single propellant instead of two. The release of energy within the chemical bonds of the propellant is initiated by the presence of a catalyst. The catalytic decomposition of one such mono-propellant—hydrogen peroxide—will be covered in detail in Chapter 4. This section will focus on a more widely used mono-propellant—hydrazine.

Chemically, hydrazine decomposes with an exothermic reaction into ammonia and nitrogen when exposed to a catalyst as follows:



Unfortunately, if the reaction is allowed to continue, the ammonia further decomposes in an endothermic reaction as follows:



Therefore, the art of hydrazine catalyst bed design is aimed at minimising the effect of this second reaction which lowers operating temperature, reducing overall engine efficiency.

Hydrazine catalyst material normally consists of iridium or cobalt deposited on porous ceramic such as aluminium oxide. These compounds are commercially available going by the trade-names Shell-405 or LCH (both of which were tested as hydrogen peroxide catalysts as discussed in Chapter 5).

Unfortunately, in some situations, hydrazine can decompose spontaneously in the absence of a catalyst. Experimental evidence indicates [Bunker 90] that hydrazine can detonate in propellant lines that are pressurised too rapidly (such as by opening a pyrotechnic valve). This adiabatic compression problem has led to costly research into slow-acting latch valves to make this pressure spike less severe.

The chief limitation on thruster lifetime is catalytic attrition caused by a variety of effects, including mechanical breakdown from thermal and pressure cycling as well as chemical poisoning by trace contaminants in the propellant. To avoid this last effect, strict requirements on the chemical purity of hydrazine are typically imposed (leading to cost implications as discussed below). A cut-away diagram of a typical hydrazine mono-propellant thruster is shown in Figure 3-5. Performance for hydrazine thrusters can differ greatly depending on the size of thruster used. The selection of an appropriate thruster for minisatellite applications will be the focus of the next subsection.

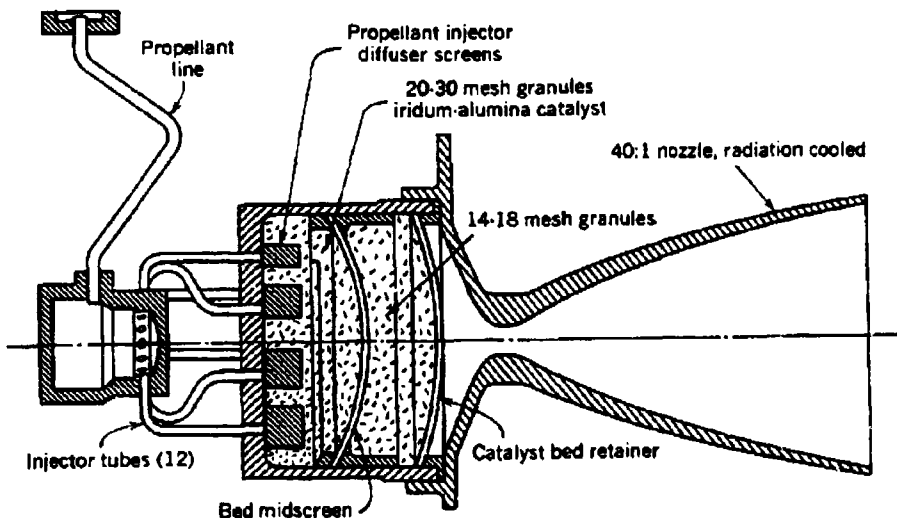


Figure 3-5: Hydrazine mono-propellant thruster shown in cut-away view (from [Sutton 92]).

3.5.2.1. Engine Selection—Price & Performance

Mono-propellant engines are available in thrust ranges from 1 - 400 N. However, to allow more realistic comparison with the LEROS-20 option, a similar thrust mono-propellant engine was selected. Such an engine is represented by the MR-106E built by Rocket Research Company, Olin Aerospace. I did not undertake the same level of detailed price negotiation with Olin as was done with RO, however, with Mr. James Bartron of Olin indicated that an MR-106E engine could be purchased at a price similar to that of the LEROS-20 (around \$40,000). Table 3-12 summarises the performance parameters for the MR-50N mono-propellant thruster.

Parameter	Value
Catalyst	LCH 227/202
Steady-state thrust (N)	11.1 - 31.2
<i>Isp</i> (sec)	228 - 235
Propellant specific gravity	1.023
Average Density <i>Isp</i> (s.g. sec)	236.8
Rated total impulse (Nsec)	124,700
Total pulses	12,405
Minimum impulse bit (Nsec)	0.56
Feed pressure (bar)	6.7 - 24.1
Chamber pressure (bar)	4.5 - 12.4
Nozzle expansion ratio	61:1
Mass flow rate (gm/sec)	5.0 - 13.1
Valve power	27 W maximum @ 28 VDC
Thruster mass (kg)	0.52

Table 3-12: MR-106E hydrazine mono-propellant thruster performance data [Olin 95b].

3.5.3. Mono-Propellant vs. Bi-Propellant

To select the most appropriate liquid engine for a given mission it is important to understand the inherent trade-offs between these competing options. Table 3-13 provides a comparison of the inherent technical advantages and disadvantages of each option. As the Table summarises, there are good technical arguments for and against each option. Of the two, mono-propellants are by far the most widely used in spacecraft application. This is primarily due to conventional wisdom which assumes that a mono-propellant system is always cheaper and simpler than a bi-propellant system. This assumption will be partly challenged by the total system cost analysis presented in Chapter 7.

Option	Advantages	Disadvantages
Mono-Propellant	<ul style="list-style-type: none"> Single propellant to handle No inherent danger of hypergolic reaction Simpler plumbing Cleaner exhaust Simpler flow trimming Fewer performance variables Better CG control Easier to use positive expulsion methods 	<ul style="list-style-type: none"> 20% Lower <i>Isp</i> 30% lower density <i>Isp</i> Displaces cold-gas system Higher freezing point propellant (2°C) means propellant heaters needed Heaters needed in catalyst pack Adiabatic compression of hydrazine in propellant lines can cause spontaneous detonation. Higher propellant cost (~10x)
Bi-Propellant	<ul style="list-style-type: none"> 20% higher <i>Isp</i> (much higher if regulated pressure) 30% higher density <i>Isp</i> Lower freezing point of propellants More growth potential for higher ΔV missions Shorter impulse bit engine 	<ul style="list-style-type: none"> Need for extra propellant loading cart (~\$15,000) Possibly less reliable engine Added compatibility issues with MON Problems with flow decay means MON purification required More performance variables Greater contamination risk

Table 3-13: Comparison between mono-propellant and bi-propellant technology options (partly based on inputs from [Wood 95]).

3.5.4. Mission Costs

The remaining dimensions of the cost paradigm with respect to both bi-propellant and mono-propellant technology will now be examined. In terms of technical risk cost, both options represent

well-proven technology with considerable flight heritage. The mono-propellant option offers a slight edge over the bi-propellant due to its inherently simpler operation.

Integration cost issues for the LEROS-20 will be addressed in greater detail in Chapter 6 as part of a complete system design exercise. For the most part, integration costs for the MR-106E engine would be almost identical. The bi-propellant option would be somewhat more complex because of the need to safely isolate the propellants which will detonate on contact. One important consideration in the choice of an engine is the cleanliness requirements imposed on the whole system, and its overall impact on integration cost. For example, AMSAT at one time considered using a 10-N thrust engine built by MBB for the OSCAR missions. Unfortunately, this particular engine had extremely small injector holes requiring very precise cleaning to remove particulate in the propellant delivery system [Meinzer 95] [MBB 81]. Fortunately, the LEROS-20 does not share this problem as its injector holes are 40 microns or larger. Thus, conventional cleaning of components, along with a 7 micron filter is sufficient to prevent particulate problems [Wood 95].

These logistical issues were very much in mind when an engine for use in the minisatellite design exercise was being selected. Because of the on-going co-operation between SSTL and RO, the LEROS-20 was chosen specifically because of the integration and logistics advantages offered by working directly with RO and leasing their facilities in the UK.

The most important mission cost to consider for liquid propellant options is safety. It must be emphasised that all of these propellants—hydrazine, MMH and MON—are VERY dangerous. [CPIA 74] provides a complete description of their toxicity, flammability and corrosive hazards. [GSC 87] gives a useful overview of safety precautions taken for propellant handling operations at Kourou. Extensive infrastructure has been put in place at this, and other Western launch sites to ensure safe handling and to mitigate the effects of spills. Workers wear special suits (referred to as a self-contained aspirated protection ensemble or SCAPE-suit) with self-contained breathing apparatus for complete isolation from the propellant. Because these facilities are already in place, the additional cost to lease them would not add significantly to safety or logistics costs. However, research into similar facilities at Russian and Chinese sites indicates a completely different standard exists with regards to safety [RMD 94], [Valentine 94]. This creates the potential for extremely high safety costs associated with using hypergolic propellants from these launch sites. As indicated in Chapter 2, Information provided by [Astrotech 96] indicates that over \$400,000 has been spent to deliver a complete safety infrastructure to one such site.

These potentially high safety costs spill over into logistics costs as well. For launch operations from Western sites, the transportation infrastructure is in-place to deliver these propellants. Thus, the logistics cost would be roughly equivalent to that of a cold-gas system. However, once again for non-Western sites this is not the case. None of the propellants needed for the either the LEROS-20

(MMH/MON) or the MR-106E (ultra-pure hydrazine) are readily available at Russian or Chinese sites (both of which typically use UDMH/MON-27). Furthermore, even if these propellants were provided by the launch authority, their chemical composition and purity would have to be accepted on faith as there is no practical means of verifying either in the field. Moreover, the extremely hazardous nature of these propellants makes their transportation to geographically remote launch sites extremely expensive, if not impossible (preliminary inquiries were made by SSTL for the transport of MMH and MON to Baikonur, but no freight carrier could be located).

Table 3-14 summarises the costs for both the bi-propellant and mono-propellant options based on a worst-case scenario of operating from a geographically remote site with little or no support infrastructure currently in place. It is interesting to note that, except for mass, this analysis shows the two options have essentially the same cost for each dimension. This is somewhat contrary to conventional wisdom which generally assumes the mono-propellant option is always less expensive than the bi-propellant. This difference will be further analysed in Chapter 7.

Cost Dimension	Bi-propellant	Mono-propellant
Mass Cost	Low	Moderate
Volume Cost	Moderate	Moderate
Time Cost	Low	Low
Power Cost	Very low	Very low
Engine Price	~\$40,000	~\$40,000
Technical Risk	Low	Low
Safety Cost	Very high	Very high
Integration Cost	Moderate	Moderate
Logistics Cost	Very high	Very high

Table 3-14: Summary of bi-propellant and mono-propellant technology costs.

3.6. Hybrid Motors

A hybrid rocket normally consists of a solid fuel and a liquid oxidiser (however, “reverse hybrids” using solid oxidiser and liquid fuel have been investigated [Humble 95] but with limited success). The configuration for a typical system is shown in Figure 3-6. Motor start-up involves opening a single valve, allowing the pressurised oxidiser to flow into the fuel/combustion chamber where combustion takes place either spontaneously or with an ignitor. Hybrids can operate using a variety of readily available fuels such as HTPB (rubber) or polyethylene (plastic) and oxidisers such as liquid oxygen (LOX) or hydrogen peroxide.

The simplest hybrid combustion chamber is a solid rod of fuel with a cylindrical port down the centre. A suitable oxidiser is injected into the port and, in the presence of an ignitor (or with pre-heated oxidiser) the fuel vaporises and starts to burn. The hybrid motor can be easily turned off by stopping the flow of oxidiser and then restarted at a later time. Laying somewhere between a traditional liquid engine and a solid motor, it is often said that a hybrid “combines the best of both worlds” [Goldberg 91].

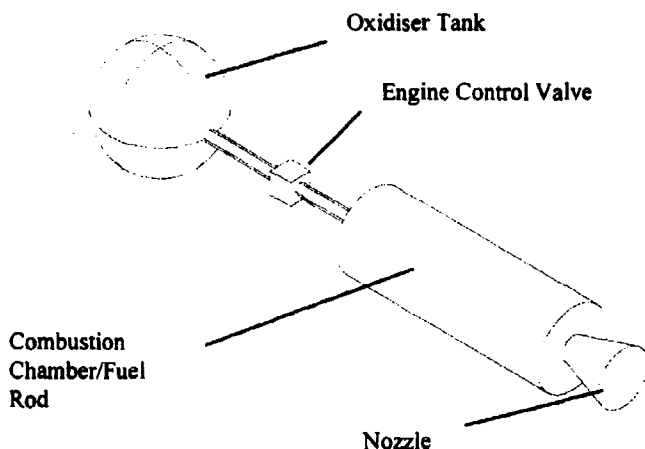


Figure 3-6: Typical hybrid rocket configuration. A liquid oxidiser is fed into a solid fuel combustion chamber.

The principle metric used for discussing the hybrid combustion process is the rate at which the fuel burns. This speed of fuel consumption is called the *regression rate*. Theory describes the regression rate as a function of the concentration of fuel and oxidiser. The standard regression rate formula is normally given as

$$\dot{r} = aG^n x^m \quad \text{Eqn. 3-4}$$

where

\dot{r} = fuel regression rate (m/s)

G = total propellant (fuel plus oxidiser) mass flux ($\text{kg/m}^2\text{s}$)

x = distance along the port (m)

a, n, m = regression rate constants, characteristics of the propellants (appropriate units)

Hybrid combustion differs from liquid and solid combustion in that the process occurs as a macroscopic diffusion flame. That is, combustion occurs in a region near the fuel surface where the fuel and oxidiser concentrations allow it. Typically, fuel is concentrated near the solid fuel wall while oxidiser is concentrated near the centre of the port. The two mix through the diffusion process. While oxidiser to fuel ratio, O/F , is basically constant for liquid and solid rockets, for hybrids this ratio gradually decreases down the length of the port. That is the reason regression rate is shown as a function of x in Eqn. 3-4.

Theory, backed up by experimental evidence, indicates that the rate of heat transfer to the fuel and its heat of decomposition are the controlling factors in combustion. The rate of heat transfer is controlled by the rate of flow of the oxidiser which, in turn, determines the rate of heat generated in the combustion zone. In practice, this combustion or flame zone exists within the boundary layer above the solid fuel (from fluid dynamics, the rate of flow of a fluid over a surface is zero at the surface and increases to a maximum at the boundary layer [White 86]). Oxidiser enters the flame

zone by diffusion from the centre of the port. Fuel enters as a result of vaporisation from the solid surface. A schematic of this process is shown in Figure 3-7. For a complete theoretical derivation of the regression rate equation refer to [Green 63] [Netzer 72] or [Humble 95].

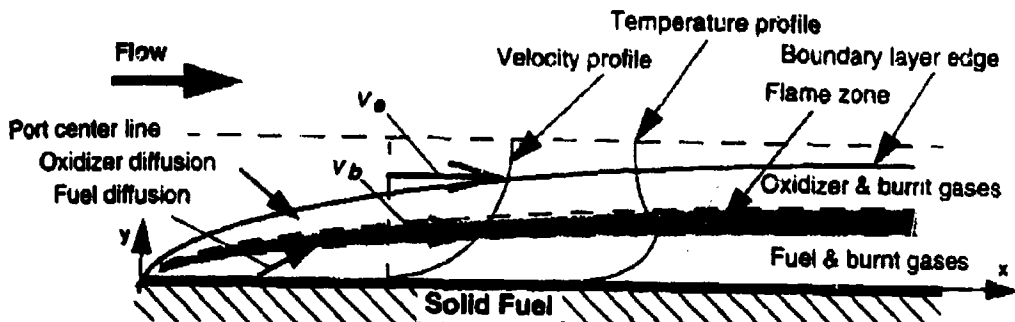


Figure 3-7: Schematic of Combustion zone above hybrid fuel (from [Humble 95]).

In experimental practice, Eqn. 3-4 has some basic limitations. To begin with, regression rate is shown to vary along the length of the port. Ideally, we would like to determine an average value which could be easily determined by measuring the mass of fuel before and after combustion. Fortunately, regression rate is actually a very weak function of x (except near the oxidiser inlet port where a very thin boundary layer is formed leading to higher heat transfer and therefore higher fuel vaporisation rate). This is a result of two compensating factors:

1. While the total mass flux increases down the length of the port due to added fuel, it is approximately balanced by the decrease in heat flux due to the growth of the boundary layer.
2. There is a self-regulating feature whereby a spurious, higher local cross section leads to a reduced total mass flux which tends to level the contour.

The other experimental drawback of Eqn. 3-4 is the dependence on total mass flux (fuel plus oxidiser). In practice, one can easily control and measure the instantaneous oxidiser flux rate, however, the fuel flux rate can only be measured on-average, after the experiment, by weighing the fuel rod. Thus, experiments often use a simplified burning expression that lends itself better to experimental data interpretation [Humble 95]

$$\dot{r} = a_{ox} G_{ox}^n \quad \text{Eqn. 3-5}$$

where

a_{ox} = simplified regression rate coefficient

G_{ox} = oxidiser mass flux rate ($\text{kg}/\text{m}^2\text{s}$)

n = regression rate exponent (constant)

Prediction of regression rate is fundamental to hybrid rocket motor design. Knowing the regression rate, along with thermochemistry variables, the mass flow rate, O/F and C^* can be computed using fundamental propulsion relationships. Regardless of whether you use the expanded Eqn. 3-4 or simplified Eqn. 3-5 form of the regression rate equation, the regression rate constants can only be

determined empirically due to the number of variables involved in the combustion process. Therefore, the primary goal of all basic hybrid rocket combustion research is to determine the regression rate constants for a given propellant combination. With these numbers in hand, the designer can then tailor a hybrid motor to support specific mission objectives.

3.6.1. Costs

In terms of performance costs, Table 3-15 demonstrates that hybrid rockets compare quite favourably to the other chemical options. Hybrids have a comparable theoretical *Isp* to storable bi-propellants, greater than that of solids or mono-propellants. Furthermore, because hybrids operate at much higher oxidiser/fuel ratios (O/F) their density specific impulse, *dIsp*, is greater than liquid bi-propellant systems, although not as high as solids. Typical bi-propellant systems for orbit manoeuvring operate at thrust levels of up to 400 N. Similar mono-propellant systems are available at these thrust levels. As we have seen, solids operate at thrust levels many times higher than this, 16000 N or greater. Hybrids, on the other hand, can be tailored to deliver thrusts over a wide range, 10's to 100,000's N.

System	Isp (sec)	Oxidiser specific gravity	Fuel specific gravity	O/F	Average propellant S.G.	dIsp (s.g. sec)	Thrust (N)	Power (W) (approx.)
Bi-Propellant	347	1.447	0.8788	1.65	1.16	403	up to 400	2
Mono-Propellant	225	-	1.023		1.023	232	up to 400	1
Hybrid	330	1.3663	0.9	6	1.27	420	up to 500+	1
Solid	287	1.661	-	-	1.66	476	16000+	0

Table 3-15: Comparison of System Performance Parameters. Bi-propellant and hybrid data computed using *Isp* computer program [Selph 92]. Mono-propellant data based on [Olin 95b]. Solid data assumes a STAR-17A motor [Thiokol 93].

Before proceeding to an evaluation of other hybrid costs, it is useful to compare hybrids to the solid and liquid chemical systems previously discussed. By the nature of their design and operation, hybrids offer a number of inherent advantages over these other options. These are summarised below (adapted in part from [Humble 95]):

- *Safety*—Hybrids are inherently safe.
 - *Inert fuel*—Typical fuels such as HTPB or PE are completely inert. As a result, they can be safely handled and installed into the spacecraft during integration.
 - *Non-toxic oxidisers*—Oxidisers such as LOX or high test peroxide (HTP) are not toxic as are bi-propellant oxidisers such as NTO.
 - *No fuel burn-throughs*—In solid rocket combustion, the propellant can burn along any crack or defect in the grain (this feature directly led to the Space Shuttle *Challenger* accident). Hybrid combustion takes place perpendicular to the flow of the oxidiser so burn-throughs are not possible.
 - *Hybrids can not explode*—Because combustion takes place only along the surface of the fuel grain, it is virtually impossible to create an explosive combination of fuel and oxidiser. A hybrid may burn in an accident, but it will not explode.
 - *Safe exhaust products*—Hybrid fuel/oxidiser combinations such as PE/HTP produce very benign exhaust products. In contrast, solid motors produce hydrochloric acid in

their exhaust (leading to acid rain near launch sites) and common liquid combinations e.g. MMH/MON are extremely toxic.

- *Simplicity*—Hybrids are inherently simple to design and operate.
 - *Low temperature sensitivity*—Like liquids, hybrid combustion burn rate is not significantly influenced by temperature. As a result, there is no need to apply additional margin to the combustion chamber design to account for operating pressure variation due to ambient temperature as with solids.
 - *No combustion chamber cooling*—The combustion chamber is automatically cooled by the ablative action of fuel combustion. Furthermore, the fuel itself acts as insulation to the chamber outer wall. Thus, no complex regenerative or film cooling system is needed.
 - *Robust grain design*—Because the grain can not burn-through as with solid motors, hybrid fuel grains are less prone to design or manufacturing defects unlike solids which typically require X-ray examination of the grain prior to flight.
- *Operational flexibility*—Hybrids offer other operational advantages.
 - *Controlled Shutdown and restart*—Because motor operation involves the opening/closing of single valve, the entire combustion process can be more easily controlled than with solids or liquids.
 - *Easy throttling*—Theoretical work discussed in [Williams 66] indicates a hybrid rocket can be throttled over thrust ratios of 10 to 100 with only a 10% loss in performance by simply varying the flow rate of oxidiser. In contrast, liquids can be throttled but require the precise co-ordination of two valves and liquid flow rates. Throttling a solid rocket can only be done *a priori* during the grain design.
 - *System testing*—A large part of a flight hybrid system, notably the oxidiser delivery system (tanks and valve, etc.) can be tested prior to flight, unlike solid motors.
 - *Propellant versatility*—The liquid oxidiser employed by a hybrid allows for higher energy levels than those used in solid propellants. Furthermore, the hybrid solid fuel allows for the introduction of various additives, such as aluminium powder, to increase *Isp*. This is much more difficult to do with liquid fuels.

Unfortunately, all these advantages do not come without some disadvantages. These are listed below:

- *Low regression rate*—Because the fuel burns relatively slowly, combustion chambers must either be fairly long or have multiple ports.
- *Low bulk density*—Because all the oxidiser is injected at the top end, there is insufficient port volume to allow mixing. This gives hybrids a lower mass density than liquids or solids. This is especially problematic for in-space applications where volumetric loading within a spacecraft can be difficult.
- *Combustion efficiency*—Because mixing of fuel/oxidiser is less efficient than with liquids or solids, their impulse efficiency is 1%-2% less. However, the delivered *Isp* is higher than solids because of higher performance propellants.
- *O/F shift*—During the course of a relatively long burn, the O/F ratio can change significantly. Depending on where combustion begins on the O/F vs. *Isp* curve this can lead to a decrease (or increase) in efficiency throughout the impulse.
- *No flight heritage*—No hybrid has been used or even tested in space. As a result, users face a potential up-hill battle with launch authorities for the first use of hybrids on a spacecraft. Furthermore, this lack of heritage may make it more difficult to obtain flight components (e.g. those compatible with HTP).

These relative advantages and disadvantages of hybrids are summarised in Table 3-16.

Option	Advantages	Disadvantages
Solid	<ul style="list-style-type: none"> • Long heritage • Simple • Reliable 	<ul style="list-style-type: none"> • Lowest <i>Isp</i> • Highest <i>dIsp</i> • One-shot only • Can not test the flight article • Hazardous exhaust products • Sensitive to manufacturing flaws and mishandling • Difficult to throttle
Liquid (storable bi-propellant)	<ul style="list-style-type: none"> • Long heritage • High <i>Isp</i> • Industry standard propellants • Industry standard components • Multiple ignitions • Flight article can be tested • Can be throttled 	<ul style="list-style-type: none"> • Toxic and expensive propellants • difficult to transport and handle • Toxic exhaust products • Complex designs, sensitive to manufacturing flaws
Hybrid	<ul style="list-style-type: none"> • Moderate <i>Isp</i> and <i>dIsp</i> • Multiple ignitions • Non-toxic propellants • Non-toxic exhaust products • Simple, robust design • Flight system can be tested (with fuel rod and nozzle replacement) • Easy to throttle 	<ul style="list-style-type: none"> • No heritage • Not an industry standard <ul style="list-style-type: none"> • Up-hill qualification battle • Fewer off-the-shelf components

Table 3-16: Comparing Propulsion Systems—Hybrids vs. Solids vs. Liquids

Based on these potential advantages of hybrids, we can now evaluate hybrids along the remaining dimensions of the cost paradigm beginning with system price. Because of the great reduction in failure modes, hybrids lend themselves to the use of commercial grade components and ingredients. Furthermore, hybrid systems can tolerate much larger design margins (and margins = money as discussed in Chapter 2). Both of these qualities imply that total system price of hybrids could be lower than competing commercial propulsion system options.

Unfortunately, before my research, there was no way to fully assess the real potential price of a hybrid system. There are no commercially available hybrid systems designed for satellite applications. In fact, the only hybrid systems available off-the-shelf are for small hobby sounding rockets. These toy systems have only been gaining in popularity during the last few years. Relying on a N₂O oxidiser and cellulose or rubber fuel, these systems are designed for fairly low total impulse (< 1000 N) and atmospheric operation. While low in price (around \$200 for a complete system) [Kilby 96], they could not be easily adapted and scaled up for space use. Therefore, I was forced to conclude that additional research was needed to fully evaluate the true potential for hybrid upper stages.

As stated earlier, no hybrid has ever been used or even tested in space. For this reason, hybrids have a potentially high technical risk cost until they can be successfully demonstrated in space. Once that is accomplished, their technical risk would be comparable to solid systems or mono-propellant liquid systems.

Turning to safety, because a hybrid literally can not explode, storage and handling procedures can be relatively simple. The inert fuel can be safely handled in the clean room during spacecraft integration

with no additional safety precautions. Furthermore, because the oxidiser used is safer than hypergolic NTO, complex and expensive safety equipment (e.g. SCAPE suits) are not needed.

The integration costs of a hybrid system associated with the components themselves should be roughly equivalent to that of a mono-propellant system. The fuel/combustion chamber can be integrated along with the rest of the spacecraft prior to shipment to the launch site. However, there is a potential integration cost due to the thermal control of the hybrid inside the spacecraft. In addition, due to the relatively high thrust, payload operations would have to be interrupted for all manoeuvres and additional requirements placed on the ADCS system.

Hybrid logistics requirements consist of the transportation and handling of a single propellant, the oxidiser. This cost should be somewhat less than that of a mono-propellant system due to the less toxic nature of hybrid oxidisers.

In summary, based on the discussion presented in this section, it appears that along all nine cost dimensions, hybrid rockets are roughly equivalent or better than competing chemical systems. These costs are summarised in Table 3-17. Perhaps most important, the inherent simplicity and design robustness of hybrids make them ideal for safe experimentation. Thus, hybrids not only have the inherent technical characteristics that offer a cost-effective option, they offer the best potential for in-house development within the context of a university environment. Given all their potential advantages, the most obvious question to arise from this discussion is why have hybrid not seen more wide-spread use? This question will be addressed in detail in Chapter 4.

Cost Dimension	Hybrid
Mass Cost	Low
Volume Cost	Low
Time Cost	Low
Power cost	Very low
System Price	Potentially Low
Technical Risk	High
Safety Cost	Low
Integration Cost	Moderate
Logistics Cost	Low

Table 3-17: Potential costs for hybrid propulsion technology.

3.7. Electric Engines

From the discussion in Section 3.2, all possible electric options were reduced to one type of electrothermal system—resistojets—and one electromagnetic system—pulse plasma thrusters (PPTs). This section will examine these two options with respect to the nine dimensions of the total cost paradigm.

3.7.1. Resistojets

Resistojets use resistive heating elements to convert electrical energy to heat. This heat is imparted to a working fluid which is then expelled from a nozzle to produce thrust. Figure 3-8 shows a simplified schematic of resistojet operation. Note that resistojets depend on convective heat transfer from the

heating elements to the fluid, therefore they must have high surface area of contact and are limited in total flow rate. Despite these limitations, resistojets have seen a variety of applications on spacecraft since the late 1960s [Greco 72] primarily using nitrogen, ammonia and hydrogen as propellant. The next section will present basic performance calculations for resistojet thrusters.

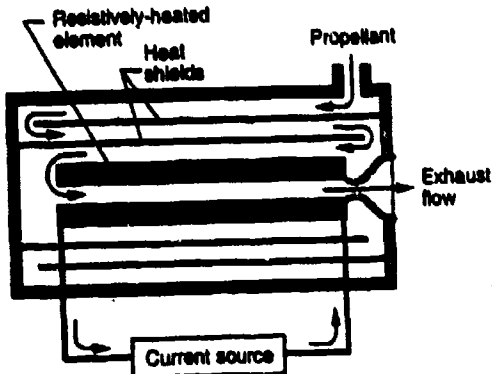


Figure 3-8: Schematic diagram of a simple resistojet [Humble 95].

3.7.1.1. Performance

The performance costs of a resistojet depend on two things, the chemical properties of the working fluid (primarily the density, ρ , and ratio of specific heats, γ) and the thruster chamber temperature. From fundamental rocket concepts, a direct relationship for characteristic exhaust velocity, C^* , as a function of γ and chamber temperature, T_c can be derived.

$$C^* = \frac{\sqrt{\gamma R T_c}}{\gamma \left(\frac{2}{\gamma + 1} \right)^{2(\gamma - 1)}} \quad \text{Eqn. 3-6}$$

where

C^* = characteristic exhaust velocity (m/s)

R = Gas constant (J/kgK)

γ = ratio of specific heats

T_c = chamber temperature (K)

The thrust can be determined from the thrust coefficient, c_F , as follows:

$$c_F = \left\{ \frac{2\gamma^2}{\gamma - 1} \left(\frac{2}{\gamma + 1} \right)^{\frac{\gamma+1}{\gamma-1}} \left[1 - \left(\frac{P_{exit}}{P_c} \right)^{\frac{\gamma-1}{\gamma}} \right] \right\}^{\frac{1}{2}} + \frac{(P_{exit} - P_{ambient}) A_e}{P_c A_t} \quad \text{Eqn. 3-7}$$

$$F = c_F A_t P_c \quad \text{Eqn. 3-8}$$

where

- P_{exit} = nozzle exit pressure (bar)
- $P_{ambient}$ = ambient pressure (bar)
- A_e = nozzle exit area (m^2)
- A_t = nozzle throat area (m^2)
- P_c = chamber pressure (bar)

The specific impulse is then found using:

$$Isp = \frac{C * C_F}{g_c} \quad \text{Eqn. 3-9}$$

With Isp , density and thrust known, propellant mass, volume and time can be determined for a given propellant and ΔV requirement.

The fourth performance cost dimension, power, depends on the initial and final propellant temperatures, the mass flow rate, and the heat capacity of the propellant.

$$P = (T_c - T_{initial})\dot{m}C_p \quad \text{Eqn. 3-10}$$

where

- P = Power (W)
- T_c = Operating chamber temperature (K)
- $T_{initial}$ = Initial propellant temperature (K)
- \dot{m} = Mass flow rate (gm/sec)
- C_p = Propellant heat capacity (cal/gmK)

To optimise overall performance, an ideal resistojet would have the following design requirements:

- High temperature
- Low molecular weight propellants
- High density propellants
- High thrust
- Low power

These requirements conflict. High operating temperatures demand either very high power or very low flow rate (or both). Power is limited by the spacecraft bus. Flow rate is limited by the minimum practical thrust. One way around this dilemma is with the choice of propellants. In theory, practically any gas or liquid could be used in a resistojet. However, if the initial temperature of the propellant is already high, then the total power needed to raise it to a given level will be lower. For this reason, (along with logistical reasons associated with its general availability) hydrazine is currently the most widely used propellant for resistojet applications (sometimes referred to as an "augmented hydrazine" engine).

In operation, the hydrazine is first decomposed using a catalyst bed in exactly the same way as it is done for mono-propellant applications producing an exhaust gas at temperatures of $\sim 700^\circ C$. The

exhaust gas is then electrically heated using simple resistive elements to temperatures $>1000^{\circ}$ C. The MR-501 thruster produced by Olin Aerospace, for example, requires 350 - 500 W to produce 0.01 - 0.02 N thrust at an *Isp* of 280 - 304 seconds [Olin 96b]. Thus, in terms of mass and volume costs, the hydrazine resistojet is roughly equivalent or superior to a conventional bi-propellant system. However, with the very low thrust, the time cost will be considerably higher. Finally, as with any electric propulsion option, the power cost is very high. In the case of the Olin thruster, it is about 100 times greater than that of a conventional chemical system.

3.7.1.2. Price and Mission Costs

The other costs for a resistojet depend, to a large extent, on the propellant used. Because the hydrazine thruster is the only one currently available off-the-shelf, the other costs are based on that option. According to Olin, the ROM price for this thruster is \$150,000 [Olin 96b]. Because this is well-proven thruster design, the technical risk would be roughly the same as that of a normal mono-propellant thruster. Safety and logistics costs would also be the same.

Integration costs, however, would be somewhat different. With respect to the spacecraft's attitude determination and control system (ADCS), the integration cost of resistojets should be roughly equivalent to that of cold-gas systems because of their relatively low thrust. This means that integration costs with respect to payload operations would be low as well. However, due to the very high power requirements and demands on battery capacity, the integration costs with respect to the power system would be relatively high. Furthermore, because of the high power requirement, the duty cycle would have to be carefully balanced so as not to interfere with payload or other bus operations. Therefore, the overall integration costs for a resistojet would be somewhat higher than for cold-gas systems and equivalent to or slightly less than much higher thrust mono-propellant systems.

Price and integration costs aside, the primary costs for the hydrazine resistojet are the same as those discussed for a mono-propellant systems. Therefore, for purposes of comparison, I have computed the performance for a similarly powered resistojet using water as the working fluid. The results of this analysis compared to the MR-501 hydrazine thruster appear in Table 3-18.

While a water resistojet has never been tested in space, it has received preliminary attention from NASA researchers for Space Station application [Manzella 89], [Morren 88], [Morren 93a] and [Morren 93b] with some success. These results indicate the performance shown in my own analysis are practically attainable. Unfortunately, this NASA work was discontinued due to lack of funding [Myers 95] as well as a preference to focus only on technologies with higher specific impulse [Myers 94]. In chapter 7, the water resistojet option will be re-examined in comparison to other options. The relative costs of both types of resistojet are summarised in Table 3-19.

Parameter	MR-501 Hydrazine Resistojet	Water Resistojet
Power Required (W)	350 - 500	459
Thrust (N)	0.01 - 0.02	0.282
Mass flow rate (gm/sec)	0.06 - 0.13	0.155
Propellant specific gravity	1.023	1.0
Chamber Pressure (bar)	3.4 - 6.6	8
Specific Impulse (sec)	280 - 304	185
Chamber Temperature (K)	-1700 (Derived)	1000

Table 3-18: Comparison of off-the-shelf hydrazine resistojet [Olin 96b] to a theoretical water resistojet.

Cost Dimension	Hydrazine Resistojet	Water Resistojet
Mass Cost	Moderate	Moderate
Volume Cost	Moderate	Moderate
Time Cost	Very high	Very high
Power Cost	Very high	Very high
Thruster Price	\$150,000	Potentially Low
Technical Risk	Moderate	High
Safety Cost	Very high	Very Low
Integration Cost	Moderate	Moderate
Logistics Cost	Very high	Very Low

Table 3-19: Summary of resistojet costs for both hydrazine and water propellant options.

3.7.2. Pulsed Plasma Thrusters

Unlike the resistojet, and all other propulsion systems discussed so far in this chapter, the pulsed plasma thruster (PPT) does not rely on the conversion of thermal energy to kinetic energy via expansion of a gas through a nozzle. Instead, a high energy plasma is accelerated mainly by the interaction of propellant charge with the electromagnetic field. This $J \times B$ force density is created during a short, high-current discharge. The basic operating principle of PPTs currently in use is described by Turchi writing in *Space Propulsion Analysis and Design* [Humble 95]. He explains:

"A PPT uses an electrical discharge across the, rectangular end-face of a block of Teflon propellant. The Teflon surface initially supports a high voltage between two electrodes in a vacuum. Two semiconductor sources in one electrode of the PPT provide sparks that ignite the discharge. A single, high-voltage capacitor supplies the initial voltage and powers the discharge. As heat transfer from the discharge causes the Teflon surface to ablate, a negator spring pushes the block into the discharge chamber. Because heat transfer to the propellant is an important feature of PPT operation, some electrothermal component of thrust is always present."

A schematic of PPT operation is shown in Figure 3-9. This technology has been available for nearly 25 years. PPT system have flown on a variety of U.S. and Soviet spacecraft. The first use was on the Lincoln Experimental Satellite LES-6 in the 1960s [Greco 72]. A flight qualified PPT operating at only 30 W with a total mass including controls, structure, thermal control, propellant and propellant feed system of only 5.85 kg was developed in 1974 [Myers 94]. Despite their development heritage, they have yet to see very wide-spread application in the satellite community. While the reasons for this are not entirely clear, an examination of their costs may offer some clues.

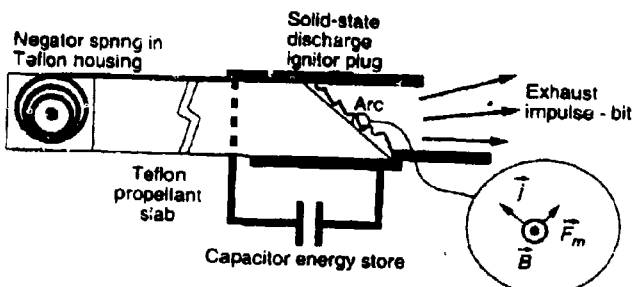


Figure 3-9: Schematic of a Pulsed Plasma Thruster (PPT) operation [Humble 95].

3.7.2.1. Performance

Because PPTs depend on Lorenz forces (the combined effect of electric and magnetic fields) rather than pure thermodynamic effects, their performance calculations are markedly different to the technologies previously discussed in this chapter. The electromagnetic force acting on the plasma can be estimated by assuming the discharge geometry is a simple flat sheet of width, w , and length, h . Let z be the distance between the first sheet and the sheet serving as the return conductor for the discharge current. The inductance can be estimated from

$$L = \frac{\mu_0 h}{w} \quad \text{Eqn. 3-11}$$

The component of the inductance gradient in the z -direction is

$$L' = \frac{\mu_0 h}{w} \quad \text{Eqn. 3-12}$$

The force on the plasma discharge is then (adapted from Turchi [Humble 95])

$$F_z = \frac{\mu_0 J^2 h}{2w} \quad \text{Eqn. 3-13}$$

where

F_z = Thrust in the z -direction (N)

J = Discharge current (A)

μ_0 = Permeability of free space ($4\pi \times 10^{-7}$ henries/m)

Integrating this force over the pulse duration (on the order of 3 μ sec) gives the total impulse, I :

$$I = \mu_0 \left(\frac{h}{2w} \right) \int J^2(t) dt \quad \text{Eqn. 3-14}$$

Performance values for a PPT currently under development by Olin Aerospace, funded by NASA are shown in Table 3-20. This system is aimed at flight qualification by mid-1997 [Olin 96a]

Parameter	Value
Propellant	Teflon (CF ₂)
Input Power	20 W
Voltage	28 V from spacecraft bus
Thrust	7 x 10 ⁻⁴ N
Specific Impulse	1200 - 1500 sec
Total thruster mass	3.5 kg
Total impulse available	20,000 Nsec

Table 3-20: Typical performance values for a pulsed plasma thruster (adapted from [Olin 96a])

Therefore, from a performance standpoint, PPTs seem nearly ideal. With an *Isp* nearly 10 times that of chemical or resistojet technology, the required propellant mass for a given ΔV would be correspondingly smaller. Furthermore, the relatively high density of the Teflon propellant (specific gravity 2.16 [Eschbach 90]) means the propellant volume requirement is small as well. In terms of power, the data from [Olin 96a] indicates requirements of only 20 W. The primary downside from the standpoint of performance is the very low thrust. This would create very long transit times for large orbit manoeuvres. Other potential costs of PPTs will be examined in the next section.

3.7.2.2. Price and Mission Costs

According to Mr. Joe Cassidy [Olin 96a], the estimated price for the PPT discussed in the previous section is expected to be about \$200,000 each when 2 to 5 units are purchased. Economies of scale could drop this price to \$100,000 when 5 to 10 units are ordered. Cassidy adds that if these thrusters were included as part of very large LEO constellations such as *Teledesic* (which envisions over 700 satellites) then the unit costs could be reduced dramatically to as little as \$20,000 each. However, for purposes of comparison in Chapter 7, I will use the higher cost estimate of \$200,000 per 20,000 Ns unit as most realistic in the near-term.

In terms of safety and logistics costs, PPTs look extremely attractive. The Teflon propellant is completely inert and can be safely handled in the clean room. This also simplifies logistics cost as the thruster can be completely integrated into the spacecraft prior to shipment to the launch site with no transport restrictions on the thruster or propellant.

Integration costs for PPTs are somewhat more difficult to determine. Certainly, their low thrust and low power would make their integration with respect to ADCS, payload operations and the electrical power system relatively simple. Furthermore, while high temperatures exist in the exiting plasma, the very low flow rates should make thermal stand-off easier to achieve and overall thermal control no more difficult than for a resistojet or small liquid thruster. Unfortunately, because of the nature of PPT operation, very high electromagnetic fields are produced during each pulse. There have been no reported problems caused by these EM fields on spacecraft that have flown PPTs. However, because of the fairly limited data base on this subject, very careful analysis of these effects would be necessary as part of a PPT integration exercise.

These potential integration costs of PPTs cloud their technical risk costs as well. Again, while there is flight heritage with the technology, the potential for EM radiation to cause in-flight problems raises the spectre of greater technical risk. Until PPTs see more widespread usage, their technical risk cost must be assumed to be higher than that of more proven technology such as cold-gas or liquid systems. All the potential costs for PPT technology are summarised in Table 3-21

Cost Dimension	PPT
Mass Cost	Very low
Volume Cost	Very low
Time Cost	Very high
Power Cost	Moderate
Thruster Price	\$200,000 per 20,000 Ns
Technical Risk	High
Safety Cost	Very low
Integration Cost	Moderate to High
Logistics Cost	Very low

Table 3-21: Summary of potential costs for pulse plasma thruster (PPT) technology.

3.8. Conclusions

Table 3-22 summarises the relative costs of each of the propulsion technology options reviewed in this chapter. Of these options, only hybrids are not available commercially for satellite application. Solids and liquids are available from a variety of sources with extensive heritage. Resistojets, especially hydrazine resistojets, are becoming more and more popular for station keeping applications. PPT systems, while not so widely used, have seen experimental applications on some satellites and may enter the market in the near future.

In contrast, hybrids have never been used in space. Thus, while there appears to be sufficient data available to evaluate the other options, to assess the utility of hybrids for small satellite application will require an extensive basic research and development program. The aim of this program would be to prove the accessibility of this untried technology, characterise its performance and amass a database of experience from which to credibly evaluate its total system cost. Why bother? As the above discussion indicates, hybrid rockets promise a simple, safe high-thrust rocket technology. Once fully developed, hybrids could be a cost-effective alternative to the other technology options.

Therefore, Chapters 4 and 5 will be devoted to evaluating the hybrid option. These chapters will present the results from a dedicated hybrid research and development effort completed as part of my research, summarising fundamental background on hybrid combustion theory, the design and implementation of a prototype hybrid system, experimental results of regression rate characterisation, and a realistic evaluation of hybrid system costs based on the extensive engineering experience gained.

Chapter 6 will return to the other side of the cost driver paradigm to consider the system engineering side of propulsion and its impact on total cost. A minisatellite propulsion system design case study

will be presented as a means for quantifying total system cost issues in greater detail. All technology options will be re-examined as complete systems in Chapter 7 as part of a parametric approach for determining the most cost-effective option for a given mission scenario.

Cost Dimension	Cold-gas	Solid	Bi-propellant	Mono-propellant
Mass Cost	Very high	Moderate	Low	Moderate
Volume Cost	Very high	Low	Moderate	Moderate
Time Cost	High	Very low	Low	Low
Power Cost	Very low	Very Low	Very low	Very low
Thruster Price	\$4000	\$125,000 - \$710,000	\$40,000	~\$40,000
Cost Dimension	Hybrid	Hydrazine Resistojet	Water Resistojet	PPT
Mass Cost	Low	Moderate	Moderate	Very low
Volume Cost	Low	Moderate	Moderate	Very low
Time Cost	Low	Very high	Very high	Very high
Power Cost	Very low	Very high	Very high	Moderate
Price	Unknown, Potentially Low	~\$150,000	Potentially Low	\$200,000 per 20,000 Ns
Technical Risk	High	Moderate	High	High
Safety Cost	Low	Very high	Very Low	Very low
Integration	Moderate	Moderate	Moderate	Moderate
Logistics	Low	Very High	Very Low	Very low

Table 3-22: Summary of propulsion technology option costs.

3.9. References

- [Allied 95] Allied Signal, Inc., *AlliedSignal Aerospace Capabilities in Satellite Systems*, Corporate Handout, June 1995.
- [Arde 96] Arde, Inc., UoSAT Minisatellite Propulsion System Phase-1 Contract Deliverable, component price quotations, SSTL Proprietary Information, 1996.
- [AstroTech 96] AstroTech, Inc., Cape Canaveral Florida, personal communication, Mr. Dwight Light, 8 January 96.
- [Bunker 90] Bunker, R.L., Baker, D.L., Lee, J.H.S., "Explosive Decomposition of Hydrazine by Rapid Compression of a Gas Volume," American Institute of Aeronautics and Astronautics, 1990.
- [Chang 89a] Chang, I., *Rocket Propulsion Fundamentals*, AA280 Notes, Stanford University, Spring 1989.
- [Chang 89b] Chang, I., *Advanced Space Propulsion*, AA286 Notes, Stanford University, Spring 1989.
- [Clark 72] Clark, John, *Ignition: An Informal History of Liquid Rocket Propellants*, Rutgers University Press, New Brunswick, N.J. 1972.
- [CPIA 70] Chemical Propulsion Information Agency, *Chemical Rocket/ Propellant Hazards*, Vol. III, *Liquid Propellant Handling, Storage and Transportation*, JANNAF Propulsion Committee, The JANNAF Hazards Working Group, May 1970.
- [Eschbach 90] Eschbach's *Handbook of Engineering Fundamentals*, 4th Edition, Tapley, B.D. (ed.), John Wiley & Sons. 1990.
- [Goldberg 91] Goldberg, B.E., Wiley, D.R., "Hybrids: Best of Both Worlds," *Aerospace America*, June 1991.

Chapter 3: Propulsion Technology Options

- [Greco 72] Greco, R.V. et al, "Resistojet and Plasma Propulsion System Technology," AIAA-72-1124, AIAA/SAE 8th Joint Propulsion Specialist Conference, New Orleans, Louisiana, November 29 - December 1, 1972.
- [Green 63] Green, L. jr, "Introductory Considerations on Hybrid Rocket Combustion," Heterogeneous Combustion, edited by Wolfhard, H.G., Glassman, I., and Green, L., jr., based on papers at Heterogeneous Combustion Conference, Palm Beach, Florida, December 11-13, 1963.
- [GSC 87] Guyana Space Centre, Safety Training, S3B Facility, ArianeSpace, CNES, 1987.
- [Humble 95] Humble, R., Henry, G.N., Larson, W.J., *Space Propulsion Analysis and Design*, McGraw-Hill, Inc., College Custom Series, 1995.
- [Kilby 96] Kilby, B., "The Great Hybrid Flyoff," *High Power Rocketry*, January 1996.
- [Manzella 89] Manzella, D.H., Carney, L.M., "Investigation of a Liquid-Fed Water Resistojet Plume," NASA Technical Memorandum 102310, AIAA-89-2840, Prepared for the 25th Joint Propulsion Conference, Monterey, California, July 10-12, 1989.
- [MBB 81] MBB, Proposal for 10-N Thrust Engine for AMSA III-B, TN RT351-2 1981.
- [Meinzer 95] Meinzer, K., Personal communication, May 1995.
- [Morren 88] Morren, W.E., Stone, J.R., "Development of a Liquid-Fed Water Resistojet," AIAA-88-3288, AIAA/ASME/SAE/ASEE 24th Joint Propulsion Conference, Boston, Massachusetts, 11 - 13 July 1988.
- [Morren 93a] Morren, W.E., "Gravity Sensitivity of a Resistojet Water Vaporiser," NASA Technical Memorandum 106220, AIAA-93-2402, 29th Joint Propulsion Conference, Monterey, California, June 28-30, 1993.
- [Morren 93b] Morren, W.E., MacRae, G.S., "Preliminary Endurance Tests of Water Vaporizers for Resistojet Applications," AIAA-93-2403, 29th Joint Propulsion Conference, Monterey, California, June 28-30, 1993.
- [MS 1522A] MIL-STD-1522A Standard General Requirements for Safe Design and Operation of Pressurized Missile and Space Systems, United States Air Force, 28 May 1984.
- [Myers 94] Myers, R.M., Oleson, S.R., "Small Satellite Propulsion Options," AIAA 94-2997, 30th Joint Propulsion Conference, Indianapolis, Indiana, June 27-29, 1994.
- [Myers 95] Myers, R., NASA Lewis Research Center, Private communication, November 1995.
- [NASA 93] NASA, "Ultra-Low-Power Arcjet Thruster Performance", NASA TM 106400, November 93.
- [Netzer 72] Netzer, D.W., "Hybrid Rocket Internal Ballistics," Naval Postgraduate School, Prepared by CPIA, January 1972.
- [Olin 95a] Olin Aerospace Company, Cost information on MR-106E Hydrazine Thruster, Mr. Jim Bartron, personal communication, 11 October 1995.
- [Olin 95b] Olin Aerospace Company, Information on MR-106E Hydrazine Thruster, Mr. Jim Bartron, FAXed personal communication, 12 October 1995.
- [Olin 96a] Olin Aerospace Company, email personal communication on pulsed plasma thruster (PPT) performance and cost, 10 January 1996.
- [Olin 96b] Olin Aerospace Company, MR-510 Electrothermal Hydrazine Thruster, ROM cost and performance data, FAXed personal communication from Mr. J.J. Galbreath, 6 February 1996.
- [RMD 94] British Aerospace Rocket Motors Division, "Baikonur Launch Site Visit," Internal Report 200 972-TR/1/E000, August 1994.
- [RO 94] Royal Ordnance, personal communication Ref: PDC/JE/313, 30 November, 1994.
- [Sellers 94a] Sellers, J.J., Astore, W.J., Crumpton, K.S., Elliot, C., Giffen, R.B., Larson, W.J. (ed), *Understanding Space: An Introduction to Astronautics*, McGraw-Hill, New York, N.Y., 1994.
- [Selph 92] Selph, C., *Isp Computer Code*, Personal communication to Dr. Ron Humble, 1992.

Chapter 3: Propulsion Technology Options

- [Sutton 92] Sutton, G.P., *Rocket Propulsion Elements*, 6th Edition, John Wiley & Sons, Inc., 1992.
- [Thiokol 93] Thiokol Corporation, *Space Motor Catalog*, Tactical Operations, Elkton Division, 1993.
- [Thiokol 96] Thiokol Corporation, Personal Communication, EP612-96 [PO29], ROM Prices for Small STAR Motors, W. Lloyd McMillan, 1 March 1996.
- [Valentine 94] Valentine, A., "Kazakhstan: Radiation and Chemical Hazard Conditions/Precautions General Health Precautions," Prepared by The Delphi Group, Inc., Austin, Texas, for Motorola, Inc., Phoenix, Arizona, August 1994.
- [White 86] White, F.M., *Fluid Mechanics*, McGraw-Hill, Inc., USA, 1986.
- [Williams 66] Williams, F. A., "Grain Design and Throttling of Hybrid Rocket Motors," Chemical Engineering Progress Symposium Series, No. 61, Vol. 62, 1966.
- [Wood 90] Wood, R.S., "Development of a Low Cost 22N Bi-propellant Thruster," AIAA 90-2056, AIAA/SAE/ASME/ASEE 26th Joint Propulsion Conference, Orlando, Florida, 16-18 July 1990.
- [Wood 95] Wood, R.S., Royal Ordnance Rocket Motors Division, Westcott, Personal communications during system design effort, 1995.
- [Zube 95] Zube, D., Messerschmid, E.W., Dittmann, A., "Project ATOS—Ammonia Arcjet Lifetime Qualification and System Component Test," AIAA 95-2508, 31st AIAA/ASME/SEA/ASEE Joint Propulsion Conference and Exhibit, 10-12 July 1995.

Chapter 4

Hybrid Research Program

- 4.1. HISTORICAL DEVELOPMENT**
- 4.2. RESEARCH PROPOSAL**
- 4.3. HYBRID DESIGN PROCESS**
- 4.4. SYSTEM REQUIREMENTS**
- 4.5. BASIC DESIGN DECISIONS**
- 4.6. PERFORMANCE ESTIMATION**
- 4.7. COMPONENT DESIGN**
- 4.8. SYSTEM DESCRIPTION**
- 4.9. CONCLUSIONS**
- 4.10. REFERENCES**

This chapter continues the second major research goal, that of fully characterising propulsion technology options for small satellites. One important conclusion from Chapter 3 was that hybrid rockets offer great promise for cost-effective satellite application. In this chapter, a thorough examination of the hybrid rocket propulsion option is begun that will extend through Chapters 5. The historical development of hybrids is first outlined with emphasis on why, despite their potential advantages, hybrids have enjoyed only limited attention. From this discussion, the chapter lays out the goals of a thorough hybrid research and development program undertaken to fully assess the true potential of hybrids for low-cost applications. The chapter goes on to describe the implementation of this program. A step-by-step hybrid rocket system design process is outlined. A discussion of how this process was applied to the design of a complete prototype hybrid system including system requirements, basic design decisions, performance estimation and system component design, is given. A complete description of the system concludes the chapter.

4. Hybrid Research Program

4.1. Historical Development

If hybrid rockets offer so many advantages then why have they not been used in space before? It is impossible to answer this question conclusively, but a brief review of the history of rocket development gives us some clues as to why this potentially useful system has languished in the background.

The hybrid rocket concept emerged at the dawn of rocket development in the early 20th Century along with most of the other modern options. The earliest recorded work was in the 1930s at I.G. Farben in Germany. In 1937, Farben, along with O. Lutz and W. Noeggerath, tested a 10-kN hybrid using coal and gaseous nitrous oxide. At about the same time, Oberth experimented with LOX/graphite combinations. However, both of these fuels have very low burning rates so their efforts met with little success. BMW also experimented with hybrids in 1944-45 [Clark 72].

The California Rocket Society (CRS) in the United States experimented with a LOX hybrid in combination with fuels such as wood, wax and rubber in the early 1940s. Unfortunately, their hybrid work was interrupted by World War II. Soon afterwards, however, in 1951, the CRS flew an experimental rocket to 9 km altitude using the LOX/rubber combination. But the most significant work done in the early 1950s (from the standpoint of my research) was done by G. Moore and K. Berman at General Electric using 90% hydrogen peroxide and polyethylene [Moore 56]. The results of their work will be discussed in greater detail later in this chapter.

In the 1960s, several European organisations engaged in hybrid research. ONERA (with SNECMA and SEP) in France worked on hypergolic combinations including nitric acid with amine-based fuels [Humble 95]. In addition, M. Pugibet and H. Moutet looked at hypergolic combination using hydrogen peroxide whereby a catalyst material was added to the surface of the fuel grain so no separate decomposer was needed [Pugibet 70]. In Sweden, B. Ankarsward and U. Magnusson working with the Royal Swedish Air Force Board and Flygmotor looked at combinations of nitric acid and a proprietary fuel they called tagaform (polybutadiene plus aromatic amine). They successfully flew a 20kg payload to an altitude of 80 km using a sounding rocket powered by this combination [Ankarsward 79] [Humble 95].

Back in the U.S., work on hybrids continued during the 1960s at United Technologies, Chemical Systems Division. Together with Beech Aircraft they developed a supersonic target drone called Sandpiper using MON-25 (75% N₂O₄ plus 25% NO) and PMM-Mg. A later version called HAST experimented with IRFNA-Pb/PMM. This version was able to throttle over a 10:1 thrust range. The *Firebolt* programme, which continued into the 1980s, grew out of this work using the same propellant combination [Humble 95].

Looking at these historical developments in the context of overall progress in the rocket industry, one can infer several possible explanations which, when taken together, shed some light on why hybrid rockets have remained largely a footnote (partly adapted from [Holzman 94])

1. *Major rocket developments have been driven by military requirements*—Faced with solid, hybrid and liquid options, solid motors were selected for their long-term storability and quick response time on ICBMs. Liquids too had been given a development boost during World War II and subsequent work on V-2 related technology for missiles. Once military and large government programs decided to spend development money on solids and liquids, there was little money left for hybrids. No individual program could justify the research and development cost on its own. In addition, the operational success of F-1 (liquid engine for the Saturn V) and the solid rocket motors for Titan III caused hybrid interest to wane.
2. *Historically, space missions have been performance driven; price and mission costs were willingly sacrificed for performance*—Designers turned to fully liquid systems for the greatest performance. Because performance was the primary driver, the other advantages of hybrids did not factor in, thus they tended to be ignored.
3. *Volume constraints*—Hybrid density *Isp* once again falls between solids and liquids. Because of the requirement of achieving full combustion of a vaporising oxidiser within the fuel/combustion chamber, these motors tend to be long and thin, thus making their packaging into short, squat spacecraft somewhat more difficult.
4. *Politics*—All the 1960s and 70s work in hybrids was done primarily by liquid and solid propulsion companies. Not surprisingly, in any selection process for upcoming systems, hybrids were always perceived as second best. “Political factors interfered with technical factors.” [Holzman 94]

Despite the historical precedent, hybrids have enjoyed a renaissance within the last ten years. In the 1980s, hybrid work was primarily focused on developing a viable alternative for solid rocket boosters on launch vehicles. The American Rocket Company (AMROC) led the way in this effort. Their H-500 motor used LOX/HTPB and demonstrated thrust levels of 312,000 N for 70 seconds. A later version, the H-250F was tested at over 1,000,000 N [Estey 92] [Humble 95]. AMROC also completed preliminary work on a hybrid upper-stage. In the early 1980s, AMROC’s efforts were mainly a lone voice in the wilderness. However, in the wake of the *Challenger* accident, followed closely by the failure of a U.S. Air Force Titan 34-D (both linked directly to inherent drawbacks of solid motors) hybrids began to receive renewed attention. These safety concerns, coupled with increasing pressure to decrease cost and environmental impact, led to NASA-funded hybrid research.

Much of this work is centred at the Marshall Space Flight Centre [Griener 92] [Marshall 95]. Initially, AMROC greatly benefited from this new attention. NASA awarded them \$22.2M to develop a prototype booster system [Davis 94]. Initial results impressed even the sceptics at NASA [Tucci 94]. Unfortunately for AMROC, this new interest in hybrids was too little, too late and they were forced to declare bankruptcy in 1995 [Boyer 95] [Dasch 95]. Despite this commercial failure, the American Institute of Aeronautics and Astronautics (AIAA) subsequently endorsed hybrids as safe and simple propulsion option for the future, deserving of further research and development [Space News 95].

Hybrid rockets have also enjoyed astounding success in the classroom. Cadets at the U.S. Air Force Academy, under the guidance of Air Force Officers and enlisted personnel, constructed and launched the first U.S. Department of Defence hybrid rocket in 1990 powered by gaseous oxygen and HTPB. Building on this success, the Academy team went on to launch a LOX/HTPB hybrid sounding rocket, *Chiron*, to over 4,500 metres altitude in January 1994 [Lydon 93]. Research at the Academy continues to exploit the relative ease of manufacture and safety of hybrid rockets for experimental and educational purposes. Hybrid research is also going on at Purdue University in the U.S. [Ventura 93] and at Bristol University in the UK [Grigorian 94].

Outside the U.S., hybrids have also recently gained renewed interest in recent years. A 1988 European Space Agency (ESA) paper study examined the advantages of a hybrid upper stage [Jansen 88]. Preliminary interest has been shown by researchers in India [Nagappa 91] and Europe [Kuentzmann 91]. In March 1995, I attended a meeting at TNO, The Netherlands along with about 20 researchers from all over Europe interested in hybrid research. TNO was awarded a hybrid research contract by ESA in 1995 [Vincent 95]. British Aerospace Royal Ordnance has also recently started their own dedicated hybrid program (derived, in part from our own work) aimed primarily at tactical applications. Finally, the inherent safety of hybrids are making them increasingly popular for hobby rocket enthusiasts. Several makes and models have come on the market in the last few years. [Kilby 96]

4.2. Research Proposal

Chapter 3 revealed inherent technical advantages of hybrids which give them great potential for cost-effective applications. The last section revealed that the political environment and the performance-driven demands of previous space missions, not purely technical issues, have prevented hybrids from being used in space. However, within the environment of a small satellite development centre such as CSER, it is possible to give hybrids a fresh start to fully evaluate their potential for spacecraft application. Never before have hybrids been critically examined in this context. A program to establish the real, not potential, costs of hybrids would contribute significantly to the basic understanding of this important propulsion option.

Therefore, understanding this critical need at the outset of my work, I proposed a hybrid research and development program aimed at characterising their combustion performance and other costs dimensions. The overriding objective of this research was to establish whether or not hybrid rockets really live up to their expectations. After all, it is sometimes the case in engineering that a particular technology application looks great in theory, but is sorely lacking in practice.

Beginning in April 1994, supported by UoSAT/SSTL, I undertook this hybrid rocket research programme. The goals of the program were established as follows:

1. *Proof-of-concept*—demonstrate the accessibility of hybrid rocket technology for continued research, development and exploitation for low-cost satellite upper stages. In the process, identify and solve the critical engineering problems of the technology.
2. *Performance characterisation*—recognising that the actual performance of a given hybrid propellant combination depends on empirical data, establish through experimental investigation, the regression rate characteristics for a prototype motor and use this data as a basis for preliminary upper stage design calculations.
3. *Total cost assessment*—based on the experience gained through hands-on hybrid rocket work, fully assess the system price and mission costs for future hybrid upper stage applications.

With these goals in mind, a research programme encompassing the following tasks was laid out:

- *Motor design*—Design a prototype hybrid motor capable of eventual integration into a small spacecraft.
- *Support system design*—Design an oxidiser delivery system along with data collection and control apparatus to ensure safe, efficient experimental testing.
- *Component acquisition and fabrication*—Locate and acquire necessary system components (pipes, valve, tanks, regulators, etc.). Fabricate motor and test rig components.
- *System integration*—Assemble and test all rig “plumbing” and integrate data collection and control system. Develop safe operational procedures.
- *Hybrid performance characterisation*—Perform sufficient tests to determine fuel regression rate equation to enable accurate motor design.
- *Cost assessment*—Gain sufficient practical experience with hybrid rocket design and operations to allow for a realistic assessment of performance and other cost dimensions and enable realistic mission planning and critical comparisons with competing propulsion options.

The remainder of the chapter will be devoted to a discussion of the design process used for my prototype hybrid motor and a detailed description of the system. Chapter 5 will describe the extensive testing done with this motor, focusing on experimental results and conclusions.

4.3. Hybrid Design Process

The basic design process for a hybrid rocket propulsion system can be outlined as follows (adapted from [Larson 92] and [Humble 95]):

Step 1: Define system requirements

Step 2: Decide on basic design parameters

- Choose propellants
- Choose O/F
- Determine oxidiser flow rate
- Determine pressure levels for combustion chamber and feed system
- Size the system
- Design combustion port

Step 3: Estimate Performance

Step 4: Design Components

- Fuel grain
- Nozzle
- Combustion chamber

- Oxidiser delivery system
- Support structure and parts

Step 5: Iterate as required

The following sections will go through these steps to summarise the process used to design the experimental hybrid system.

4.4. System Requirements

Recall, the primary objective of the hybrid research was a critical characterisation of combustion performance and other costs dimensions as well as support system architecture to evaluate the suitability of hybrids for low-cost application on small satellites. To that end, a prototype hybrid system was needed to allow flexible experimentation and data capture while being representative of an eventual flight system. From these objectives, a detailed set of system requirements emerged as summarised below in order of importance:

1. *Safety*—The overriding requirement in the system design was safety. Even though hybrids themselves are inherently safer to work with than other types of rockets, there is still a need to work safely with extremely high temperatures and pressures, as well as potentially dangerous oxidisers. Many of these safety concerns were alleviated by the selection of the test site. This will be addressed in Section 4.8.
2. *Low Price*—This was the single most important driver in my prototype system design. The entire programme budget was constrained to under £20,000. Many basic system design decisions were made based primarily on price. Low price also mandated several related requirements such as:
 - Simple to fabricate—This helped keep manufacturing cost low
 - Use of available materials and components
3. *Approximate operating configuration of a flight demonstration motor*—To the greatest extent practical, the prototype motor should resemble an actual flight motor. This eliminates the problem of trying to scale data from a very small motor to predict performance of a much larger motor. Designers of hybrid motors for booster application often have no choice. Fortunately, the size of a flight motor for a minisatellite is approximately the same physical size as a typical test motor. Operating pressure for the prototype motor was partly selected for spacecraft compatibility. (Note: thrust is primarily a function of expansion conditions. Therefore, for expansion to atmosphere vs. vacuum it was not necessary to match the thrust requirement for a flight engine).
4. *Easy to test*—an experimental motor will differ markedly from an operational flight motor because of the inherent requirement of making it easy to assemble and disassemble.
5. *Robust and flexible*—In the experimental environment, it is essential that a test motor be of robust and flexible design to accommodate large pressure fluctuations and design loads to enable it to operate well beyond the initially predicted envelope.
6. *Representative flight propellants*—While it may be easier to work with some propellant combinations than others, to validate the experience base and allow me to extrapolate to flight operations it is necessary to work with the same basic propellants.

The next section moves on to step 2 in the hybrid system design process, illustrating how these requirements helped to drive basic system design decisions.

4.5. Basic Design Decisions

Given these basic requirements, the next step was to make basic system design decisions. The most fundamental of these decisions for a hybrid system is the choice of propellants. This decision will be the subject of the following subsections.

4.5.1. Oxidiser Selection

For satellite applications, an ideal hybrid oxidiser should have the following characteristics:

- High storage density
- Space storability
- Handling, storage and launch safety
- Readily available
- Ease of ignition
- Acceptability by launch agency and primary payload
- Environmentally friendly combustion products

The total potential list of hybrid oxidisers include:

- oxygen (gaseous, GO₂ or liquid, LOX)
- nitrogen tetroxide, NTO (N₂O₄)
- nitrous oxide ("laughing gas," N₂O)
- hydrogen peroxide (H₂O₂)

Of these, gaseous O₂ must be eliminated because of its very low storage density. Cryogenic LOX is not a viable candidate for an upper stage because of the problems of long-term storability. NTO at first appears to be a likely candidate because of its wide availability in the space industry. Unfortunately, as a hybrid oxidiser it is less desirable because of its toxicity and the problem of initiating combustion with the fuel. An ignition device would be required which is less desirable than a spontaneous reaction. N₂O has the additional advantage of being potentially "self-pressurising" due to its very low vapour pressure. A nitrous oxide/HTPB was investigated by AMROC for use as an upper stage [AMROC 94]; however, all data is proprietary and has not been published [Witinghill 94]. This is also the oxidiser favoured for hobby rocket applications as noted in Chapter 3 [Kilby 96]. Unfortunately, N₂O has the drawback of requiring an ignition system like all the others listed. This makes multiple start-ups significantly more difficult. The exception is hydrogen peroxide. For space applications, hydrogen peroxide is generally in excess of 80% concentration and is referred to as *high test peroxide* or *HTP*. When first passed through a suitable catalyst, HTP breaks down into super heated (>600°C) steam and oxygen. At this high temperature, combustion is spontaneous with most conventional fuels. The following subsections will take a closer look at this oxidiser option.

4.5.1.1. Hydrogen Peroxide Background

In one respect, hydrogen peroxide could be called the most natural of rocket propellants. There is a small beetle of genus *Brachinus* that makes its home in the chalky areas of southern England. Known as the "Bombardier Beetle," this six-legged rocket scientist fires a cloud of caustic vapour at its

enemies, expelled by an explosive mixture of 10% hydroquinone and 23% hydrogen peroxide! [Cambridge 91].

Outside the insect world, hydrogen peroxide was first discovered by Louis-Jacques Thenard and reported to the Paris Academy of Science in July 1818. Thenard had been conducting research into voltaic cells when he discovered that barium peroxide reacted with cold nitric acid to form what he called "oxygenated water." Thenard spent considerable effort testing this new substance. He cited reactions with 130 elements, oxides, salts, acids and bases. He sometimes noted that in "in these decompositions, chemical action is evidently missing; it is necessary then, to attribute these actions to a physical cause; but the actions are dependent on neither heat nor light, whence it follows that they are probably due to electricity." [HPHB 67] His unexplained reactions were later explained by Berzelius in 1836 who first described the process of catalysts and catalytic reactions.

At first, hydrogen peroxide was used only for removing sulfide deposits from oil paintings and as a skin irritant for medical purposes. Later, industrial grade hydrogen peroxide (less than 52% H₂O₂ by weight) was found useful in a variety of commercial processes including textile and pulp bleaching, synthesis of chemical derivatives, manufacture of foam rubber, oxidation of dyes, and the treatment of metal surfaces.

Hydrogen peroxide (60%) was first used for propulsion applications in Germany in 1934 for underwater vehicles. Later, it was used to drive the turbo-pumps in the V-2. After the War, hydrogen peroxide in even higher concentrations were used for space propulsion applications, both as an oxidiser and as a mono-propellant. Hydrogen peroxide fell out of favour in the late 1950s primarily due to "bad press" and the emergence of more storable oxidisers such as nitrogen tetroxide. Hydrogen peroxide's "bad press" centred on its instability during storage. Even contemporary sources [Sutton 92] quote storage decomposition of >1%/year. Even though, as of 1967, storage decomposition rates of < 0.1%/year were readily attainable and in-space storage in excess of 2 years had already been demonstrated. [HPHB 67]

Hydrogen peroxide has seen service on the following space missions [HPHB 67]:

- Mercury spacecraft
- Scout launch vehicle
- Little Joe II sub-orbital vehicle
- Burner II
- SATAR satellite
- ASSET satellite
- Lunar landing simulator
- Astronaut manoeuvring unit (Gemini program)
- SYNCOM spacecraft
- COMSAT spacecraft
- HS-303A "Blue Bird" spacecraft

- ATS spacecraft
- Personal rocket belt
- X-15 rocket plane
- *Black Arrow* launch vehicle

All of these missions relied on “propellant grade” peroxide or “high test peroxide (HTP).” Table 4-1 lists some important characteristics of HTP.

Parameter	Value
Density (kg/m ³)	1388
Freezing Point (°C)	-17.9
Boiling Point (°C) 1 atmosphere	136.6
Specific Heat 20° to 60°C (kg/kg-K)	2.83
Viscosity at 20°C (N-s/m ²)	1.26 × 10 ⁻³
Latent Heat of Fusion (pure) (kJ/kg)	367.64

Table 4-1: High Test Hydrogen Peroxide (HTP) characteristics (adapted from [Andrews 90])

Despite its excellent chemical properties, the main criticisms of peroxide are related to its stability. Clark in *Ignition: An Informal History of Liquid Rocket Propellants* [Clark 72] calls HTP “the oxidiser that never made it.” H_2O_2 will decompose in an exothermic reaction into H_2O (steam) and O_2 in the presence of a suitable catalyst or when heated. Virtually any organic substance is a potential catalyst, thus any contamination in a storage container can initiate decomposition, releasing heat and further aiding the decomposition. In this way, run-away reactions can begin. However, according to Mr. E.G. David Andrews [Andrews 90] who had extensive experience working with HTP on the *Black Arrow* project in the 1960’s, much of this criticism came from engineers who actually had little experience with HTP and are, in some cases, “unbalanced and dismissive, presenting much too negative a view.” One could equally argue that no oxidiser, LOX, NTO, etc. is perfectly safe to work with. In fact, safe rocket propellant is, chemically speaking, an oxymoron. That being said, the safety issues surrounding the use of HTP must be thoroughly understood before one should attempt to use it. References [HPHB 67] and [Davis 52] give a comprehensive discussion of the safety procedures, material compatibility issues and other important information for HTP handling.

In operation, the HTP is injected into a *catalyst pack*—a small decomposition chamber containing the catalyst material capable of high temperature and pressure. Within the catalyst pack, the HTP chemically decomposes into superheated (>600°C) oxygen and steam. The decomposition products are then directed into a combustion chamber where the oxygen-rich mixture can be combined with any number of liquid or solid fuels. The decomposition products can also be expanded as-is through a nozzle giving a mono-propellant rocket with an *I_{sp}* of approximately 170 seconds. This is an added advantage of using HTP for a spacecraft application, it can be used alone for attitude control and minor orbit corrections.

By far, the most extensive work done on HTP was conducted in the UK during the 1950s and early 1960s. Much of this work was for classified military applications, however, HTP was also used for

the *Black Arrow*—Britain's first and only space launcher [Andrews 90] [Gould 91]. Much of this work was conducted at Westcott, England at what was then the Royal Aircraft Establishment. At that time, HTP was being delivered to Westcott by the rail cart load. Between 1954 and 1956 alone, 462 tons of non-stabilised HTP were used [Maggs 56] (no figures are available for the amount of stabilised HTP used during the same period, presumably an equal or greater amount). A vast army of researchers investigated HTP catalysts, the effects of various stabilisers and additives in addition to basic rocket development using HTP in combination with various fuels (all work was with liquid fuels such as RP-1, there is no record of HTP hybrid work being conducted at Westcott at that time).

Unfortunately, because this work was in support of military programmes, all technical reports were either confidential or secret. I was only able to obtain some key documents relatively late in my research programme. These are discussed in Chapter 5 in the context of my own catalyst pack development.

In the late 1960s, work on HTP basically died out all together due to the success of “packaged liquids,” primarily combinations of hydrazine with the oxidiser nitrogen tetroxide, NTO. Still today, NTO remains the most popular oxidiser for space applications [Clark 72]. However, in the last several years, HTP has gained new attention. Among the various new ideas for single-stage to orbit is one by Kistler Aerospace Corporation. Their sub-orbital test vehicle the K-0, (originally planned for testing in late 1995) plans to use hydrogen peroxide for sub-orbital tests [Kross 95] [Hudson 95].

Another radical new idea for getting payloads into space also envisions leveraging from the inherent advantages of HTP. *Black Horse* is a U.S. Air Force sponsored programme which would use a winged orbiting vehicle that would take off like a conventional aeroplane using air-breathing engines powered by normal jet propellant (JP). However, once the space plane reaches cruising altitude at around 12,000 metres it would rendezvous with a conventional tanker such as a KC-135 or KC-10A but instead of loading fuel, it would load hydrogen peroxide oxidiser. The JP/HTP would then be burned in rocket engines to take the space plane into orbit. HTP was a key enabling technology for this particular applications because it “is very dense, allowing a lightweight, compact airframe to hold a lot of it; it is non toxic, and is much cheaper than any other oxidiser except for cryogenic liquid oxygen. The fact that hydrogen peroxide is non-cryogenic is a major plus—it allows existing tankers to be used for aerial propellant transfer with only minor modifications.” [Zubrin 95]

For the reasons discussed above, HTP was chosen as the oxidiser for the prototype hybrid system. The following subsection explores details of HTP thermochemistry.

4.5.1.2. Hydrogen Peroxide Thermochemistry

Hydrogen peroxide decomposition can be represented chemically by



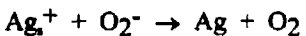
This is an exothermic, irreversible process and while this formula represents the end result of the decomposition, there are an estimated 10 to 20 intermediate reactions chemists have identified [HPHB 67]. Considering both the liquid and vapour phases, there are total of 5 types of decomposition reactions possible:

1. Homogeneous reaction in the liquid phase between the hydrogen peroxide and the dissolved catalytic or oxidisable components.
2. Heterogeneous reaction of the liquid phase with surfaces of the container and/or suspended particles.
3. Heterogeneous reaction of a film of condensed hydrogen peroxide on the surfaces in contact with a vapour phase.
4. Heterogeneous reaction of the vapour phase on dry surfaces.
5. Homogeneous decomposition of the vapour phase.

As my work is focused on the controlled decomposition of HTP via a catalyst, reactions 2, 3 and 4 are the most important. D. Sutton [Sutton 60] provides an extensive summary of the theoretical and experimental work done to investigate the mechanisms of hydrogen peroxide decomposition in the presence of a catalyst (in this case silver). According to Sutton, the most likely initiating reaction is



Assuming purely heterogeneous decomposition, then the subsequent reactions are, in order:



Where Ag^+ stands for charged site on the metal surface.

Because of the complex nature of HTP chemical decomposition, performance predictions relied on the U.S. Air Force *Isp* computer programme [Selph 92]. The program provides several key parameters including characteristic exhaust velocity, C^* , ratio of specific heats, γ , and chamber temperature, T_C . These values are listed in Table 4-2 based on the following assumptions:

- 85% HTP (0.85 H_2O_2 /0.15 H_2O)
- Chamber Pressure = 17.2 bar (250 psi)

Parameter	Value
C^* (m/s)	885
Temperature (K)	907.4
Molecular Weight (kg/kmole)	21.829
Moles gas/100 gm	4.581
Ratio of specific heat, γ	1.275
Heat capacity (cal)	42.204
Entropy (cal)	233.325
Enthalpy (cal)	-169.018
Density (gm/cc)	0.004987

Table 4-2: Theoretical performance of 85% HTP decomposition at 17.2 bar (250 psi) based on the USAF *Isp* program.

While this describes the theoretical result from the standpoint of pure chemistry, achieving this reaction with high efficiency is the engineering challenge. The effort expended towards meeting this challenge is described in Chapter 5.

4.5.1.3. HTP Supply

Hydrogen peroxide can be made in very high concentrations (up to 99%) but, in practice, can never be made completely pure. There are always some concentrations of contaminants left over from the manufacturing process. In addition, other compounds, most notably tin, are normally added as stabilising agents. For propulsion applications, these stabilising agents offer both advantages and disadvantages. On one hand, you would like the propellant to be as stable as possible for safe handling and long-term storage. On the other hand, if it is too stable it will not react as required.

To clarify the limits on contaminants and stabilisers, the U.S. Military defined propellant grade hydrogen peroxide using MIL-P-16005D "Propellant, Hydrogen Peroxide." (18 March 1965) This specification is summarised in Table 4-3.

Property	Minimum	Maximum
Weight Percent H ₂ O ₂	90.0	91.0
Aluminium		0.5 mg/litre
Chloride		1.0 mg/litre
Ammonium		3.0 mg/litre
Nitrate	3.0 mg/litre	5.0 mg/litre
Phosphate		0.2 mg/litre
Sulphate		3.0 mg/litre
Tin	1.0 mg/litre	4.0 mg/litre
Carbon		200.0 mg/litre
pH	n/a	n/a
Surface Tension, dynes/cm	n/a	n/a
Evaporative residue		20.0 mg/litre
Stability, percent		5

Table 4-3: Specifications for propellant grade hydrogen peroxide per MIL-P-16005D (adapted from [HPHB 67]).

As noted earlier, 40 years ago HTP was in abundant supply. It was inexpensive as well. In 1967, the USAF paid only \$0.23/lb. Unfortunately, those days are gone. Very early in my research I learned that HTP is no longer cheap or plentiful.

The problem of locating a reliable supply of HTP slowed down the program by several months. Fortunately, I was eventually put in contact with Air Liquide in France. They produce high purity, 85% "electronic grade" hydrogen peroxide for the semiconductor industry and, after only a few months, the first shipment of 80 litres arrived at Westcott in two small stainless steel drums (a far cry from the good old days when I am sure engineers routinely wasted this amount with little care).

The chemical assay for the Air Liquide HTP is shown in Table 4-4. Comparison to MIL-P-16005D is also provided where applicable. While Air Liquide said they would be able to produce 90% hydrogen peroxide if required, the electronic grade at 85% was readily available at a much lower price. For

basic research work, this was deemed acceptable. Notice that all contaminant and stabiliser parameters are well within the MIL-SPEC with the exception of phosphates. The potential effects of this contaminant are described in Chapter 5.

Characteristic	Value
Concentration	85% (Spec >90.0%)
Density	1.37 kg/m ³
Residue @ 110°C	2 mg/kg
Chlorides, Cl ⁻	450 µg/kg (Spec < 729.9 µg/kg)
Nitrates, NO ₃ ⁻	2000 µg/kg (Spec < 3649.6 µg/kg)
Phosphates, PO ₄ ³⁻	540 µg/kg (Spec < 145.98 µg/kg)
Sulphates, SO ₄ ²⁻	150 µg/kg (Spec < 2189.7 µg/kg)
Lead, Pb	180 µg/kg
Silicon, Si	25 µg/kg
Tin, Sn	15 µg/kg (Spec < 2919.6 µg/kg)

Table 4-4: Characteristics of hydrogen peroxide provided by Air Liquide, France. All other elements are below 5 µg/kg [AL 94]. Specification is based on MIL-P-16005D.

4.5.2. Fuel Selection

With HTP selected as the candidate oxidiser, I then turned to selection of a fuel. The list of possible fuels is virtually endless as nearly all polymers fall into this category. Typical examples that have been used are hydroxyl terminated polybutadiene (HTPB), polyethylene (PE), nylon, Araldite, Plexiglas and Stratyl [Moore 56][Pugibet 70]. Because of the experimental success enjoyed by Moore and Berman [Moore 56] with the HTP/polyethylene combination, as well as its inexpensive commercial availability and ease of machining, it was chosen as the primary candidate fuel. Generally speaking, the theoretical performance of polyethylene is virtually identical to gasoline (petrol).

4.5.3. O/F Ratio

For spacecraft application, it would be desirable to design a motor to operate at or near the *optimum oxidiser/fuel ratio (O/F_{optimum})* (sometimes called the *stoichiometric* ratio). Figure 4-1 shows the relationship between O/F and *I_{sp}* for HTP/PE. The optimum point is O/F_{optimum} = 8.1. Realise that as the burn progresses, the port area increases. Thus, for a fixed oxidiser flow rate, the actual O/F will increase during the firing. As a result, a flight motor would be designed to begin combustion at an O/F somewhat lower than the optimum value so the efficiency would be increasing over time with a near optimum integrated efficiency achieved.

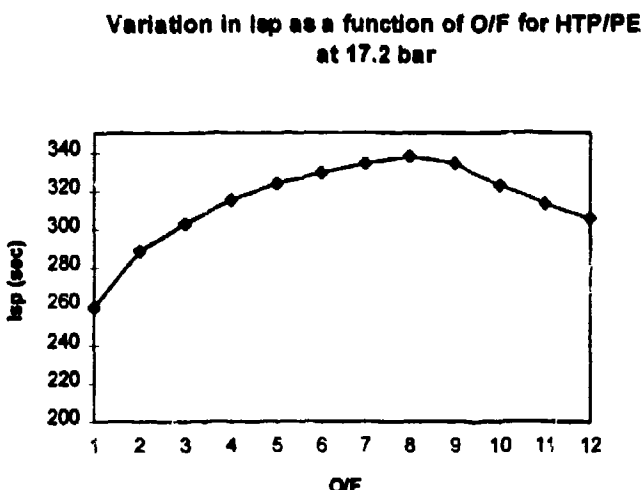


Figure 4-1: The graph shows the relationship between O/F and Isp (vacuum) for HTP/PE. Maximum Isp is achieved for an O/F of approximately 8. Data computed for constant $P_c = 17.2$ bar and 85% HTP (assumes near vacuum expansion to 10^{-4} bar).

As discussed in Chapter 3, the regression rate can be modelled as a direct function of oxidiser flux rate, G_{ox} ,

$$\dot{r} = a_{ox} G_{ox}^n \quad \text{Eqn. 4-1}$$

Note that G_{ox} , in combination with the port area, determines O/F. However, the regression rate constants, a_{ox} and n are independent of O/F. Therefore, as part of the experimental design, it was desirable to test a range of O/F greater than or equal to the optimum in order to have a sufficiently large spread of data to more accurately estimate a_{ox} and n . As an arbitrary starting point, an O/F = 10 was chosen.

4.5.4. Operating Pressure

In selecting an operating pressure for the prototype engine it was necessary to trade-off the basic relationship between chamber pressure, P_c , and Isp as shown in Figure 4-2. As you can see, higher P_c delivers slightly higher performance. However, this desire for high P_c must be traded off against the practical limitation of the system design. The higher the P_c , the more massive the combustion chamber and propellant tank must be. Typically, spacecraft propulsion systems operate in the 15 to 35 bar range. However, while Isp is a direct function of P_c , over this range the effect is not so dramatic. From Figure 4-2 you can see that doubling P_c from 17 to 34 bar only increases Isp by about 6%. Therefore, for the sake of simplicity and safety, a nominal P_c of around 17 bar (250 psi) was chosen.

Variation in Isp as a function of chamber pressure for HTP/PE at O/F = 8

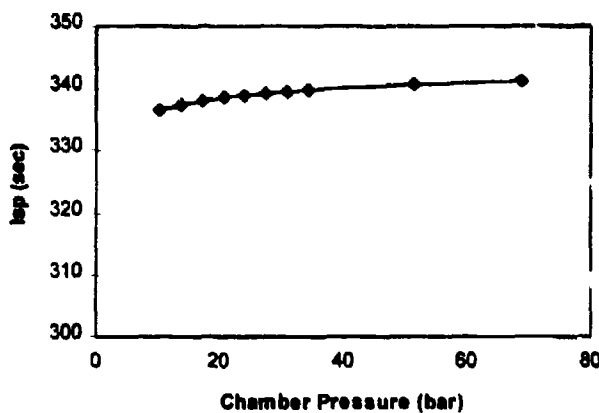


Figure 4-2: The graph shows the relationship between chamber pressure and Isp for HTP/PE at an O/F of 8 (assumes near vacuum expansion to $P_e = 10^{-4}$ bar (0.0015 psi)).

4.5.5. Port Design

The hybrid fuel port must be designed such that sufficient surface area is exposed to injected oxidiser to achieve the desired O/F at a reasonable regression rate. There are virtually an infinite number of ways to design the port geometry—rod & tube, wagon wheel, double-D, 7-cylinder cluster and the simplest, cylindrical. These geometries are illustrated in Figure 4-3. The multi-port options offer promise for more efficient packaging within the confines of a satellite. However, because characterising combustion was one of the primary objectives, the cylindrical port was chosen as the simplest and cheapest option.

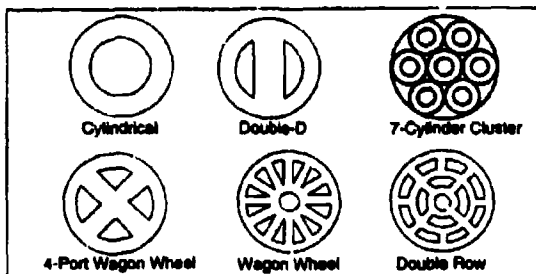


Figure 4-3: Port geometry options for a hybrid motor (from [Humble 95]).

With a port shape chosen, the next consideration was port size and length. Keeping in mind that the physical dimensions of the motor had to approximate what could reasonably be packaged inside a spacecraft, and further that this port would be drilled into a solid tube of polyethylene, an initial port diameter with a convenient, reasonable size of 2.5 cm (1 inch) was chosen.

An important parameter in hybrid design is the port length to diameter ratio (L/D). L/D must be selected to provide sufficient total surface area as well as volume to allow proper mixing of vaporised

fuel and oxidiser. L/D for most hybrids lies between 20 and 30, with smaller L/D normally used for smaller motors [Humble 95]. Unfortunately, it was not cost effective to have a different combustion chamber length for every different port diameter to be tested. Thus, to keep the motor relatively short, an initial L/D of 15 was chosen. This gave a constant port length of 36 cm and allowed for greater L/D values for smaller port tests (L/D varies as port diameter varies).

4.5.6. Oxidiser Flow Rate

Ideally, the oxidiser flow rate, \dot{m}_{ox} , would be selected to provide the desired O/F ratio. In practice, however, \dot{m}_{ox} , and port design are intimately related by the regression rate equation. G_{ox} is determined by \dot{m}_{ox} divided by the port cross-sectional area.

$$G_{ox} = \frac{\dot{m}_{ox}}{A_{port}} \quad \text{Eqn. 4-2}$$

where A_{port} = port cross-sectional area (m^2)

Thus, once the port diameter is fixed a given \dot{m}_{ox} will give the desired O/F, but only if a specific regression rate is achieved. Unfortunately, as will be discussed in the following section, there was no completely reliable regression rate equation available. Therefore, I had to use an iterative approach for my hybrid motor design process that relied heavily on estimated performance as described in the next section.

4.6. Performance Estimation

Performance estimation for system came from two primary sources

- Theoretical results based on combustion thermochemistry
- Empirical results based on previous work

Because of the scarcity of empirical results, design analysis relied chiefly on theoretical predictions, using those previous empirical results available as a guideline only.

4.6.1. Theoretical Results

Theoretical results for rocket performance must be obtained using standard thermochemistry analysis methods. All of my results are based on the *Isp* program developed by the USAF [Selby 92]. The assumptions on which this program are based are sufficient to produce results within 1% - 5%.

Theoretical results for HTP decomposition where presented earlier. Theoretical results for hybrid combustion based on the thermochemistry analysis is shown in Table 4-5. These results are based on the earlier assumptions for HTP decomposition at an O/F of 10 (8.5 H₂O₂:1.5 H₂O:1.0 PE).

Combustion Parameter	Value
Characteristic exhaust velocity, C^* (m/sec)	1522
Temperature (K)	2505.5
Molecular Weight (kg/kmol)	22.05
Moles gas/100 gm	4.535
Ratio of specific heat, γ	1.183
Heat capacity (cal)	58.386
Entropy (cal)	286.38
Enthalpy (cal)	-157.769
Density (gm/cc)	0.001824

Table 4-5: Theoretical performance of 85% HTP/Polyethylene hybrid motor with O/F = 10 at 17.2 bar based on the USAF *Isp* program.

In practice, the primary indication of combustion efficiency is theoretical vs. measured C^* . Chapter 5 will compare these theoretical results to experimental data.

4.6.2. Previous Empirical Results

This section focuses on empirical results for hybrid combustion only. Empirical results for HTP decomposition will be discussed in Chapter 5 in the context of catalyst pack development.

While theoretical results for hybrid combustion can tell you expected C^* and other combustion parameters, they do not give you the all-important regression rate parameters needed to reliably design a hybrid motor. These parameters can only come from empirical results. Therefore, regression rate data is often treated as closely guarded, proprietary information. There have been only three published reports of other HTP hybrid work. These are summarised in the following subsections.

4.6.2.1. Moore/Berman (1956)

The definitive paper which pre-dates the work described in this thesis was published by George Moore and Kurt Berman in the November 1956 issue of *Jet Propulsion* [Moore 56]. Their paper describes work conducted several years earlier at the General Electric Company as part of an Army Ordnance contract. Moore and Berman used the same HTP/PE combination used in my work (although they used 90% HTP instead of 85%). At the outset, they list several desirable characteristics of this particular hybrid combination:

1. Good theoretical specific impulse, *Isp*
2. High average propellant density
3. Spontaneous ignition, usually after < 0.5 seconds. In this way the fuel combustion can be thought of augmenting the HTP mono-propellant performance. "Ignition is generally reliable and smooth over a wide range of oxidiser/fuel ratios."
4. With proper design of the engine and fuel charge "hard" starts should never occur; the peroxide decomposition product is a gaseous oxidiser and therefore cannot accumulate in the combustion chamber prior to ignition.
5. Intermittent operation and throttling can be accomplished by means of a single valve in the peroxide line.
6. The system has the simplicity of a mono-propellant, but with a safety, at a given performance, probably unattainable with most liquid mono-propellants.

7. The design and construction of the fuel charge is not very critical in regard to the presence of cracks or voids; there is very little possibility of an explosion of the entire propellant, and in these respects the system is more desirable than most solid propellants.

At the same time, they noted only a few disadvantages:

1. Relatively high freezing point and potential instability of HTP
2. Difficult to vary the fuel burning rate by more than a factor of two which can complicate the fuel charge design for some applications.

Moore & Berman go on to note many of the inherent advantages of the HTP/PE combination already explained above and of hybrids in general as explained in Chapter 3. They also point out the potential advantages of operating at higher than the optimum stoichiometric ratio ($O/F > 8$) which gives higher overall propellant density (meaning an even smaller fuel chamber) with only a slight loss in overall efficiency.

Another interesting observation that Moore and Berman noted was the longitudinal uniformity of fuel burning. They write, "there appears to be no tendency for the fuel to burn faster at one end than the other." This is consistent with own results as will be explained in Chapter 5. They go on to comment, "the combustion itself shows remarkable stability under all conditions, including very low chamber pressures and low pressure drops. It appears, in fact, that the burning solid fuel is its own flame holder and a very stable one."

The remainder of their paper outlines the results from over 300 tests (the benefits of a large-budget, government-funded operation). They used three basic chamber designs—straight tube, rod & tube and straight tubes with alternating inside diameters to generate eddy currents for better mixing. They used both extruded tube as well as stacks of 1/2" plastic wafers (the fact that the gaps between the wafers had no effect on burning underscores how insensitive hybrids are to cracks or voids in the fuel grain). [Moore 56] presents a log-log plot of their results, correlating regression rate (inches/second) to a number "which is roughly proportional to the initial mass velocity of the gas in the fuel channel."

This correlation factor is given as (in units of slug/ ft^2).

$$\left(\frac{P_c}{V^*} \right) \left(\frac{A_t}{A_{port}} \right) \quad \text{Eqn. 4-3}$$

where

P_c = Chamber pressure (psi)

V^* = (C^* it turns out) = Characteristic exhaust velocity (ft/s)

A_t = Throat area (in^2)

A_{port} = Port area (in^2)

Note that Moore/Berman use the parameter, V^* . This appears to have been a typographical error in the paper. After much trial and error, I was able to prove that $V^* = C^*$. Therefore, because

$$\dot{m} = \frac{P_c A_t}{C^*}$$

Eqn. 4-4

their correlation factor, is actually the total mass flux, G , which is in keeping with conventional hybrid analysis.

$$G = \frac{\dot{m}}{A_{pert}}$$

Eqn. 4-5

where G = Total mass flux (slug/ft²)

Unfortunately, aside from the general praises they offer about this combination, very little hard data is presented. No specific data for individual test runs was reported (run-to-run combustion efficiencies for example). The sum total of results from over 300 tests is a single graph. The only discussion of regression rate is the single statement that "the slope of the line indicates that $r \sim (G)^{0.45}$." The other regression rate constant is not offered. Therefore, the regression rate equation obtained from their data had to be interpolated from this graph.

The equation interpolated from their graph is shown below:

$$r(mm/sec) = 0.0465G^{0.454}$$

Eqn. 4-6

where G has units of kg/m²sec

However, it should be stressed that this is approximate at best. The best use I could make of their data was as a rough order of magnitude check for my own engine design calculations. Sadly, their results, while presumably valid based on the vast number of tests conducted, was insufficiently reported to allow the technology to be readily used (especially after a 40 year hiatus). Thus, to revive this combination, the technology would literally have to be re-invented.

4.6.2.2. Pugibet (1970)

Across the Atlantic, nearly 15 years after Moore & Berman, the HTP/PE hybrid once again gained some attention as documented by M. Pugibet and H. Moutet in May 1970 [Pugibet 70]. They investigated using HTP as a oxidiser with a variety of polymers. However, rather than using a separate decomposition chamber to first break-down the HTP, they investigated coating the inside of the fuel with a catalytic material. After experimenting with several possible combinations, they chose a suspension of 30% potassium borohydride in 70% paratoluidine solvent spread at a concentration of 0.05 gm/cm² over the inside of the fuel grain. The fuel they chose was 96% metalacene diamine with 4% binder (nylon made plastic with cyclohexylphthalate). They tested this combination in their micro-thruster for detailed study of ignition characteristics.

While their work is interesting from an historical perspective, it actually represents a sideline to my own research. Obviously, their technique offers a simplified ignition process without the additional

complexity of the decomposition chamber. This could be useful for large booster applications. However, because it does not offer the opportunity for a re-start, it has less appeal for spacecraft applications.

4.6.2.3. Wernimont (1994-1995)

Concurrent with my own research, E. Wernimont at Purdue University in the U.S. was also reviving U.S. HTP/PE hybrid work. His research objectives and results are summarised in two papers [Wernimont 94] and [Wernimont 95]. The Purdue research, like my own, is aimed at producing a low-cost, highly reliable rocket motor. However, theirs is aimed specifically at booster applications. The goals of their research were listed as follows in [Wernimont 94]:

1. Use hydrogen peroxide with concentrations levels typically used in industry.
2. Do not use silver screen catalytic beds because this decomposition device has several undesirable characteristics such as: increased system dry mass, increased cost of catalytic bed construction, and catalyst screen poisoning or degradation.
3. Do not use liquid injection of catalyst. A second fluid system taints the simplicity of the hybrid propulsion system.
4. If possible, use highly stabilised peroxide (defined in [Wernimont 95] as having stannates and phosphates at 10 - 100 ppm).

While I agree in principle with all these goals, the paper does not make clear (with reference to goal 2.) how any other type of catalyst system (such as the one they use) is inherently simpler or lighter in weight than a silver screen catalyst. The catalyst used is described in [Wernimont 94] as pellets of refractory cement impregnated with potassium permanganate ($KMnO_4$). A diagram of this catalyst pack is shown in Figure 4-4.

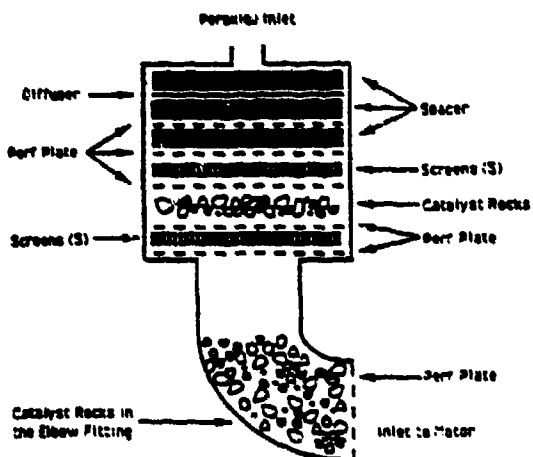


Figure 4-4: Diagram of catalyst pack configuration used by Wernimont and Meyer. Catalyst rocks were made from pellets of refractory cement impregnated with potassium permanganate ($KMnO_4$). [Wernimont 94].

[Wernimont 94] describes results from 6 different hybrid firings all at $P_c \sim 120$ psi (8.25 bar) with O/F from 3.2 to 4.6 and reports combustion efficiencies ranging from 87% to 98.3%. The paper also

presents a regression rate equation based on 6 data points as follows (note the equation was left in the original imperial units to preserve imbedded units on the constants).

$$\dot{r}(\text{in/sec}) = 0.0535G^{0.8}$$

Eqn. 4-7

where G = Total mass flux ($\text{lbf/in}^2/\text{s}$)

[Wernimont 95] reports somewhat different results from a more recent series of about 20 tests. For these tests, efficiencies are reported somewhat lower, ranging from 77% to 89%. Problems with nozzle erosion are also reported. The regression rate equation for the more recent tests is somewhat different from the first series:

$$\dot{r}(\text{in/sec}) = 0.034G^{0.88}$$

Eqn. 4-8

The results from both these tests are plotted in Figure 4-5. These results will be compared to those of Moore/Berman and my own results in Chapter 5.

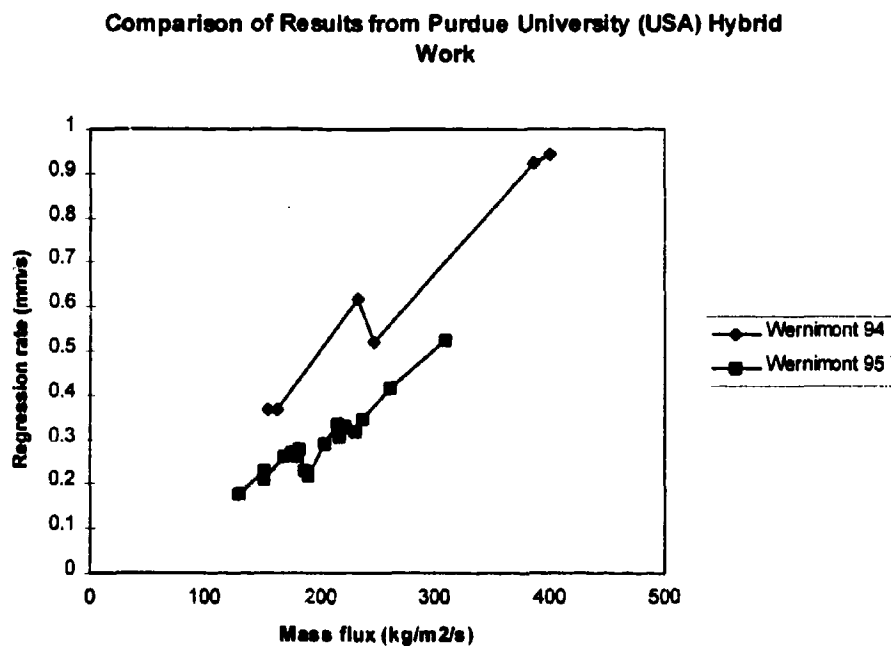


Figure 4-5: Results from Purdue University, USA, HTP/PE hybrid tests [Wernimont 94] [Wernimont 95].

4.6.2.4. Conclusions

Realise that at the outset of my design work only Moore & Berman's results were available. Therefore, performance estimation primarily relied on theoretical thermochemistry results from the *Isp* computer program with approximate results from [Moore 56] used as a guideline to bound design results.

4.7. Component Design

This section will discuss specific design issues associated with important components of the experimental hybrid system. Fuel grain design will first be addressed followed by a discussion of nozzle design and material issues, the combustion chamber, oxidiser delivery system and the overall support structure.

4.7.1. Fuel Grain

From a practical standpoint, once the basic system was designed and fabricated, there were only limited degrees of freedom in terms of the final fuel grain design. This was especially true after the cavitating venturi was added (see Sections 4.7.4 and 4.8.4.5). The most important parameters which were fixed by the basic system design were the nozzle throat area, A_t and the motor length, L . Table 4-6 gives a list of fixed design values for the system.

Parameter	Value
Port length (m)	0.36
Ambient Pressure (bar)	1.0
Nozzle throat radius (m)	0.0065
Nozzle expansion ratio	3.408
Cavitating Venturi flow number (kg cm ^{3/2} sec ⁻¹ bars ^{1/2} gm ^{-1/2})	0.02189
Cavitating Venturi pressure recovery factor	72.5%
Injector pressure recovery	80%
Polyethylene fuel density (kg/m ³)	930
HTP (85%) oxidiser density (kg/m ³)	1370

Table 4-6: Fixed motor design parameters.

This left the following variables for further design iteration:

- Feed Pressure, P_{tank} (over a practically limited range 0 to 50 bar) which determines:
 - Oxidiser flow rate, \dot{m}_{ox} (over a limited range with the cavitating venturi in place).
 - Chamber pressure, P_C (up to a practical limited of about 20 bar).
- Port radius, R_p (practically limited by standard-sized drills, non-standard sizes available at greater expense) which determines:
 - Oxidiser/Fuel ratio, O/F

The iterative motor design process that emerged used the following steps.

- Step 1: Select initial port radius, r_{port}
- Step 2: Pick a tank feed pressure which is used to approximate actual \dot{m}_{ox}

$$\dot{m}_{ox} = FN \sqrt{(P_{Tank} - P_{atmosphere}) \rho_{ox}}$$

Eqn. 4-9

where

FN = Cavitating Venturi Flow Number

P_{Tank} = Oxidiser tank pressure (bar)

$P_{atmosphere}$ = Atmospheric pressure = 1 bar

ρ_{ox} = Oxidiser density

- Step 3: Determine maximum possible chamber pressure

$$P_c = P_{\text{Tank}} CV_{PR} I_{PR}$$

Eqn. 4-10

where

 P_c = chamber pressure CV_{PR} = Cavitating venturi pressure recovery = 72.5% I_{PR} = Injector pressure recovery = 80%

- Step 4: Assume value for initial O/F
- Step 5: Compute thermochemistry parameters using *Isp* program
- Step 6: Compute theoretical mass flow rate for given O/F at 100% C^* using Eqn. 4-4
- Step 7: Compute required average fuel regression rate

$$\dot{m}_{ox} = \frac{O/F}{(O/F + 1)} \dot{m}$$

Eqn. 4-11

$$\dot{m}_{fuel} = \frac{1}{(O/F + 1)} \dot{m}$$

Eqn. 4-12

$$\dot{v}_{fuel} = \frac{\dot{m}_{fuel}}{\rho_{fuel}}$$

Eqn. 4-13

$$Vol_{fuel} = \dot{v}_{fuel} \cdot time$$

Eqn. 4-14

$$\Delta r = \frac{\sqrt{\frac{Vol_{fuel}}{\pi L} + r_{port}^2} - r_{port}}{time}$$

Eqn. 4-15

where

 \dot{v}_{fuel} = Volume flow rate of fuel ρ_{fuel} = Fuel density Vol_{fuel} = Total volume of fuel consumed

time = Total burn time

 Δr = Required average fuel regression rate L = Port length

- Step 8: Compare required regression rate to Moore/Berman results [Moore 56] for "sanity check." Iterate as required.
- Step 9: Compute all performance parameters using basic rocket relationships from Chapter 3.

To simplify the tedious nature of iterative calculations, this design process was implemented using MathCAD. Table 4-7 gives the parameters for an example motor design and predicted performance

parameters which result. Notice that the required regression rate is approximately 8% less than that predicted by Moore/Berman. This is about as close as one can practically interpolate from their data.

Parameter	Value
Feed Pressure, P_{tank} (bar)	30
Oxidiser flow rate (kg/sec)	0.143
Chamber Pressure (bar)	17.4
O/F	9:1
Motor Port Radius (m)	0.01
Ratio of specific heat, γ	1.181
Chamber Temperature (K)	2581
Molecular weight (kg/kmole)	21.94
Theoretical Characteristic Exhaust Velocity, C^* (m/sec)	1534
Burn time (sec)	15
Total mass flow rate (kg/sec)	0.151
Average Fuel Regression Rate (m/sec)	5.16×10^{-4}
Predicted fuel regression rate (Moore/Berman) (m/sec)	5.588×10^{-4}
Thrust (N)	314
Total Oxidiser used (litre)	1.484
Total Fuel used (kg)	0.226

Table 4-7: Hybrid Motor Design Characteristics

With the basic motor geometry established, the next step was to design the remaining components of the motor and oxidiser delivery system.

4.7.2. Nozzle

The nozzle represented one of the most challenging aspects of the entire system design. It had to perform its function of expanding the exhaust from chamber pressure to ambient conditions under the following harsh conditions:

- Throat temperatures > 2340 K
- Multiple thermal cycling without fracturing
- > 18 bar chamber pressure
- Relatively high concentrations of super-heated oxygen and steam

On top of these performance requirements were laid the basic constraints of the programme. The nozzle had to be:

- Inexpensive (or if relatively expensive, reusable)
- Easy to manufacture
- Easy to integrate into the system

Arguably, I could have opted for a simple, disposable choke—perhaps made from stainless steel or copper. After all, if you are only interested in combustion characteristics there is no need for an expanding nozzle. However, because the system was meant as a prototype for a spacecraft motor, I chose to include all the necessary components. This would provide valuable insight into what type nozzle to eventually pursue for space applications.

4.7.2.1. Nozzle Shape

The most fundamental decision in nozzle design is the shape. [Humble 95] and [Sutton 92] give details on several types of nozzle shapes. Figure 4-6 gives four basic shapes and there are literally hundreds of possible variations on these themes.

	Cone	Contracted or Bell-Shaped	Plug	Expansion-Diffusion
Shape				
Flow with deflection angle at altitude				
Flow with decompression (Sea level)				
Mass flow distribution at exit				

Figure 4-6: Four different nozzle configurations and their flow effects (from [Sutton 92]).

Initially, considerable time was spent looking at the plug-type nozzle. It has several inherent advantages, especially for space applications, which made it an interesting candidate [Berman 60]. However, in the end, a simple cone was chosen due to its ease of manufacture.

The nozzle shape was designed to give optimum expansion to 1 bar (14.5 psi) for a chamber pressure of 18 bar.

- Exit radius = 0.012 m
- Throat radius = 0.0065 m
- Expansion ratio = 3.41
- Cone angle = 15°
- Length = 0.021 m

4.7.2.2. Nozzle Material & Cooling

Design of the nozzle shape was relatively easy, given that it depends only on straightforward calculations of supersonic flow. In comparison, selection of the nozzle material was much more difficult given that it had to withstand temperatures up to 2100° C. Therefore, material selection ultimately depended on the type of cooling mechanism to be used. There are four basic cooling options to choose from:

1. Ablative
2. Radiative
3. Regenerative
4. Heat Sink

With *ablative* cooling, the phase change process of subliming a solid into a gas absorbs large quantities of heat. However, this would mean the nozzle would gradually wear away with use, changing the exit area and distorting C^* calculations. ([Wernimont 95] noted this problem with the ablative nozzle he used).

Radiative cooling was also an attractive option. This involves radiating heat into the surroundings. Unfortunately radiative heat transfer is very slow and requires large surface area. This type of cooling is appropriate for longer vacuum nozzles but not for short nozzles expanding to the atmosphere.

Regenerative cooling would involve circulating the liquid HTP (or other liquid) around the nozzle to cool it in much the same way as a car engine is cooled. However, this creates additional complexity for the plumbing involved. Furthermore, precise circulation tubes must be built into the nozzle, greatly increasing its complexity (and cost). The simplest means of regenerative cooling I considered was using water from a separate source to cool the nozzle. This was the technique employed by Moore/Berman [Moore 56]. Unfortunately, regenerative cooling would add significant complexity. Furthermore, because the objective was to match as closely as possible the configuration that would be most desirable for satellite applications a simpler, passive solution was chosen using a heat sink in combination with convective and radiative cooling.

By providing a sufficient mass of high heat capacity material, such as stainless steel, the heat generated during a short test firing could be harmlessly absorbed into this *heat sink* and then dissipated after the test through convective cooling from the ambient air and radiation. However, even with a heat sink, some means of slowing the heat transfer rate, especially at the throat, had to be found or even stainless steel could begin to melt before sufficient heat had been conducted away. Thus, a refractory material with very slow heat transfer was desired. Discussions with Advanced Furnace Technologies in Cambridge led to the selection a solid graphite throat insert coated in pyrolytic graphite.

4.7.3. Combustion Chamber

The combustion chamber design was a logical outgrowth of the motor design. A cylindrical pressure vessel was needed that could contain the fuel rod and withstand the necessary pressure and temperature. For ease of machining and convenience, the entire system was planned to be made from stainless steel. However, even stainless steel would melt when faced with +2000° C combustion temperature. Here, one of the inherent design advantages of hybrids saw direct benefit. Because the fuel itself could act as insulation for the chamber walls, the fuel rod diameter could be oversized without having to resort to more complex active cooling techniques.

4.7.4. Oxidiser Delivery System

With the exception of the cavitating venturi, the design of the oxidiser delivery system was a straightforward fluid mechanics problem. The success of the final system lay-out was due primarily to the help of Mr. Malcolm Paul formally of Royal Ordnance, a renown expert in test rig design, construction and operation. One of the biggest problems encountered was in finding HTP-compatible components. Virtually all solenoid valves on the market contain at least some 400-series stainless steel (slightly magnetic, used in the plunger) which is not completely compatible with HTP. Therefore, pneumatically-actuated ball valves were selected which were 100% compatible. The complete system is summarised in Section 4.8.

The cavitating venturi (CV) was added to the oxidiser delivery system part way through the test program as described in Chapter 5. The CV serves two purposes:

1. Restricts maximum flow rate to eliminate wet-starts of the catalyst pack
2. Provides a calibrated means of measuring HTP flow rate

Without a CV in the system, oxidiser flow rate is a function of the square root of the pressure difference between the tank and catalyst pack. This means that at start up, when the chamber pressure is 1 bar (absolute), the flow rate is highest and then decreases to a steady-state value as chamber pressure increases due to the catalytic reaction. As described in Chapter 5, this situation proved to be undesirable for cold start conditions as it caused the catalyst pack to initially be flooded, leading to a "wet start" condition whereby liquid HTP was ejected until the reaction could reach a steady-state condition. The CV virtually eliminated this problem by creating the condition whereby flow rate is a function of upstream pressure only, independent of downstream pressure.

CV's are a common feature in many experimental rocket test rigs. A basic CV consists of a narrow orifice in the oxidiser flow line with a relatively sharp converging section (15° half-angle) and gentle diverging section (6° half-angle). Their use for this application was first advocated as early as 1951 by L.N. Randall in the *American Rocket Society Journal*. He explains their basic operating principle as follows:

"As the pressure drop across a conventional venturi is increased, a point is reached at the throat where substantially all of the upstream head is converted into velocity head. The only static head remaining is that of the fluid vapour pressure. If, under these conditions the upstream head is maintained constant, a further increase of the pressure drop obtained by decreasing the downstream pressure cannot result in increased flow." [Randall 51]

In other words, once upstream pressure is sufficiently high, the flow through the CV will cavitate. At this point, the maximum flow rate is fixed, independent of the pressure difference across the CV.

4.7.5. Support Structure

The support structure was designed with the help of Mr. Maarten Meerman and Mr. David Montgomery of SSTL. This design effort was driven by low-cost fabrication considerations and ease

of experimentation. We wanted an adaptable system that would allow reconfiguration if needed while including a minimum number of total parts allowing for ease of manufacture.



Figure 4-7: Photograph showing all parts of the hybrid test apparatus, the motor, test stand, oxidiser delivery system and data collection/control system.

4.8. System Description

This section offers a summary of the hybrid test infrastructure. The complete test apparatus is shown in Figure 4-7. It consists of four parts: hybrid motor, test stand, oxidiser delivery system and data collection/control system. This section begins with a brief description of the test site itself, followed by a summary of each part of the test apparatus.

4.8.1. Test Site

As discussed above, the overriding system design requirement was safety. Initially, we briefly considered conducting all testing at the University of Surrey. However, lack of facilities within CSUR to safely support rocket testing ruled out this option. Fortunately, Mr. John Harlow of British Aerospace, Royal Ordnance (RO), Westcott had suggested to Prof. Sweeting at a chance meeting that they may be interested in co-operating in various types of research. Seizing on this opportunity, I presented a complete test plan to Mr. Harlow and Dr. Bonner, the RO safety officer. They graciously offered the use of test cell J-4 which had been unoccupied for several years. Figure 4-8 shows a picture of J-4 site. It consists of a firing bay, separated from the control room by a thick concrete wall. Blast-proof windows allow viewing of the firing bay. The site also offered plenty of running

water (necessary for safe handling of HTP), power and pressurised nitrogen to drive and control the oxidiser delivery system. A memorandum of agreement was formalised between SSTL and RO outlining the co-operative nature of this basic research.



Figure 4-8: Test site J-4 at British Aerospace, Royal Ordnance, Westcott.

4.8.2. Motor

Figure 4-9 shows a cut-away diagram of the hybrid motor attached to the test stand. The motor consists of four basic components: the catalyst pack, combustion chamber, fuel element, and nozzle. Each of these is described in the following sections.

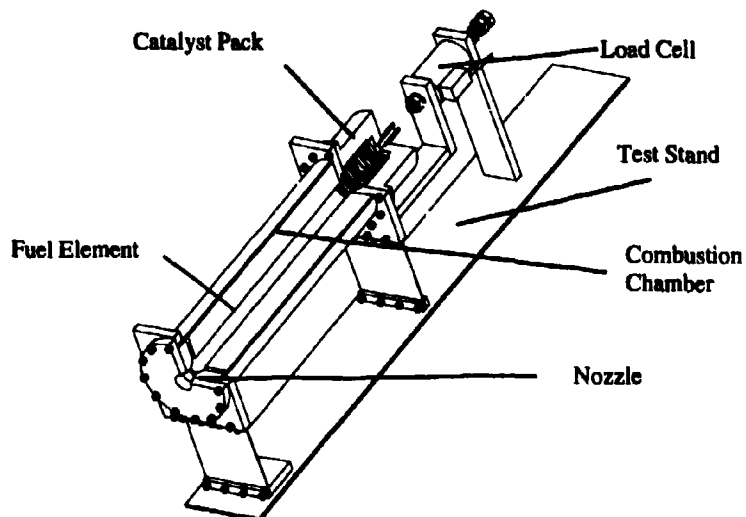


Figure 4-9: Hybrid motor cross-section attached to the test stand showing load cell, catalyst pack, combustion chamber, fuel element and nozzle.

4.8.2.1. Catalyst Pack

The catalyst pack is designed to fully decompose HTP into superheated steam and oxygen. It consists of four parts: the housing, injector plate, sleeve, and spacers. The stainless steel housing provides structural support, heat sink mass and interface to the hybrid motor and test stand. A close-up diagram of the catalyst pack is shown in Figure 4-10. The injector plate acts as a "shower head" for the HTP entering the pack. This thin plate has 1.8 mm holes covering 25% of the surface. Upon passing through the injector plate the oxidiser experiences approximately a 20% decrease in pressure.

The sleeve is a thin-walled, stainless steel cylinder into which the catalyst material is packed. The catalyst materials used are fully described in Chapter 5. They consisted mostly of nickel or silver mesh disks which were stacked and compressed into the sleeve with the spacers at the top and bottom.

The catalyst pack is mounted to the motor via a flange. A large opening in the top of the combustion chamber allows decomposition products to flow into the centre of the fuel element.

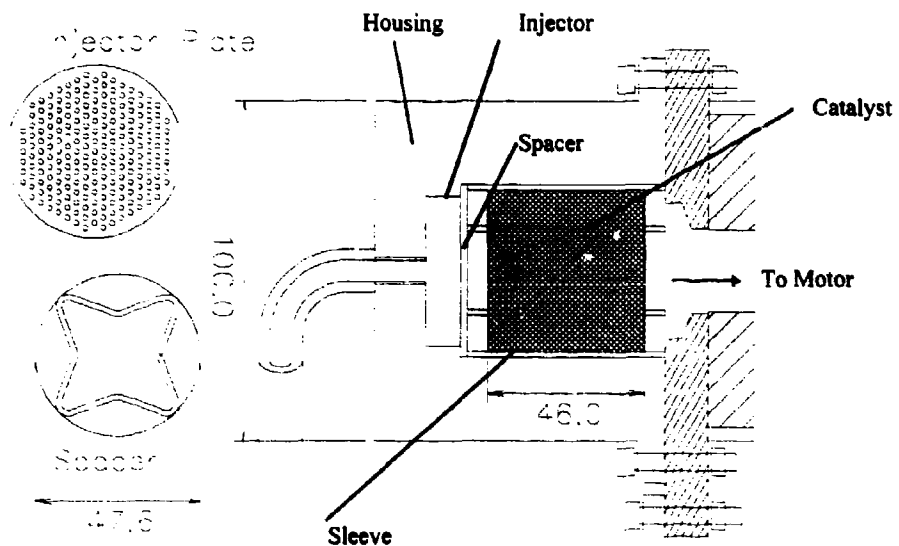


Figure 4-10: Diagram of the catalyst pack showing the housing, injector plate and the "star-shaped" spacers. The sleeve containing the catalyst itself is inserted into the pack. Dimensions are in mm.

4.8.2.2. Combustion Chamber

The combustion chamber is constructed of 316 stainless steel seamless tube with a 4 inch (0.1016 m) outer diameter. The casing is 10G (3.175 mm) in thickness. Nominal operating pressure is 18 bar. At twice this pressure, the hoop stress safety factor is 3.7. Flanges were welded to the chamber for attachment to the test stand.

4.8.2.3. Fuel Element

The fuel elements used were made from polythene rods with a combustion port drilled into them and machined to fit into the combustion chamber. The nominal rod length was 0.36 m. The motor was purposely oversized in diameter to provide insulation for the combustion chamber. For a 10 second

test firing, only about 0.013 m of fuel is consumed. Figure 4-11 shows a photograph of a fuel rod standing next to the combustion chamber.

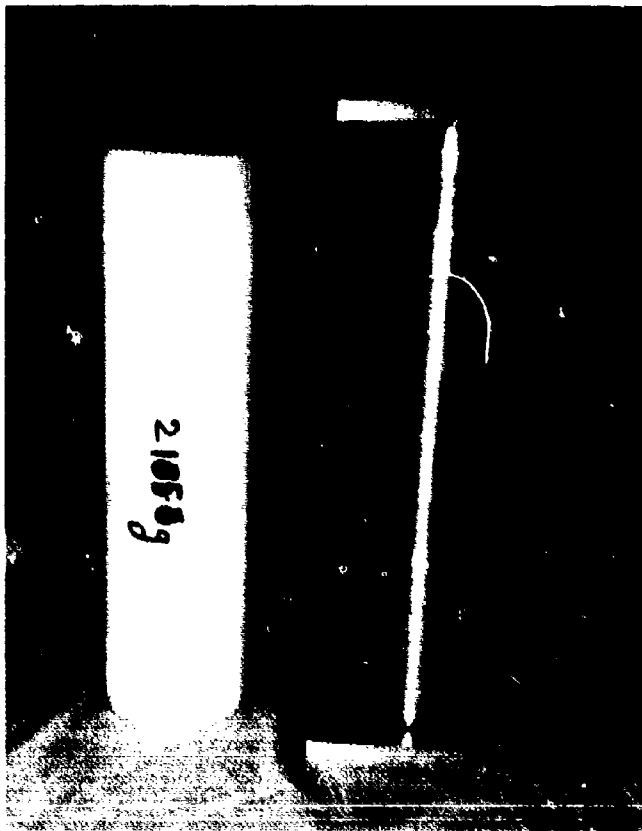


Figure 4-11: Photograph of a hybrid fuel rod standing next to the combustion chamber.

4.8.2.4. Nozzle

The nozzle assembly consists of a throat insert and outer cone/assembly flange. The throat insert is formed from machined bulk graphite coated in pyrolytic graphite. It is fitted into the combustion chamber, separated from the fuel by rubber gaskets to provide for fuel rod expansion during firing. A stainless steel flange secures the pyrolytic graphite/graphite throat insert and forms the last half of the nozzle expansion cone. A diagram of the nozzle is shown in Figure 4-12.

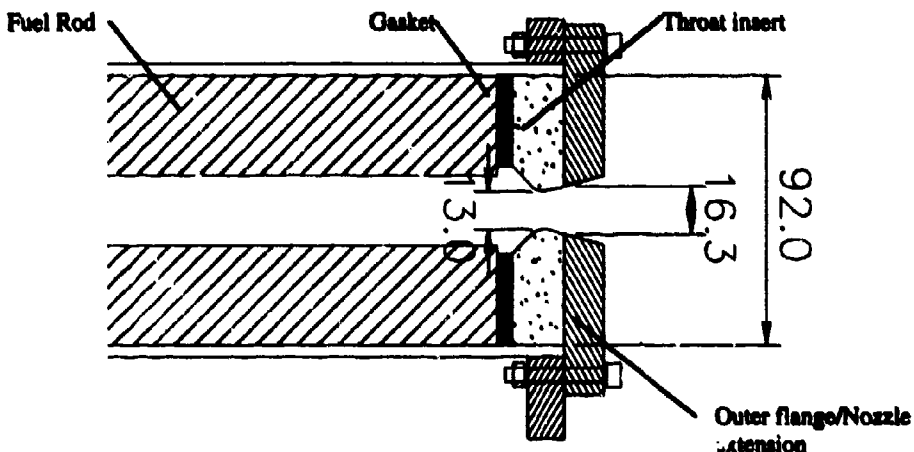


Figure 4-12: Cross-sectional view of the nozzle showing the graphite/pyrolytic graphite insert and the nozzle extension section which acts as a heat sink. Dimensions are in mm.

4.8.3. Test Stand

The complete test stand consists of a mounting bracket, motor support brackets and HTP delivery system "plumbing" shelf. A photograph of the complete test stand installed in J-4 site is shown in Figure 4-13.

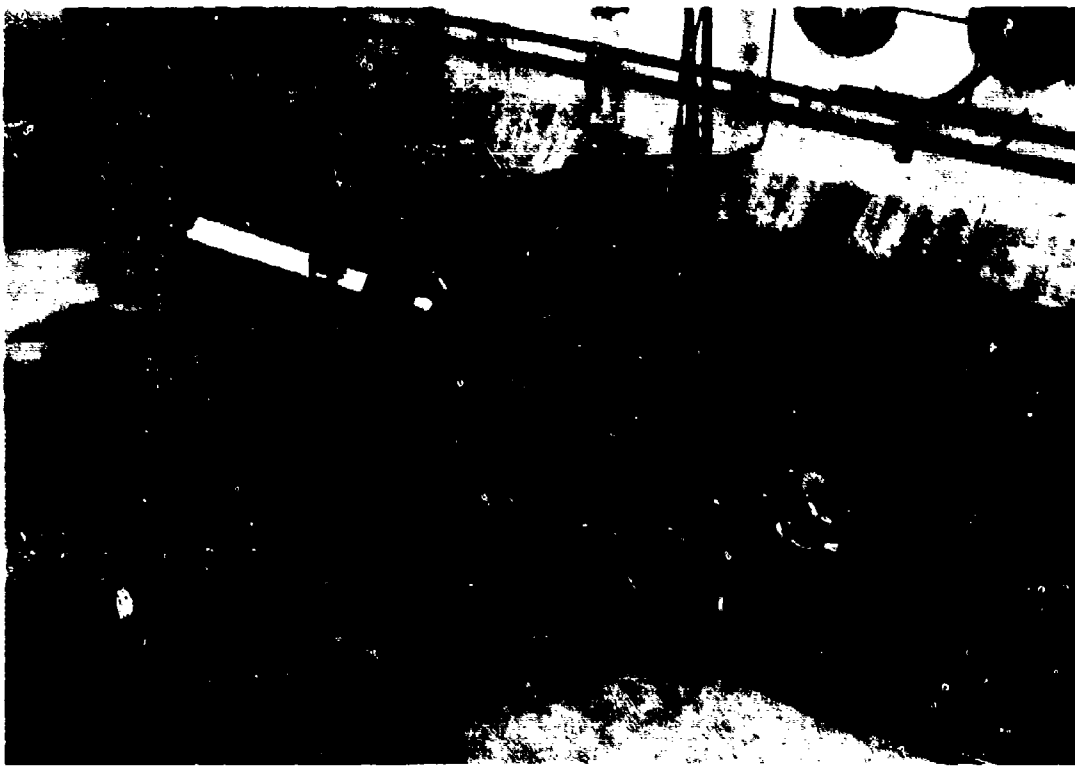


Figure 4-13: Test stand installed into test cell J-4 at Royal Ordnance, Westcott.

The I-shaped mounting bracket is bolted directly to the floor of the test cell into grooved rails built-in for that purpose. The mounting bracket acts as a spine to which the motor support brackets and plumbing shelf is attached. The motor is supported and attached to the support plate using two spring-

steel flexures. The attachment point at the rear of the motor can be moved along the test stand, allowing the motor length to be varied if necessary. The oxidiser delivery system uses high pressure nitrogen gas to deliver HTP to the catalyst bed and to allow for system purging and dumping following tests. This "plumbing," consisting of the oxidiser tank, valves and lines, is attached to a separate plumbing shelf which is bolted to the end of the test stand. It is described in the next subsection.

4.8.4. Oxidiser Delivery System ("Plumbing")

A schematic of the oxidiser delivery system is shown in Figure 4-14. Major components are described in the following subsections.

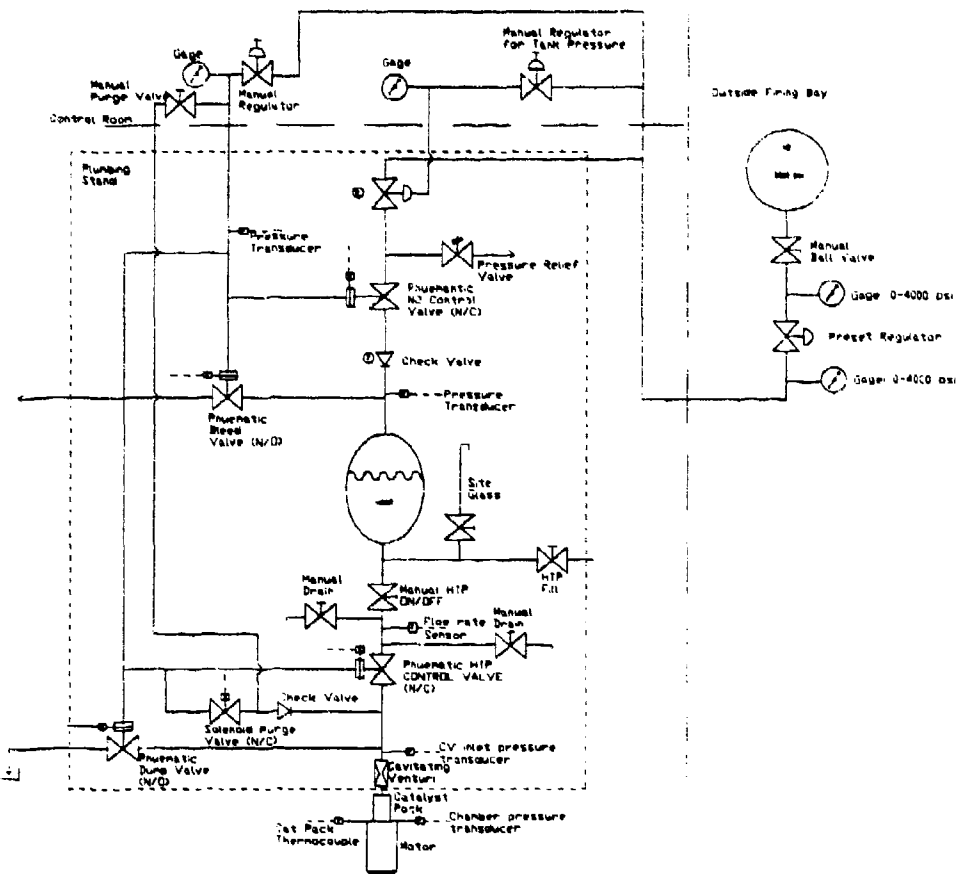


Figure 4-14: Oxidiser Delivery System

4.8.4.1. Oxidiser Tank

The oxidiser tank was constructed as a pressure vessel from 316 stainless steel and tested to 2000 psi (over 6 times the predicted operating pressure). It has a volume of approximately 5 litres and is roughly 15 cm in diameter and 33 cm long. Prior to use with HTP, the tank was "pacified" by filling with 45% nitric acid for 1 hr. After this period it was filled with 50% hydrogen peroxide for an

additional 1 hour. The tank was then repeatedly flushed with distilled water. The tank was only used with distilled water and HTP after the pacification process.

4.8.4.2. Lines and Fittings

Standard stainless steel lines were used throughout the system. These lines are pressure rated to 350 bar (5000 psi). No dedicated pacification process was used with the lines. The majority of fittings were 1/4" Swagelok.

4.8.4.3. Nitrogen Supply

N₂ is supplied by a set of 200 bar (3000 psi) bottles outside the J-4 site provided by RO.

4.8.4.4. Components

As you can see from Figure 4-14, a wide variety of different valves and other components were needed to complete the plumbing system. The primary driver for component selection downstream of the oxidiser tank was HTP compatibility. Upstream of the tank, and in separate N₂ supply lines for pneumatic valves, compatibility was not an issue.

System pressure is regulated from 200 bar inlet over a controllable range 0 - 60 bar using one Hale-Hamilton dome regulator donated by RO. The regulator is protected from HTP damage by a non-return valve downstream. The output pressure of the regulator is determined by the pressure applied to the top of the dome via a needle valve from inside the control.

Whitey Series 40 ball valves (SS-43S4-31C) with pneumatic actuators (A-SVMF4-C24D) were used for HTP compatible applications. These include the engine control valve and the dump valve. These valves require solenoid actuation as well as a minimum of 5 bar pressure in order to actuate. The choice of this particular design was based on recommendations from Mr. Malcolm Paul. Unlike similar ball valves available, this design precludes liquid from being trapped in voids around the ball itself, a potentially dangerous problem with active oxidisers.

There are two Hale-Hamilton NRS-1 non-return valves in the system. These valves are HTP-compatible. They are designed to prevent HTP from migrating up stream to the N₂ control valves in the pressure line and in the purge line. One pressure relief valve set at 48 bar was used for emergency release of pressure in the event of inadvertent HTP decomposition.

4.8.4.5. Cavitating Venturi

The design principles for the cavitating venturi (CV) were described earlier. Figure 4-15 shows a diagram of the CV used on the test rig. For cost reasons, three CV's were made to the same specification. These were calibrated in the RO flow lab by Mr. Henry Eggleston. Table 4-8 lists the relevant parameters for the CV used in testing. As described earlier, the CV served the dual purpose of limiting the flow rate to eliminate wet start conditions and acting as a means of measuring oxidiser flow rate.

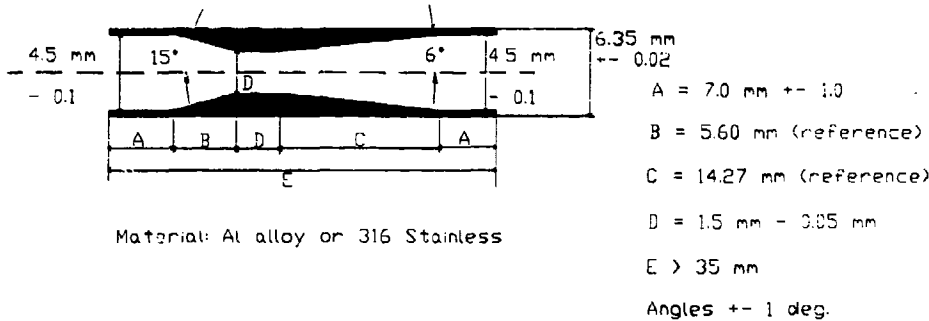


Figure 4-15: Cavitating venturi (CV) diagram. With the CV installed in the system the maximum flow rate was restricted thus virtually eliminating wet starts. The known calibration of the CV was also used to accurately determine oxidiser flow rate.

Parameter	Value
Length (mm)	35
Outer diameter (mm)	6.35 (+ 0.02)
Inner diameter (mm)	4.5 (- 0.1)
Throat radius (m)	1.5 (-0.05 on diameter)
Converging cone angle	15° (+ 1°)
Diverging cone angle	6° (+ 1°)
Cavitating Venturi flow number (kg cm ^{3/2} sec ⁻¹ bars ^{-1/2} gm ^{-1/2})	0.02189
Cavitating Venturi pressure recovery factor	72.5%

Table 4-8: Cavitating venturi design parameters (with margins) and calibration parameters.

4.8.5. Data Collection and Control

The system makes the greatest possible use of remote data collection and control using PC-based software. As part of the initial system design trade-offs, a detailed industry trade study was conducted to locate a low-cost, easy to use system. For the most part, the system chosen was very good. It was easy to install and quite simple to program and change. Data collection and control was also straightforward. The primary drawback with the system was its slow data rate running in the Microsoft Windows environment. This restricted data collection to < 2 Hz which was often inconvenient for very accurate data analysis as will be described in Chapter 5. A brief description of the system follows.

The system hardware consisted of a 486DX rack-mounted PC with 8 MB RAM. The rack-mounted system was selected because it was initially thought the system would be moving frequently back and forth to RO and so a rugged system was needed (in actual fact, once installed in the control room at RO, the PC was not moved).

Data input and control output from the PC was accomplished using an Integrated Measurement Systems model PCL-813H plug-in PC board. In addition, a PCLD-780 and PCLD-789 were used for data collection. A PCLD-786 AC/DC Power solid-state relay (SSR) and relay driver board were used to interface to the valve solenoids.

Primary wiring to and from the PC was done through two 25-way screened cables. A sensor cable was used to interface the PC data collection card to the load cell, pressure transducers and flow meter (when it was used). In addition, it provided excitation voltage to all these sensors. A control cable was used to connect the PCLD-786 SSRs and all valves with the exception of the HTP control valve which is wired separately. The thermocouples were also wired separately with special thermocouple extension cable. The data collection boards, SSRs, amplifiers and power supply was assembled in a rack mounted container. Interface to the Sensor and Control Cables on both ends was through 25-pin D-connectors.

Sensors included pressure transducers, thermocouples and a load cell. A standard wheel-type flow meter was used initially in the system but was abandoned when the CV proved to be a more reliable and accurate means for flow rate measurement. Pressure transducers were supplied by RO. K-type thermocouples are used to measure temperature in the catalyst pack and record ambient temperature. Temperature inside the hybrid combustion chamber is far too high to measure using conventional sensors. A load cell was also installed on the system to record thrust. However, for the following reasons, the data from this sensor was largely used as a secondary indication of performance only.

- Thrust is primarily a function of expansion condition. Therefore, thrust measurements tell you more about the nozzle performance than actual combustion performance
- Load cell data proved to be quite noisy due to vibrations even with a pre-load
- Load cell data resolution was quite low (± 20 N) due to the resolution of the data collection system.

4.8.5.1. Software

Data collection and system control was done on the PC using Integrated Measurement System's *Genie* software. This software allows for real-time data collection, display and control. Figure 4-16 shows the interface screen used for all rocket testing. The screen allows for control of all valves via mouse-activated virtual push buttons. Rocket firing is set on a user-defined timer. Real-time display of oxidiser flow rate, catalyst pack temperature, thrust and chamber pressure are displayed.

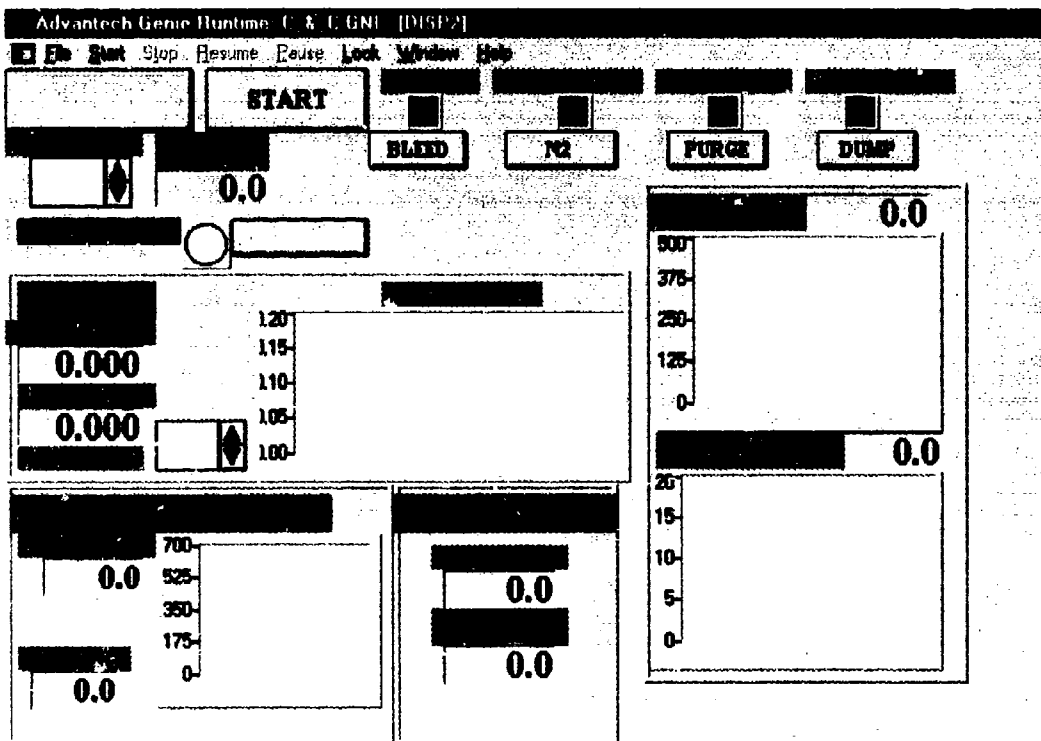


Figure 4-16: Real-time rocket control and data monitoring screen from the *Genie* software package.

4.9. Conclusions

This chapter has presented the detailed background of my hybrid research program. Historical development of hybrids was reviewed, revealing why, despite their many potential advantages, they have remained largely in the background of propulsion research. The need for a dedicated hybrid research program aimed specifically at satellite applications was demonstrated. The goals of this program were established:

1. Proof-of-concept
2. Performance characterisation
3. Total cost assessment

A detailed technical discussion examined the process of hybrid motor design. Fundamental design decisions for my own system were presented and justified. Estimates of performance, both theoretical and empirical, were summarised. Design issues for critical system components and the complete system that resulted was described. Chapter 5 will present experimental results and important conclusions from this program.

4.10. References

- [AL 94] Air Liquide, Specification sheet for hydrogen peroxide, electronic grade, July 1994.
- [AMROC 94] AMROC, "Aquila Launch Vehicle Family," American Rocket Company, Ventura, California, June 1994.
- [Andrews 90] Andrews, David "The Advantages of Hydrogen Peroxide as a Rocket Oxidant," *Journal of the British Interplanetary Society*, Vol. 43, No. 7 July 1990
- [Ankarsward 79] Ankarsward, B., Magnusson, U., "Presentation of the Hybrid Rocket Engine HR 4," Svenska Flygmotor Aktiebolaget, Trollhattan, Sweden, 7 December 1979.
- [Berman 60] Berman, K., "The Plug Nozzle: A New Approach to Engine Design," *Astronautics*, April 1960.
- [Boyer 95] Boyer, W., "Lack of Financing Cripples AMROC," *Space News*, 10-16 July 1995.
- [Cambridge 91] Cambridge Encyclopaedia, 1991.
- [Clark 72] Clark, John, *Ignition: An Informal History of Liquid Rocket Propellants*, Rutgers University Press, New Brunswick, N.J. 1972.
- [Dasch 95] Dasch, P., Kross, J., "Amroc Sinks in Sea of Red Ink," *Ad Astra*, November/December 1995.
- [Davis 52] Davis, N.S., Keefe, J.H., "Equipment for Use with High-Strength Hydrogen Peroxide," *Journal of the American Rocket Society*, Vol. 22, No. 2, March-April 1952.
- [Davis 94] David, L. "U.S. Defence Conversion Effort Buoyed Amroc Hybrid Fuel Work," *Space News*, 7-13 February, 1994.
- [Estey 92] Estey, P., "Hybrid Rockets," *Aerospace America*, December 1992.
- [Gould 91] Gould, R.D., Harlow, J., "Black Arrow—The First British Satellite Launcher," IAA91-639, 42nd Congress of the International Astronautical Federation, Montreal, Canada, 5 - 11 October 1991.
- [Greiner 92] Greiner, B., Frederick, R.A. jr, "Results of Lab-scale Hybrid Rocket Motor Investigation," Propulsion Research Center, University of Alabama, AIAA 92-3301, 1992.
- [Grigorian 94] Grigorian, V., "Propellant Characterisation and Design of a Hybrid Rocket Engine," 45th Congress of the International Astronautical Federation, Jerusalem, Israel, 9-14 October 1994.
- [Holzman 94] Holzman, A. L., "Hybrid Rocket Propulsion," United Technologies Chemical Systems, Presentation by the Hybrid Propulsion Industry Action Group, Received as part of a private communication, 1994.
- [HPHB 67] Hydrogen Peroxide Handbook, Chemical and Material Sciences Department, Research Division, Rocketdyne—a division of North American Aviation, Inc., Canoga Park, California, Technical Report AFRPL-TR-67-144, July 1967.
- [Hudson 95] Hudson, G.C., Personal email communication, 21 March 1995.
- [Humble 95] Humble, R., et al, *Propulsion System Analysis and Design*, To be published, Fall 1995.
- [Jansen 88] Jansen, D.P.L.F., Kletzkine, P., "Preliminary Design for a 3 kN Hybrid Propellant Engine," *ESA Journal*, Vol. 12, 1988.
- [Kilby 96] Kilby, B., "The Great Hybrid Flyoff," *High Power Rocketry*, January 1996.
- [Kross 95] Kross, J., "These Are Not Your Father's Rocketships Anymore," *Ad Astra*, pp. 22-29, March/April 1995.
- [Kuentzmann 91] Kuentzmann, P., Sternfeld, H.J., "What Future for Hybrid Rocket Propulsion?," Proceedings from the Symposium on Launcher Propulsion Toward the Year 2010, Bordeaux, France, 11-12 June 1991.
- [Larson 92] Larson, W.J., Wertz, J.R. (ed), *Space Mission Analysis and Design*, 2 ed., Microcosm, Inc. Torrance, California and Kluwer Academic Publishers, Dordrecht, The Netherlands, 1992.

Chapter 4: Hybrid Research Program

- [Lydon 93] Lydon, M., et al, "Hybrid Sounding Rocket Development at the United States Air Force Academy," AIAA Paper 93-2264, 29th Joint Propulsion Conference Monterey, CA, June 1993.
- [Maggs 54] Maggs, F.T., Avery, M.J., "A Preliminary Investigation of the Loss of Efficiency of an HTP Decomposer During Use," Technical Memo No. RPD 53, RAE, Farnborough, June 1954.
- [Marshall 95] Marshall Star, "Hybrid Motor Development Accelerates at Marshall," NASA, Vol. 36, No. 7, 18 October 95.
- [Moore 56] Moore, G. E., Berman, K., "A Solid-Liquid Rocket Propellant System," *Jet Propulsion*, November, 1956.
- [Nagappa 91] Nagappa, R., Deepak, D., "Hybrid Propulsion—Capabilities and Potentials," *Journal of the Aeronautical Society of India*, Vol. 43, 1991.
- [Pugibet 70] Pugibet, M., Moutet, H. "On the Use of Hydrogen Peroxide as Oxidizer in Hybrid Systems," NASA Technical Translation, NASA TT F-13034, May 1970.
- [Randall 52] Randall, L.N., "Rocket Applications of the Cavitating Venturi," *American Rocket Society Journal*, January-February 1952.
- [Selph 92] Selph, C., *Isp Computer Code*, Personal communication to Dr. Ron Humble, 1992.
- [SpaceNews 95] Space News, "Hybrid Rocket Draws Attention," 13-26 November 1995.
- [Sutton 60] Sutton, D., "Some Aspects of the Catalytic Decomposition of Hydrogen Peroxide by Silver: Part IV. The Rate of Decomposition," RPE Technical Note No. 197, Rocket Propulsion Establishment, Westcott, December 1960.
- [Sutton 92] Sutton, G.P., *Rocket Propulsion Elements*, 6th Edition, John Wiley & Sons, Inc., 1992.
- [Tucci 94] Tucci, L., "Hybrid Rocket Tests Impress NASA Skeptics," Space News, 20-26 July 1994.
- [Ventura 93] Ventura, M., Heister, S., "Hydrogen Peroxide as an Alternate Oxidizer for a Hybrid Strap-on Booster," AIAA/SAE/ASME/ASEE 29th Joint Propulsion Conference and Exhibit, Monterey, California, June 28-30, 1993.
- [Vincent 95] Vincent, B., "Hybrid Rockets," *Aerospace America*, Vol. 33, No. 12, December 1995.
- [Wernimont 95] Wernimont, E.J., Heister, S.D., "Performance Characterisation of Hybrid Rockets Using Hydrogen Peroxide Oxidiser," AIAA-95-3084, 31st AIAA/ASME/SAE/ASEE Joint Propulsion Conference and Exhibit, San Diego, California, 10-12 July 1995.
- [Wernimont 94] Wernimont, E.J., Meyer, S.E., "Hydrogen Peroxide Hybrid Rocket Engine Performance Investigation," AIAA 94-3147, 30th Joint Propulsion Conference, Indianapolis, IN, June 1994.
- [Witinghill 94] Witinghill, G., AMROC, Personal Communication, 26 July 1994.
- [Zubrin 95] Zubrin, R.M., Clapp, M.B., "Black Horse: Winging it to Orbit," *Ad Astra*, pp. 40-43, March/April 1995.

Chapter 5

Hybrid Program Results

- 5.1. PROOF-OF-CONCEPT**
- 5.2. CATALYST PACK DEVELOPMENT & TESTING**
- 5.3. HYBRID PERFORMANCE CHARACTERISATION**
- 5.4. HYBRID COST ANALYSIS**
- 5.5. CONCLUSIONS**
- 5.6. REFERENCES**

This chapter summarises the results of the hybrid research program and demonstrates how the program objectives were fulfilled. The chapter begins by addressing the first objective—proof-of-concept demonstration—by presenting an overview of the project budget and schedule. A discussion of the most difficult engineering challenge that had to be overcome—catalyst pack design—follows. The various catalyst options investigated and the experimental results are presented with specific conclusions for future satellite applications. The second program objective, performance characterisation of hybrid combustion, is then discussed, with experimental results summarised. The empirically derived regression rate equation is presented and assessed. A variety of other results from this experimental work that relate to hybrid performance are also presented including: combustion uniformity, start-up and re-start characteristics, combustion stability, fuel selection and throttling. A hybrid upper stage motor design process emerges which is presented along with results for an example minisatellite mission. The chapter concludes with an overall assessment of hybrid rocket technology for cost-effective small satellite application by evaluating price and mission costs.

5. Hybrid Program Results

5.1. Proof-of-Concept

The first objective of the hybrid program was to prove the basic concept of hybrid technology for small satellite applications. The aim was to demonstrate the overall accessibility of hybrids for cost-constrained research and development within a University environment. Basically, hybrids had to be shown to be cheap and easy to work with. In these respects, the program was an overwhelming success.

Table 5-1 summarises the complete budget for the program, labour costs are not included(e.g. those of Mr. Malcolm Paul, or Mr. Maarten Meerman. My own labour, of course, was "free"). The bottom line indicates the relatively low-level of funding required to get the program up and running. At ~£13,000, this represents a very small investment considering it encompasses the entire program. Similar programs run at government funded research organisations would spend many times this amount (perhaps with slower or fewer results). It is important to remember that at the outset of the project, the University of Surrey had no propulsion infrastructure. Everything had to be developed. In this, we were greatly aided by the generous use of facilities at British Aerospace, Royal Ordnance, Westcott. The use of a test cell there for safe testing with ample running water and power overcame one of the first big programmatic hurdles.

Item	Cost
Mechanical & Electrical Components	£1,917.85
Valves	£1,234.46
Data Collection & Control System	£3,943.00
HTP	£2,059.14
Catalyst	£1,514.28
Fuel	£278.61
Cavitating Venturi	£240.00
Nozzle Insert	£352.00
Misc. Labour & Components	£1,070.00
Total	£12,609.34

Table 5-1: Summary budget for complete hybrid research program.

The program schedule is shown in Figure 5-1. For purposes of discussion, the test program has been divided into two phases. The differences between the phases relate to catalyst pack development as discussed later in the chapter. Hybrid firing days are shown as significant milestones in the schedule. Despite the many months in the program dedicated to solving a single engineering problem (discussed in the next section), the overall pace of the schedule underscores the essential simplicity of hybrid technology. Note that only 7 months elapsed from project go-ahead to the first successful hybrid firing. During this time, the entire system was designed, fabricated, integrated and ready for testing. To be sure, this schedule greatly benefited from the expert advice and guidance of Mr.

Chapter 5: Hybrid Program Results

Maarten Meerman, David Montegomery and, especially, Malcolm Paul. However, over that time period, their overall time contribution adds to less than 5 man-months. The important conclusion from this information is that hybrid technology is easy to use. The margins on design requirements are large enough to allow the use of standard industrial practices with excellent performance at very low cost.

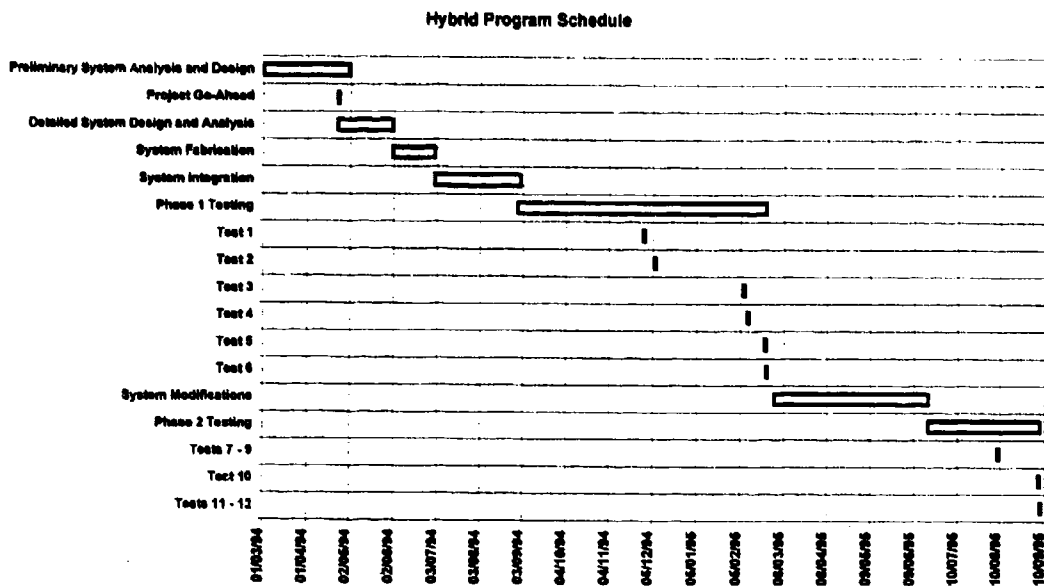


Figure 5-1: Summary Hybrid Program Schedule.

It is interesting to note another direct result of proving the basic concept of hybrid rocket technology for low-cost applications—the keen interest generated in the press. After the first successful test, the University issued a press release which received a startling response. Many different articles appeared in newspapers and magazines around the world heralding our results as a unique approach to rocket motors. We were also the subject of several radio interviews. The BBC were very interested in featuring a hybrid firing as part of children's science program but unfortunately we were unable to coincide with their production schedule. Below are a sample of some of the headlines generated:

- "British Develop Hybrid Rocket," *Space News* 13 - 19 March 1995.
- "Successful Test for Hybrid Rocket Motor," *Surrey Matters*, 17 February 1995.
- "Campus Boffins Cut Satellite Costs," *Surrey Advertiser*, 24 February 1995.
- "New Motor Will Cut Cost of Space Trips," *The Times*, 17 February 1995.
- "Motor Sets Satellites on Cheap Orbit," *The Times Higher Education Supplement*, 10 March 1995.
- "Satellites Enter Steam Age," *The Sunday Times*, 11 June 1995.

In addition to demonstrating the accessibility of hybrid technology, another aspect of the proof-of-concept objective was to identify and solve significant engineering problems that drive system performance. The difficulties encountered underscores the state-of-the-art for HTP hybrids prior to this research. There were no off-the-shelf manuals and very few experts to consult (and those experts

still alive had to work from memory rather than documented results). The following is a list of some of the technical problems that had to be overcome during the program.

- Designing a reliable, long-lived catalyst pack.
- Obtaining a reliable supply of HTP.
- Locating HTP-compatible valves and flow meter
- Designing, fabricating, calibrating and installing a cavitating venturi to overcome "wet-start" problems.
- Designing a low-cost nozzle insert capable of withstanding the +2300°C temperature of hybrid combustion.

Of these, all but the first one was addressed as part of the overall system design effort described in Chapter 4. This challenge proved to be the most difficult to overcome. Catalyst pack research eventually consumed a large percentage of the program schedule. Details of this effort are presented in the following section. Following this discussion, the remaining program objectives will be discussed.

5.2. Catalyst Pack Development & Testing

This section summarises experimental work conducted on HTP catalysts and catalyst packs. It should be noted that at the outset of the research program, I did not envision spending the bulk of the time on this single topic. However, developing an effective catalyst pack turned out to be the weak link in the chain. Without a reliable catalyst, reliable hybrid combustion is not possible. The section begins with a discussion of catalyst pack design issues followed by an overview of the catalyst research program, a summary of catalyst results and conclusions.

5.2.1. Catalyst Pack Design

The hybrid combustion process begins in the catalyst pack. If it does not work, the hybrid will not ignite. Within the catalyst pack, the HTP must be fully decomposed into superheated oxygen and steam before passing into the combustion chamber. Thus, as part of an over-all system, a reliable pack needs to initiate smooth, rapid and complete decomposition of HTP with minimum pressure drop across the pack. Five design goals emerge from this description:

1. *Reliable*—relatively long lifetime with little degradation in performance, working "first-time, every-time."
2. *Smooth*—no radical surges or oscillations in working pressure.
3. *Rapid*—decomposition time should be on the order of milliseconds. "Wet starts" should not be observed. A wet start condition exists when liquid HTP is ejected on start-up prior to transition to full decomposition.
4. *Complete decomposition*—as characterised by measured vs. theoretical characteristic exhaust velocity, C^* or decomposition temperature, T_C .
5. *Minimum pressure drop*—higher pressure drop requires higher delivery pressure. Drops on the order of 6 bar or less should be attainable [HPHB 67].

My research revealed that these characteristics are much more easily stated than achieved. The search for a reliable and effective catalyst pack eventually consumed the bulk of rocket development

and experimentation time. This work was quite frustrating because reliable catalyst packs had been fully developed and widely used in the 1950s and 60s. However, when HTP fell out of favour in the late 60s, this technology was abandoned. Thus, the program was forced to reinvent the technology, repeating the same mistakes of earlier researchers in the process. This was primarily due to the lack of details presented in previous work. Moore & Berman, for example, [Moore 56] provide virtually no details about their catalyst pack design. To correct this problem, it is hoped that this thesis can serve as handbook to guide further research, preventing future investigators from repeating these same mistakes.

Initially, I searched for a commercially available HTP catalyst. Unfortunately, none could be located. The latest known space application of HTP was on the NASA Scout rocket for attitude control. However, Valcor, Inc., the company that originally made these control jets, no longer knew how to make them [LaTona 94]. Therefore, I had to develop my own. The best descriptions available at the time were in [Davis 60] and [HPHB 67]. From these, some general guidelines for catalyst pack configuration were determined. To begin with [Davis 60] defines the *loading factor* as the mass flux of hydrogen peroxide as follows:

$$LF = \frac{\dot{m}}{A} \quad \text{Eqn. 5-1}$$

where

LF = Loading factor ($\text{kg}/\text{s}/\text{m}^2$)

\dot{m} = mass flow rate of HTP (m/s)

A = cross-sectional area of catalyst pack (m^2)

[Davis 60] indicated that the normal loading factor is between 60 and 235 $\text{kg}/\text{sec}/\text{m}^2$, with the smaller values used for low-temperature starts. Armed with the desired HTP flow rate as described in Chapter 4, the diameter of the pack could be determined. Unfortunately, [Davis 60] did not provide firm rules of thumb for pack depth. Therefore, the approximate length of 5 cm described in his paper was adopted.

This established the pack geometry. What remained was finding a suitable catalyst material to use. Unfortunately, descriptions of catalyst material were even more vague. [HPHB 67], for example, describes a variety of catalyst types including calcium permanganate "stones," silver gauze and silver-plated brass, nickel and stainless steel gauze, 16 - 20 mesh ("mesh" is used to describe the number of wires either per linear inch or per cm, i.e. one square inch of mesh would have a total of 40 wires woven perpendicular to each other). With only this to go on, the catalyst development program described in the next section was initiated.

5.2.2. Program Overview

This section provides an overview of the catalyst pack research program. It begins by describing the approach taken followed by a summary of the program schedule. For purposes of discussion, the program has been divided into two phases. Phase 1 comprises the first 34 catalyst tests (including hybrid tests 1 - 6). Phase 2 comprises all tests conducted after that period which includes catalyst pack tests 35 - 55 (and hybrid tests 7 - 12). Note that catalyst pack and hybrid tests are numbered sequentially, independent of catalyst type used. Results from each phase will be addressed separately below.

Catalyst efficiency was assessed by computing characteristic exhaust velocity, C^* and measuring decomposition temperature, T_C . However, early in the program some C^* values exceeded 100% of theoretical. This value was determined from the known throat area, A_t , and measured chamber pressure, P_C and flow rate, \dot{m} using the following relationship:

$$C^* = \frac{P_C A_t}{\dot{m}} \quad \text{Eqn. 5-1}$$

Extensive verification of all these parameters was repeatedly conducted to determine why C^* was so high (> 100% is, of course, impossible). The exact concentration of HTP was also measured to verify the results from the *Isp* program and was found to be accurate. Further investigation determined that the inaccuracy was caused by the choke design. For simplicity, catalyst pack testing initially used the outer flange/nozzle extension section designed for the hybrid described in Chapter 4. This component had a flat inlet for interface to the graphite/pyrolytic graphite throat insert. Unfortunately, lack of a converging inlet section in the choke used for catalyst testing was causing a *vena contracta* condition [White 86] whereby a "virtual throat" slightly smaller in diameter than the real throat, was created, artificially inflating the C^* calculation. This condition was rectified by constructing of a separate choke with contoured convergent section introduced for catalyst pack test 49 and subsequent.

Fortunately, chamber temperature, T_C , proved to be an equally effective indication of overall catalyst pack efficiency and, most important, predictor of hybrid ignition performance. Therefore, for consistency, T_C will be the primary means used in the assessment of catalyst performance reported in the following sections. It should be emphasised that C^* calculations for hybrid tests were not effected by this problem, as these tests used the nozzle insert which had a well-contoured converging section.

5.2.3. Phase 1 Discussion

Testing during Phase 1 was primarily aimed at proof-of-concept. Every effort was made to get the test rig operational in the shortest possible time to produce reasonable results and validate the basic feasibility of the program. During Phase 1, between August 1994 and February 1995, a total of 7 different catalyst pack configurations were tested.

1. *Type-1*: Maximum density silver-plated nickel gauze
2. *Type-2*: Maximum surface area silver-plated nickel gauze
3. *Type-3*: KMnO₄ crystals
4. *Type-2A*: Type-2 catalyst, sintered for 30 min at 800°C
5. *Type-4*: LCH 212
6. *Type-5*: Silver-plated gauze provided by the US Air Force Academy (USAFA)
7. *Type-4A*: LCH 212 plus Shell 405

Table 5-2 highlights significant milestones during Phase 1 testing. It is important to note that testing during Phase 1 was severely handicapped by a limited supply of HTP (only 80 litres). Thus, catalyst pack test runs had to be kept very short (as little as 5 seconds). This, coupled with the relatively low sampling rate imposed by our low-cost data collection/control system (<2 Hz), meant that collected data could only provide a good indication of performance, especially relative performance, but not exact values. It should also be noted that the cavitating venturi (CV) was added after test 18 to eliminate wet start conditions. However, this did not effect chamber temperature results.

The following subsections will discuss experimental results from each catalyst type evaluated in Phase 1. Hybrid tests conducted during Phase 1 will be addressed in a Section 5.3.

5.2.3.1. Type-1 (maximum density)

Catalyst Type-1 was made up of 84 hand-cut, 40 SWG x 40 mesh nickel gauze, silver-plated for maximum density. As described above, at the beginning of this work it was known that silver plated nickel gauze had been used with success in the past but no details were available indicating exactly what plating process to use. Initial discussions with commercial silver plating firms revealed that modern plating practices strive to achieve a very smooth, thin surface finish. However, reasoning from the standpoint that "more is better," a plating process was ordered that would deposit the maximum density of silver on the gauze. This was designated Type-1 catalyst.

Unfortunately, only 2.5 litres of HTP was available at the beginning of research. Therefore, these tests were used to verify system compatibility, oxidiser handling procedures and test procedures. Objective performance data was not available as the pressure transducer failed and the thermocouple had not been installed into the catalyst pack. However, subjective assessment of the performance based on the exhaust and lack of hybrid reactivity indicated that this configuration did not achieve good performance. The exhaust appeared as solid white steam, however super-heated steam should be invisible. This was a strong indication that decomposition efficiency was low. Furthermore, an attempt was made to ignite a hybrid motor with this catalyst configuration and no ignition or even minor erosion of the fuel was achieved, further indicating inefficient decomposition. Following these tests, a new catalyst was produced using a method to achieve the greatest overall surface area of silver and a larger supply of HTP was obtained.

Date	Milestones	Comments
March-April 1994	<ul style="list-style-type: none"> Preliminary system analysis and design 	
23 April 1994	<ul style="list-style-type: none"> Official project go-ahead 	
May 1994	<ul style="list-style-type: none"> Detailed system analysis and design 	<ul style="list-style-type: none"> Component selection Subcontractor selection for component fabrication
June 1994	<ul style="list-style-type: none"> System Fabrication 	<ul style="list-style-type: none"> System manufacture by Project Machinery Component procurement Plumbing system assembly
July - August 1994	<ul style="list-style-type: none"> System integration 	<ul style="list-style-type: none"> Integrate hardware/software data collection and control system Integrate entire test rig into test cell Sensor calibration
30 August 1994	<ul style="list-style-type: none"> Preliminary catalyst pack tests A & B 	<ul style="list-style-type: none"> Using Type-1 catalyst
September - November 1994	<ul style="list-style-type: none"> Develop catalyst Type-2 Obtain reliable HTP supply 	<ul style="list-style-type: none"> Obtained a better process for gauze plating from D. Andrews Worked with Air Liquide, France, on 80 litre supply of HTP
23 November 1994	<ul style="list-style-type: none"> Catalyst Pack tests 1 - 5 	<ul style="list-style-type: none"> Using Type-2 catalyst (maximum surface area)
28 November 1994	<ul style="list-style-type: none"> Catalyst Pack tests 6 - 7 Hybrid Test 1 	<ul style="list-style-type: none"> Using Type-2 catalyst (maximum surface area)
6 December 1994	<ul style="list-style-type: none"> Catalyst Pack tests 8 - 9 Hybrid Test 2 	<ul style="list-style-type: none"> Using Type-2 catalyst (maximum surface area)
12 December 1994	<ul style="list-style-type: none"> Catalyst Pack tests 10 - 12 	<ul style="list-style-type: none"> Using Type-2 catalyst (maximum surface area)
20 December 1994	<ul style="list-style-type: none"> Catalyst Pack tests 13 - 17 	<ul style="list-style-type: none"> Using Type-3 catalyst ($KMnO_4$)
3 February 1995	<ul style="list-style-type: none"> Install cavitating venturi Catalyst Pack tests 18 - 20 Catalyst Pack tests 21 - 22 	<ul style="list-style-type: none"> CV to eliminate "wet-start" conditions Tests 18 - 20 with catalyst Type-2A (sintered maximum surface area gauze) Tests 21 - 23 with catalyst Type-4 (LCH 212)
6 February 1995	<ul style="list-style-type: none"> Catalyst Pack tests 23 - 26 Catalyst Pack tests 27 - 30 	<ul style="list-style-type: none"> Tests 23 - 26 with catalyst Type-4 Tests 27 - 31 with catalyst Type-5 (USAFA catalyst)
7 February 1995	<ul style="list-style-type: none"> Catalyst Pack tests 31 - 32 Hybrid Test 3 	<ul style="list-style-type: none"> Tests 31 - 32 with Type-5 Hybrid Test 3 with Type-4A
10 February 1995	<ul style="list-style-type: none"> Catalyst Pack test 33 Hybrid Test 4 	<ul style="list-style-type: none"> Using Type-4A
22 February 1995	<ul style="list-style-type: none"> Catalyst Pack test 34 Hybrid Test 5 (take 1) 	<ul style="list-style-type: none"> Using Type-4A
23 February 1995	<ul style="list-style-type: none"> Hybrid Test 5 (take 2) 	<ul style="list-style-type: none"> Using new catalyst Type-4A

Table 5-2: Summary of Catalyst Pack development milestones during Phase 1.

5.2.3.2. Type-2 (maximum surface area)

Based on Type-1 testing results, several changes were made to streamline testing and improve results:

- Chamber pressure transducer changed and calibrated
- Thermocouple probe added to inside of catalyst pack
- Delivery of 80 kg of HTP from Air Liquide accepted and handling procedures developed.
- A punch and die were produced to allow gauze disks to be cut out to the exact size of the catalyst pack.

In addition, the Type-2 gauze was developed. The plating process for this gauze was based on information supplied by Mr. D. Andrews who had extensive experience with HTP in the 1960s [Andrews 94]. From his input, we tried to re-create a surface finish that would have maximum surface area of silver. The process described by Mr. Andrews was adapted by a local plating firm to yield the following procedure using 28 SWG x 40 nickel gauze:

- **Type-2 Catalyst Procedure**

- Cut 28 SWG x 40 nickel gauze into 15 x 15 cm squares
- Step 1: 1 min at 50 - 56 amp. Solution of 5 g/l silver in 60 g/l KCN
- Step 2: 15 min at 24 - 30 amp. Solution of 10 g/l silver in 60 g/l KCN
- Step 3: 2 min at 50 - 60 amp. Solution of 5 g/l silver in 60 g/l KCN
- Stamp out disks to size

This process yielded a light-beige coloured gauze which, under the microscope, had a slightly frosty appearance. Type-2 catalyst was used for catalyst pack tests 1 - 9. Five tests were done as a preliminary assessment of catalyst pack performance. Two additional tests (6 & 7 and 8 & 9) were performed before hybrid tests 1 & 2 to confirm total system performance and ensure sufficient decomposition efficiency for hybrid combustion. Experimental results for the Type-2 catalyst are summarised in Figure 5-2.

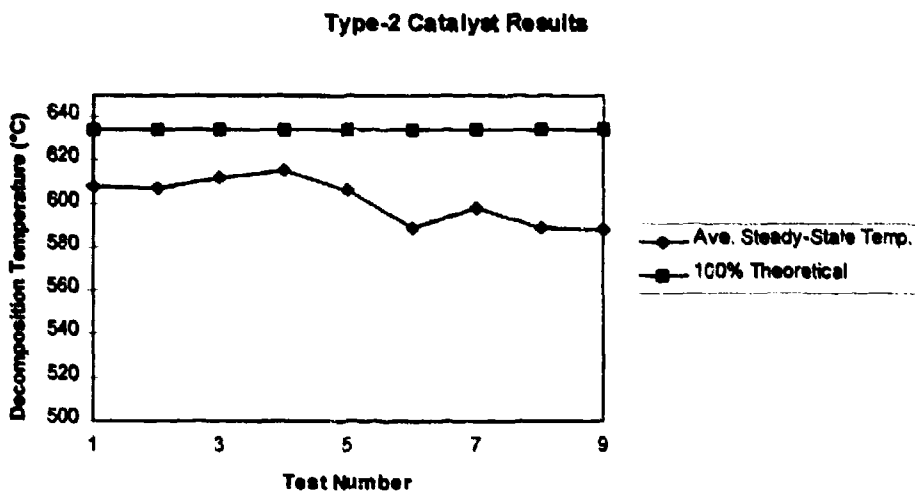


Figure 5-2: Decomposition efficiency results for Type-2 catalyst. Average steady-state decomposition temperature based on average temperature from first data point >500°C through end of run.

After the poor observed performance with the Type-1 tests, the initial results with the Type-2 catalyst were very encouraging. The exhaust was invisible a noticeable distance away from the nozzle and decomposition temperatures were reasonably high. Based on these results, we pressed ahead with two hybrid tests using this catalyst configuration (described in the hybrid results section). Ignition was very good for hybrid test 1 but hybrid test 2 presented a wet start. It was concluded that the pack had been simply "used up" (at the time, no data indicating the expected lifetime of a catalyst pack was

available, however it seemed reasonable to assume that it should be longer than the total duration of less than 2 minutes to which this one had been subjected).

Dismantling the pack it was noted that approximately the first third of the 80 gauze in the pack were stripped smooth. The appearance of fresh catalyst disks were light beige or dull white with frosty or hairy surface. The disks in the top layer of the pack (nearest the injector) were smooth in appearance with a dull copper or brown colour. In addition, there were localised darker areas. Further down the pack this transformation was less pronounced.

These results were consistent with those described by D. Sutton [Sutton 62a] (in a restricted internal Royal Propulsion Establishment (RPE) memo only released to me very late in Phase 1). Sutton clearly describes the mechanical process of HTP decomposition within a catalyst pack. At start-up, liquid HTP penetrates a considerable fraction of the entire length then rapidly retreats toward the entry end as temperature rises. When thermal equilibrium is reached, the change of phase settles down near the entry end. Understanding this process helps to explain why the front-end gauze in the pack were stripped. According to Sutton, this is due to chemical solution of the silver in the liquid HTP at the entry end. Most of the dissolved silver is re-deposited but a small fraction is blown out so gradually the total silver available decreases. Furthermore, use of HTP at low temperature and repeated stopping and starting of a pack accelerates the loss of efficiency due to increased rate of silver erosion. Since the rate of decomposition decreases with decreased temperature, the use of a pack at low temperature involves a greater penetration of liquid HTP and thus a higher erosion rate.

In addition, Sutton explains the localised darker areas on the catalyst material. This is due to *channelling*. Channelling is caused by preferential erosion of silver over certain parts of the gauze area caused by two principal factors:

1. Lack of uniform HTP distribution by injector
2. Cooling effects on gauze periphery due to heat loss

Sutton [Sutton 62a] concludes that these two effects, along with chemical poisoning of the catalyst surface by HTP contaminants such as tin and phosphates [Sutton 62b], will decrease the life time of the catalyst. As indicated in Chapter 4, phosphates were the one ingredient which exceeded the MilSPEC in the HTP supplied by Air Liquide. Thus it appeared that some or all of these effects conspired to give the mediocre lifetime of the Type-2 catalyst.

5.2.3.3. Type-3 ($KMnO_4$)

It has long been known that permanganate (as either calcium, $CaMnO_4$, or potassium $KMnO_4$) is a superb catalyst for hydrogen peroxide. The Germans used it in liquid form to decompose the peroxide used in torpedoes and in the turbo-pumps on the V-2 [HPHB 67]. Unfortunately, liquid injection of $KMnO_4$ would greatly increase the complexity of the hybrid system. [HPHB 67] describes the use poly-surfaced silicon carbide "stones" impregnated with calcium permanganate in

the gas generator of the *Redstone* missile. This is the same approach used by Wernimont at Purdue University [Wernimont 94] as described in Chapter 4. Unfortunately, such stones were not available "off-the-shelf" (however, a similar material subsequently became available during Phase 2 described below). Therefore, a simple approach was applied to construct a catalyst pack using four layers of approximately 10 gm each of KMnO₄ crystals interspersed between layers of Type-1 gauze (a total of 84 gauze).

Results with this configuration were disappointing. The chamber pressure was much lower than the results with the Type-2 catalyst (10 bar vs. 15 bar). Furthermore, both tests 11 & 12 gushed liquid HTP throughout the test.

While KMnO₄ is chemically a good catalyst (it practically explodes even with 3% hydrogen peroxide), the difficulty is in presenting sufficient surface area to a high speed flow of HTP while preventing the catalyst from being dissolved and washed away. During our tests, the KMnO₄ was effectively blown out of the pack. As a result, this approach was abandoned.

3.2.3.4. Type-2A (maximum surface area, sintered)

After the dismal results with the Type-3 catalyst, the lifetime issue of the Type-2 catalyst was reconsidered. Information on the plating process supplied by Mr. David Andrews [Andrews 94] indicated that the gauze should be sintered for 45 minutes at 850°C. For simplicity, this step had been omitted for the Type-2 catalyst. Subsequent discussions with Mr. David Andrews revealed that sintering should help to maintain the mechanical integrity of the gauze, possibly giving a longer lifetime. A 30 minute sintering at 850°C was done to the remaining batch of Type-2 catalyst creating Type-2A.

The catalyst pack using the Type-2A catalyst consisted of a total of 87 disks. The appearance of the gauze was significantly different following the sintering process. It was distinctly white rather than light beige. Under microscopic examination, the frosty, hairy appearance was replaced by a rough, granular surface.

While overall performance of the Type-2A catalyst, as indicated by average decomposition temperature as shown in Figure 5-3, was respectable (in most cases >550° C), wet starts continued to plague the operation. With an initial cold start-up of the pack, the chamber pressure remains low causing a very high liquid flow rate, exacerbating the wet start problem. Therefore, it was reasoned that if this initial flow rate could be moderated, the pack could be given time to warm up, alleviating the wet start condition. For this reason, a cavitating venturi (as described in Chapter 4) was added to the system after test 18. Results were dramatic. Along with providing a more reliable indication of flow rate, the CV practically eliminated the wet start condition. Thus, while the Type-2A catalyst configuration was abandoned, the CV was retained for all subsequent tests.

Following tests with the Type-2A catalyst, the pack was again dismantled and examined. Some stripping of the top portion of the pack was noted, but not as severe as with the unsintered Type-2. However, significant channelling was present. Ironically, subsequent discussions with Mr. David Andrews [Andrews 95] revealed that the sintering time for the process he provided in [Andrews 94] should have read 4-5 minutes rather than 45 minutes!

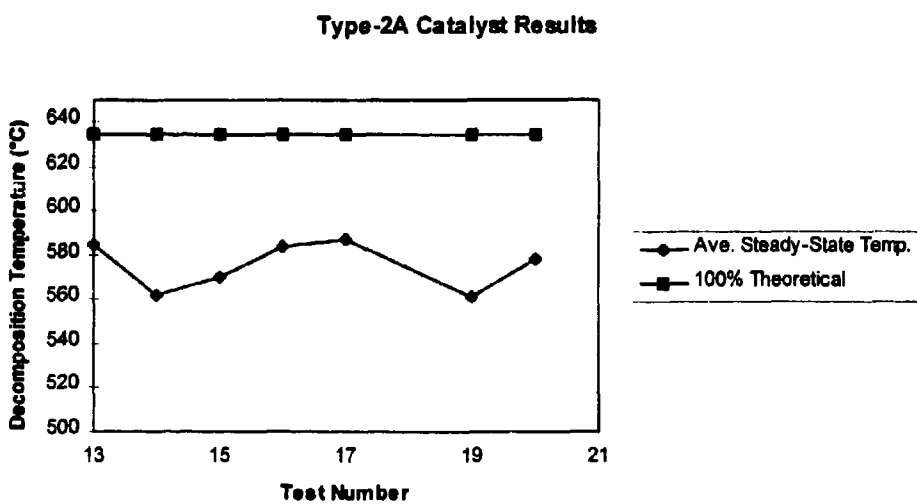


Figure 5-3: Decomposition efficiency results for Type-2A catalyst. Decomposition temperature based on average temperature from first data point $>500^{\circ}\text{C}$ through end of run. Test #18 not included due to total lack of decomposition activity. The cavitating venturi was added for test #19 and all subsequent tests.

5.2.3.5. Type-4 (LCH 212)

In the process of trying to discover a good HTP catalyst, commonly used catalysts for hydrazine mono-propellant engines were also examined. This material goes by several commercial names such as LCH 212 or Shell 405. It was reasoned that if these commercial products could be used for hydrazine, it was possible they could be equally effective with HTP. This reasoning was based on the chemical composition of these commercial hydrazine catalysts which rely on iridium as the active catalytic agent. This element was listed as possible catalyst for HTP in [HPHB 67]. Furthermore, because this material was available commercially, it would make it easier to procure at known standards. Because these products came into common use after HTP had fallen out of favour, to my knowledge they had never been tried with HTP so in that respect this investigation represents truly unique results.

The basic constituent of LCH-212 and Shell 405 is iridium on a porous ceramic substrate. The actual material used was of unknown heritage donated by RO. The catalyst pack consisted of approximately $9.0 \times 10^{-3} \text{ m}^3$ of LCH-212 granules constrained between plain nickel gauze. The granules are black,

roughly cylindrical in shape, about 3 mm in diameter by 3 mm in length. This configuration was used for tests 21 - 26.

Overall performance with the Type-4 catalyst was fair. Start-up was relatively slow (accounting for the low average T_c) but overall performance was consistent with no wet starts observed. On all runs, temperatures consistently reached nearly 600° C. Results from Type-4 tests are summarised in Figure 5-4.

After test 26, the Type-4 catalyst was examined to reveal that the glossy black finish on the pellets had taken on a white discoloration over much of the surface. This was most likely due to oxidation of the iridium by the peroxide. Because of this rapid oxidation, LCH-212 and Shell 405 had to be ruled out for long-term space applications. However, because of its consistent performance, a modified catalyst pack, Type-4A using both LCH and Shell was used for hybrid test 3 as discussed later in the chapter.

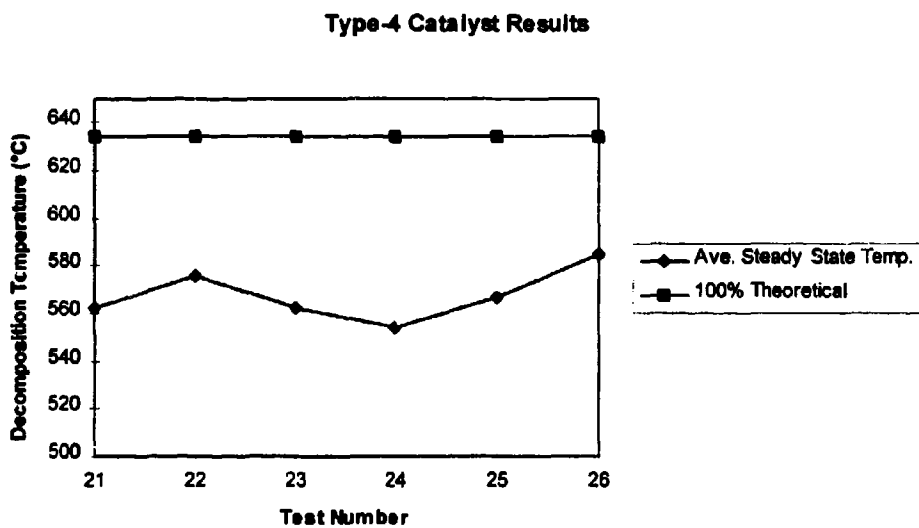


Figure 5-4: Decomposition efficiency results for Type-4 catalyst.

5.2.3.6. Type-5 (USAFA gauze)

While our work progressed at the University of Surrey, colleagues at the U.S. Air Force Academy (USAFA) in Colorado Springs were pursuing similar lines of research. The team at USAFA was headed by Capt. Mike Lydon and consisted of several other faculty members and 10 - 20 undergraduate engineering students. Because our test apparatus was already set-up and running while theirs was not, we agreed to test some silver-plated nickel gauze they had made. This was designated Type-5 catalyst. The exact manufacturing process for this gauze was not available. The Type-5 catalyst was used for tests 27 - 32. Results of these tests are shown in Figure 5-5.

Performance with the Type-5 catalyst was somewhat erratic. Temperatures eventually reached respectable values as high as 618°C on tests 29 and 30. However, start-up was very slow with wet starts observed on tests 28, 31 and 32. Therefore, the Type-5 catalyst was not considered for hybrid application and the modified Type-4, called 4A, was used for hybrid test 3.

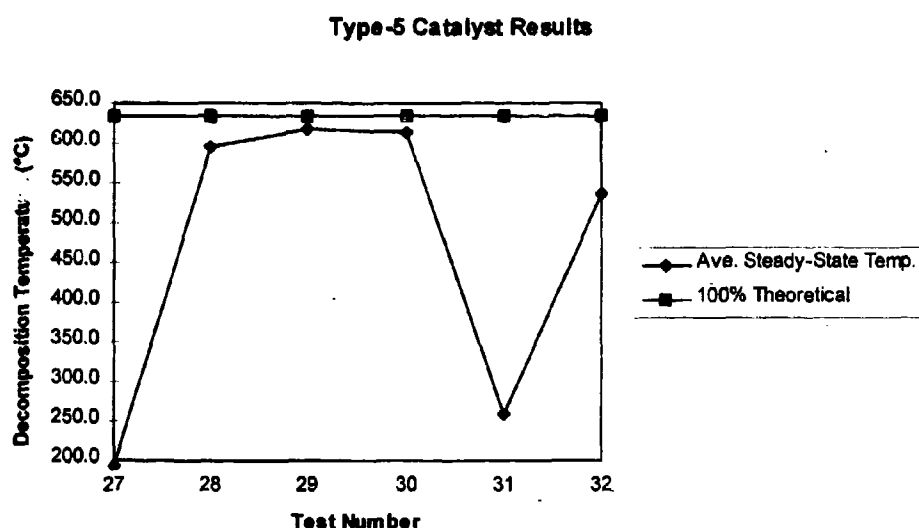


Figure 5-5: Decomposition efficiency results for Type-5 catalyst, silver-plated nickel gauze supplied by the US Air Force Academy (USAFA). Decomposition temperature based on average temperature from first data point >500°C through end of run. Note change of scale from previous results to fit lower steady-state temperatures on the graph.

5.2.3.7. Type-4A (LCH 212/Shell 405)

In an effort to keep up the pace of hybrid development concurrent with catalyst pack experiments, the partial success of the Type-4 was adapted to form the Type-4A configuration. Type-4A catalyst consisted of a combination of pellet-like LCH 212 along with small, ~1 mm beads of Shell 405. In a conventional hydrazine mono-propellant engine, a layer of the smaller grained material is placed at the inlet end of the pack with a deeper layer of the larger grains nearer the exit. This approach was adapted by putting a 1 cm layer of Shell 405 followed by the remaining 4 cm of LCH separated by 3 blank nickel gauze.

Normally, we had conducted two catalyst pack tests prior to each hybrid firing for system check-out. However, because we feared that we could use up some of the catalyst's lifetime by doing these additional tests, I chose to press ahead with hybrid test 3 (which was successful) without a separate catalyst pack test. However, test 33 was done prior to hybrid test 4 (which did not ignite reliably). Test 34 was done prior to hybrid test 5 (this time with no ignition).

The results for tests 33 and 34 indicated a rapid drop off in performance between the two. However, there were 3 attempts to ignite hybrid 4 in between the two tests, with duration of 15, 15 and 5 seconds respectively, which were only moderately successful.

5.2.3.8. Phase 1 Conclusions

Results from Phase 1 of testing were encouraging but frustrating. It was demonstrated that good decomposition could be achieved leading to hybrid ignition but achieving this reliably was an elusive goal. Toward the end of Phase 1, RO released a wealth of documents describing HTP work done in the late 1950s and 60s. The important results from the RO work and its influence for planning during Phase 2 are discussed in the next section.

5.2.4. Phase 2 Discussion

Late in Phase 1, several events happened which influenced the direction of the research and led to Phase 2.

- RO released 11 previously CONFIDENTIAL or RESTRICTED documents on HTP work from their archives dating from 1955 - 1967.
- Dr. John Rusek at USAF Edwards AFB in California developed a permanganate catalyst.
- A 1963 NASA document was obtained describing another early catalyst based on pure silver gauze.

Table 5-3 summarises the important milestones during Phase 2.

Date	Milestones	Comments
• March-June 1995	<ul style="list-style-type: none"> • Obtain Type-6 catalyst • Acquisition and review of RO documents • Type-7 catalyst development • Acquistion of [Runckel 63] report • Type-8 catalyst development 	<ul style="list-style-type: none"> • During this time several upgrades were made to the test rig • Flow rate measurement re-calibration using CV • Improved HTP handling process • Complete sensor re-calibration
19 June 1995	<ul style="list-style-type: none"> • Catalyst pack test 35 	<ul style="list-style-type: none"> • Using Type-6 catalyst • Very poor results
20 June 1995	<ul style="list-style-type: none"> • Catalyst pack tests 36 - 45 	<ul style="list-style-type: none"> • Type-7 catalyst • Excellent results
3 August 1995	<ul style="list-style-type: none"> • Catalyst pack tests 46 - 47 	<ul style="list-style-type: none"> • Type-7 catalysts • High speed data collection system added in parallel to measure chamber pressure
4 August 1995	<ul style="list-style-type: none"> • Catalyst pack tests 48 - 55 	<ul style="list-style-type: none"> • Type-8 catalyst • Excellent results • problem with inflated C* results due to <i>vena contracta</i> effect discovered
8 August 1995	<ul style="list-style-type: none"> • Catalyst pack test 56 • Hybrid tests 7 - 9 	<ul style="list-style-type: none"> • Type-8 catalyst • Very good hybrid start-up
6 September 1995	<ul style="list-style-type: none"> • Catalyst pack tests 57 - 58 • Hybrid test 10 	<ul style="list-style-type: none"> • Type-8 catalyst • Very good hybrid start-up
7 September 1995	<ul style="list-style-type: none"> • Hybrid tests 11 - 12 	<ul style="list-style-type: none"> • Type-8 catalyst • Very good hybrid start-up

Table 5-3: Summary of Phase-2 milestones.

The RO reports came at a critical time. As the discussion from Phase 1 indicates, different catalyst options were being tried with the hope that one would eventually prove effective. However, RO had been through this loop before in the 1950s. At that time, they had hundreds of people working on HTP development. There was no way one lone PhD student could hope to match the resources

dedicated to the problem back then. Fortunately, the release of documents by RO provided access to these early results. Experimental results with the updated RO catalyst are reported below.

5.2.4.1. Type-6 (Edwards AFB)

Collaboration with my colleagues at USAFA brought me into contact with Dr. John Rusek at the USAF Edwards AFB in California. The recent increase in industry interest in HTP (as described in Chapter 4) led Dr. Rusek to establish a loose co-ordination group (dubbed "Jabberwocky") which includes dozens of HTP researchers connected via the Internet. He was working on developing a cheap, reliable catalyst material that had the potential to solve the problems noted during Phase 1. He used a straight-forward chemical process to deposit $KMnO_4$ onto a molecular sieve material. A sample of his catalyst was received in May 1995 and designated Type-6.

The Type-6 catalyst material consisted of tiny (~1 mm diameter) beads with a slight dusty appearance. The single test with this catalyst type yielded very disappointing results. The HTP gushed through the pack in liquid form. No decomposition was observed. This run was aborted part way through the planned 30 second trial to save HTP. The pack was dismantled following the test and the beads were found to have been effectively turned to powder. Some of the powder had dissolved forming a purple paste in places. No further tests with Type-6 were conducted. The results from these tests were reported back to Dr. Rusek to aid his further research while other options were pursued.

5.2.4.2. Type-7 (updated S-2)

The most important bit of information to come out of the RO reports was the complete specification for their catalyst along with performance data. [Walder 55] describes the Royal Aircraft Establishment (RAE) specification for "very rough" silver-plated nickel gauze, called RPD Spec. S2. This specification is shown in Table 5-4.

Silver Plating Bath	<p>Electrolyte:</p> <ul style="list-style-type: none"> • Silver cyanide 5 gm/litre • Sodium cyanide 72 gm/litre <p>Solution should contain:</p> <ul style="list-style-type: none"> • Silver (metal) 4 gm/litre • Sodium cyanide (free) 70 gm/litre
Operating condition	Room temperature
Time and current density for total area	<p>30 sec @ 4.0 amp/dm²</p> <p>5 min @ 0.8 amp/dm²</p> <p>5 min @ 4.0 amp/dm²</p>
Sintering	Electric furnace at 800° C for 30 min

Table 5-4: RPD Specification for "very rough" silver plating of nickel gauze, RPD Spec. S2.

The S2 catalyst was not designed to provide optimum lifetime, rather it was intended as a standard for determining operating characteristics without excessive expenditure of HTP [Southern 67]. The lifetime of the S2 catalyst was designed for a total throughput of 1.055×10^4 kg/m² (15 lb/in²) [Shufflebotham 57] (which equates to a lifetime of 137 seconds for my catalyst pack design with a

nominal flow rate of 0.1 litre/sec). At least 10 start-ups were expected at this load rate. However, performance data given in [Shufflebotham 57] indicates actual performance was much better in practice with packs using this catalyst giving 20 to 30 start-ups, 30 seconds each, at load factors of around 280 kg/m²/sec (0.4 lb/in²/sec) before C* dropped below 92%.

Based on these reported results, I set about having this circa-1950s specification updated to the 1990s. With help from Mr. Richard Brown of Project Machinery, we held several meetings with Mr. Kirwood of Electro Hi-Tech. Using the S-2 specification as a starting point, Mr. Kirwood was able to update this process, making some modifications to time and current to achieve an excellent result. This catalyst was designated Type-7. Tests results are reported below.

The direct data from the RO results also reinforced the importance of controlling the initial temperature of the HTP and, to a less extent, the catalyst pack. [Shufflebotham 57] indicates a rough correlation of 1 m/s per 1° C. By pre-heating the HTP tank (with a simple hair dryer) to 20° C an increase in C* of about 2% could be expected. Furthermore, raising the initial HTP temperature may make a big difference in whether or not the catalyst works at all. [Andrews 90] indicates that "in temperate conditions, with a good pack, full decomposition was reached after 0.025 to 0.05 seconds, but at 0° C the starting delay was near 0.5 seconds, and at a temperature between -3° C and -5° C a pack became completely inactive." [Andrews 90] Therefore, temperature was more closely monitored during Phase 2 testing.

A catalyst pack was constructed using Type-7 catalyst consisting of 52 plated disks with 12 blank disks interspersed. Nine 30-second tests and one 20-second test were conducted with the Type-7 catalyst. Overall results were excellent. These results are summarised in Figure 5-6. On the very first test, the exhaust plume "disappeared" as should be expected with super-heated steam. Virtually no white steam was observed on some of the tests. However, the performance did appeared to degrade steadily throughout the trials. In addition, there was a sudden drop in performance between test 45 and 46 which then rebounded on test 47. This result seemed to indicate the pack needs to be "run-in" after being left idle for long periods (there was an approximate 6 week delay between tests 45 and 46). The reason for this performance behaviour could not be fully explained.

Had no other options been available, I would have gladly pressed ahead with hybrid testing using the Type-7 option. However, in parallel with the Type-7 catalyst plating process development, the Type-8 was being developed as a back-up option. These results are reported in the next subsection.

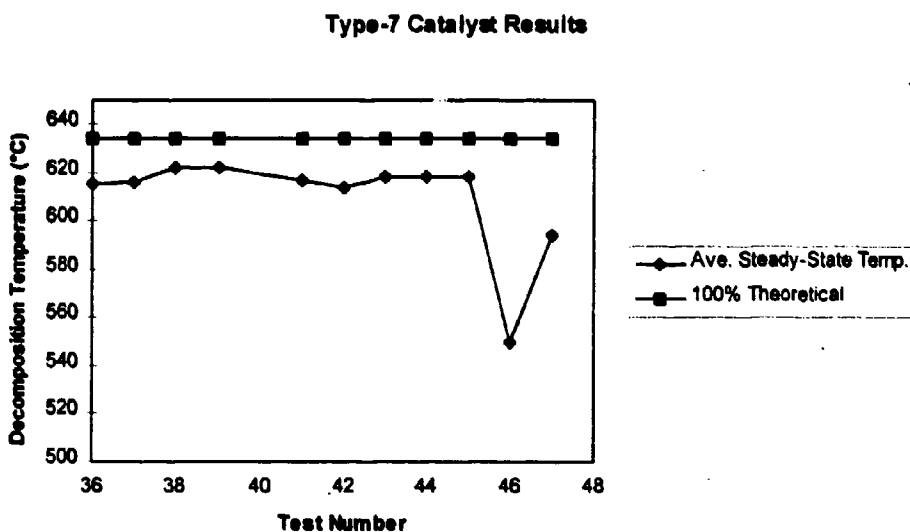


Figure 5-6: Decomposition efficiency results for Type-7 catalyst. Decomposition temperature based on average temperature from first data point >500°C through end of run. (NOTE: Tests #46 and #47 were conducted after a 6 week break.)

5.2.4.3. Type-8 (NASA spec)

What turned out to be one of the most useful references for my work was a June 1963 NASA Technical Note by Runckel, et al entitled "Investigation of Catalyst Beds for 98% Concentration Hydrogen Peroxide." [Runckel 63] This detailed report described experimental results using pure silver gauze treated with samarium nitrate as a catalyst for 90% and 98% HTP. While no details were offered describing the actual samarium nitrate treatment process, experimental results described success with both 2% and 10% solutions of the compound. In addition, results indicated better start-up characteristics with 40-mesh than with 20-mesh silver gauze. Furthermore, Runckel reported decomposition efficiencies around 90% with an average bed lifetime of about 2 hours.

With the promise of these results, I set about trying to duplicate the 30 year-old catalyst material. Because no details on the samarium nitrate process were available, I had to improvise. A 5% solution of the compound was prepared and 80 40-mesh pure silver gauze disks were soaked in it for 30 minutes. After vacuum drying, these disks were loaded into the catalyst pack. Every 5 silver disks were separated by 1 plain stainless steel disk. Even with the stainless steel disks, the pure silver pack compressed far more than silver-plated nickel disks. To make up for additional space, 25 used Type-2 disks were added to the aft end of the pack.

Figure 5-7 summarises results from the first eight of these tests. Subsequent tests were interspersed with hybrid tests so their throughput lifetime is effected by this additional usage. Figure 5-7 shows the efficiency of the Type-8 catalyst as measured by decomposition temperature. As the plot indicates, the efficiency actually improved somewhat with time. It was not possible to determine the final lifetime of this catalyst type due to lack of HTP. (It did not seem prudent to simply waste

unknown quantity of HTP in order to see how long the catalyst would eventually last.) Instead, I elected to resume hybrid testing using this catalyst to complete the characterisation of hybrid combustion.

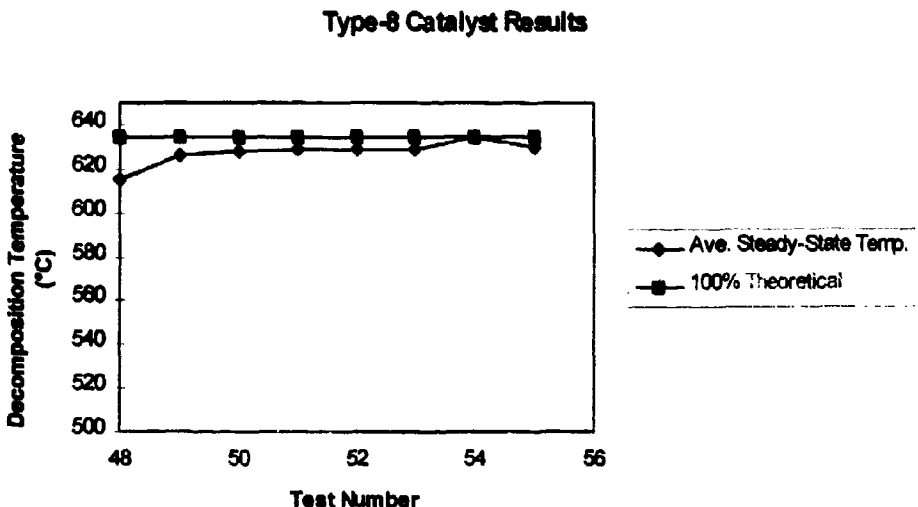


Figure 5-7: Decomposition efficiency results for Type-8 catalyst. Decomposition temperature based on average temperature from first data point >500°C through end of run.

5.2.5. Catalyst Testing Conclusions

Despite several initial difficulties, two effective and reliable catalyst materials were identified by the research. These are the Type-7 and Type-8 specifications. Figure 5-8 effectively summarises the entire catalyst development effort. The graph illustrates the relationship between efficiency and lifetime for the most active catalysts tested. The data indicates that both Type-7 and Type-8 offer superior performance with long life. Of these, the Type-8, samarium oxide treated silver, was best. It should be noted that the "dip" in performance of the Type-7 catalyst at the right side of the graph came after 6 weeks of program down-time while the catalyst was left in the catalyst pack at J-4 site. Following an initial low-performance run, it quickly regained its performance. It seems the pack needs to be "run-in" after long periods of inactivity. This is most likely due to natural oxidation of the silver over time which is largely removed by flushing with HTP. Unfortunately, due to the cost of HTP, it was not feasible to run either catalyst "to death." Thus, actual lifetime was not determined.

Given the performance demonstrated by this data, it is reasonable to baseline a spacecraft catalyst pack system using the Type-8 catalyst.

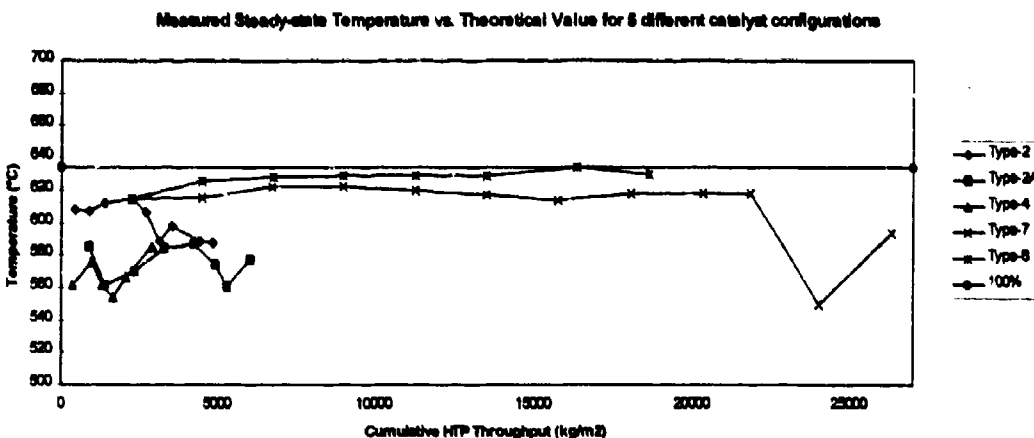


Figure 5-8: Summary of catalyst pack development tests.

5.3. Hybrid Performance Characterisation

This section addresses the second hybrid research program objective, that of experimentally characterising the HTP/PE combustion process. The aim was to derive the all-important regression rate equation which governs the relationship between oxidiser flow rate and fuel regression. Armed with this function, realistic hybrid upper stage design calculations and performance estimations could be derived. The overall program schedule was presented earlier in the chapter. Table 5-5 highlights important schedule milestones during hybrid testing.

The following subsections will summarise the results from experimental hybrid testing. The regression rate data derived from the research will be compared to empirical results presented in Chapter 4. Following this discussion, the remarks section will highlight additional interesting results that emerged from the program, including the issue of post-combustion chambers, re-start and throttling capability as well as combustion uniformity and stability. Finally, these experimental results will be used to develop a hybrid upper stage design process which will be applied to an example minisatellite mission in order to evaluate performance costs.

Date	Test	Comments
28 November 1994	Hybrid Test 1	<ul style="list-style-type: none"> • Good combustion • Catalyst—Type 2
6 December 1994	Hybrid Test 2	<ul style="list-style-type: none"> • Slightly wet start • Catalyst—Type 2
7 February 1995	Hybrid Test 3	<ul style="list-style-type: none"> • Good combustion • Catalyst—Type-4A
10 February 1995	Hybrid Test 4	<ul style="list-style-type: none"> • Unreliable ignition • Catalyst—Type-4A • Re-start capability demonstrated
22 February 1995	Hybrid Test 5	<ul style="list-style-type: none"> • Failed ignition due to unreliable catalyst • Catalyst—Type-4A
23 February 1995	Hybrid Test 6	<ul style="list-style-type: none"> • Failed ignition due to unreliable catalyst • Catalyst—Type-4A
8 August 1995	Hybrid Test 7	<ul style="list-style-type: none"> • Good combustion • Catalyst—Type-8
8 August 1995	Hybrid Test 8	<ul style="list-style-type: none"> • Good combustion • Catalyst—Type-8
8 August 1995	Hybrid Test 9	<ul style="list-style-type: none"> • Good combustion • Catalyst—Type-8 • Post-combustion chamber added
6 September 1995	Hybrid Test 10	<ul style="list-style-type: none"> • Good combustion • Catalyst—Type 8
7 September 1995	Hybrid Test 11	<ul style="list-style-type: none"> • Good combustion • Catalyst—Type-8
7 September 1995	Hybrid Test 12	<ul style="list-style-type: none"> • Good combustion • Catalyst—Type-8

Table 5-5: Summary of hybrid testing milestones.

5.3.1. Discussion

Table 5-6 summarises important data from the 9 successful hybrid tests. As noted in Table 5-5 in the previous section, tests 4, 5 and 6 demonstrated unreliable or complete lack of ignition due to poor catalyst performance and are therefore excluded from analysis. Test 4, however, was useful in demonstrating re-start capability as discussed in the following section.

Fuel regression rate was determined by measuring the difference in mass of the fuel rod before and after firing. From this information, and a knowledge of the pre-combustion port geometry, an average regression rate was derived by dividing the average change in radius by the combustion time. Unfortunately, from an experimental standpoint, one of the greatest difficulties encountered was determining the actual combustion time. The very slow sampling rate (approximately 0.5 Hz) of the low-cost data collection system used made it difficult to measure the precise time of fuel ignition. With relatively short burns (15 - 20 sec), a difference of even 1 second can be significant. The actual combustion times used represent a best estimate based on the data sampled, cross-checked by reviewing the video tape of the firing. To resolve this problem and better characterise start-up conditions, a high speed (1000 Hz) system was added to record chamber pressure for tests 7, 9, 10 and 11. These results will be addressed in the remarks section.

Despite the few instances of poor ignition and the data collection system drawbacks, the overall results of hybrid testing were excellent. Combustion efficiency as measured by C^* averaged greater than 90% over a wide range of O/F. With a good catalyst, combustion was quite reliable with an ignition delay of 1 to 2 seconds.

With the exception of the flow meter which was replaced by the simpler, more reliable cavitating venturi, all system components functioned nominally. The nozzle far outperformed expectations. Two nozzles were purchased with the expectation that one would wear out or fail after repeated firings. However, I was pleasantly surprised by the overall robustness of the graphite/pyrolytic graphite nozzle insert. Despite often abusive handling during the fuel rod extraction process, the same nozzle insert was used for all firings with virtually no sign of damage or wear. This is extremely encouraging from the standpoint of designing a flight nozzle which would be subjected to large temperature extremes and hard vacuum in the harsh space environment. It is quite possible that a similar, low-cost nozzle insert could be adapted for satellite applications.

Test	Init. Port Radius (m)	Burn Time (sec)	Steady-state P _c (bar)	Oxidiser mdot (kg/s)	Total mdot (kg/s)	G _{ex} (kg/m ² /sec)	G _{total} (kg/m ² /sec)	Average regression rate (10 ⁻⁴ m/s)	Ave. O/F	C* (m/s)	Theoretical C* (m/s)	% eff.
1	12.60	17.8	18.1	0.144	0.162	160.6	179.9	0.486	8.3	1482.2	1575	94%
2	12.60	16.9	16.9	0.155	0.170	241.8	265.4	0.502	10.2	1320.4	1522	87%
3	8.33	13.2	18.9	0.162	0.180	319.8	354.9	0.662	9.1	1395.4	1554	90%
7	12.60	17.3	16.1	0.142	0.157	168.4	186.4	0.437	9.4	1362.7	1554	88%
8	8.33	18.6	17.5	0.161	0.161	255.2	282.8	0.550	9.3	1446.8	1554	93%
9	8.33	18.3	18.2	0.143	0.164	222.4	255.7	0.653	6.7	1472.4	1568	94%
10	12.60	17.8	16.3	0.144	0.159	171.5	188.8	0.421	9.9	1366.4	1522	90%
11	8.33	18	19.3	0.163	0.181	271.1	300.9	0.612	9.1	1413.0	1554	91%
12	12.60	17.9	17.6	0.153	0.168	179.3	197.0	0.434	10.1	1389.9	1522	91%

Table 5-6: Summary of experimental results from hybrid testing. Note that Test 9 included a post-combustion chamber.

Figure 5-9 plots the average fuel regression rate vs. the total mass flux. The numerically derived regression equation is also shown. Note that for consistency, these results exclude test 9 which included a post-combustion chamber. This classic form of the equation is

$$\dot{r} = aG_{total}^n$$

Eqn. 5-2

where

$$a = 0.0205$$

$$n = 0.5869$$

G_{total} = total mass flux (kg/m²/sec)

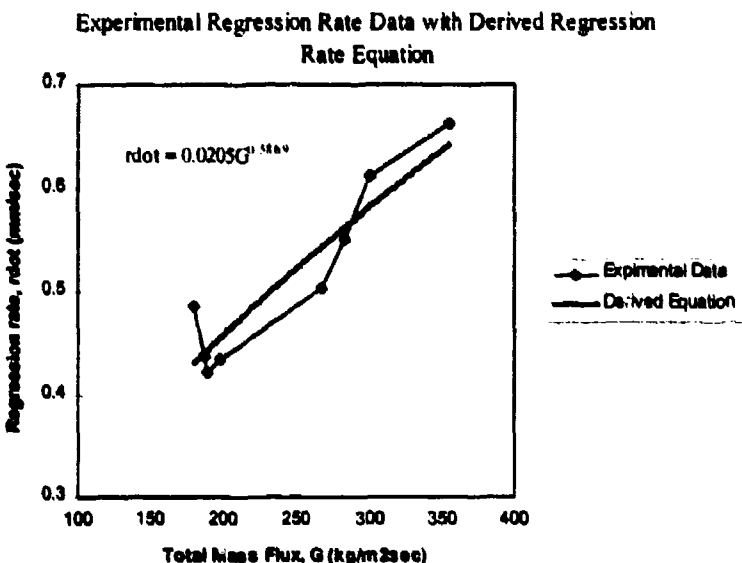


Figure 5-9: Summary of regression rate results. Plot shows measured regression rate data vs. the regression equation derived from this data.

As discussed in Chapter 3, it is sometimes more useful from a design standpoint to use the other form of the regression equation which relates regression rate only to oxidiser flux. This data is plotted in Figure 5-10 along with the numerically derived function which is also repeated in Eqn. 5-3.

$$\dot{r} = 0.0223G_{ox}^{0.5819} \quad \text{Eqn. 5-3}$$

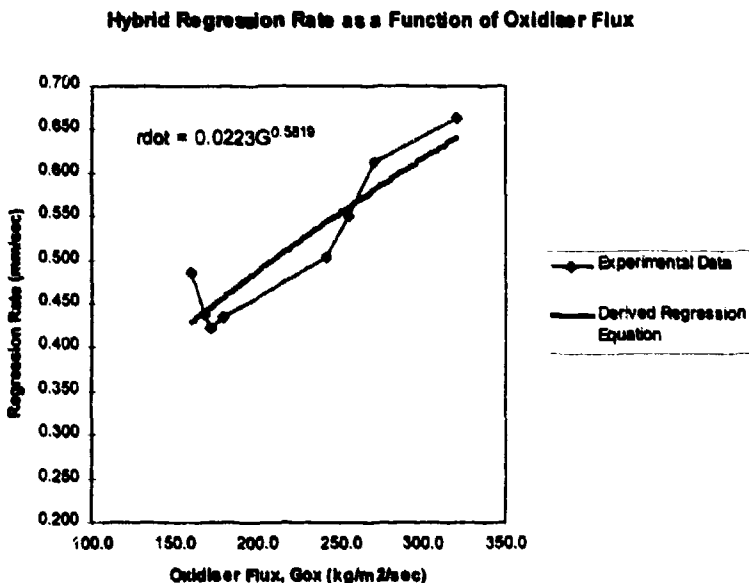


Figure 5-10: Regression rate results plotted vs. oxidiser flux. This form of the equation is somewhat more useful for motor design calculations.

Chapter 5: Hybrid Program Results

Now that a regression rate relationship has been experimentally derived, it is important to examine its validity. As discussed in Chapter 4, prior to my work there was only one other published report of HTP/PE hybrid results, Moore/Berman in 1956 [Moore 56]. Unfortunately, their results were insufficiently detailed and could only be used as a rough order of magnitude comparison for design parameters. As a result, the primary argument for the validity of my regression rate equation is the close agreement with theoretical results as evidenced by the generally high (>90%) combustion efficiencies (measured vs. theoretical C*).

However, for purposes of discussion, it is interesting to compare my results with the interpolated results of Moore/Berman. In addition, as noted in Chapter 4, Wernimont at Purdue University in the USA has been examining this same hybrid combination in parallel. Figure 5-11 plots my results along with Moore/Berman and two results from Wernimont [Wernimont 94] [Wernimont 95] published concurrently with my own. As the graph indicates, my results appear to agree more closely with Moore/Berman than do either of Wernimont's. The derived regression rate exponent of 0.5977 compares more favourably with Moore/Berman's result of 0.45 than Wernimont's values of 0.88 and 0.8 respectively.

It is interesting to note that the regression rate from [Wernimont 95] is somewhat lower than [Wernimont 94] and from Moore & Berman's results. Wernimont explains the higher regression rates of his earlier results by saying that it is "probably a result of shorter burn times used (with the earlier work of about 4 sec) in which the ignition device (catalyst pack) would have more of an influence." [Wernimont 95] However, the relatively short start-up transients (on the order of < 0.05 sec) reported with both results should imply that start-up conditions reach steady state very quickly even for a short burn which seems incongruous with the explanation. Furthermore, he offers no explanation for his relatively large differences with Moore & Berman.

I would offer that the higher regression rate reported in [Wernimont 94] is possibly a result of using slightly higher concentration of HTP than with his later results (88% HTP rather than 85%). No explanation is offered for this change in percentage. Another explanation which also addresses the somewhat low combustion efficiencies is simply a lower efficiency catalyst pack.

From this discussion, I would conclude that the regression rate relationship derived from my work is valid. Furthermore, it is, in fact, the most reasonable data currently available. Therefore, this data can be confidently used for preliminary upper stage design work with reasonable accuracy.

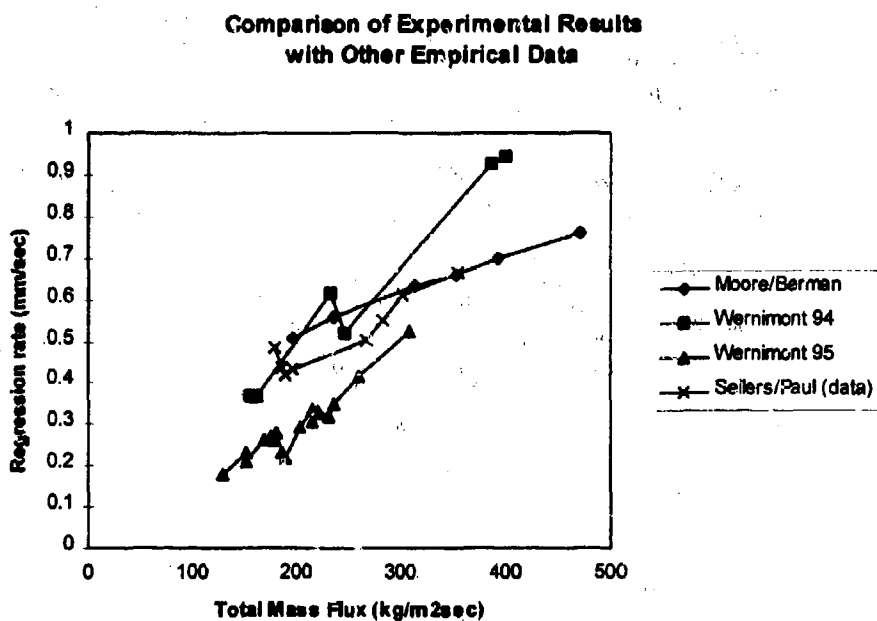


Figure 5-11: Comparison of regression rate data. Plot shows results from Moore/Berman and Wernimont [Wernimont 94] and [Wernimont 95] vs. our experimental data.

5.3.2. Remarks

This section will summarise various performance-related observations that emerged during the hybrid test program. These include combustion uniformity and stability, the efficacy of post-combustion chambers, re-start demonstrations and experience with throttling and alternate fuels.

5.3.2.1. Combustion Uniformity

Recall from Chapter 4 the summary of conclusions from Moore & Berman's work [Moore 56] which commented on the uniformity of combustion for the HTP/PE. My own results confirm this observation. Figure 5-12 shows sectioned fuel rods from tests 11 and 12. As you can see, the port widens slightly at the injector end (left-hand side of photo) but overall regression is quite uniform. This implies good homogeneous mixing along the length of the port which means regression rate is a weak function of length along the port. This important feature of the combustion process supports the validity of the derived regression rate equation and lends credibility to using it for preliminary upper stage designs.

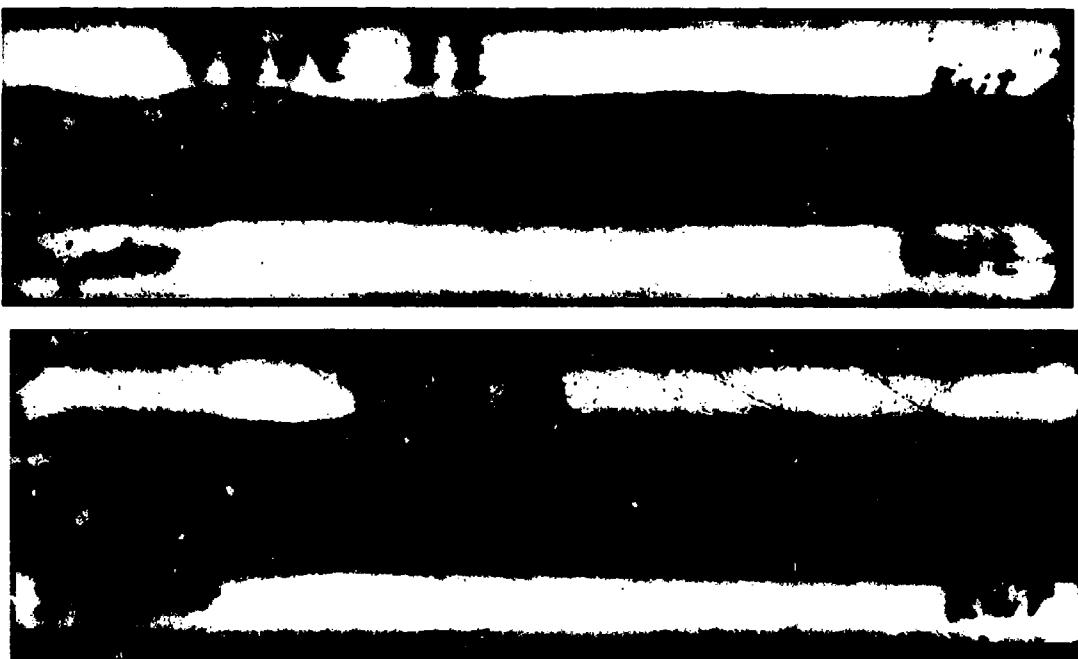


Figure 5-12: Cross-sectional views of spent fuel rods showing the overall uniformity of combustion.

5.3.2.2. Start-up Characteristics

To better understand and characterise hybrid start-up characteristics, a high speed data collection system (1000 Hz) was added in parallel with the primary system to measure chamber pressure for tests 7, 9, 10, 11 and 12. Figure 5-13 shows the plots from the four runs for which this system was available. These graphs indicate dimensionless chamber pressure as a function of time. Notice similar start-up characteristics for each run. As the HTP control valve is opened, pressure tends to spike as the catalyst reaction begins. A transient steady-state condition is then reached as the catalytic reaction stabilises. Once sufficient pressure and, probably most important, temperature is reached, fuel ignition begins as evidenced by the second well-defined pressure spike. This entire process took up to nearly 3 seconds in some cases.

Recall, Moore/Berman [Moore 56] noted start-up delays of only around 0.5 second. I cannot completely explain the relatively large difference with my own results. However, I would offer that for my experiments, no effort was made to raise the initial temperature of the HTP or the catalyst pack. Anecdotal evidence offered by [Brown 96] suggests that this start-up delay can be significantly reduced by first "priming" the catalyst pack with a short duration pulse of HTP to raise its initial temperature. This operation was not attempted for my experimental runs. While start-up characteristics are important to understand for future space applications, the fact that the delay itself may be relatively long (a few seconds) is less important than being able to predict its effect. For relatively long hybrid firings in support of large ΔV missions, a few seconds start-up delay would not present significant operational concerns.

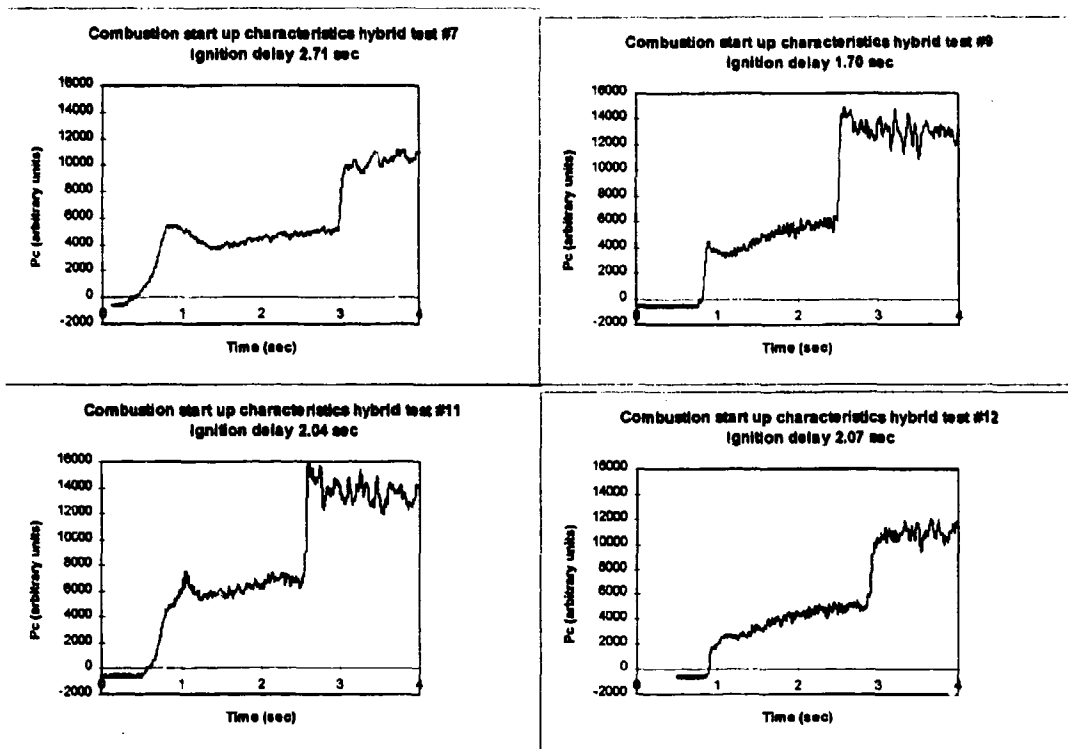


Figure 5-13: Hybrid combustion start up characteristics represented by chamber pressure for hybrid tests 7, 9 - 11. Data was captured at 1000 Hz.

5.3.2.3. Re-start

The capability to reliably re-start a hybrid motor is one of its principle operational advantages over a solid motor. By splitting a large burn into several smaller ones, the overall margins imposed on the orbit determination and pointing system are wider and easier to meet. In other words, margin for error is introduced such that if determination or pointing is slightly off during the first portion of the burn, there is an opportunity to correct it during the next portion. This, of course, is impossible with a solid motor. Being able to re-start a hybrid also allows for the simple fact of orbital mechanics that dictates for large orbit manoeuvres that two separate manoeuvres be done: one to raise (or lower) apogee, the other to raise (or lower) perigee. Again, missions relying on solid motors (such as FREJA described in Chapter 6) must use two separate solid motors in order to carry out the desired orbit change. The same manoeuvre can easily be done with a single, re-startable hybrid motor.

Hybrid motor re-start is identical to initial start-up. The only difference is the initial size of the port which changes initial *O/F* and *L/D*. However, if a hybrid motor is designed to do a total ΔV of 200 m/s, for example, from a performance standpoint, there would be little impact to dividing this into 4, 50 m/s burns. The primary concern would be in efficiency losses during start-up phase which would accumulate over the total number of start-ups. However, for a reasonably long total burn time (on the order of 2 minutes for a 200 m/s ΔV motor) split into a few start-ups (~ 4) this effect would be insignificant compared to the gain in operational flexibility.

Re-start capability was demonstrated during hybrid test #4. As noted, earlier this particular test exhibited unreliable ignition due to problems with the catalyst pack. Therefore, because the ability to reliably measure regression rate was already compromised, this test was used to demonstrate re-start. No problems specific with re-start were noted. In fact, because the start/re-start sequence was relatively close in time (on the order of a few minutes) the catalyst pack was still quite warm making the re start somewhat faster than the initial start-up.

Based on this experimental experience, it is quite reasonable to plan a series of burns with a hybrid upper stage motor. Ideally, the operational mode for a given upper stage design would be defined initially allowing for the actual sequence of firings to be tested sufficiently to enable reliable modelling and performance prediction.

5.3.2.4. Combustion Stability

Another important feature of any type of rocket motor combustion is stability. [Greiner 93] provides a good introduction and overview of the literature pertaining to the combustion instability problem as applied to hybrids. [Jenkins 95] provides a theoretical basis for modelling its causes.

While some localised variation in combustion chamber pressure is inevitable due to the dynamic nature of the process, large variations are undesirable because of the potential effects on performance and the danger of interaction with the natural frequency of the oxidiser delivery system or other system components. In liquid booster systems, such instabilities have led to the so-called "Pogo" effect. Classically, a rocket motor is said to present unstable combustion if the steady state chamber pressure oscillates by greater than 5% to 30%. For hybrid motors, instabilities have most often been noted in relative low frequency range (0 - 1000 Hz). Greiner notes four potential causes of instabilities in hybrid rockets:

1. Incomplete atomisation and mixing of the oxidiser
2. Chuffing—periodic accumulation and breaking off of char or melted layers of the fuel surface
3. Pressure-coupled combustion instabilities (nominally, regression is only very weakly dependent on pressure but localised boundary layer effects can increase this dependence)
4. Vortex shedding—vortices are formed in shear layers between high and low speed streams. This can occur in regions of sudden expansion such as near the injector and in post-combustion chambers.

The conclusion of Greiner's study was that, overall, little research has been done to fully characterise combustion instabilities in hybrids. Certainly, in the case of my work, this was not the major focus. Furthermore, the high speed nature of the phenomenon (up to 1000 Hz) made it impossible to capture with the low speed data collection system used.

However, as discussed above, a high speed data collection system (1000 Hz) was added in parallel to the primary system for the last few runs of the test series to measure chamber pressure. While the original purpose of having access to the high speed data was to provide better insight into the hybrid

start-up process, this data also provides some initial clues to the instability problem. Note from Figure 5-13 that while tests 7 and 12 appear to be relatively stable, tests 9 and 11 exhibit pressure fluctuations that approach 15%. While characterising this instability was not the focus of the program, it is important to note that potential instability modes have been identified. Future work aimed at specific upper stage applications need be aware of this potential problem and seek to avoid or mitigate its effects.

5.3.2.5. Post-Combustion Chambers

According to [Humble 95], a simple straight tube combustion port may not provide sufficient mixing of products to insure complete combustion. To enhance mixing, designers can undertake any one or combination of the following options:

1. Add length to the motor (increase L/D)
2. Provide a physical mixing surface (vortex generators)
3. Use a submerged nozzle
4. Inject a gas or more oxidiser at the end of the combustion chamber

From a practical engineering standpoint, the easiest approach is to increase the length of the motor and submerge the nozzle by adding an aft mixing chamber (sometimes called a *post-combustion chamber*) with an L/D of 0.5 to 1.0.

To investigate the effect a post-combustion chamber would have on the combustion process, one was added for hybrid test #9 to measure the difference in performance. The simplest means of doing this was to drill out a section at the aft end of the fuel rod, 5 cm diameter by 2.5 cm deep. To allow for true comparison, test #8 was identical in all respects except for the addition of the post-combustion chamber. Table 5-7 repeats the performance summary data for these two tests. Note that there was no significant effect on overall combustion performance. The primary effect was on O/F ratio which shifted from 9.3 to 6.7. From this data I would conclude that our initial L/D was sufficient to provide adequate mixing such that the post-combustion chamber made no measurable increase to efficiency. However, for shorter motors, especially for multi-port configurations, the post-combustion chamber may be essential to ensure adequate mixing.

Test	Init. Port Radius (m)	Burn Time (sec)	Steady-state P_c (bar)	Oxidiser mdot (kg/s)	Total mdot (kg/s)	G_{ox} (kg/m ² /sec)	G_{total} (kg/m ² /sec)	Average regression rate (10^{-4} m/s)	Ave. O/F	Measured C* (m/s)	Theoretical C* (m/s)	% eff.
8	8.33	18.6	17.5	0.145	0.161	255.2	282.8	0.550	9.3	1446.8	1554	93%
9	8.33	18.3	18.2	0.143	0.164	222.4	255.7	0.653	6.7	1472.4	1568	94%

Table 5-7: Post-combustion chamber effects. Tests 8 and 9 were identical except for the addition of a post-combustion chamber for test 9.

5.3.2.6. Alternate Fuels

As discussed in Chapter 4, virtually any polymer is a potential hybrid fuel. Perhaps the most widely used hybrid fuel has been hydroxyl-terminated polybutadiene (HTPB). This compound is basically common rubber. In practice, the HTPB is prepared as a soft dough-like compound. It is then poured into moulds and allowed to harden. This is a relatively simple industrial process requiring only a few basic kitchen-like tools such as a standard food mixer. Table 5-8 compares the theoretical combustion parameters for HTPB vs. PE. As you can see, their performance is essentially the same (less than 1% difference).

Parameter	PE	HTPB
C^* (m/s)	1575.1	1567.2
Isp (sec)	319	322

Table 5-8: HTPB vs. PE performance comparison assuming 85% HTP, 17.5 bar P_o , O/F = 8 and 150:1 vacuum expansion.

However, HTPB has several potential integration and operational advantages over PE as a hybrid fuel:

- *Flexible Port geometry*—because HTPB can be cast into a variety of shapes it is far easier to form complex port geometries (wagon wheel, double-D, etc.).
- *Increased fuel performance*—Flexibility to supplement the basic composition of the fuel through the use of additives. Carbon black, for example, has been added to fuel rods made at the Air Force Academy to enhance radiative heat transfer during combustion. Aluminum powder or other metals can also be added, increasing the combustion temperature and thus performance.
- *Higher regression rate*—because HTPB is significantly softer and more volatile than PE, it sublimes and combusts faster giving a higher overall regression rate which can be useful for some applications.

Despite these basic advantages, PE was chosen for proof-of-concept testing for the reasons discussed in Chapter 4. However, as part of on-going co-operative research with RO, there was an opportunity to do some limited testing with HTPB. RO is primarily interested in tactical applications for hybrid technology. Their facility at Stevenage, UK already has the equipment for doing HTPB casting as part of their work with solid motors. To help jump-start the RO hybrid program, we agreed to do some initial tests with HTPB to demonstrate basic combustion potential and throttling capability. Their test rig was modelled after my own, so the combustion chambers were of identical dimension, allowing an HTPB fuel rod to be easily inserted and removed. Figure 5-14 shows the computed regression rate for the two HTPB runs for which data was collected. As expected, the HTPB demonstrated significantly higher regression rate than PE. Unfortunately, due to lack of time and supply of HTPB rods, it was not possible to fully characterise its regression rate equation. However, these results have been partially corroborated by anecdotal data from [Brown 96].

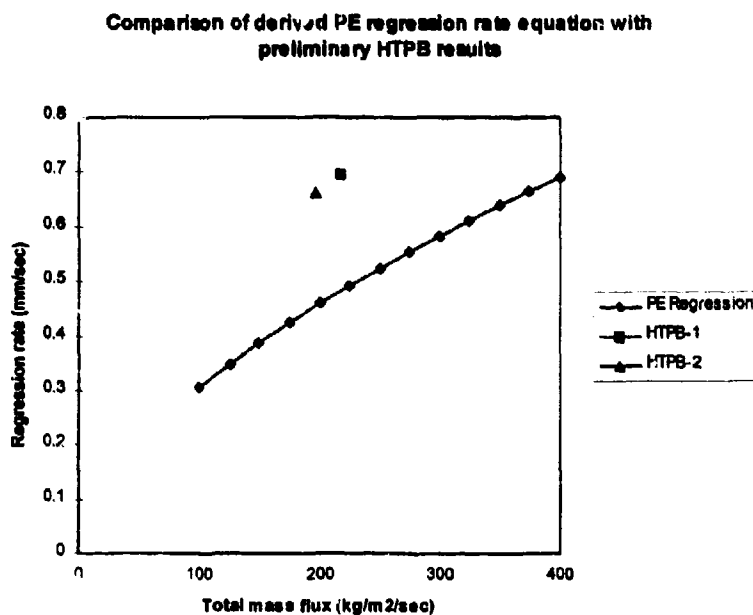


Figure 5-14 Comparison of derived PE regression rate relationship with preliminary results from HTPB testing. Note the significantly higher regression rate for HTPB.

Future research aimed at developing an upper stage motor would probably use HTPB or a similar derivative. Special attention needs to be given to selecting a particular fuel with known outgassing properties in order to comply with launch agency requirements as discussed in Chapter 2. The cost and time necessary to develop the in-house capability to cast HTPB motors would not add significantly to the overall program schedule and brings all the advantages discussed above.

However, one potential disadvantage of HTPB was noted during our preliminary work with this fuel. Subjective assessment of the combustion characteristics of PE vs. HTPB indicates the HTPB produces far more particulate in the form of black smoke and other residue than the cleaner burning PE. This could be an important integration issue for this fuel as it may lead to contamination of spacecraft sensors and solar panels. Quantifying the extent of this problem would be part of the full-scale development program for a hybrid upper stage.

5.3.2.7. Throttling

As part of the HTPB tests conducted for RO, the feasibility of throttling a hybrid motor was also evaluated. Work cited in Chapter 4 [Willis 60] indicates that 10:1 throttling of hybrids is possible with only about 10% loss in efficiency. This capability is one of the primary advantages of hybrids over solids for tactical applications. To demonstrate the proof-of-concept for this capability, the oxidiser delivery system was modified to allow a decrease in flow rate in order to reduce chamber pressure and thrust. Figure 5-15 shows the results from this test. A 3:2 throttling capability was achieved with a relatively crude flow reduction system.

While the ability to throttle has little practical use for upper stage applications, the success of these tests was greeted with enthusiasm by the tactical hybrid researchers. Perhaps most significant, these tests further demonstrates the inherent flexibility of this versatile technology.

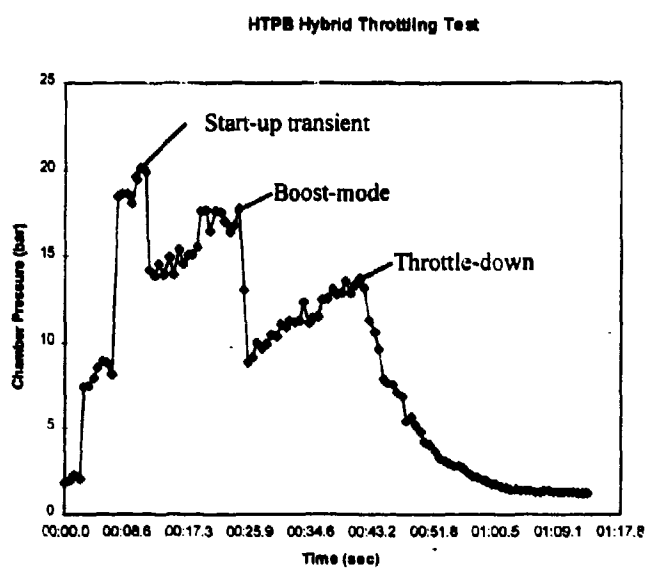


Figure 5-15: Throttling experiment using HTPB fuel. Plot shows chamber pressure, P_c , over time. Throttle down occurred at approximately 24 seconds as evidenced by the 30% reduction in P_c .

5.3.3. Upper Stage Motor Design

As described in Chapter 3, the reliable estimation of hybrid motor performance depends on empirical data, specifically the regression rate equation. Determining that equation was one of the primary objectives of the hybrid research. This relationship can now be used to develop a process for designing spacecraft motors. Along with the regression rate equation, two other tools are also needed:

1. Models of thermochemistry parameters.
2. Simulation of fuel regression and other parameters during the course of a burn.

The first of these can be derived using data produced by the *Isp* program. Figure 5-16 shows the relationship between O/F and *Isp* for an 85% HTP/PE hybrid. This combination was chosen to correspond to data derived during the test program.

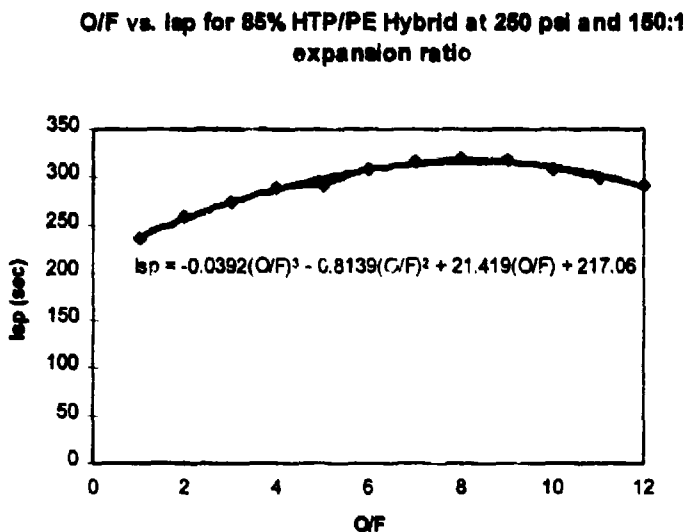


Figure 5-16: Relationship between O/F and Isp for 17.5 bar (250 psi) chamber pressure, 150:1 expansion and 85% HTP. Darker line indicates derived 3rd order polynomial relationship between the parameters used in simulation results.

From this data, a polynomial approximation of *Isp* vs. *O/F* can be derived as follows:

$$Isp = -0.0392(O/F)^3 - 0.8139(O/F)^2 + 21.419(O/F) + 217.06 \quad \text{Eqn. 5-4}$$

This relationship, along with the regression rate equation and other fundamental rocket equations, can then be used to develop a simulation tool as called for above. The entire design process is summarised in Table 5-9. For the simulation described in Step 4, I developed a simple tool using a Microsoft Excel spreadsheet running a Newton-Raphson iteration scheme. Details of this simulation algorithm are summarised in Table 5-10.

Table 5-11 summarises the results of applying this process to a sample mission with the following requirements:

- Deployed spacecraft mass = 250 kg
- HTP concentration = 85%
- Maximum thrust = 400 N
- Maximum motor length = 0.3 m
- Average O/F = 8 (for optimum performance)
- Initial L/D = 25

It is interesting to highlight two important results from this process. Figure 5-17 shows the O/F shift that occurs during a 120 second burn and Figure 5-18 the change in regression rate. These results illustrate the necessity for numerical analysis. An analytic approach must assume average values for these parameters. The numerical simulation allows these parameters to be modelled much more accurately. These results indicate the real performance costs for a typical hybrid motor.

Design Step	Outcome
1: Define mission requirements & design goals:	<ul style="list-style-type: none"> Total ΔV Deployed spacecraft mass HTP concentration Maximum thrust Maximum motor length Average O/F
2: Assume initial values	<ul style="list-style-type: none"> Chamber pressure, P_c Motor configuration (e.g. tube, Double-D, etc.) Initial port radius Oxidiser flow rate Initial L/D Expansion ratio, ϵ
3: Derive I_{sp} vs. O/F relationship	<ul style="list-style-type: none"> Eqn. 5-4 (for example)
4: Iterate using simulation (see Table 5-10)	<ul style="list-style-type: none"> Actual oxidiser flow rate Actual average O/F, I_{sp} Actual average thrust Total burn time Total propellant required
5: Continue analytic modelling	<ul style="list-style-type: none"> Actual nozzle dimensions Total motor dimensions
6: Compare results to Step 1 and iterate if required	

Table 5-9: Summary of steps in the hybrid motor design process.

Iteration step	Equation
Compute instantaneous port radius, r	$r_{i+1} = r_i + \dot{r}\Delta t$
Compute oxidiser flux, G_{ox}	$G_{ox_{i+1}} = \frac{\dot{m}_{ox}}{\pi r_{i+1}^2}$
Compute regression rate, \dot{r}	Eqn. 5-3
Compute fuel mass flow rate, \dot{m}_{fuel}	$\dot{m}_{fuel_{i+1}} = \frac{(r_{i+1}^2 - r_i^2)\pi L \rho_{fuel}}{\Delta t}$
Compute O/F	$(O/F)_{i+1} = \frac{\dot{m}_{ox}}{\dot{m}_{fuel_{i+1}}}$
Estimate I_{sp}, c	I_{sp} per Eqn. 5-2 $c_{i+1} = I_{sp_{i+1}} g_0$
Compute thrust, F	$F_{i+1} = \dot{m}_{i+1} c_{i+1}$
Compute cumulative oxidiser & fuel mass consumed	$m_{i+1} = m_i + \dot{m}_{ox} \Delta t + \dot{m}_{fuel_i} \Delta t$
Update spacecraft mass	$s/c_mass_{i+1} = s/c_mass_{init} - m_{i+1}$
Compute cumulative ΔV	$\Delta V_{i+1} = \Delta V_i + c_i \ln \frac{s/c_mass_i}{s/c_mass_{i+1}}$
Increment step	$t_{i+2} = t_{i+1} + \Delta t$

Table 5-10: Hybrid motor design simulation algorithm and governing equations.

Chapter 5: Hybrid Program Results

Parameter	Value
Initial port radius (m)	0.008
Initial L/D	25
Ave. Isp (sec)	299.6
Ave. O/F	8.4
Total propellant mass (kg)	16.5
Fuel mass (kg)	1.8
Oxidiser flow rate (kg/s)	0.123
HTP volume (litre)	10.8
Ave. Thrust (N)	404
Thrust time (sec)	120
Total impulse (Ns)	48,480
Throat diameter (m)	0.0062
Expansion Ratio	150:1
Nozzle length (m)	0.268
Motor length (m)	0.25

Table 5-11: Results of spacecraft hybrid motor design exercise. Performance is assumed to be 95%. Port geometry is assumed to be "double-D."

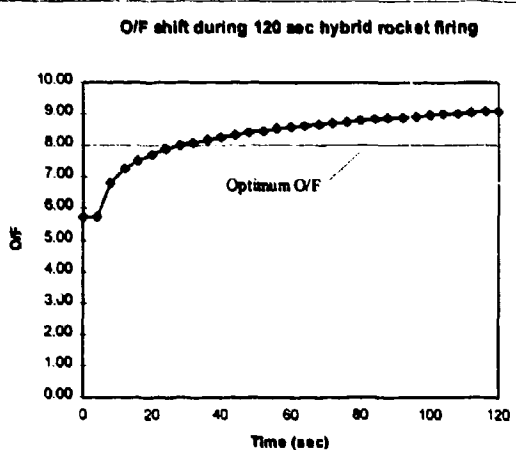


Figure 5-17: O/F shift during 120 sec hybrid rocket firing.

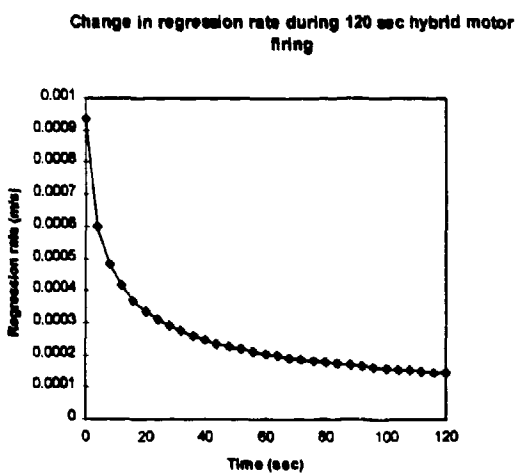


Figure 5-18: Simulation results for regression rate change during a 120 sec hybrid motor firing.

5.4. Hybrid Cost Analysis

With realistic performance costs established in the previous section, we can now turn to address the price and mission costs for hybrid motor technology. The assessment of these costs is based on my own engineering judgement, tempered by two years of detailed hybrid research and hands-on experience with HTP handling and hybrid testing. Mr. Malcolm Paul collaborated in this costing exercise.

5.4.1. Motor Price

Motor prices were estimated based on rapid development of an engineering model for qualification testing in parallel with construction of the flight article. The primary differences between the two would be in the way the nozzle is integrated. Ease of qualification testing would dictate a removable nozzle (e.g. bolted flanges) while the flight article would be of all-welded construction. This development program assumes continued access to J-4 site at RO and is "success oriented," in that no significant development problems are anticipated. Program costs are summarised in Table 5-12. As you can see from the bottom line, even with the significant head-start given to the program by my own work, an additional £60,000 investment would be needed along with over two man-years of effort. However, this is for the first flight article. Subsequent flight articles of identical design would cost approximately £15,000 with a requirement for about 5 man-months for fabrication, assembly and testing. Significant deviations from the base-line design would require additional qualification testing adding to the cost.

Program Requirement	Man-Power	Monetary Cost
Facilities Improvement:		
• Test Rig Upgrade	4 man-months	£5,000
• Data Acquisition System Upgrade		
Consumables (HTP, Fuel and Catalyst Material)	1 man-month	£3,000
Engineering model motor	4 man-months	£4,000
Flight model motor	1 man-month	£6,000
Nozzles (experimental plus flight article)	4 man-months	£10,000
Environmental test facilities:		£10,000
• Vacuum firing chamber		
• Vibration test facility		
Ground Support Equipment	1 man-month	£12,000
Qualification Testing:	12 man-months	£5,000
• 10 start-ups (ambient)		
• 10 start-ups (vacuum)		
• 5 full-duration		
• Vibration testing		
Totals:	27 man-months	£60,000

Table 5-12: Summary of development costs for a proto-flight hybrid motor.

5.4.2. Mission Costs

This section will address the unique mission costs associated with hybrid upper stage motor applications. Technical risk cost will first be discussed, followed by integration, safety and logistics costs.

5.4.2.1. Technical Risk

The first flight of any new propulsion technology creates technical risk for the mission. Fortunately, the inherent nature of hybrids makes the chance of a catastrophic failure extremely low. In addition to the failure scenarios that accompany any chemical system (such as nozzle structural failure or burn-through, causing thrust vectoring and potential loss of control) there are only two significant ones unique to the hybrid configuration:

1. Failure to ignite or very poor ignition
2. Oxidiser contamination leading to run-away decontamination requiring venting of all oxidiser.

Both of which lead to partial or total loss of ΔV capability in the worst case. However, the inherently simple nature of hybrid technology, as demonstrated by this research, indicates the real likelihood of failed or poor ignition is rather low. Experimental results indicate that with a reliable catalyst, ignition is almost assured. Furthermore, the extensive work on catalyst development has shown that both pure silver and specially plated nickel gauze offer reliable options.

Unfortunately, the second failure scenario could not be fully addressed by the research. It is well known that any organic contamination can lead to HTP decomposition. If this decomposition were to begin in a sealed tank, the growing pressure could further fuel the process leading to a run-away condition. To safeguard against this contingency, relief valves would be prudent, set above the operating tank pressure but below the minimum burst pressure. Nevertheless, background information such as [HPHB 67] discussed in Chapter 4 indicates that HTP has been reliably stored in space for years without mishap. To re-gain confidence in this capability, long-term ground storage tests using flight tanks are recommended. Such an experiment is planned to begin in the Spring of 1996 using tanks donated by Arde, Inc. Unfortunately, the data from this experiment will take over one year to accumulate.

Despite these potential failure scenarios, it must be emphasised that the hybrid technology this work has developed is inherently simple. When the oxidiser valve is opened, ignition begins. In operation it is both safe and reliable. Once hybrid technology has overcome the stigma of being untried in space, these inherent features would make its overall technical risk roughly equivalent to mono-propellant technology.

5.4.2.2. Integration Costs

The combined thermal control and ADCS aspects of hybrid motor integration costs would be roughly the same as those discussed for solid motors. Thermal control issues would be somewhat more demanding due the relatively hot ($>600^{\circ}\text{C}$) catalyst pack that would most likely be integrated within the spacecraft. The insulation properties of the fuel would protect the spacecraft from high temperatures in the motor. The nozzle, of course, would have to be fully exposed to space to allow for radiative cooling. Compared to solid motors, ADCS issues would be significantly less demanding because of much lower thrust levels (~400 N vs. ~16,000 N).

In addition, hybrids have a significant overall integration advantage over solids in that the motor can be fully integrated within the spacecraft prior to shipment. Launch site preparation would require only the loading of oxidiser. Figure 5-19 gives a cut-away view of the hybrid motor described earlier installed in the minisatellite structure. The mechanical integration complexity for a hybrid would be similar to a mono-propellant system in terms of overall requirements for support systems (tanks, valves, etc.).

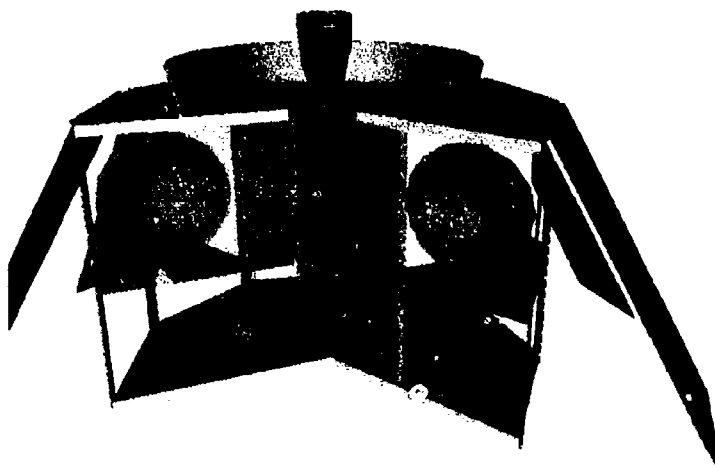


Figure 5-19: Cut-away diagram showing possible configuration of a hybrid motor and support tanks within the minisatellite structure.

5.4.2.3. Safety and Logistics Costs

Safety issues associated with small satellite applications for hybrids arise from two sources:

1. Storage and handling of high pressurant gas
2. Storage and handling of HTP

The first safety issue is not unique to hybrids and must be addressed as part of cold-gas or other liquid propellant options (bi-propellant, mono-propellant or resistojet). As discussed in Chapter 4, procedures and regulations governing high pressure gasses are well established. References such as [MS 1522A] specify design criteria for tanks and lines to ensure safe operation.

The second issue is the most important to address. A fair assessment of the safety aspects of HTP must be done in context with other propellant options such as hydrazine, MMH or MON. Both [CPIA 84] and [HPHB 67] provide extensive background on HTP safety requirements. There is also a 1950s vintage safety film produced by Royal Aircraft Establishment that is both informative and amusing (the viewer is shown the actual effects of using HTP as a hair bleach). Of these, concluding remarks from [HPHB 67] in particular are worth noting:

“The potential safety hazards in dealing with hydrogen peroxide fall into the following general categories: detonation and/or explosion, uncontrolled decomposition, fires, and personnel injury. While these hazards may sound ominous, it must be remembered that similar hazards exist for various other compounds which are in widespread use and safely handled by industry. If operating personnel are armed with knowledge of the potential hazards and how to avoid them, there is no reason why concentrated hydrogen peroxide cannot be safely employed in commercial processes.”

While HTP can cause skin irritation, [HPHB 67] classifies it as non-toxic in sharp contrast to other liquid propellants. This greatly alleviates demands on the necessary safety infrastructure as “respiratory protection is ordinarily not required” [CPIA 84] in sharp contrast to hypergolics which, as Chapter 4 describes, require the use of full SCAPE suits. For HTP handling, much less expensive and complex vinyl-coated trousers, coats and hoods with Plexiglas face protection are sufficient. Ordinary rubber gloves offer adequate protection for equipment handling.

The single most important equipment for safe handling of HTP is a capability for water deluge. In the event of a spill, rapid dilution with water can prevent or contain reactions with the environment. In our experience at Westcott, HTP was routinely spilled on the surrounding concrete. These spills were routinely washed with water, however, even when the dilution was delayed several minutes, no spontaneous reactions observed. (In fact, attempts to initiate reaction of HTP with organic material such as paper met with no success).

For these reasons, from a safety cost standpoint, HTP operations even at remote launch sites would bring relatively small additional cost. Assuming water of any kind is available at the site, the launch campaign would require:

- *Personal safety equipment*—vinyl-coated suit, boots, face protection, hood and gloves)
- *Ground support equipment*—self-contained cart for pressurising HTP into flight tanks. Nominally, this system would be designed such that the HTP is never directly exposed to the environment. Safety equipment would be for contingency only.
- *Water pump*—hand or electrically operated pump for directing supplied water onto spills and for washing personnel after exposure.

The biggest potential impact of safety considerations on mission costs relates to logistics. HTP must either be delivered to the launch site by the supplier (e.g. Air Liquide) or directly to the satellite manufacturer for shipment as part of the overall launch campaign. According to [CPIA 84], HTP is authorised for transport aboard military aircraft when packaged in accordance with DOT regulations

which defines it as an oxidiser under UN2015. Unfortunately, it cannot be carried on commercial aircraft in any quantity. However, discussions with supplier Air Liquide [Tremblot 96] indicates that the rules governing HTP ground transport are the same that apply to 70% hydrogen peroxide which is used world-wide in the pulp and paper industry. Therefore, ground transportation of even very large quantities virtually anywhere in the world would be relatively easy to arrange given sufficient delivery notice.

5.4.3. HTP Mono-Propellant Option

One advantage of the HTP hybrid (as discussed in Chapter 4) is the possibility of using HTP alone in a mono-propellant mode. Table 5-13 summarises the performance costs for such a thruster operating at the 1.0 N level for station keeping or lunar mid-course correction applications. Higher or lower thrust engines over an approximate range of 0.5 N to 10 N would be practical.

Parameter	Value
Propellant	85% HTP
Chamber pressure (bar)	17.3
Specific impulse, Isp (sec)	149.3
Density specific impulse, $dIsp$ (s.g.sec)	204.5
Thrust, N	1.1
Mass flow rate, gm/sec	0.75
Throat diameter, cm	0.66
Nozzle exit diameter, cm	7.0
Expansion ratio	110:1
Nozzle length, cm	1.2
Total HTP required for 250 kg spacecraft, $\Delta V = 200$ m/sec	31.9 kg (23.3 litre)

Table 5-13: HTP mono-propellant thruster design option. Isp value assumes 90% decomposition efficiency.

The potential price for an HTP mono-propellant engine would be significantly less than a hybrid for first use. The lower price would be due to the reduced complexity of building a thruster to operate at maximum temperatures of <700°C, a regime where conventional materials such as stainless steel relying on radiative cooling could be used for the nozzle rather than more complex refractory metals or ceramics. Based on the experience gained from building and operating the catalyst pack for the hybrid program, the estimated price for a prototype HTP thruster would be <\$30,000.

The mission costs for a mono-propellant HTP thruster would be identical to those of the hybrid discussed below. The important exception is the integration costs which would be more similar to those of the hydrazine mono-propellant engine as discussed in Chapter 3 due to the lower thrust and thermal demands.

5.5. Conclusions

This chapter has demonstrated that the primary objectives for the hybrid research program have been met:

Concept proven—hybrids represent a readily accessible technology allowing full-scale research and development in a budget-constrained, University environment. The program demonstrated rapid results with minimal cost, and addressed and solved a number of fundamental engineering problems, most notably catalyst pack technology.

Performance characterised—the prototype hybrid motor was used to fully characterise the PE/HTP combination and publish the first-ever regression rate relationship applied specifically to small satellite upper stages. The resulting design process will enable mission analysis critical to future applications.

Total cost assessed—price and mission cost issues for hybrid applications on small satellites were identified and analysed from the basis of practical knowledge and experience. The total cost and schedule for a first-use hybrid upper stage mission was outlined. Technical risk, integration costs, safety and logistics issues for such a mission were thoroughly assessed and recommendations for future research given.

All near term technology options have now been fully characterised. The next chapter returns to the other side of the total cost equation to assess the impact of system architecture and acquisition on total system cost. Chapter 7 will return to consider the hybrid technology and compare it to competing options to determine the most cost-effective system for a given application. Specific recommendations for future hybrid research aimed at developing an upper stage are summarised in Chapter 8.

5.6. References

- [Andrews 90] Andrews, David "The Advantages of Hydrogen Peroxide as a Rocket Oxidant," Journal of the British Interplanetary Society, Vol. 43, No. 7 July 1990.
- [Andrews 94] Andrews, D., Personal Communication, 15 June 1994.
- [Andrews 95] Andrews, D., Personal Communication, 6 March 1995.
- [Brown 96] Brown, R. Project Machinery, Personal Communication, 15 February 1996.
- [CPIA 84] Chemical Propulsion Information Agency Publication 394, Vol. III, Hazards of Chemical Rockets and Propellants, Johns Hopkins University, Applied Physics Laboratory, Laurel, Maryland, September 1984.
- [Davis 60] Davis, N.S., jr., McCormick, J.C., "Design of Catalyst Packs for the Decomposition of Hydrogen Peroxide," Liquid Rockets and Propellants, Bollinger, L.E., Goldsmith, M., & Lemmon, A.W., jr., (eds.), A Symposium of the American Rocket Society, Ohio State University, Columbus, Ohio, 18-19 July, 1960.
- [Greiner 93] Greiner, B., Frederick, R.A. jr, "Hybrid Rocket Instability," AIAA 93-2553, 29th AIAA/ASME/SAE/ASEE Joint Propulsion Conference, Monterey, California, 28 - 30 June 1993.

Chapter 5: Hybrid Program Results

- [HPHB 67] Hydrogen Peroxide Handbook, Chemical and Material Sciences Department, Research Division, Rocketdyne—a division of North American Aviation, Inc., Canoga Park, California, Technical Report AFRPL-TR-67-144, July 1967.
- [Humble 95] Humble, R., et al, *Propulsion System Analysis and Design*, To be published, Fall 1995.
- [Jenkins 95] Jenkins, R.M., Cook, J.R., "A Preliminary Analysis of Low Frequency Pressure Oscillations in Hybrid Rocket Motors," AIAA 95-2690, 31st AIAA/ASME/SAE/ASEE Joint Propulsion Conference, San Diego, California, 10 - 12 July 1995.
- [LaTona 94] LaTona, A., Valcor, Inc., private communication, 7 September 1994.
- [Moore 56] Moore, G. E., Berman, K., "A Solid-Liquid Rocket Propellant System," *Jet Propulsion*, November, 1956.
- [MS 1522A] MIL-STD-1522A Standard General Requirements for Safe Design and Operation of Pressurized Missile and Space Systems, United States Air Force, 28 May 1984.
- [Runckel 63] Runckel, J.F., Willis, C.M., Salters, L.B.jr, "Investigation of Catalyst Beds for 98-Percent-Concentration Hydrogen Peroxide," NASA Technical Note D-1808, June 1963.
- [Shufflebotham 57] Shufflebotham, N., Walder, H., "Decomposition Tests of Non-Stabilised HTP on Silver Catalyst," Technical Memo No. RPD 134, RAE, Farnborough, June 1957.
- [Southern 67] Southern, G.R., Sutton, D., "Some Aspects of the Catalytic Decomposition of Hydrogen Peroxide by Silver: Part X. Decomposer Tests Using HTP at Concentrations up to 98% w/w," RPE Technical Report No. 67/9, RPE, Westcott, August 1967.
- [Sutton 62a] Sutton, D., "Some Comments on the Efficiency and Life of the Silver Catalyst Pack for the Decomposition of HTP," Technical Memo No. 248, RPE, Westcott, February 1962.
- [Sutton 62b] Sutton, D., Bennett, C.R., "Some Aspects of the Catalytic Decomposition of Hydrogen Peroxide by Silver: Part VIII. The Effects of Additives," RPE Technical Note No. 211, RPE, Westcott, February 1962.
- [Tremblot 96] Tremblot, A., Air Liquide, private communications, February/March 1996.
- [Walder 55] Walder, H., Spalding, E.G., "Influence of HTP stabiliser (sodium stannate) on the silver catalyst," Technical Memorandum No. RPD 68, Rocket Propulsion Department, Westcott, January 1955.
- [Wernimont 94] Wernimont, E.J., Meyer, S.E., "Hydrogen Peroxide Hybrid Rocket Engine Performance Investigation," AIAA 94-3147, 30th Joint Propulsion Conference, Indianapolis, Indiana, June 1994.
- [Wernimont 95] Wernimont, E.J., Heister, S.D., "Performance Characterisation of Hybrid Rockets Using Hydrogen Peroxide Oxidiser," AIAA-95-3084, 31st AIAA/ASME/SAE/ASEE Joint Propulsion Conference and Exhibit, San Diego, California, 10-12 July 1995.
- [White 86] White, F.M., *Fluid Mechanics*, McGraw-Hill, Inc., USA, 1986.
- [Willis 60] Willis, C. M., "The Effect of Catalyst-Bed Arrangement on Thrust Buildup and Decay Time for a 90 Percent Hydrogen Peroxide Control Rocket," Langley Research Center, Langley Field, Virginia., NASA Technical Note D-516, September 1960.

Chapter 6

System Costs

6.1. BACKGROUND

6.2. SYSTEM DEVELOPMENT

6.3. TOTAL SYSTEM COST

6.4. CONCLUSIONS

6.5. REFERENCES

The preceding chapters have concentrated on characterising the total cost of propulsion technology. The research goal described in this chapter shifts the focus to characterise the total cost of propulsion systems. The aim was to apply the design justification process by developing a versatile, cost-effective system to meet specific mission requirements while, in parallel, deriving a realistic understanding of total cost trade-offs. Using off-the-shelf bi-propellant and cold-gas technology, this system design case study examined the influence of each mission phase—definition, design and acquisition—on the nine dimensions of the total cost paradigm. The minisatellite mission on which the study was based is first described, highlighting the critical cost drivers. A baseline system architecture is then presented derived from standard industry practices. This baseline served as a starting point from which to minimise total system cost. From this background, the system development is described. Propulsion systems on other low-cost missions are examined to learn from their experiences with cost-constrained systems engineering. System requirements for the case study, including the trade-offs and acquisition process used, are then described. The results of this effort are presented and unique aspects of the final system architecture are highlighted. The most important conclusion to emerge from this research was that a complete understanding of costs can only come by looking beyond technology to assess the influence of mission definition, system architecture and acquisition on the critical aspects of a total propulsion system. By focusing on these cost drivers, total propulsion system costs can be drastically reduced. In addition, the research resulted in a flexible, cost-effective “generic” system design that can be readily adapted to a variety of technologies and effectively integrated on small satellites with easily quantifiable total cost. These results will enable a more realistic comparison of system options for various mission scenarios.

6. System Costs

6.1. Background

This section begins by defining the mission cost drivers for the propulsion system developed during the case study. A baseline system architecture is then described that was derived using standard industry practices. Cost estimating relationships (CERs) are then applied to this baseline design in order to quantify system price. This analysis is complemented by results from a market survey.

6.1.1. Mission Cost Drivers

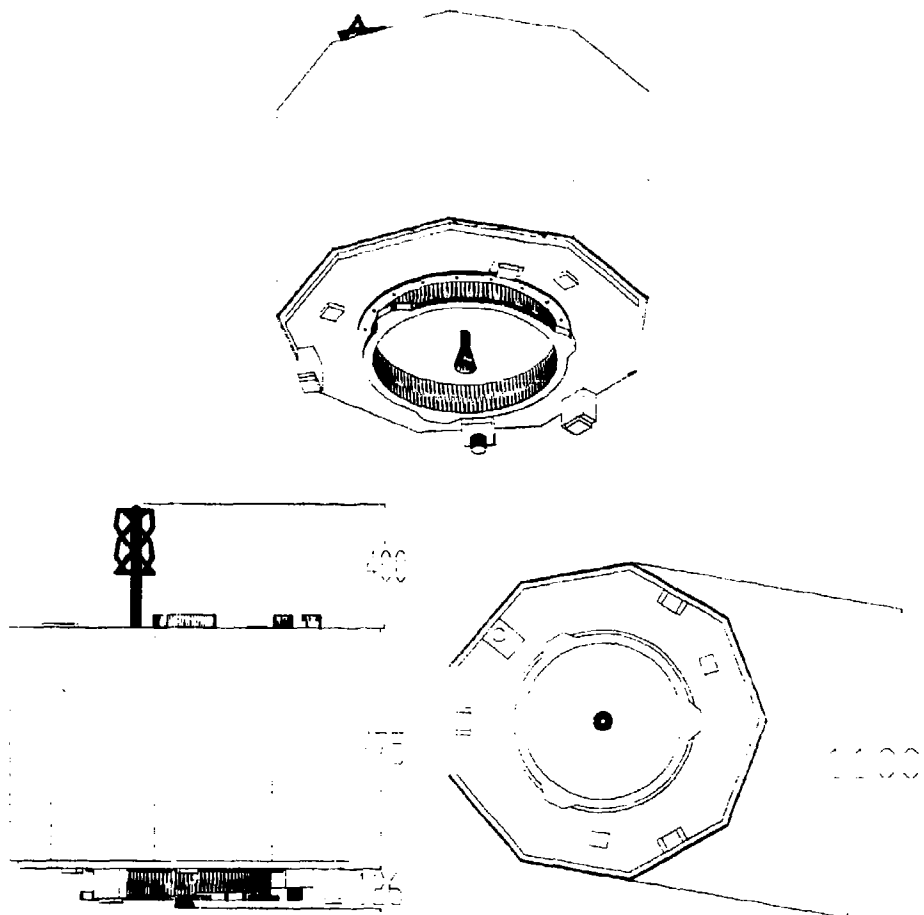


Figure 6-1: Configuration of the UoSAT/SSTL Minisatellite used for the design case study. Dimensions are in mm.

This section provides a brief overview of the cost driver environment during the phases of the mission used in the case study. The purpose is to understand the restrictions imposed by these drivers so that steps can be taken to minimise overall system cost whilst complying with their mandates. These particular mission parameters were defined to reflect those of the real UoSAT-12 minisatellite mission being developed in parallel with this research as defined by SSTL Technical Director, Dr. Jeff Ward [Ward 95]. The mission objective is stated below:

Mission Objective—demonstrate advanced technology including on-orbit manoeuvre and attitude control capability on an experimental UoSAT minisatellite in LEO.

The mechanical design and dimensions for the minisatellite are shown in Figure 6-1. Restrictions imposed on the design study that follow from this mission objective as they effect each mission phase are summarised in Table 6-1.

Mission Phase	Cost Driver	Case Study Restrictions
Definition	Political Environment	<ul style="list-style-type: none"> • University-funded mission • Spacecraft deployed mass 250 kg • Main Engine: LEROS-20, Thrust = 20 N • Propellants: MON/MMH, nitrogen pressurised • Cold-gas thrusters for attitude control: Thrust = 0.1 N, nitrogen propellant
	Launch & Space Environment	<ul style="list-style-type: none"> • All system components capable of withstanding standard LEO vacuum and radiation environment. • Final launch vehicle to be defined.
Design	Performance Requirements/ Margins	<ul style="list-style-type: none"> • ΔV: sufficient to develop and demonstrate proficiency in orbit manoeuvring, guidance and navigation. • Component integration constrained to integrate entirely on the minisatellite attach frame. • System in compliance with Vandenberg AFB range safety restrictions • Total loaded mass of propulsion system < 50 kg
	Quality Level	No special restrictions
	System Architecture	To be determined by case study
Hardware Acquisition	Hardware Source	All components purchased, no in-house development
	Procurement process	To be determined by case study
	Space qualification requirements	No special requirements

Table 6-1: Summary of mission lifetime phases for the hypothetical minisatellite mission indicating cost drivers and specific restrictions imposed on the case study.

6.1.2. Baseline Architecture

As a starting point for a discussion of the system design process, a configuration based on commercial spacecraft propulsion systems such as CPS, Cluster and EuroSTAR [Paul 94] was defined. This architecture is shown in Figure 6-2. Interesting features to note in this design are:

- Mechanical regulator to drop pressure from the 240 bar supply tank to the 24 bar propellant tanks.
- Redundant cold-gas thruster attitude control branches
- Use of latch valves
- Use of pyrotechnic valves

The next subsection begins to address the question of system price.

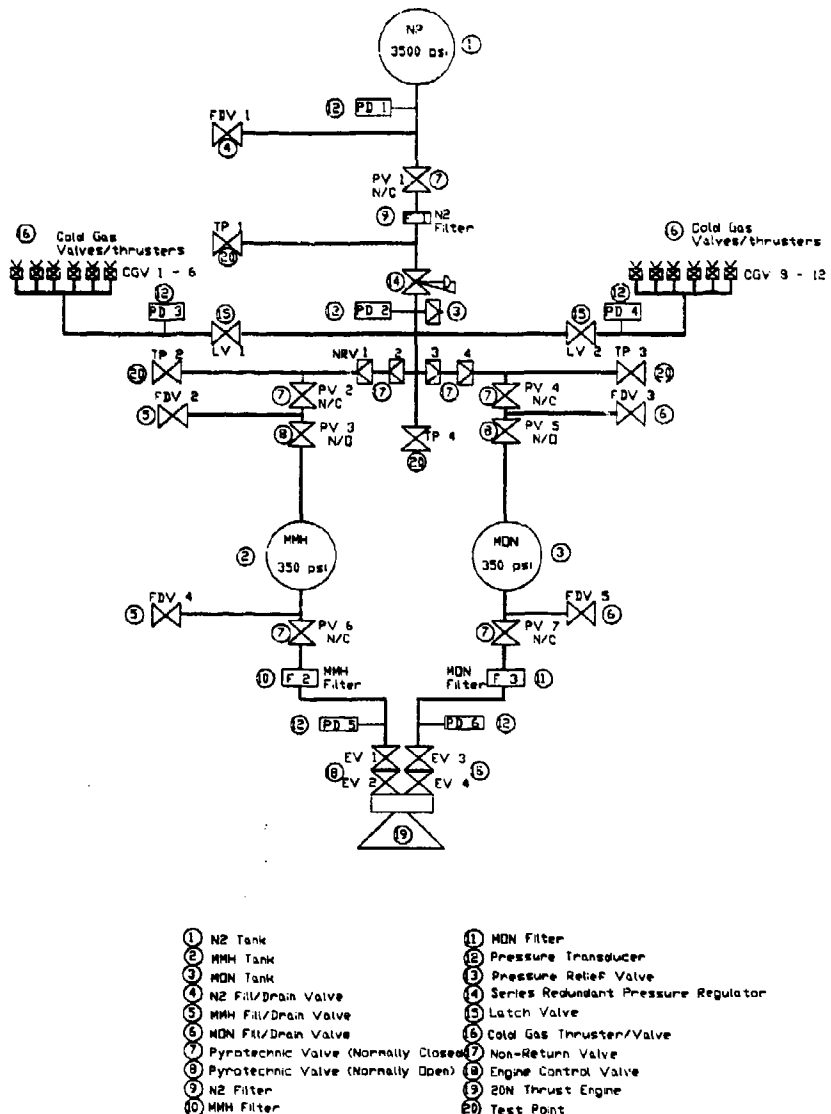


Figure 6-2: Baseline system architecture for the Minisatellite Propulsion System.

6.1.3. Cost Estimating Relationships

The most important question to be answered before designing a “low-cost” system is “what does a high-cost system cost?” The first place to turn in order to answer that question is industry. Over the years, the aerospace industry has developed cost estimating relationships (CER) for both subsystems and entire missions. These CERs are widely used by mission sponsors as planning tools prior to committing large funds to a project. This section presents results from analysis based on two such models, one developed in the early 1980s based on large satellite programs and the other in 1995 based on small satellite programs.

6.1.3.1. Smith & Horton Model

In 1984, Smith and Horton [Smith 84] performed a comprehensive survey of available propulsion systems and developed cost functions to allow realistic cost estimates of liquid propulsion systems. They established ROM costs and mass estimates for critical system components and simple cost functions for tanks in terms of diameter, D, in cm as follows.

$$\text{Shell Tank Cost} = 20D^2 (\text{recurring}) + 4000D(\text{non-recurring})$$

Eqn. 6-1

Applying their cost relationships to the following baseline assumptions:

- Spacecraft deployed mass = 250 kg.
- Shell tanks for oxidiser, fuel (10 litre each @ 20 bar, 27.18 cm diameter, 1.65:1 oxidiser/fuel (O/F) ratio) and pressurant gas (10 litre @ N₂, 200 bar, 27.18 cm diameter).
- Orbit Correction ΔV = 200 m/s.

gives an overall propulsion system cost estimate as summarised in Table 6-2. ([Smith 84] worked in ESA accounting units where 1AU = \$1US.

Component	Qty.	Unit Mass (kg)	Total Mass (kg)	Recurring Cost	Non-Recurring Cost	Total First spacecraft cost
20-N Thrust Engine	1	0.60	0.60	\$833,600	\$96,000	\$929,600
Propellant Tank	2	1.02	2.05	\$14,775	\$108,720	\$138,270
Nitrogen Tank	1	4.18	4.18	\$14,775	\$108,720	\$123,495
Regulator	1	0.84	0.84	\$30,000	\$100,000	\$130,000
Pressure Transducer	6	0.23	1.38	\$6,500	\$20,000	\$21,495
Pyrotechnic Valve	7	0.15	1.02	\$2,500	\$50,000	\$67,500
Relief Valve	1	0.45	0.45	\$10,000	\$80,000	\$90,000
Filter	3	0.23	0.68	\$4,000	\$30,000	\$42,000
Fill/Drain Valve	3	0.15	0.44	\$2,700	\$10,000	\$18,100
Cold-Gas Thruster	12	0.10	1.20	\$20,000	\$100,000	\$340,000
Thruster Isolation Valve	2	0.15	0.29	\$2,500	\$50,000	\$55,000
Total			11.63	\$1,352,020	\$603,440	\$1,955,460

Table 6-2: Smith & Horton [Smith 84] cost model applied to a 250 kg spacecraft with a 200 m/s ΔV requirement along with cold-gas thrusters based on baseline system architecture. Engine cost estimate based on "thruster to suit typical spacecraft industry requirement" [RO 94].

We would conclude from this analysis that a small satellite designer is faced with a propulsion system price of >\$1.3M in non-recurring mission design costs in addition to around \$600k per mission. For total mission cost targeted for around \$7M, this means the propulsion system would consume nearly 30% of the budget, an unacceptable scenario. Furthermore, looking at these results from a system standpoint, it would appear that of the total system price, nearly one-half (47.5%) comes from the price of the engine alone.

6.1.3.2. Aerospace Corp. Model

Recall, the approach developed by [Smith 84] was based on data from large, commercial satellite missions and therefore may not have direct applicability to small spacecraft. This has been

substantiated by recent studies at the Aerospace Corp. which have shown that “cost-reduction techniques employed on modern small-satellite programs result in system costs that are substantially lower than those estimated by traditional weight-based parametric CERs.” [Burgess 95] Realising this bias of industry cost models toward large satellites, engineers at Aerospace Corp. developed new models based solely on small satellite historical data. Their propulsion system CERs, published in [Burgess 95] was based on data from 15 modern (post-1990) small satellites. The CERs were derived using a general-error regression model assuming constant percentage error. Of the 15 satellites in the study, only 6 included propulsion systems. These were

- MICROSAT—US Defence Advanced Research Project Agency sponsored communication satellite built by DSI (now CTA) launched in July 1991.
- STEP 0—USAF Space Test Programs (STP) Office sponsored experimental satellite built by TRW/CTA launched in March 1994.
- STEP 1—STP sponsored atmospheric physics satellite built by TRW/CTA launched in June 1994.
- SEASTAR—NASA sponsored oceanographic satellite built by OSC launch TBD.
- MSTI-1—US Strategic Defence Initiative Office sponsored experimental satellite built by Spectrum/JPL launched in November 1992.
- FREJA—Swedish National Space Board sponsored plasma measurement satellite built by Swedish Space Corp. launched in October 1992.

The Aerospace team developed two separate CERs, one based on system dry mass (Eqn. 6-2) and the other based on total number of thrusters (Eqn. 6-3):

$$\text{Cost(FY94\$k)} = 76.3 \cdot \text{System_dry_mass(kg)} \quad \text{Eqn. 6-2}$$

$$\text{Cost(FY94\$k)} = 264 \cdot \text{Number_thrusters} \quad \text{Eqn. 6-3}$$

Of these, the first is the more applicable to the case study as the second approach assumes the same type of thrusters throughout the system (while the minisatellite system has both bi-propellant and cold-gas thrusters). Using the system mass estimate from [Smith 84] presented above and applying mass-based Aerospace Corp. CER to the baseline system yields a system price estimate of \$887k, about 50% less than the price results of [Smith 84].

This value provides a realistic criteria by which to evaluate the total system cost savings realised by focusing on the hardware cost drivers. The final system cost determined by the case study will be compared to this value in order to quantify the efficacy of this approach. System mass estimates from [Smith 84] will be used to assess that cost dimension.

6.1.4. Market Analysis

While the results of CER data presented in the last subsection provide a good starting point for assessing propulsion system costs, a more realistic analysis requires that we turn to the market place itself. To quantify price ranges and availability of propulsion system components, I prepared a formal

Request for Quotation (RFQ) which was sent to nearly 30 aerospace companies. The RFQ component requirements were established by the baseline system described earlier.

The covering letter in the RFQ tried to establish a rapport with suppliers in order to have them work as part of a team to lower costs. In part, the letter explained "Our experience in building other satellite systems has demonstrated that there are ways to lower component costs by relaxing performance requirements and judiciously modifying the procurement and parts production process. We know that a \$50,000 component can't simply be changed into a \$20,000 component by changing the amount of paperwork that gets shuffled. We recognise that the less expensive component can not have the same assured quality as its more expensive counterpart, however, in many cases it may be sufficient for our higher-risk, low-cost missions. We are asking you to tell us how best to reduce the cost of each component with understandable consequences."

Companies were given an abbreviated set of component requirements and asked to provide two separate quotations:

1. Individual components in compliance with all typical industry standard performance requirements and acceptance testing (usually provided in a document several inches thick e.g. NASA, ESA or DoD programme specifications).
2. Individual components at minimum possible cost as the result of relaxation of requirements as addressed in the attached RFQ and modification of normal production processes.

Unfortunately, response to this RFQ was not overwhelming. Only 12 companies provided serious responses to any components. These responses are summarised in Table 6-3 (because most companies only provided the second type of bid asked for, minimum cost, only those results are reported).

It is interesting to note the wide range of responses for some components. Tanks in particular span nearly a difference of nearly 10:1. The results of this market analysis provided two useful results:

1. High-cost component prices (those at the high end of the range) agree roughly with those predicted by [Smith 84].
2. A working relationship was established with a supplier team, Arde and EG & G Wright, for further evolution of the design as part of the minisatellite case study.

By working with Arde as part of a team effort, as this Chapter will demonstrate, tank and support system prices were reduced still further and a true lowest-cost solution was achieved. The results of this effort are discussed in greater detail in subsequent sections.

Chapter 6: System Costs

Component	Bids
N2 Tank	<ul style="list-style-type: none"> • Arde, Inc: \$15,000 • Dowty: \$160,000 NRC + \$48,000 RC = \$208,000 1st unit
MMH Tank	<ul style="list-style-type: none"> • Arde, Inc: \$15,000 • Dowty: \$16,000 NRC + \$11,200 RC = \$27,200 1st unit
MON Tank	<ul style="list-style-type: none"> • Arde, Inc: \$15,000 • Dowty: \$16,000 NRC + \$11,200 RC = \$27,200 1st unit
N2 Fill/drain valve	<ul style="list-style-type: none"> • Moog: \$4,000 • Dowty: \$19,200 NRC + \$6,400 RC = \$25,600 1st unit • OEA: \$6,000 NRC + \$4,000 RC = \$10,000 1st unit • Raufoss: \$16,000
Propellant Fill/drain valve	<ul style="list-style-type: none"> • Moog: \$4,000 • Dowty: \$9,600 NRC + \$6,400 RC = \$16,000 1st unit • OEA: \$3,750 NRC + \$6,000 RC = \$9,750 1st unit • Raufoss: \$16,000
Pyrotechnic valve	<ul style="list-style-type: none"> • OEA: \$6,000 NRC + \$6,000 RC = \$12,000 1 unit
N2 or Propellant Filter	<ul style="list-style-type: none"> • Dowty: \$19,200 NRC + \$6,400 RC = \$25,600 1st unit
Pressure Transducers	<ul style="list-style-type: none"> • Lucas: \$350
Pressure Relief valve	<ul style="list-style-type: none"> • Carleton: \$30,000 • Hale Hamilton: \$675 • R&D Institute of Mech. Eng.: \$ 2,770
Pressure regulator	<ul style="list-style-type: none"> • Carleton: \$30,000 • R&D Institute of Mech. Eng.: \$3,950
Cold-gas thruster isolation valve	<ul style="list-style-type: none"> • EG & G Wright: \$3,750 • Moog: \$4,000 • Valcor: \$3,100 • MMS: \$1,623 NRC + \$9,494 NRC = \$11,117 1st unit • R&D Institute of Mech. Eng.: \$7,500
Cold-gas thruster valve	<ul style="list-style-type: none"> • EG & G Wright: \$2,525 • Moog: \$4,000 • Valcor: \$3,100 • MMS: \$693 NRC + \$9,518 NRC = \$10,211 1st unit • R&D Institute of Mech. Eng.: \$12,560
Propellant check valves	<ul style="list-style-type: none"> • Moog: \$24,000
Engine control valve	<ul style="list-style-type: none"> • Moog: \$36,800 • Valcor: \$1,250 NRC + \$4,600 RC = \$5,850 1st unit
Engine	<ul style="list-style-type: none"> • R&D Institute of Mech. Eng.: \$35,470
High pressure N2 valve	<ul style="list-style-type: none"> • EG & G Wright: \$3,750 • Valcor: \$5,800 • Hale Hamilton: \$1,440
Engine isolation valve (latch valve)	<ul style="list-style-type: none"> • Moog: \$19,250 • Valcor: \$1,400 NRC + \$8,000 RC = \$9,400 1st unit • R&D Institute of Mech. Eng.: \$7,500
HTP valve	<ul style="list-style-type: none"> • No bids
HTP tank	<ul style="list-style-type: none"> • No bids

Table 6-3: Results of market analysis.

6.2. System Development

This section will summarise the development of the minisatellite propulsion system. Here, the cost driver lessons described in Chapter 2 will be implemented in order to achieve the most cost-effective system overall. Recall the design justification concept was defined whereby the system design and its cost model are developed concurrently. The aim of this case study is to put this concept into practice by designing a complete system and fully characterising its cost along the nine dimensions of the total

cost paradigm. In this way, system trade-offs can be better characterised and the resulting design adapted to other applications with predictable, quantifiable results.

Chapter 2 described the primary cost drivers during each mission phase—definition, design and acquisition. While this was discussed as a sequential process, the results of this case study confirm the importance of the interrelationships between each mission phase. By understanding the mission environment and trading system requirements and architecture layout with the realities of the acquisition process, a lowest-cost solution was achieved that was safe, simple and easy to integrate.

The mission was defined in the previous section. From this definition, the propulsion system gradually evolved, modified by focusing on the key cost drivers and quantifying real cost trade-offs with our acquisition partner. To describe this iterative process as it actually unfolded would be redundant and potentially confusing. Therefore, for purposes of discussion, the philosophy behind the system architecture will first be described by defining the system design requirements. To provide important background for the design process, system engineering techniques employed on other low-cost propulsion systems will then be summarised. With this understanding as background, technical trade-offs for the case study are addressed. The acquisition process adopted with the prime contractor will then be summarised. The section concludes with a description of the resulting minisatellite system, highlighting its unique features.

6.2.1. Design Requirements

The primary design requirements for the system architecture were:

- Mechanical interface restrictions
- Liquid/gas pressures & flow rates
- Range safety requirements

Each of these is addressed below.

The minisatellite configuration along with dimensions was shown in Figure 6-1. As this mission is one of technology demonstration, mass budgets were not overly constrained. However, the minisatellite design imposed inflexible constraints on the mechanical envelope for which considerable effort was expended to ensure compliance. As noted as part of the mission performance requirements, the entire system had to be contained on the attach frame of the satellite. This attach frame is the bottom honeycomb panel on which the module boxes are stacked. The attach frame also provides the launch vehicle interface. This requirement was intended to make spacecraft integration easier allowing for independent installation and testing of the propulsion system separate from the rest of the satellite. The available envelope for tanks and associated plumbing is shown in Figure 6-3 and summarised below:

- Allowable tank envelope—maximum diameter 311 mm (equates to maximum volume of 15.75 litre for spherical tank)

- Allowable component envelope—integration within standard module box. Available footprint 290 x 298 mm with total module box height 100 mm.

Liquid and gas pressure as well as flow rates follow directly from the mission requirements for the main engine and cold-gas thrusters. Table 6-4 shows these requirements for the LEROS-20 main engine and the EG&G Wright cold-gas thrusters.

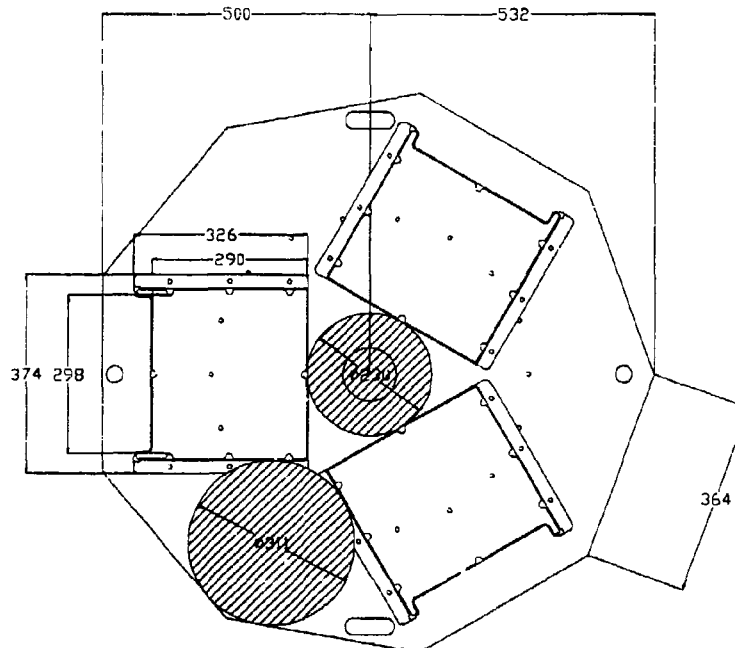


Figure 6-3: Mechanical drawing showing the inside surface of the minisatellite attach frame on which all propulsion system components must be integrated. Envelope limitations are indicated in mm.

Parameter	LEROS-20	EG&G Wright Cold-gas Thrusters
Thrust (N)	20 N	0.1
Chamber Pressure (bar)	8.88	4.0
Propellant flow rate (gm/s)	7.8	0.016
Inlet Pressure Range (bar)	10 - 20	0 - 13.8

Table 6-4: Nominal pressure and flow rate requirements for the Minisatellite propulsion system.

Because the launch site for the spacecraft was unknown, the system had to be safe enough to operate from virtually any site. Therefore, Vandenberg AFB range safety requirements were chosen as the most constraining. These rules are governed by WRR 127-1 Range Safety Requirements [WRR]. In addition to this regulation, MIL-STD-1522A [MS 1522A] covers “Standard General Requirements for Safe Design and Operation of Pressurised Missile and Space Systems.” These regulations make the following specific design impacts:

- At least 2 physical breaks between high pressure gas tanks and the outside.
- At least 3 physical (and electronic) breaks between propellant tanks and the engine (1 pyrotechnic valve counts as 2 breaks).
- All components proof tested to 1.5 x maximum expected operating pressure (MEOP).
- Pressure relief valves set to 1.5 x MEOP.

The initial design criteria were established using these VAFB requirements with the belief they would be the most stringent that could be expected. Regulations at Russian sites, for example, were not expected to be more demanding than this and would, in all probability, be less restricting. Before proceeding to a discussion of system trade-offs, the next subsection will examine experiences from previous low-cost missions to gain insight into the potential applications for various system engineering techniques.

6.2.2. Previous Examples

Before designing a cost-effective propulsion system for the minisatellite, it was useful to examine previous experiences in this area to avoid re-inventing the wheel. Chapter 1 described the emerging need for propulsion systems on small satellites. Unfortunately, this need is relatively new. Therefore, there is little previous experience to draw upon. In fact, there are only three missions which I believe can justifiably be placed in the category of truly low-cost missions that depended on propulsion. These are ARSENE, FREJA and the OSCAR series spacecraft. With the exception of FREJA built by the Swedish Space Corporation for the Swedish National Space Board, these fall in the category of "amateur" satellite projects. It is important to note, however, that most of the so-called "amateurs" working on these satellites are actually experts with regular jobs within the aerospace community. They donate their valuable time to projects such as ARSENE and OSCAR.

6.2.2.1. ARSENE

The ARSENE project was begun by the French Radio Amateur Club d l'Espace (RACE) in 1981. Its mission was to provide packet radio communication for users around the world. As the project developed, it grew beyond the scope of the resources available to RACE, so CNES agreed to take over sponsorship with financial help from the French Space ministry. The spacecraft was hexagonal shaped, 785 mm in diameter and 618 mm high. At separation, the total spacecraft mass was 157 kg. The ARSENE propulsion system consisted of a 74 kg (propellant mass) carbon fibre-wound solid apogee kick motor donated by Société Européenne de Propulsion (SEP) of France and a nitrogen cold-gas system consisting of four nitrogen tanks (donated by Air Liquide of France), four spin/despin thrusters and two tilt thrusters. [ARSENE 92]

After deployment into GTO, the spacecraft was spun up using the cold-gas thrusters to 60 rpm. Following measurement and correction of the satellite's attitude, it was spun up further to 90 rpm. The solid motor was then fired, raising perigee to 20,000 km. The spacecraft was then de-spun to 60 rpm and the spin vector precessed to point out of the orbit plane, again using the cold-gas thrusters. [Pidoux 92]

Following initial orbit insertion and commissioning, ARSENE appeared to be functioning nominally. Unfortunately, after 9 September 93 it stopped sending telemetry [OSCAR 93]. The final cause of the failure has not been completely identified [Llareus 94].

While the limited success of ARSENE demonstrated that propulsion systems could be effectively deployed on an "amateur" satellite, it did little to advance the cause of low-cost propulsion. Because all major propulsion system components were donated, there was no need to rigorously analyse or reduce costs.

6.2.2.2. FREJA

FREJA was a magnetospheric research spacecraft built by the Swedish Space Corporation for the Swedish National Space Board. As such, it represents a commercial endeavour with real cost data. The low-cost (under \$16M) design, construction and launch of this 214 kg spacecraft is another good example of the high quality engineering that can be done by a small group (8 people) working in a "skunk works" environment. It was launched on 6 October 1992 from the Chinese Jiuquan Satellite Launch Centre into 213.7 x 317.4 km with an inclination of 63°.

The FREJA propulsion system consisted of two solid rocket motors for orbit adjust (a STAR 13-A and a STAR 6-B manufactured by Thiokol, Inc., USA) providing a total impulse of over 110,000 Ns. In addition, a total of 4 solid spin-up/spin-down rockets with a propellant mass of 370 gm and total impulse of 750 Ns each were employed. These were made by the Beijing Institute of Space Machine and Electricity under the Chinese Academy of Space Technology.

Following deployment from the second stage, small solid rocket motors were fired to spin-up the spacecraft to 50 RPM. The STAR 13A rocket motor was then fired, raising apogee to 1756 km. One-half orbit later, the STAR 6B motor (mounted on the spacecraft to point in the opposite direction to the first motor) was fired to raise perigee to 601 km. Once this operational orbit was achieved, the remaining two small solid rocket motors were fired reducing the spin rate to 10 RPM.

[Grahn 93] provides detailed cost data for the FREJA mission. Converting to \$US based on (\$1 = 6.6 SEK) the total mission cost was \$15M. Of this, the spacecraft cost (including equipment, subsystems, engineering management and labour) was \$7.7M of which \$520,000 represented the total propulsion system cost. This value roughly agrees with the solid motor cost estimates presented in Chapter 3 and is somewhat less than what would be predicted by standard CERs. Thus, while FREJA offers a very good example of a low-cost propulsion system on a commercial mission, there are no unique lessons that can be applied to the design of a more flexible minisatellite system using liquid propellants. For these insights we must look to the OSCAR series satellites.

6.2.2.3. The OSCAR Series

Since their first spacecraft in 1961, the OSCAR (the Orbiting Satellite Carrying Amateur Radio) series has grown in size and sophistication. Built by ham radio enthusiasts and other "amateurs" in the space industry, these spacecraft have had a long and distinguished career providing radio relay and

store-and-forward communications for ham operators world-wide and have gone a long way toward advancing the cause of low-cost spacecraft engineering.

It is the latest series of OSCAR spacecraft which have included propulsion capability that are most relevant to my research. These include the "Phase III" series of spacecraft (which have corresponding OSCAR designations). The first three spacecraft in this series are briefly described below.

- *Phase IIIA*—lost in *Ariane* launch failure 23 May 1980.(First OSCAR to fail to reach orbit) [Clark 80]. Propulsion system relied on a TE-345 solid motor donated by Thiokol.
- *Phase IIIB (OSCAR 10)*—Launched aboard *Ariane* 16 June 1983. Main engine donated by MBB used N₂O₄ and UDMH [Daniels 87].
- *Phase IIIC (OSCAR 13)*—Launched aboard *Ariane* 15 June 1988. MBB engine, N₂O₄ and AZ-50 [Daniels 87].

The latest and most ambitious OSCAR design is Phase III-D (P3D). At 400 kg, the P3D spacecraft will dwarf its predecessors as shown in Figure 6-4. Launch is planned on the second flight of the new Ariane V booster in 1996 into GTO (200 km x 36,000 km, inclination ~ 7°). From there, it will use its main propulsion system to raise perigee to 4000 km, apogee to 47,000 km and change its inclination to 63°. This 16 hour modified Molniya orbit will offer optimum coverage to amateur radio operators in the northern hemisphere.

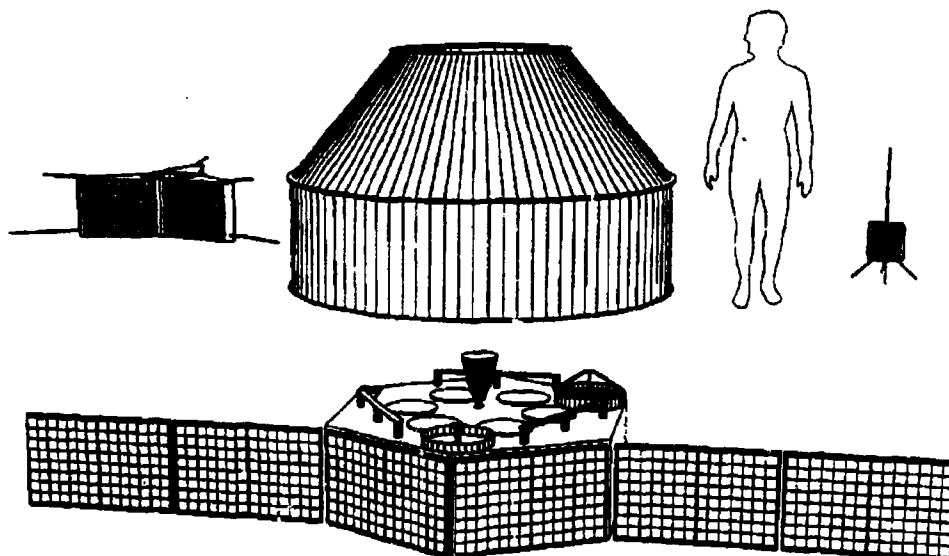


Figure 6-4: OSCAR Phase III-D spacecraft built by the AMSAT community for launch in late 1996. Its propulsion system design provided important lessons in the art of low-cost systems engineering.

From the standpoint of my research, the Phase III spacecraft offer useful insight into low-cost propulsion systems engineering practices. According to the propulsion system designer, Mr. Richard Daniels, "the design is an absolutely bare-bones approach emphasising simplicity and economy." [Daniels 87] While the OSCAR team has benefited from the generous donations of critical components, they have done this only after carefully minimising the complexity (and cost) of the overall system so as not to be overly dependent on such generosity.

For gas pressure regulation, P3B relied on a standard mechanical regulator. In contrast, for cost reasons P3C used a “bang-bang” pressure control approach as does P3D. The schematic for the P3D propulsion system is shown in Figure 6-5. The main propulsion system uses a 400-N thrust bi-propellant engine (MMH/N₂O₄) donated by MBB (now DASA) of Germany. Propellant pressurisation is provided by a single 400 bar helium tank. Helium isolation and pressure regulation is accomplished using two series-redundant solenoid valves. Pressure is regulated by a “bang-bang” system whereby the solenoid valves are pulsed on/off with feedback from a pressure transducer to maintain the desired pressure in the propellant tanks, buffered by a manifold/accumulator. Orbit maintenance will be accomplished using a 100-millinewton ammonia arc-jet thruster developed at the University of Stuttgart. Power requirements for the thruster are approximately 750 W [AMSAT 95] [Zube 95].

I had the unique opportunity to take part in the propulsion system integration campaign for P3D at the AMSAT facility in Orlando, Florida. Under the guidance of subsystem manager Mr. Richard Daniels, Mr Malcolm Paul and I were able to help with the mechanical integration of system pipes and tanks. In the process, we gained valuable insight into the engineering techniques employed by the OSCAR team to reduce costs while maintaining safe, effective performance.

A detailed study of the P3D propulsion system schematic in Figure 6-5 reveals several important lessons in low-cost systems engineering.

- *Reduced performance requirements*—typical space industry design criteria specify tight performance margins. By relaxing these requirements, even by a relatively small amount, potentially large cost savings can be realised. On P3D, this is evident by the use of a bang-bang pressure regulation scheme instead of a more precise (and much more expensive) regulator. This of course leads to a potentially higher risk level for mission performance, however, on missions like P3D spending more money may reduce the risk by some unspecified amount but may price the mission out of existence.
- *Use of terrestrial components*—to the largest extent possible, the system depends on commercial-grade components. These are evident in the high pressure iso/bang-bang solenoid valves, check valves, pressure transducers, filters (He, fuel and oxidiser) and 37° flare fittings (in place of orbit welds). These terrestrial components are far cheaper than their “space qualified” equivalents. Typically, the major drawback of such components is higher mass or less efficient power consumption.
- *Reduced documentation*—Because the entire system design, assembly and operations is conducted by “amateurs” donating their spare time to the project, and because the project management does not have to answer to a “higher power” i.e. a government agency, documentation is kept to the minimum amount needed to communicate within the team and comply with launch agency requirements.
- *“Build-your-own” approach to hardware*—High pressure helium tanks for both P3B and C used modified fire extinguisher tanks. The propellant tanks for both P3B and C were designed and built by AMSAT-DL engineers. These tanks consisted of a common bulkhead separating fuel and oxidiser. The design took maximum advantage of available spacecraft volume. [Daniels 87]

Chapter 6: System Costs

Table 6-5 contains cost data for various components of the P3D spacecraft and Table 6-6 for earlier Phase III spacecraft. As you can see, many of the significant cost items have been donated or offered at a reduced price. Therefore, while the Phase III spacecraft design experience offers much to learn in low-cost systems engineering, their experience in selecting low-cost components cannot be directly applied to commercial missions. Furthermore, the nature of each Phase III mission was essentially a "one-off," taking advantage of whatever cheap or free components happen to be available at the time. Thus, there was no requirement to establish long-term relationships with component suppliers on a commercial basis.

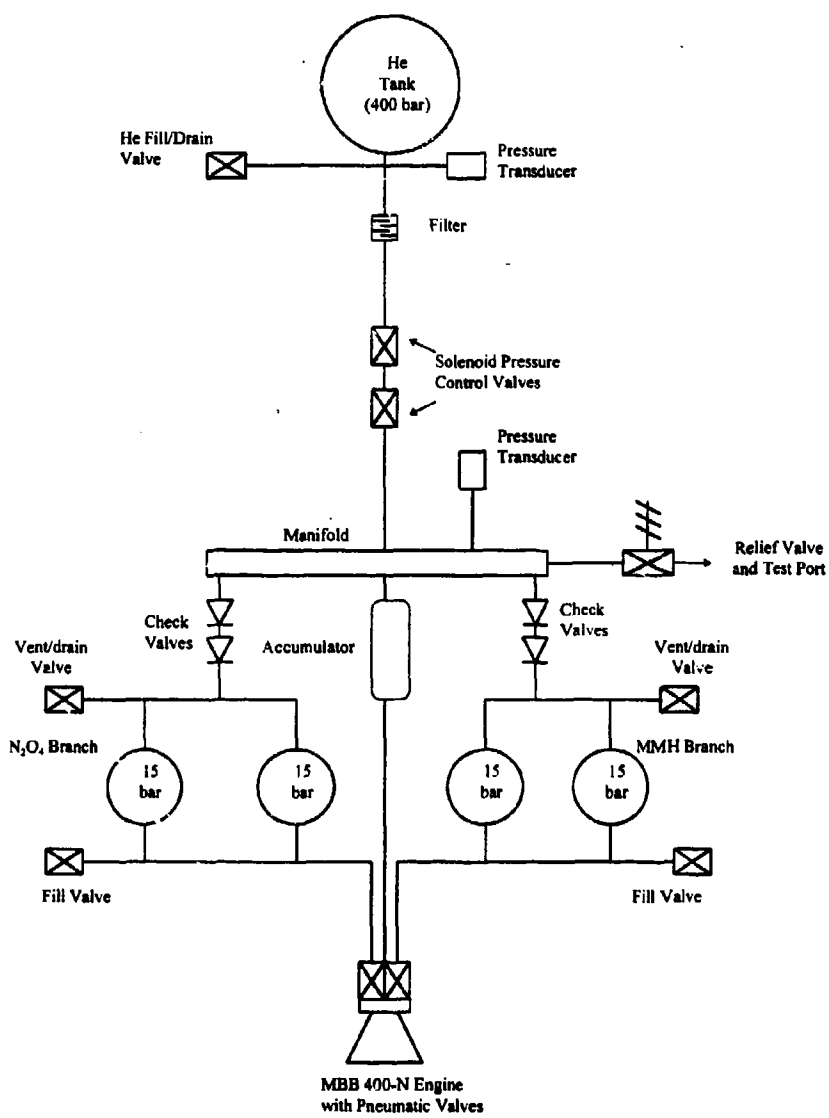


Figure 6-5: Main propulsion system schematic for Phase IIID spacecraft.

Chapter 6: System Costs

Component	Source	Cost
Phase IIIC Fill/Drain	MBB (DASA)	\$0 (Donated)
Phase IIID He Fill/Drain	OEA	\$2841
Phase IIID prop Fill/Drain	Circle Seal K220T-4TB 6 total (LOX cleaned) (modified check valves)	\$251 each
Phase IIID He isolation/bang-bang solenoid valve	Steering Engineering	\$2000 total (refurbish one left over plus two new, price reduced from quoted value of \$3500)
Phase IIID He filter	Steering Engineering	\$0 (Donated)
Phase IIID pressure transducers	Lucas P1241-0004	\$350 each
Phase IIID check valve	Circle Seal 2x K220T-4TT 2x K220T-4BT LOX cleaned	\$304.90 each \$325.80 each
Phase IIID He tank	Russian source 1 flight, 1 test 200 bar MEOP	Cost data proprietary
Phase IIID propellant tanks	Russian source 6 flight, 1 test 15 bar MEOP	Cost data proprietary
Phase IIIB, C & D engines	MBB	\$0 (Donated)
Phase IIIC & D tubes and fittings	Parker Hannifin Corp. 37°-flared fittings. Tubing "scrounged"	\$750 (estimated)
Phase IIIB, C & D welding	AMSAT-NA	\$0 (Donated)
Phase IIIB, C & D cleaning and testing	AMSAT-NA	\$0 (labour and facilities donated)
Phase IIIB, C & D ground support equipment (fill/drain)	MBB	\$0 (loaned by MBB, operations supervised by their personnel)

Table 6-5: Available cost data for OSCAR/P3D spacecraft propulsion system components [Daniels 95].

Component	Source	Cost
Phase IIIC pressure transducers	Shavevitz (Lucas) P2503-0001	Leftover from OSCAR 10
Phase IIIC relief valve	Circle Seal 5120A-4T	\$237
Phase IIIC relief valve	Circle Seal 5120A-4T	\$372.55
Phase IIIC check valve	Circle Seal 2x K220T-4TT 2x K220T-4BT	\$183.45 each \$231 each
Phase IIIC He isolation /bang-bang solenoid valve	Sterer Engineering	\$0 (Donated, estimated value \$3,325 each)
Phase IIIB and Phase IIIC He tank	AMSAT-DL	Total cost unknown. Design used a modified fire extinguisher
Phase IIIB & C propellant	Launch Site	\$0 (Donated)
Phase IIIC propellant tanks	AMSAT-DL	Total cost unknown Common bulkhead tank machined from Al billets
Phase IIIA solid rocket motor	Thiokol TE-345	\$0 (Donated by USAF)

Table 6-6: Propulsion system components for other OSCAR spacecraft [Daniels 95]

While the OSCAR missions provide little insight into low-cost components, their on-orbit experience with the cost-effective systems engineering techniques described above have direct application to the minisatellite case study. The trade-offs associated with applying these techniques will be described in the following subsections.

6.2.3. Trade-offs

During the initial system design phase, the following trade-offs were encountered that effected the eventual architecture

- Liquid propellant expulsion method
- Liquid propellant pressurisation margin
- Pressure regulation method
- Propellant flow control and isolation methods

The following subsections will step through each of these major trade areas to analyse the critical factors involved in the final decisions. Following this discussion, the system acquisition process will be addressed.

6.2.3.1. *Expulsion Method*

There are two types of expulsion methods used for propellant tanks: passive and active. Passive methods refer to simple, free-surface expulsion whereby inertial forces (either spacecraft spin rate or acceleration from cold gas jets or the engine itself) orient liquid at the exit end of the tank and the less dense gas at the other. Obviously, this is the simpler and cheaper method but requires that the spacecraft be spun or that a short, propellant-settling pulse is given prior to main engine ignition. However, using spacecraft spin to achieve passive orientation of the propellant requires careful consideration be given to the exact location of the tank outlet line so it is roughly parallel to the effective liquid surface. This requires calculating the resultant total acceleration seen by the propellant due to both centripetal acceleration and engine thrust which was done for the actual tank designed.

Active expulsion methods use either pistons, diaphragms or propellant management devices (PMDs) to ensure the propellant stays at one end while the pressurant gas stays at the other. The operation of pistons, diaphragms or bladders is fairly easy to envision. The primary disadvantages of these methods is the extra ullage volume needed (meaning wasted propellant) and the necessity of finding a material compatible with the reactive propellants (this is especially difficult for MON). PMDs rely on surface tension to ensure the liquid remains over the exit port. In the simplest case, a PMD can be a "bubble trap" screen over the exit which will keep at least some liquid over the exit at all times with inertia combined with surface tension forces maintaining a steady flow of liquid toward the bubble trap. PMDs can also be much more complex, including wings and various shapes of screen to funnel the liquid to the outlet.

As cost and component availability were the primary drivers in tank selection, the design started from a free-surface tank developed by Arde as described below. This particular tank, designed for another mission, included a simple bubble trap which would have allowed propellant expulsion in a non-spinning mode. The design was then modified to incorporate a "dip leg" to allow propellant feed from a spinning mode as well.

6.2.3.2. Pressurisation Margin

Rocket engines are designed to function over a specified input pressure and flow rate. Depending on the particular engine, this range can be very narrow or relatively wide. In either case, optimum design performance is achieved at only one specific input pressure and flow rate. For this reason, virtually all space missions choose to precisely control the gas pressure in the propellant tanks to ensure that optimum performance is achieved. This approach requires the flow of pressurant gas from a high-pressure upstream reservoir to be carefully controlled throughout all propulsion system operations. However, even during Space Shuttle missions, a point is reached when there is sufficient ullage volume in the tanks to close off gas supply and complete engine operations in *blow-down* mode.

Once a blow-down capability is achieved, the propellant will continue to be supplied to the engine at a gradually decreasing inlet pressure. As long as this inlet pressure range is within the performance specifications of the engine, it is a perfectly acceptable practice with only a small, quantifiable loss in overall performance. Normally, the need for sufficient ullage volume to begin blow-down operations is far outweighed by the competing requirement to maximise propellant tank loading for mission lifetime. Thus, few missions begin in a blow-down mode. Blow-down is normally initiated only after the first major series of orbit manoeuvres when the remaining tank pressure is sufficient to meet attitude control requirements.

For the purposes of the Minisatellite propulsion system design, it was initially planned to operate in a regulated mode to maximise propellant loading. However, subsequent trade-off considerations led us to go to a unique complete blow-down system accepting the loss of ΔV capability (about 7%) in exchange for enhanced safety as well as integration and operational simplicity. This design approach will be discussed in greater detail later in the chapter.

6.2.3.3. Pressure Control

While it is acceptable in terms of performance and advantageous in terms of system safety to operate the liquid part of the propulsion system in a blow-down mode, this is not practical for the cold-gas portion. For this system, some means of reliable pressure control is essential.

There are two approaches to reducing a high-pressure supply gas to a lower specified operating pressure:

- Pressure regulator
- "Bang-bang" pressure control

A pressure regulator is a mechanical device which takes in high pressure gas at one end, and using mechanical feedback within the body of the regulator, delivers gas at a lower, constant pressure out the other end. Pressure regulators are the preferred approach in traditional systems.

A "bang-bang" pressure control scheme uses one or more valves in series with a pressure transducer downstream to close the loop. In operation, the valves are pulsed on/off to slowly bleed pressure downstream, usually into a buffer volume known as a plenum or accumulator. The valves are pulsed on and off until the desired downstream pressure is reached. A pressure transducer in the accumulator senses the downstream pressure and feeds this information to a controller that decides when and for how long to pulse the valves open. This "bang-bang" approach has been used on the OSCAR P3 spacecraft as already discussed. The advantages and disadvantages of each type of pressure regulation method are summarised in Table 6-7.

Pressure Regulation Method	Advantage	Disadvantages
Pressure Regulator	<ul style="list-style-type: none"> • Reliable • Accurate • Light weight • Requires no external feedback 	<ul style="list-style-type: none"> • Very expensive • Leak rates may be too high for a small ullage volume system • Once downstream pressure is set, can not be changed • Difficult to design, build and test
"Bang-bang" control system	<ul style="list-style-type: none"> • Inexpensive • Flexible, positive control over downstream pressure • Potentially lower leak rate • Easy to build and test 	<ul style="list-style-type: none"> • Heavy • More complex • Potentially less accurate • Requires additional flow restriction and accumulator volume

Table 6-7: Comparison of Pressure Regulation Methods.

It is important to note that with a bang-bang system, the accuracy of the regulated pressure is based on a feedback control system using the pressure transducer information. The longer it takes for the downstream pressure to reach the desired value the greater the potential for accuracy. Figure 6-6 shows the downstream pressure in a 1.3 litre accumulator as a function of time immediately after the bang-bang valves are opened to a 240 bar reservoir. As you can see, a desired downstream pressure of 20 bar is reached in less than 20 ms! To increase this time, flow restriction such as a Lee Visco Jet can be easily and inexpensively added to the system to insure a specific, specified gas flow rate to increase the time between valve opening and reaching desired downstream pressure [Lee 84]. Figure 6-7 shows the effect of limiting the flow rate to 2.0×10^{-4} kg/s using either a 1.3 litre or 0.5 litre accumulator. As you can see, the time to reach 20 bar increased to between 50 and 150 sec depending on the accumulator volume. An added advantage of the Visco Jet is that its predictable flow rate provides a limited but effective means of doing open loop pressure control in the event of a transducer failure.

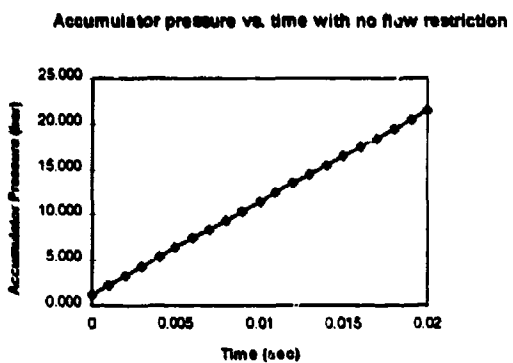


Figure 6-6: Rate of downstream pressure increase from 240 bar reservoir without flow with a 1.3 litre accumulator.

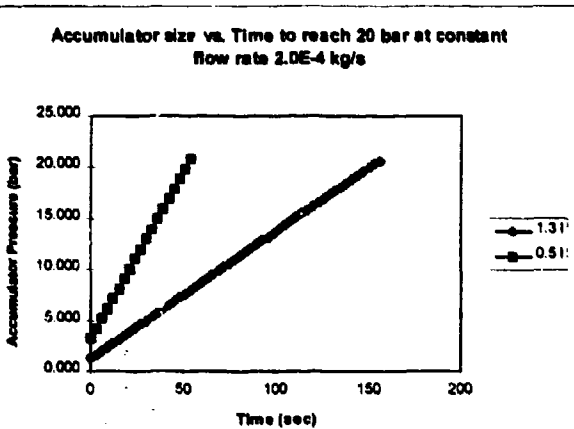


Figure 6-7: Downstream pressure as a function of time for a system employing a flow restrictor and various sizes of accumulator.

Because of the massive cost savings associated with a bang-bang system, its ease of implementation and testing, and the flight heritage demonstrated by the OSCAR P3 spacecraft, this method was selected for the minisatellite system design.

6.2.3.4. Flow Control & Isolation

Components used for propellant flow control and isolation include valves, lines and connectors. This section will address the trade-offs confronted in the system architecture for these components beginning with valves. The primary function of a valve is to control flow (ON/OFF). Typically, there are three types of valves used in spacecraft systems:

1. Solenoid (normally open or closed)
2. Solenoid latch valves
3. Pyrotechnic valves (normally open or closed)

Solenoid valves are perhaps the most widely used. They are spring-loaded into a normally open or normally closed position. When current is provided to the solenoid, a stem is pulled against the

spring to open or close. This means the non-default condition can only be maintained while current is applied. Solenoid valves are used most often in engine valves and cold-gas thrusters.

Because it is wasteful to provide constant power to energise a solenoid valve for long periods, latch valves are sometimes used to isolate branches within a system. A latch valve is also powered by a solenoid but has no default position. It will latch into either the open or closed position and remain there without the need for additional power. While the operational nature of latch valves make them an attractive option, their main drawback is expense. Quotations for latch valves were on the order of \$20,000 each and up. For this reason, they were not considered seriously for the system design case study.

The final type of valve commonly used is a pyrotechnic valve. Again, these can be configured either normally open or closed. When power is provided to the pyrotechnic charge, it changes configuration—permanently. Therefore, pyrotechnic valves can only be used once. The main advantage over latch valves is their lower cost and perceived reliability. They are mainly used to provide isolation of propellant tanks either prior to or after a mission manoeuvre phase. Because they provide a positive metal-to-metal seal, they are preferred by range safety offices for isolating propellant tanks from the engine during ground operation and launch. However, pyrotechnic valves have several drawbacks which caused them to be dismissed from consideration for the system:

1. Pyrotechnic valves are expensive (~\$8000 each)
2. They require more complex pre-flight operations to install
3. They can not be tested as part of the entire system
4. They have recently been linked to several expensive failures of spacecraft propulsion systems [AWST 95]

With latch valves and pyrotechnic valves dismissed from consideration, this left only solenoid valves. Recall, range safety requirements dictate there be three physical breaks between the propellant tanks and the engine. The dual-redundant LEROS-20 engine solenoid valves provide two of those breaks but a third was still needed. It was initially planned to use an additional solenoid valve in this application and accept the operational requirement of providing extra power to keep them open during engine firing (meaning a total of 6 valves would have to be on in order to fire the engine, one isolation valve and two engine valves in each line). Fortunately, there was another option to consider—burst disks.

Burst disks are commonly used in ground systems to provide emergency pressure relief. They consist of a metal housing containing a perforated metal disk designed to burst at a given pressure ($\pm 10\%$). They can be used to provide reliable propellant isolation during ground operations and launch, then burst when the tanks are pressurised in-orbit allowing propellant to flow to the engine valves. Thus, the additional power and reliability impacts of extra solenoid valves could be avoided at lower cost. The primary drawback was the need to accept the additional testing complexity and expense of a bolt-

up version of the burst disk housing to allow disks to be changed during system integration and testing. Disks would have to be changed after each ground test. A welded version with the disk pre-installed would be added prior to close-out of the system before launch. However, because of the cost savings and additional reliability, these integration problems were deemed to be an acceptable trade-off.

Another important flow-control decision to be made was the selection of propellant lines. Frequently, spacecraft propulsion systems use titanium lines to accommodate high pressure with the lowest possible mass. However, titanium lines are very expensive and require complicated and expensive transition welds from components which normally end in stainless steel stubs. Thus, for the minisatellite system it was decided to use standard, industrial stainless steel lines, 6 mm outer diameter. These are normally proof-tested in excess of 400 bar and are more than adequate for this application at far less cost.

Finally, there are two viable options for component-to-component connections in a spacecraft propulsions system:

- Welded
- Standard aerospace 37° flared fittings, sometimes called "AN" fittings used for a variety of commercial applications including military and civilian aircraft

Table 6-8 lists the advantages and disadvantages of each option

Option	Advantages	Disadvantages
Welded	<ul style="list-style-type: none"> • Standard approach used on virtually all spacecraft • High reliability • Robust, less susceptible to vibration • Lower weight 	<ul style="list-style-type: none"> • High cost (special orbit weld equipment needed) • Fixed configuration makes changes difficult and expensive • Orbit welding equipment limits size, bend and location of joints • Common metal transition pieces may be needed e.g. Ti to stainless steel • X-ray of joints often required
Flared fitting	<ul style="list-style-type: none"> • Inexpensive • Easy to use • Flexible and adaptable to changing plumbing layout • An industry standard outside of spacecraft applications 	<ul style="list-style-type: none"> • Inherently less leak-tight than a welded joint • Wire locking needed to protect against vibration • Higher overall parts count in system • More likely to introduce particulates into system • Higher weight

Table 6-8: Advantages and disadvantages of connector options.

The propulsion system team spent considerable time debating these options. In the end, flared fittings were selected primarily because of price and flexibility. This decision was aided by the knowledge that OSCAR spacecraft have used this approach for many years with no problems. Another important

consideration was that certain low-cost components only come with screwed fittings. To adapt these to a welded joint would require additional complexity and cost.

6.2.4. Acquisition Process

The ultimate proof for the utility of the cost-saving techniques developed in the research would be in realistically evaluating the acquisition process for the system. This effort was undertaken in parallel with the system architecture design effort as indicated above. System manufacturers at Arde, Inc., teamed with EG&G Wright Systems, were selected as the prime contractor for support systems (everything except the LEROS-20 engine). In working with Arde, the aim was to apply the cost driver lessons identified during the Hardware Acquisition Phase discussed in Chapter 2.

At the outset of our working relationship, the following cost-saving options were listed for the team to consider:

1. *Use of terrestrial hardware*—Nearly every single component in a spacecraft propulsion system (filters, relief valves, etc.) has a terrestrial, industrial-standard equivalent.
2. *Reduced requirements for acceptance testing*—Typically, all components, regardless of heritage, undergo final acceptance testing prior to delivery. They are then tested again as part of in-house screening and system integration. Reducing, or in some cases eliminating, redundant tests could realise real cost savings with a quantifiable risk.
3. *Reduced vibration and thermal/vacuum testing*—In many cases within the aerospace industry, individual components, such as engine valves, undergo separate vibration and thermal/vacuum testing. The valves are then installed on the flight engine, and together they undergo additional vibration and thermal/vacuum tests. Finally, the engine and valves are integrated into the spacecraft which undergoes yet another round of testing. Arguably, (especially in the case of engines and valves which have already been flight proven) the only vibration and thermal/vacuum tests which are necessary are the final ones.
4. *Elimination of unnecessary documentation*—The primary purpose of most documentation associated with component procurement is to manage the uncertainty in its performance. A large amount of the documentation generated as part of component procurement is intended to ensure no incorrect materials or procedures are used and to provide a clear paper trail in case of failure. Failure modes and effects analysis (FMEA), parts lists, materials lists, etc. give programme managers a “warm fuzzy” feeling that the part will work, but can not guarantee it. By their very nature, small, low-cost missions accept higher levels of risk than much larger programmes. Thus, much of the documentation associated with the traditional approach becomes unnecessary in light of the overall risk level of the mission.
5. *Relaxing performance requirements and margins*—As discussed in Chapter 2, the stricter the performance requirement and the tighter the margin, the higher the cost of the component.

The philosophy which eventually evolved was incorporated into the system design process and emphasised the use of:

- Standard, proven designs for essential modules
- Simple interfaces
- Careful selection of components from established volume production items.

The propulsion system requirements were carefully evaluated in conjunction with Arde and relaxed when possible to arrive at an effective design solution. Ensuring that the system could be delivered on schedule and at low cost was a major driver in the selection of the final approach and specific components. To the greatest extent possible, the propulsion system team used existing hardware and selected only those suppliers with a known record for good quality products to reduce risk during ground testing and in flight.

The systems requirements were evaluated from the very beginning of the design phase to allow the inclusion of selected key space-grade components. These components would require little or no analytical effort to determine their structural and thermal compatibility to the space environment. The history of each component was used to preclude unnecessary testing and its associated cost.

Actual component selection was made using experienced engineering judgement based on traditional space programs. Specific cost reduction guidelines were determined for the component procurement process:

- Flexible system specification
- Relaxed component specifications (data requirements sheets, if necessary)
- No formal configuration management required
- No supplier data items (other than a certificate of compliance)
- Supplier standard practices and procedures
- Balance performance against cost and perform trade-offs (This was aimed at taking advantage of large production runs, in some cases these may already be in place to support larger, more formal programs).

Another feature of the component selection and procurement process used by Arde was the use of a network of suppliers and customers developed over numerous formal space programs. Knowledge of production lines and previous performance were a major consideration in component selection. A key element was the formation of a strategic alliance to support small satellite propulsion system requirements. This alliance essentially committed the suppliers of the two major cost elements of the system (tanks and valves) to the team. This achieved a favourable reduction in unit cost, as well as control of that cost for the duration of the project.

Simple and easily manufactured work packages characterised the design of the propulsion system. The entire system was broken into the following subassembly kits:

- *Module box kits*—containing valves, ullage/accumulator bottles, pressure transducers and filters, flow restrictors, burst disks
- *Propellant tank kits*—containing propellant tanks ready to mount
- *Cold-gas thruster kits*—containing a valve/nozzle assembly plus connectors
- *Fill/Drain kits*—containing all fill and drain valves

Each kit could be assembled and tested at the factory. The kits would contain all necessary connectors. Spacecraft integration would require the addition of lines and mechanical brackets to

hold the components in place. This overall approach was designed to support rapid system assembly and testing and thus reduce cost as well as program risk.

6.2.5. Results

With an understanding of the critical performance drivers, the effects of various system trade-offs and an appreciation for the component acquisition process as discussed above, numerous changes were made to the baseline design presented in Section 6.2.2. Throughout the system development, those dimensions of cost controlled by the architecture were constantly in mind. Safety cost was paramount while performance (specifically system mass and volume) was traded-off to minimise integration cost, technical risk and the bottom-line price. The resulting final system architecture, shown in Figure 6-8 evolved considerably from the baseline presented at the beginning of the chapter and incorporates the following unique features and design goals:

1. Complete de-coupling of cold-gas system from bi-propellant system
2. Total blow-down liquid propellant delivery allowing for complete de-coupling of oxidiser and fuel tanks
3. Replacement of mechanical regulator with "bang-bang" pressure control
4. Elimination of all pyrotechnic valves
5. Use of burst disks
6. Use of Lee Visco Jets for flow restriction
7. Elimination of unnecessary redundancy i.e. additional cold-gas branch
8. Addition of two cold-gas thrusters for a total of 8 to provide 3 axis-control while keeping all components on the attach frame
9. Maximum use of off-the-shelf components
10. Reliance on flared fittings
11. Maximum re-use of standard components to minimise total parts count
12. Dual propellant extraction modes, spinning and non-spinning
13. Identical sized nitrogen and propellant tanks for identical bracket design

The detailed engineering design work and discussions with the acquisition partner Arde, Inc. culminated in a critical design review (CDR) of the entire system held at their offices in New Jersey and attended by Mr. Maarten Meerman, Mr. Malcolm Paul and myself. Following the resolution of open items from the CDR, final component selections were made. Detailed descriptions of each component with engineering drawings were part of Arde's contractual deliverable items with SSTL. Important specifications for tanks are summarised in Table 6-9. Specifications for valves and other components are summarised in Table 6-10.

Chapter 6: System Costs

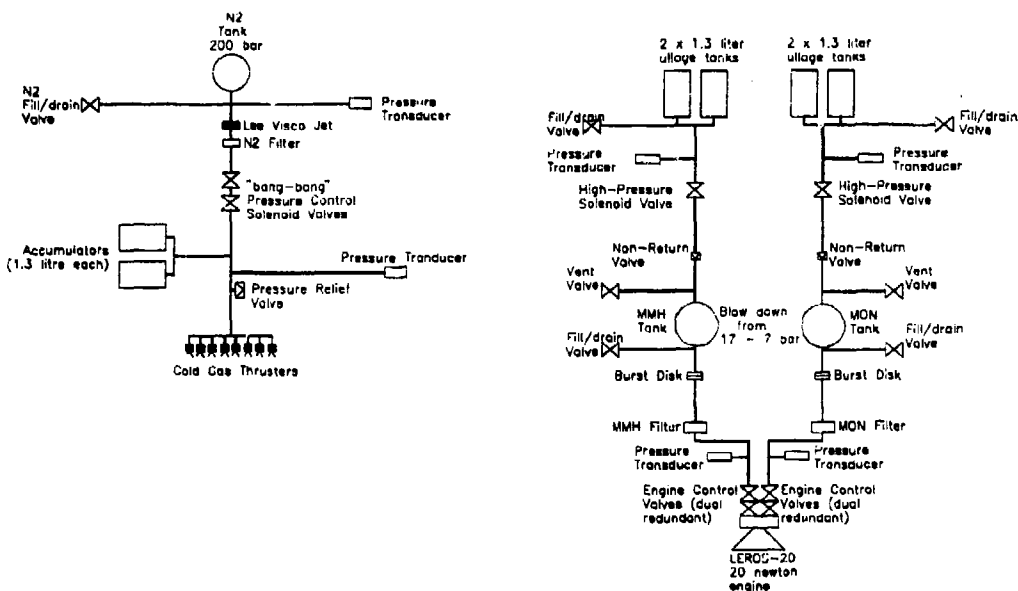


Figure 6-8: Final system architecture for minisatellite propulsion system.

Tank	Volume	MEOP	Mass	Dimensions
Accumulator/ Ullage	82 in ³ (1.344 litre)	500 psi (35 bar)	2.25 lb (1.021 kg)	Cylindrical, O.D.: 3.5 in (0.089 m) Length: 11.4 in (0.29 m)
Nitrogen	628 in ³ (10.291 litre)	3000 psi (206.8 bar)	9.6 lb (4.354 kg)	Spherical, O.D.: 10.8 in max (0.274 m) (dome to boss 11.6 in (0.295 m))
Propellant	628 in ³ (10.291 litre)	247 psi (17.03 bar) (designed for 600 psi (41.4 bar))	3.5 lb (1.588 kg)	Spherical, O.D.: 10.8 in (0.274 m) (boss to boss 12.5 in (0.318 m))

Table 6-9: Specifications for minisatellite propulsion system tanks.

Component	Supplier	Specifications
High Pressure "bang-bang" valve	EG&G Wright	MEOP = 241 bar
Ullage tank isolation valve	EG&G Wright	MEOP = 34.5 bar
Cold-gas thruster	EG&G Wright	0.1 N thrust at 4 bar operating pressure MEOP 13.8 bar
Relief Valve	Circle Seal	Set at 12.8 bar relief
Lee Visco Jet	Lee	Lohm = 25,000
Propellant Filter	Nupro	7 micron
Nitrogen Filter	Nupro	7 micron
Check Valves	Circle Seal	
Nitrogen Fill/Drain Valve	OEA	
Propellant Fill/Drain Valve	OEA	
Pressure Transducers	Taber	High pressure 0 - 200 bar Low pressure 0 - ? bar

Table 6-10: Specifications for minisatellite propulsion system components.

6.3. Total System Cost

With the system architecture fully defined and system components selected, the total cost of the system can now be assessed. Analysis of operational performance along with recommended operational configuration will first be summarised. System price will then be addressed including the additional costs for support hardware and manpower. Integration costs will then be addressed followed by safety, technical risk and logistics.

6.3.1. Performance

Of the four performance dimensions of cost, volume was fixed by the minisatellite envelope, time and power by the decision to use the LEROS-20 engine and cold-gas thrusters. Therefore, the most important dimension to be assess was system mass. Table 6-11 gives the total dry system mass break down. Notice the bottom line of 22.75 kg is more than 10 kg greater than that estimated by [Smith 84] as presented in Table 6-2. This represents about 4% of the total spacecraft mass and proves a rough estimate of the “mass cost” of this system architecture.

Component	Number	Unit Mass (kg)	Total Mass (kg)
Accumulator	2	1.1	2.2
Ullage tanks	4	1.1	4.4
Propellant tanks	2	1.6	3.2
Nitrogen tank	1	4.35	4.35
Bang-bang valves	2	0.54	1.08
Isolation valves	2	0.54	1.08
Cold-gas thrusters	8	0.32	2.56
Filters	2	0.05	0.1
Visco Jets	1	0.05	0.05
Pressure Transducers	6	0.35	2.1
Burst Disks	2	0.2	0.4
Non-Return Valves	2	0.1	0.2
Fill/Drain or Vent Valves	5	0.045	0.225
Relief Valve	1	0.2	0.2
LEROS-20 Engine (w/valves)	1	1	0.6
Total			22.745

Table 6-11: Mass break-down for minisatellite propulsion system.

Another important aspect of performance cost to consider is the mass efficiency of the system. For the cold-gas system this was relatively easy to determine. MEOP of the tank was designed to be 200 bar because this is the easiest standard pressure to work with. Higher operating pressures would require the use of pressure intensifiers which would greatly complicate launch logistics from remote launch sites. Therefore, the mass performance of the cold-gas system was solely a function of the *Isp* of the thrusters.

The propellant loading for the bi-propellant system, however, was not so simple. The following parameters were fixed by the system architecture:

- Propellant tank volume = 10.291 litre
- Ullage tank volume = 1.344 litre
- Number of ullage tanks per tank = 2
- Maximum ullage tank pressure = 35 bar

The actual mission ΔV was then determined by the following interrelated parameters which define a trade-space:

1. Initial ullage tank pressure.
2. Initial ullage in propellant tank (which determines available propellant).
3. Engine performance as a function of tank pressure.

The first two items in this trade-space determine the initial and final blow-down pressure as well as the total propellant available. The third item relates this blow-down pressure to instantaneous performance which must be integrated over the total available propellant to get mission ΔV . Obviously, the design goal was to maximise total ΔV . This means we want to maximise the initial propellant loading (minimise the propellant tank ullage) while maximising performance. Unfortunately, a compromise is needed. To achieve the greatest amount of pressurant gas, it was decided to operate the ullage tanks at their maximum operating pressure of 35 bar. This established the first variable in the trade-space and left the remaining two.

Looking at the second item in the trade-space (initial ullage in the propellant tank) Table 6-12 shows the initial and final blow-down pressures for various initial ullage volume options.

Initial Propellant Tank Ullage (litre)	Initial Blow-down Pressure (bar)	Final Blow-down Pressure (bar)
1	25.8	7.3
2	20.29	7.45
2.5	18.40	7.49
3	16.86	7.53

Table 6-12: Propellant tank blow-down ranges at various initial ullage volumes assuming 35 bar ullage tank pressure.

Using these blow-down ranges as options, the final key to optimising the design was to analyse the performance as a function of tank pressure and integrate over the blow-down range. According to [Wood 90], the LEROS-20 engine specification allows for a blow-down range of 20 to 10 bar. Typically, orifices are placed downstream of the propellant tanks to create an additional pressure drop in the system both to better de-couple engine pressure from the rest of the system and to “tune” the blow-down performance range [Wood 95]. This orifice arrangement has the effect of dropping actual inlet pressure.

Additional data provided by RO [Wood 95] allowed me to derive actual engine performance as a function of tank pressure. In practice, the analysis requires you to pick a *set-point* at the initial blow-down pressure. An orifice is then placed in the engine to give maximum performance at this set-point

pressure and drops off correspondingly from there. Analytic performance relationships were derived from this data to allow performance simulation over various blow-down ranges. Figure 6-9 shows the performance drop-off in terms of *Isp* for the 1 litre ullage option which delivers an inlet pressure blow-down range of 25.8 - 7.3 bar. Based on the results from my systems analysis, this loading option was selected to deliver maximum total ΔV . Table 6-13 summarises performance for both the cold-gas and bi-propellant systems. Notice the total ΔV available from the bi-propellant system operating in blow-down is 239.8 m/s. Operating in a regulated system at constant inlet pressure, the average *Isp* would be 290 sec for a total ΔV 257 m/s with this propellant loading. This equates to a loss of about 7% for using the total blow-down method. The next subsection will address the total system price.

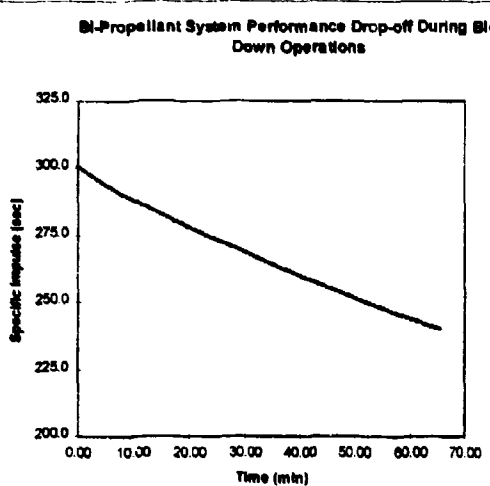


Figure 6-9: Bi-propellant System performance drop-off during blow-down operations. Simulation assumes 1 litre initial ullage in propellant tanks with initial ullage tank pressure of 35 bar.

Parameter	Cold-gas System	Bi-Propellant System
Propellant(s)	Nitrogen	MMH/MON
Propellant mass, kg	2.367	21.61 (MMH = 8.16, MON = 13.44)
Feed pressure, bar	4.0	25.8 - 7.3
Thrust, N (Torque, Nm)	0.1 (0.048 Nm)	14.6 (average)
Average specific impulse, sec	65	267.4
Total impulse	695 Nmsec	57,173 Nsec
ΔV , m/sec	n/a	239.8
Approximate Total thrust time available, min	243	65

Table 6-13: Summary of propulsion system performance parameters.

6.3.2. System Price

Perhaps more important than the system engineering issues negotiated with the prime contractor were the detailed component prices. Table 6-14 summarises these prices for each part of the system and provides subtotals for the cold-gas and bi-propellant systems separately. Price information for the LEROS-20 engine was provided by RO through separate negotiation as discussed in Chapter 3.

It is interesting to note the percentage of total system price represented by the thrusters alone. These results indicate that thrusters (cold-gas and bi-propellant) account for only 35% of total system cost. Stated another way, support system hardware accounts for at least 65% total system price, relatively independent of actual technology used. This is a significant shift from that predicted by the standard model which indicated a rough parity between thruster and support system price.

However, the hardware price represents only part of the story. Once delivered, this hardware must be fully integrated into the spacecraft and subjected to a variety of operational testing prior to flight. The budget for this effort, both in price and manpower, is summarised in Table 6-15.

Component	Number	Unit Cost	System Cost
<i>Cold-gas Attitude Control System</i>			
Nitrogen tank	1	\$10,627	\$10,627
Accumulator	2	\$2,447	\$4,894
Bang-bang valve	2	\$5,100	\$10,200
Cold-gas thrusters	8	\$4,046	\$32,368
Lee Visco Jet	1	\$1,066	\$1,066
Nitrogen fill/drain valve	1	\$1,443	\$1,443
Pressure relief valve	1	\$1,836	\$1,836
Nitrogen filter	1	\$160	\$160
Pressure transducer	2	\$1,442	\$2,884
<i>Subtotal</i>			\$65,478
<i>Bi-propellant Orbit Control System</i>			
LEROS-20 Engine	1	\$36,160	\$36,160
Ullage tanks	4	\$2,447	\$9,788
Propellant tanks	2	\$12,728	\$25,456
Isolation valves	2	\$5,100	\$10,200
Check valves	2	\$2,538	\$5,076
Filter	2	\$160	\$320
Vent valve	2	\$5,856	\$11,712
Fill/drain valve	2	\$5,856	\$11,712
Pressure transducer	4	\$1,442	\$5,768
Burst disk holder	2	\$410	\$820
Burst disk	2	\$304	\$608
<i>Subtotal</i>			\$117,620
<i>Miscellaneous</i>			
Shipping containers	4	\$401	\$1,604
Program management	1	\$11,784	\$11,784
<i>System Total</i>			\$196,486

Table 6-14: Detailed cost data for minisatellite propulsion system. Adapted from [Arde 96] [RO 94].

Item	Cost	Man-power (mandays)
Total System Cost	\$196,486	
RO Facility Hire	\$5,000	
Proto-flight Mech. Model Development	\$41,837	123
Ground Support Equipment	\$74,160	76
Additional Flight Hardware	\$1,280	39
Consumables	\$2,440	
Flight Model Integration		61
Flight Model Testing		148
Misc.	\$9,200	
Hardware Total	\$330,403	447
Labour at \$100,000/man-year	\$122,466	
Bottom Line	\$452,869	

Table 6-15: Estimated budget for minisatellite propulsion system acquisition, integration and testing including ground support equipment for launch support.

6.3.3. Integration Cost

This section addresses the integration costs that were identified and addressed during the system design case study. Figure 6-10 shows an estimated schedule for completing mechanical and electrical integration and all testing prior to launch. Further details of mechanical integration and electrical interface will be addressed in the following subsections, followed by a summary of attitude and orbit control system and payload operations issues.

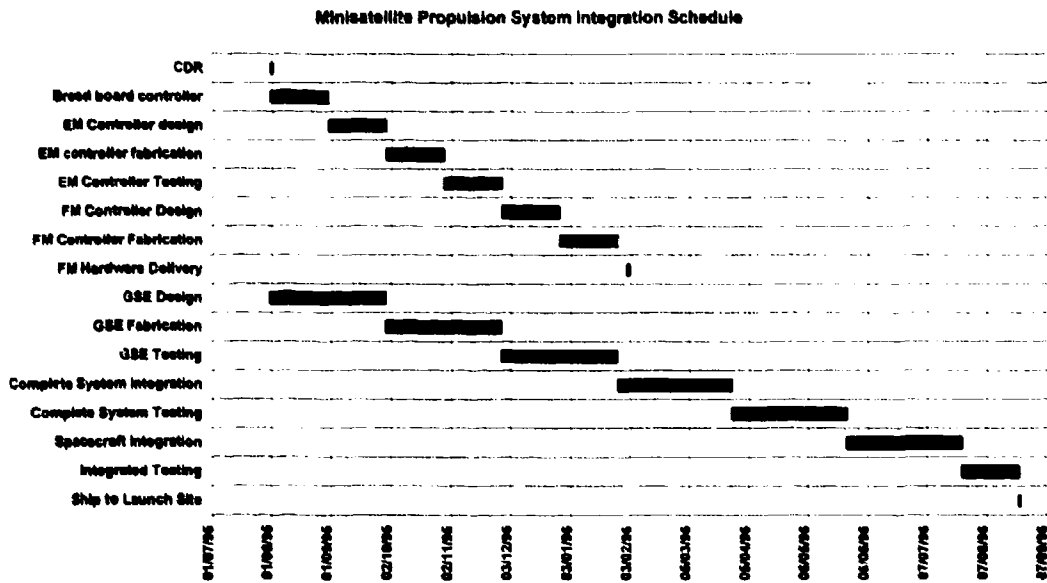


Figure 6-10: Proposed spacecraft integration schedule for the minisatellite propulsion system.

6.3.3.1. Mechanical Integration

A substantial effort was put into defining the mechanical interface for the propulsion system components within the minisatellite structure. Much credit is owed to Mr. Richard Williams and Mr.

Andy Currie for their ideas and wizardry with *AutoCAD*. Recall, one of the primary mechanical constraints was to restrict all propulsion system integration to the minisatellite attach frame. In addition, the structure of the minisatellite is based on the module box configuration. Working with the mechanical design team, we decided to integrate all system components (valves, burst disks, etc.) into 100 mm high module boxes. The LEROS-20 engine would be in the centre of the attach frame. The cold-gas thrusters would be on the underside of the attach frame. The configuration for the module boxes and tanks is shown in Figure 6-11 with the underside of the attach frame below it revealing the cold-gas thruster locations.

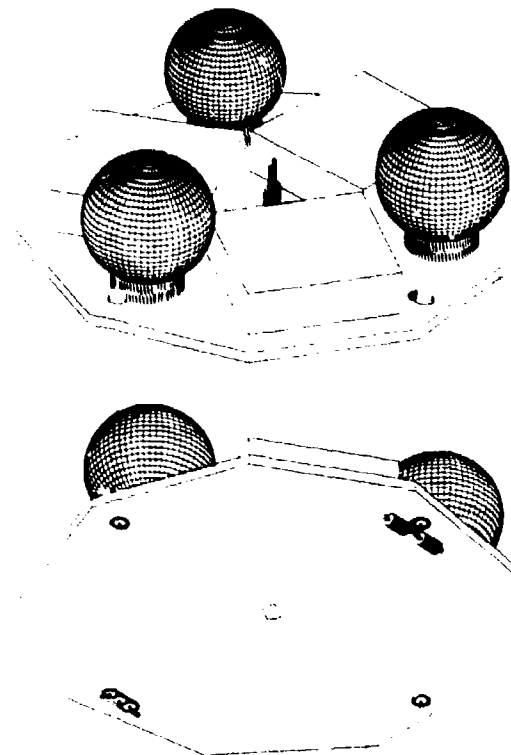


Figure 6-11: Two views showing the configuration of the minisatellite attach frame where the propulsion system is to be integrated. On the top see the three module boxes which contain the system components with the tanks in between. The LEROS-20 engine can be seen in the centre. The bottom figure shows the underside of the attach frame with locations for cold-gas thrusters.

To simplify mechanical integration while maintaining low-cost, our guiding principle was to minimise total parts count by re-using mechanical bracket designs. We were greatly aided in this effort by the inherently elegant symmetry of the system architecture itself. By design, the three main tanks, 2 propellant and one nitrogen, have identical outer diameter allowing for 3 identical tank mounting brackets. Associated with each tank are identical sets of components:

- 1 (or 2) solenoid valves
- 2 pressure transducers
- 2 accumulator/ullage tanks

This allowed us to configure two, completely identical, module box layouts with associated brackets (one for each branch of the liquid system) and one nearly identical module box for the cold-gas system. The symmetry of this layout is shown in Figure 6-12. Figure 6-13 and Figure 6-14 offer different perspectives of the same layout. The conclusions of the mechanical design team was that this configuration would allow rapid, modular integration and testing with minimum impact to other spacecraft systems.

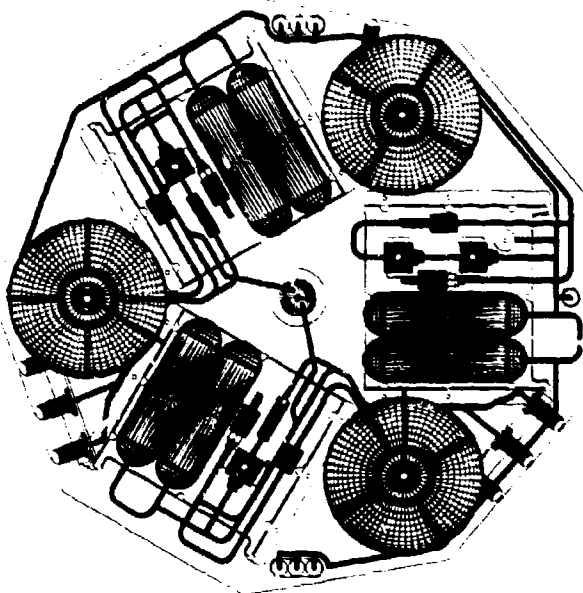


Figure 6-12: Diagram showing a top view of the propulsion system mechanical layout. Notice the system is split into three, nearly identical module boxes for ease and economy of integration.

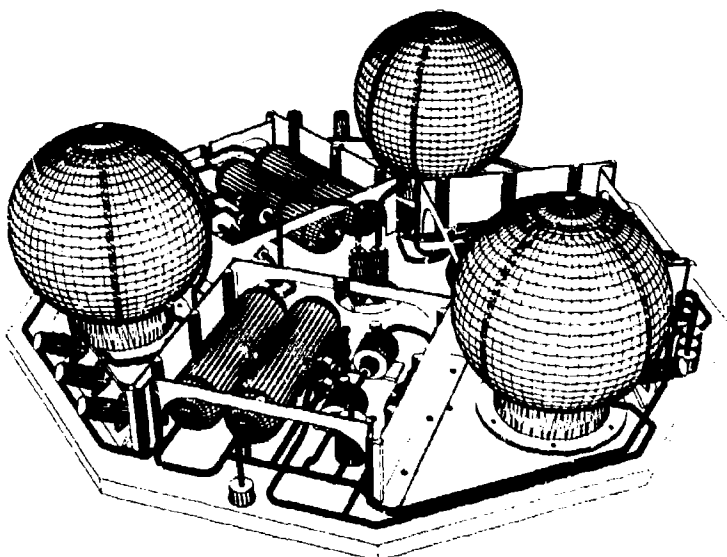


Figure 6-13: Side view of propulsion system mechanical integration onto the attach frame.

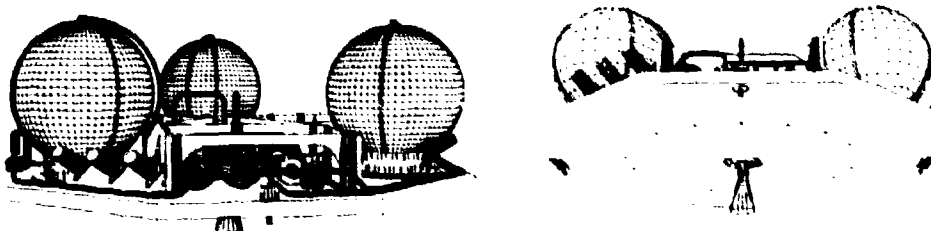


Figure 6-14: Two additional perspectives on the propulsion system mechanical integration.

6.3.3.2. Electronic Integration

Power supply and control of all 16 of the system's valves, as well as sensing of the 6 pressure transducers, would be via two dedicated electronic module boxes. These would be placed on top of two of the component boxes shown in the last section. Initial design architecture envisions that each electronic module box would contain a single control area network (CAN) interface microcontroller, 8 relay drivers and 5 analogue signal inputs. These would be configured such that either microcontroller could command all 16 valves to allow for some degraded functional redundancy. The electrical interface requirements for the valves are listed in Table 6-16.

Parameter	Cold-gas Thruster	Bang-bang Valve	N2 Isolation Valve	Engine Valve (model 18212-1)
Number	8	2	2	2 (series redundant)
Power	• 30 W @ 28 VDC, 68°F	34 W	34 W	
Voltage	• 28±4 VDC • Pull-in voltage: 20 VDC, 68°F • Drop-out voltage: 2 VDC, 68°F	28±4 VDC	28±4 VDC	• 22-35 VDC • Pull-in voltage 22 VDC per series pair • Drop-out voltage 0.75 VDC per series pair
Resistance				11 Ohms per coil min @ 0°C (total of 4 coils per valve)
Response	• Opening 18 ms max., closing 10 ms max.	0.15 sec maximum opening and closing	0.15 sec maximum opening and closing	
Flow	• Thrust: 0.0225 lbf (0.1 N) @ 58 +10 psia (4±0.7 bar), 68°F, GN ₂ • Expansion Ratio: 100:1 • Flow: 0.000357 lbm/sec (1.619 x 10 ⁻⁴ kg/sec)	Equivalent to 0.0394 in (1 mm) diameter orifice (CD = 0.8)	Equivalent to 0.0787 in (2 mm) diameter orifice (CD = 0.8)	
Duty		Continuous at 16 VDC, 10 sec min. at 32 VDC	Continuous at 16 VDC, 10 sec min. at 32 VDC	Continuous with flow, 120 sec. no flow.

Table 6-16: Electrical interface requirements for propulsion system valves.

6.3.3.3. Attitude & Orbit Control

A key consideration for main engine operations is the attitude control scheme during manoeuvres and the corresponding integration issues imposed on the spacecraft attitude determination and control system. The purpose of this discussion is not to present the complete answer to the problem of pointing and stabilising the platform during manoeuvres. Rather, this subsection is intended to identify the sources of disturbance torques and apply fundamental analytic techniques in an attempt to bound the complexity of the problem.

The primary sources for disturbance torque during main engine firing are:

- *Engine misalignment angle (θ)*—causes torque about an axis in the transverse plane
- *CG offset/movement during flight*—causes torque about an axis in the transverse plane

These are illustrated Figure 6-15 where

F_{engine} = Engine thrust

F_{miss} = Force due to engine misalignment

F_{cg} = Force due to CG movement

d_{miss} = Distance to CG (moment arm of misalignment torque)

dcg = Movement of CG

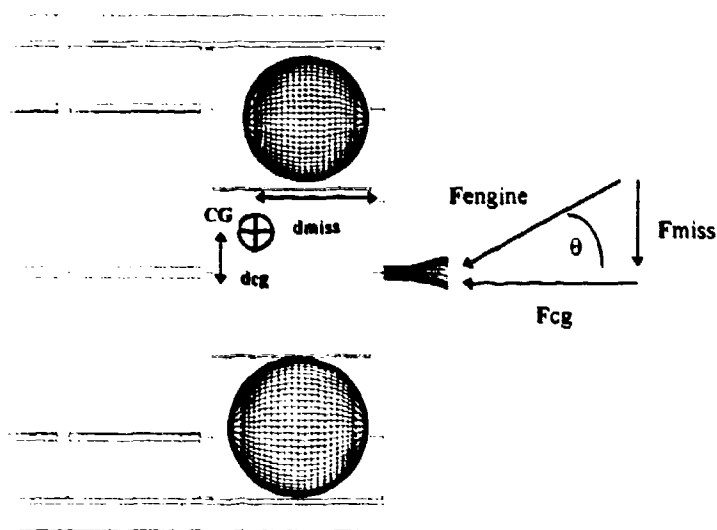


Figure 6-15: Simplified lay-out showing potential sources of disturbance torque for the minisatellite.

For analysis purposes, the following assumptions can be made:

- I_a = Axial moment of inertia = $20 \text{ kg}\cdot\text{m}^2$
- I_t = Transverse moment of inertia = $22 \text{ kg}\cdot\text{m}^2$
- No off-diagonal components of moment of inertia
- d_{miss} = Distance from engine to CG = 0.288 m
- Thrust = 20 N

Using these parameters as a starting point, both open loop control (i.e. no stabilisation) and 3-axis control using the cold-gas system were considered. Even using best-case assumptions, neither option was practical. In open loop mode, disturbance torques quickly cause the platform to spin out of control. While the cold-gas system has the control authority to maintain pointing against the disturbance torques, there is not sufficient cold-gas propellant onboard to maintain pointing throughout the lifetime of the bi-propellant system. Therefore, the only remaining control option is inertial stabilisation attained by either spinning the entire spacecraft or spinning a momentum wheel aligned with the thrust axis. For simplicity, the spinning option was assumed in order to determine the total system momentum needed to provide sufficient platform stiffness. However, from an operational standpoint, it may be more desirable to use the momentum wheel approach. This makes attitude determination less complex and eliminates the potential problem of propellant sloshing which can lead to system energy damping and potentially unstable modes [Wertz 95].

Using the above assumptions, a technique for determining the nutation cone angle of a spinning mass subjected to a constant torque described in [Greenwood 88] was adapted to the problem. This analysis determined the minimum spacecraft spin rate to provide inertial stiffness in the face of a moderate disturbance torque from CG displacement and engine misalignment. Figure 6-16 shows the relationship between spin rate and maximum cone angle for a constant 1 cm CG displacement and 1° engine misalignment. As the figure shows, maximum cone angle decreases dramatically as spin rate is increased from zero to about 15 RPM. Diminishing returns is reached as the spin rate is increased beyond about 15 RPM.

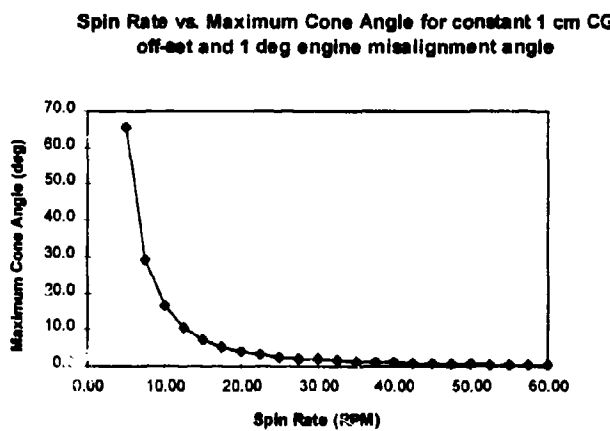


Figure 6-16: The effect of spin rate on maximum cone angle for a constant disturbance torque caused by a 1 cm CG displacement and 1° engine misalignment.

Taking 15 RPM as the minimum spin rate to provide stability, we can look at the trade-off between CG displacement and engine misalignment as shown in Figure 6-17. This allows us to define a trade-space for these two design budgets which dictates a requirement for a maximum 2 cm CG displacement throughout the mission and a maximum 1.5° engine misalignment angle. These

requirements result in the following worst-case disturbance torques induced during main engine firing:

- $\text{Torque}_{\text{cg}} = (20 \text{ N})(0.02 \text{ m}) = 0.4 \text{ Nm}$
- $\text{Torque}_{\text{mis}} = (20 \text{ N})(\sin 1.5^\circ)(d_{\text{cg}}) = 0.151 \text{ Nm}$

We can construct a worst-on-worst case by adding the two to get a combined disturbance torque of

- $\text{Torque}_{\text{total}} = \text{Torque}_{\text{cg}} + \text{Torque}_{\text{miss}} = 0.551 \text{ Nm}$

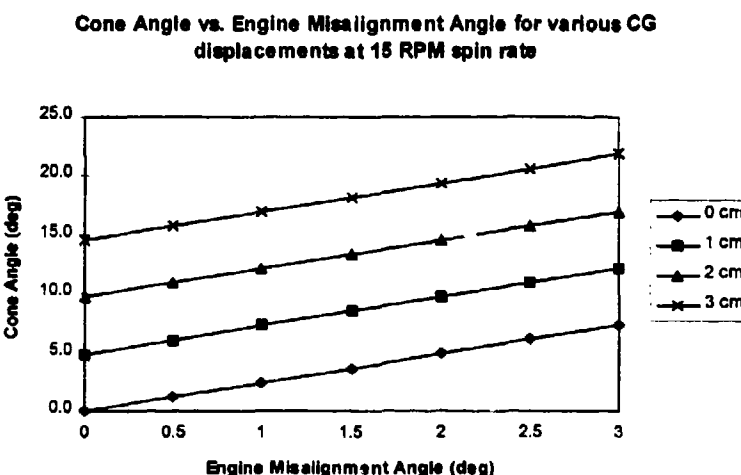


Figure 6-17: Trade space for CG displacement and engine misalignment angle for a constant 15 RPM spin rate.

It is important to note the sensitivity of these results to the assumed values for axial and transverse moment of inertia. Figure 6-18 shows the variation in maximum cone angle for a spin rate of 15 RPM with a 1.5° engine misalignment and 0.01 m CG displacement. As you can see, the maximum cone angle changes by a factor of 4 between I_t values of 21 to 25 kgm^2 . Obviously, all these results would have to be re-analysed when more precise moment of inertia data becomes available for the actual spacecraft configuration.

Assuming the spacecraft is inertially stabilised during manoeuvres, ignition time must be planned such that it takes place when the inertial attitude coincides with the desired thrust attitude. For pro-grade manoeuvres, this will occur only at one point per orbit when the thrust axis will be pointed directly along the orbit velocity vector. Unfortunately, this perfect alignment occurs for only an infinitesimal length of time while the practical manoeuvre time is of finite duration. Thus, we must accept that all inertially targeted manoeuvres can only bracket the ideal attitude with less than ideal pointing before and after.

Effect of Transverse Moment of Inertia value on Maximum Cone Angle (with $I_a = 20 \text{ kgm}^2$)

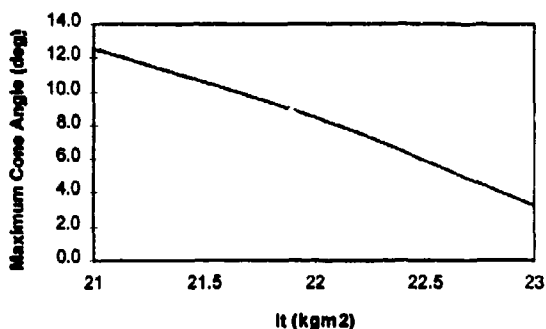


Figure 6-18: Sensitivity of maximum cone angle to assumed value of transverse moment of inertia (I_t) for a 15 RPM spin rate, 1.5° engine misalignment and 0.01 m CG displacement.

To minimise these losses due to non-optimal pointing, we would like to keep the burn length quite short. However, practical aspects of manoeuvre targeting, monitoring and execution would argue that burns should be as long as possible. To help balance these conflicting requirements we can look at the actual effect of off-nominal pointing for a hypothetical manoeuvre to quantify the losses. Assuming an initial circular orbit at an altitude of 700 km, the period would be 5926 seconds. This implies the velocity vector rotates at a rate of 0.0607°/sec. Thus, during a 10 minute manoeuvre, the orbit velocity vector would rotate about 36.4°. Assuming we bracketed the ideal point in the middle of the manoeuvre, we would begin and end the manoeuvre with about 18.2° misalignment. In other words, the manoeuvre starts out with an 18.2° misalignment, gets better until it is optimum half way through, then gradually gets worse again.

Optimally, a 10 minute burn with 20-N thrust would give 12,000 N-sec of impulse along the velocity vector. However, integrating throughout the 10 minute burn produces an effective total impulse of 11,798 N-sec which equates to a loss of only about 2%. However, for a 20 minute burn this loss increases to almost 7%. Therefore, given that attitude control pointing losses must be added on top of this misalignment error, a 10 minute limit for manoeuvres is recommended.

6.3.3.4. Payload Operations

The preceding discussion on attitude control during orbit manoeuvres has important implications for payload operations. Note that analysis indicates that the spacecraft requires some type of stabilisation during main engine firing to compensate for induced disturbance torques. Unfortunately, this attitude control mode will be somewhat different from that used for nadir-pointing payload operations. Furthermore, the engine location is on the opposite facet from the Earth-pointing side of the spacecraft. As a result, payload operations will have to be interrupted for manoeuvres which are targeted parallel to the velocity vector. In addition, this necessitates two separate attitude control

modes, one for engine firing and one for payload pointing. This would have additional cost implications for the entire mission.

6.3.3.5. Other Mission Costs

The remaining mission costs to consider for the minisatellite system are technical risk, safety, and logistics. The technical risk for the first flight of any new system is difficult to quantify. While the system architecture itself is unique, the majority of components have proven flight heritage. Therefore, the majority of risk is tied to integration and operation of the system. Here, the fact that UoSAT/SSTL personnel must climb a learning curve adds some overall risk to the program. Fortunately, the simplicity of the system provides a large margin for error. By de-coupling the cold-gas system from the bi-propellant system, a failure in one will have no effect on the other. Furthermore, the blow-down arrangement for the bi-propellant system virtually eliminates the chance of oxidiser and fuel mixing outside the engine. While it is possible that one or both could leak, they would most likely sublime harmlessly into space without creating a catastrophic situation.

A final consideration of the system design is its safety and logistics costs. The system fully complies with USAF safety requirements with the assumption that this represents the minimum acceptable level. Additional features could be added at greater expense but with little additional contribution to overall safety. While the system is as safe as possible in design, there is still the inherent safety cost associated with handling and using hypergolic propellants as described in Chapter 3. Furthermore, the necessary propellant and ground support equipment must be delivered to the launch site. It should be noted that until relatively late in the program, the system described in this chapter was intended for the UoSAT-12 mission in early 1997. However, because this mission is planned for launch on a Russian ROCKOT launch vehicle, uncertainties associated with the actual launch site greatly increased the potential for high safety and logistics costs to the point where the bi-propellant system was eliminated, leaving only the cold-gas system.

6.4. Conclusions

This chapter has presented the results of a propulsion system design case study. The goal of this effort was to look beyond the technology chosen, to fully characterise the influence of mission definition, system design and acquisition on total cost. This research effort represented significant engineering development aimed at defining the actual system for a real mission. The resulting design represents a completely new system that now exists on-the-shelf with well-defined costs and performance.

From the cost analysis in the last section, we can conclude that the system delivers good performance, well within 200 m/s ΔV requirement called for in the mission definition. More significantly, the system design presents a quantifiable trade-off between total system mass, performance and price.

Compared to more conventional systems using all space-qualified hardware and regulated pressure, this system adds only about 4% to total spacecraft mass and sacrifices about 7% in delivered ΔV .

Furthermore, armed with the price data derived, the effectiveness of the steps taken as part of the system design case study can also be evaluated. Recall from Section 6.2.3, the best target cost available was based on the CER developed by Aerospace Corp. which gave a projected system cost of \$887,000. To be the most conservative, one can assume this CER price includes integration and testing costs in addition to hardware. However, because this CER was based on the orbit control system requirement alone, for comparison the cost of the cold-gas attitude control system must be removed from the bottom-line price (for simplicity, other integration costs will not be changed as a result of removing the cold-gas system). In Table 6-14, the hardware price for the cold-gas system was shown to be \$65,478. Removing this price from the bottom line leaves a total price for the orbit control system alone of \$387,391. This is about 44% of the amount predicted by the CER or a cost reduction of greater than 50%.

The point of this pricing exercise is not to get into a "bean counting" argument over which numbers are correct. The objective is to evaluate the design justification process described in Chapter 2 whereby system design and cost data are established concurrently. By comparing the price reached through this process with that predicted by the CER, we arrive at an indication of the potential effectiveness of applying the cost reduction strategies outlined in this thesis. The results indicate that these cost reduction strategies are effective and can significantly reduce total system price with a quantifiable trade-off in mass and performance.

Another important result from this exercise was quantifying the contribution to total system price from thrusters vs. support hardware. This analysis reveals that the thruster itself represents only about 35% of total system price. In other words, the majority of system price is in the support components—tanks, valves, etc. These costs are somewhat independent of engine technology. This implies there is far more leverage to lowering overall system price by focusing on architecture and acquisition issues than in building cheap thrusters alone.

Equally important, this research now provides a "generic" system that can be readily adapted to support mono-propellant, hybrid or resistojet applications with realistic and predictable total cost. The detailed analysis of system performance and integration issues highlights how the system could be effectively used in orbit, as well as how it will interact with other subsystems including mechanical, electrical, ADCS and payload operations. This "generic" system will be adapted to various technology options for further comparison in Chapter 7.

In summary, the research goal of this chapter has been fully met. The minisatellite case study has allowed the complete characterisation of the costs that are driven by the systems engineering issues of propulsion design. The important conclusions from this research are:

- A complete understanding of propulsion system costs can only come by looking beyond technology to assess the influence of mission definition, system design and acquisition on the critical aspects of systems engineering. By focusing on these cost drivers, total system price can be drastically reduced with quantifiable trade-offs in performance.
- Thruster price accounts for only about 35% of total system price. Thus, total system price and performance depend, in large part, on the actual system design used. In other words, a cheap technology does not necessarily deliver a cheap system.
- A flexible, cost-effective "generic" system was developed that can be readily adapted to a variety of technologies and effectively integrated on a small satellite with easily quantifiable total cost data.

6.5. References

- [AMSAT 95] The Phase 3D Design Team, "Phase 3D, A New Era For Amateur Satellites," *The AMSAT Journal*, March/April 1995.
- [Arde 96] Arde, Inc., UoSAT Minisatellite Propulsion System Phase-I Contract Deliverable, component price quotations, SSTL Proprietary Information, 1996.
- [ARSENE 92] "ARSENE Satellite," Publicity handout prepared by CNES, 1992.
- [AWST 95] Aviation Week & Space Technology, "NOAA-14 To Restore Forecasting Capability," 9 January 1995.
- [Burgess 95] Burgess, E.L., Lao, N.Y., Bearden, D.A., "Small-Satellite Cost Estimating Relationships," Presented at the 9th Annual AIAA/Utah State University Conference on Small Satellites, 18-21 September 1995.
- [Clark 80] Clark, T., Kasser, J., "Ariane Launch Vehicle Malfunctions, Phase IIIA Spacecraft Lost!" *Orbit*, June/July 1980.
- [Daniels 87] Daniels, Richard L., W4PUJ, "The Propulsion System of the Phase-III Series Spacecraft," Presented at the 1st Utah State Conference on Small Satellites, reprinted in AMSAT-NA Technical Journal, Vol. 1, No. 2, Winter 1987-88.
- [Daniels 95] Daniels, R., Private communication, 9 February 95.
- [Grahn 93] Grahn, S., "The FREJA Magnetospheric Research Satellite Design and Flight Operations," Presented at the 7th Annual AIAA/USU Conference on Small Satellites, 13 - 16 September 1993, Logan, Utah.
- [Greenwood 88] Greenwood, D.T., *Principles of Dynamics*, Prentice-Hall, Inc., Englewood Cliffs, NJ, 1988.
- [Lee 84] Lee Company, *Technical Hydraulic Handbook*, Westbrook, Connecticut, USA, 1984.
- [Llareus 94] Llareus, M., ENSAE, Phone conversation with author, 5 January 1994.
- [MS 1522A] MIL-STD-1522A Standard General Requirements for Safe Design and Operation of Pressurized Missile and Space Systems, United States Air Force, 28 May 1984.
- [OSCAR 93] "ARSENE, The End?" *OSCAR NEWS*, AMSAT-UK, October 1993, Number 103.
- [Paul 95] Paul, M., Propulsion Systems Engineer, SSTL, Personal communication, 1995.
- [Pidoux 92] Pidoux, B., "The Mission of the Amateur Radio Satellite ARSENE," Proceedings of the 7th AMSAT-UK Colloquium, University of Surrey, July 1992.
- [RO 94] Royal Ordnance, personal communication Ref: PDC/JE/313, 30 November, 1994.
- [Smith 84] Smith, P., Horton, M.A., "Advanced Propulsion Systems for Geostationary Spacecraft—Study Results," The Marconi Company, AIAA-84-1230, 1984.
- [Ward 95] Ward, J., "Minisatellite Program Objectives," SSTL internal memo, 1995.

Chapter 6: *System Costs*

- [Wertz 95] Wertz, J. President Micrososm, Inc., Spacecraft attitude control and determination consultant, private communication, 1995.
- [Wood 90] Wood, R.S., "Development of a Low Cost 22N Bi-propellant Thruster." AIAA 90-2056, AIAA/SAE/ASME/ASEE 26th Joint Propulsion Conference, Orlando, Florida, 16-18 July 1990.
- [Wood 95] Wood, R.S., Chief Engineer, Royal Ordnance Liquid Motors Division, Results of technical meetings and correspondences, 1995.
- [WRR] WRR 127-1, *Range Safety Requirements*, 30th Space Wing, United States Air Force, 30 June 1993.
- [Zube 95] Zube, D., Messerschmid, E.W., Dittmann, A., "Project ATOS—Ammonia Arcjet Lifetime Qualification and System Component Test," AIAA 95-2508, 31st AIAA/ASME/SEA/ASEE Joint Propulsion Conference and Exhibit, 10-12 July 1995.

Chapter 7

Comparing Propulsion

System Costs

- 7.1. OVERVIEW**
- 7.2. DESCRIBING TOTAL COST**
- 7.3. COMPARING TOTAL COST**
- 7.4. RESULTS & CONCLUSIONS**
- 7.5. REFERENCES**

The final goal of the research was to develop a useful metric for evaluating the cost-effectiveness of propulsion system options by using the results from the previous objectives to derive a total cost figure of merit and demonstrate its utility for future mission planning. To that end, a process was derived to provide a useful technique for quantifying and comparing propulsion technology options in terms of total mission cost. This process produces a figure of merit for competing options to allow one-to-one comparisons and provide important insight into fundamental system-level trade-offs. The derivation of this figure of merit is first described in terms of the design justification concept that has been applied throughout this thesis. The dimensions of the total cost paradigm used to assess propulsion technology are reviewed and a means of combining these dimensions parametrically is described. The technique is then applied to a series of different scenarios to provide an indication of the most cost-effective option for a given mission. Results indicate that this technique provides a useful tool for research and mission planning that gives new insight into real propulsion system costs.

7. Evaluating Propulsion System Costs

7.1. Overview

The primary objective of my research was to evaluate hybrid rockets and other cost-effective propulsion system options for small satellites. The first research goal to be attained on the way toward this objective was an understanding of the fundamental sources of spacecraft hardware costs. Chapter 2 presented a methodical approach for viewing the development of a mission in order to understand where the primary cost drivers were for system hardware. From there, the nine dimensions of the propulsion system cost paradigm were derived. It was found that the values for these dimensions were determined by the technology chosen and the system architecture designed to support it.

Chapters 3, 4 and 5 first focused on the technology aspects of this problem. The goal was to analyse and characterise all near-term options with respect to the total cost paradigm. From this analysis, hybrid rockets emerged as a promising technology with the potential for cost-effective application. The lack of previous research into hybrid applications for small satellites prompted a dedicated program of study aimed at understanding all aspects of hybrid rockets. The results of this program proved the basic concept of hybrid rocket upper stages and demonstrated the accessibility of the technology. Experimental results served to characterise important parameters fundamental to describing the hybrid combustion process and essential for realistic design work on satellite motors. Finally, the hybrid research program fully assessed the price and mission costs of the technology and concluded that hybrid motors offer a safe, simple technology option.

In the previous chapter, the influence of the systems engineering aspects of propulsion costs were examined. A detailed system design case study was documented. The results of this study demonstrated the importance of considering the complete system design when trying to reduce overall costs. Support systems account for the majority of total system price and strongly influence final performance and other dimensions. The "generic" system developed during this study can be readily adapted to support any liquid or gaseous propellant technology and its total price readily estimated.

The purpose of this chapter is to take all these important results one step further by combining them in a cogent way to simplify future applications. The research goal described here was to develop a simple method for synthesising my results and applying them to preliminary mission planning to enable important conclusions about cost-effective propulsion systems to be drawn. It should be emphasised that the results described in the previous chapter can stand on their own merit. This chapter represents additional work intended to ease the interpretation of these results and make them accessible to a wider community.

Previous work on propulsion system costs as described in Chapter 2 [Myers 04] has focused exclusively on a single aspect of performance—mass—in the pursuit of low-cost systems. Figure 7-1 compares the relative performance of the technology options analysed in this thesis based on this single criteria. From this analysis alone, mission planners would be motivated to pursue the best performing option which is clearly pulsed plasma thruster (PPT) technology. At an I_{sp} of 1500 sec, it far surpasses cold-gas and chemical options as well as other less efficient electric options such as resistojects.

Comparison of Propellant Mass Requirements for 300 m/s ΔV

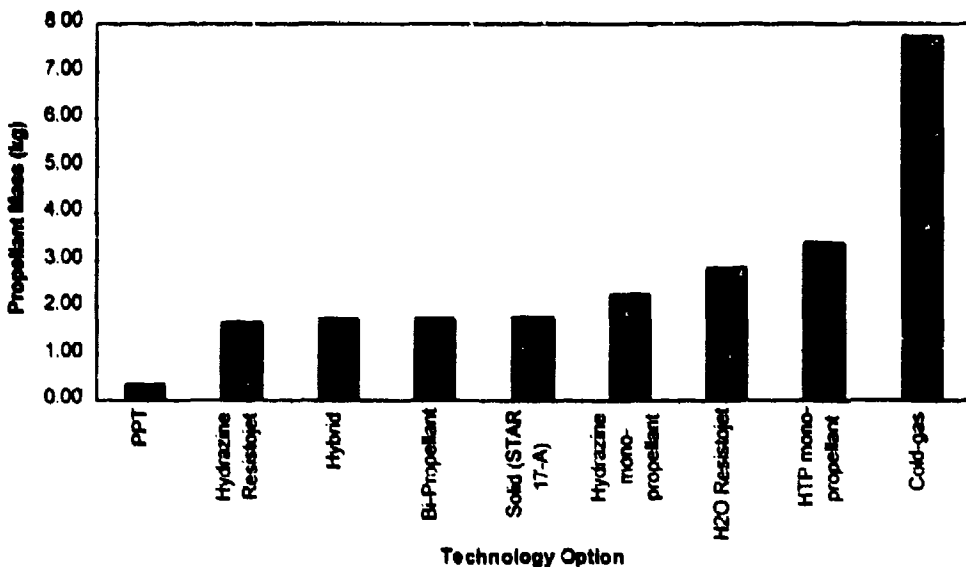


Figure 7-1: Comparison of propulsion technology options in terms of propellant mass needed to complete 300 m/s ΔV for an initial 250 kg satellite.

However, as this thesis has repeatedly emphasised, in the pursuit of cost-effective systems, mass alone is not the answer. In fact, as pointed out in Chapter 2, focusing solely on reducing mass may actually raise system costs due to the increase in overall system complexity. This fact is supported by Figure 7-2 which plots the same technology options described above with respect to thruster price alone. Here, the conclusions from the mass analysis are turned upside-down. The cheapest thruster in terms of price (cold-gas) was actually the most expensive in terms of mass. Similarly, the best performing option in terms of specific impulse, PPT, is one of the most expensive in terms of price.

Propulsion System Thruster Costs

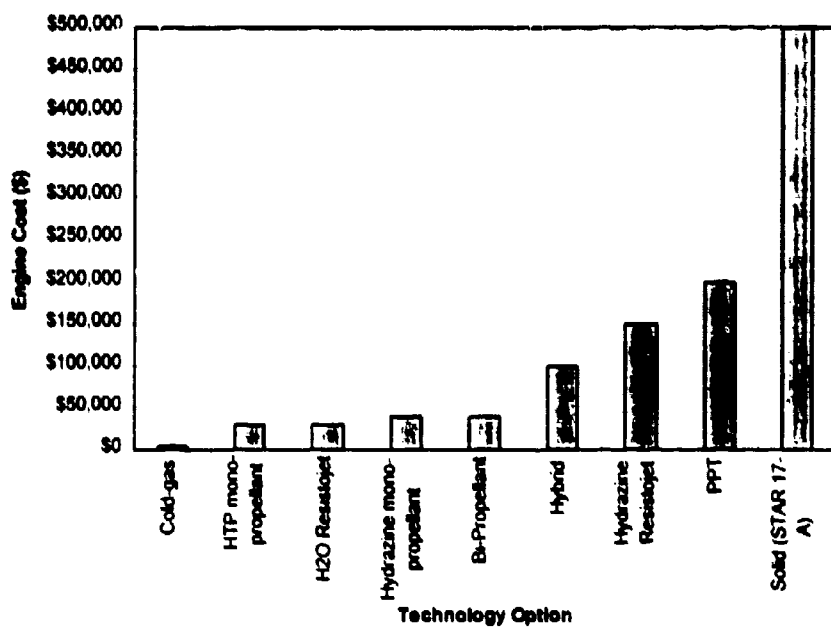


Figure 7-2: Estimated thruster costs for various propulsion technology options. Cost data adapted from results presented in Chapter 3.

Clearly, neither mass nor thruster price alone can provide the complete answer. Instead, a simple means of comparing and trading all aspects of system cost is needed. To accomplish this aim, the chapter begins by developing a simple means of describing total system cost. Obviously, there are a variety of ways that one could approach this problem. However, a complete parametric analysis could easily consume another thesis. Therefore, the purpose of this research was to develop a simple, useful method for performing a systematic trade-off between the various cost dimensions. Improving on this approach to enable it to cope with more detailed mission planning will be left to future research.

To demonstrate the utility of this method, the chapter applies it to a standard commercial station keeping mission. This mission is examined from two difference perspectives. The first takes a traditional approach which places a premium on system mass. The second is a budget-constrained perspective which places the highest priority on low price, sacrificing performance to meet that aim. The flexibility of the method is then demonstrated by applying it to both a low ΔV experimental mission and a high ΔV , high risk lunar mission. The system architectures for each propulsion system option are presented. Performance characteristics are developed and the total system cost figure of merit for each option is computed and compared. Conclusions are then drawn from these results.

7.2. Describing Total Cost

This section develops a simple method for succinctly describing the total system cost for a given propulsion technology option. The design justification concept is first outlined and each of the cost function dimensions are reviewed. A total cost figure of merit is then derived and discussed.

7.2.1. Design Justification

In Chapter 2, the three phases of a mission were discussed and the cost drivers in each were examined. The *design justification* concept was also presented which relates to the process of developing a cost model concurrently with system design. This discussion led to the definition of the nine dimensions of the propulsion system cost paradigm that include performance, price and mission costs:

1. Mass
2. Volume
3. Time
4. Power
5. System price
6. Technical risk
7. Integration
8. Safety
9. Logistics

This concept of design justification was applied to the examination of technology options presented in Chapters 3-5 in order to characterise their performance and other costs. Chapter 6 extended this process by undertaking a design case study which developed a versatile system architecture and a corresponding system price model. Figure 7-3 illustrates this process as it has developed throughout the thesis.

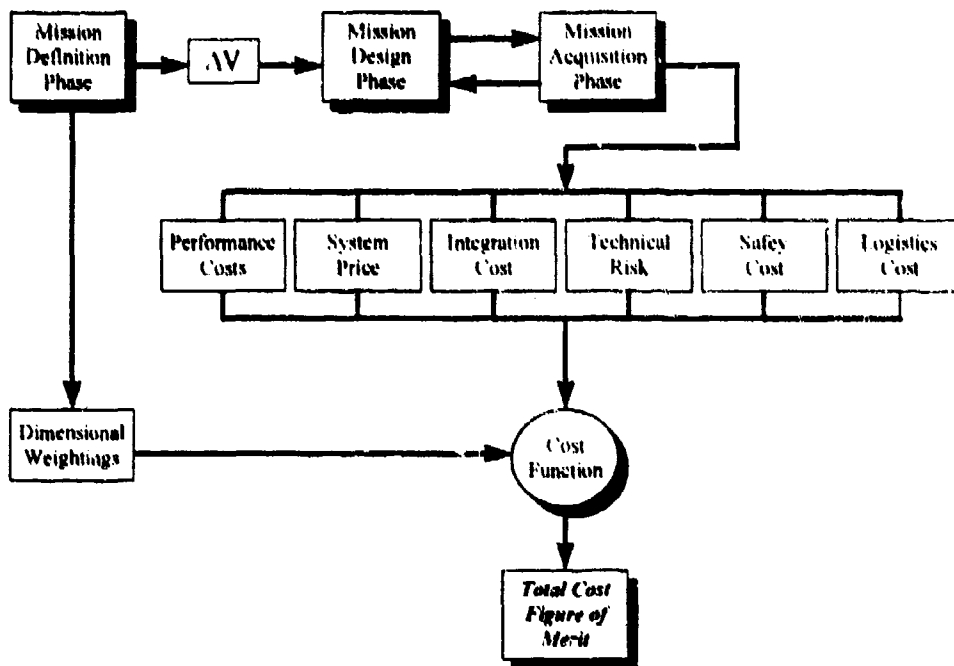


Figure 7-3: The diagram illustrates the design justification process developed throughout the thesis.

7.2.2. Total Cost Figure of Merit

We can now develop a method for combining the nine dimensions of the cost paradigm to derive a single figure of merit. As stated earlier, this figure of merit is intended as a useful method for comparing and trading off the various dimensions which comprise total propulsion system cost. It was derived from research into cost estimating relationship development and operations research techniques. The basic background for the cost function will first be discussed followed by a presentation of the final equation and discussion of variables.

7.2.2.1. Background

As discussed in Chapter 6, cost estimating relationships (CERs) are widely used tools for management planning within the aerospace community. The primary purpose of CERs is to allow managers to predict final system or program costs based on a few variables known at the outset. [Mandell 92] provides a good overview of mathematical derivation of CERs and their historical development. As he points out, there are two basic paradigms currently used in CER development. The *Rand Paradigm* produces a statistical correlation between estimating variables such as mass or volume and the final system or program cost. This approach was used by [Burgess 95] presented in Chapter 6. However, due to the difficulty in developing CERs for entirely new technology programs without historical precedent, the *PRICE Paradigm* was developed which bases the CER on data from similar systems or programs in other industries.

Unfortunately, according to [Christensen 92] "it is widely agreed that good cost estimates for technology programs are difficult to derive and the bases of estimates typically used have many

flaws." Another basic problem with CERs is their total reliance on only one or two variables from which to estimate system cost. My research has clearly emphasised the importance of considering all aspects of system cost, not focusing on mass or the bottom-line price alone. However, my literature searches were unable to reveal any previous research on this specialised aspect of total system cost estimation.

Taking a broader view, the research led me to consider techniques employed in the science of operations research. This specialised branch of statistics attempts to model and predict organisational operations to optimise processes and aid decision making. The process of parametrically combining the various cost dimensions into a single figure of merit is based on the same methodology used in linear programming techniques [Hillier 86]. This development is summarised in the next section.

7.2.2.2. Figure of Merit

The variables used for the nine cost dimensions are listed below:

Prop_Mass = Propellant mass (scaled 0 - 100)

Prop_Vol = Propellant volume (scaled 0 - 100)

Time = Total thrust time (scaled 0 - 100)

Power = Power consumed (scaled 0 - 100)

Logistics = Logistical cost factor (0 - 100)

Integrat = Integration cost factor (0 - 100)

Safety_Cost = Personal risk cost factor (0 - 100)

Tech_Risk = Technical risk cost factor (0 - 100)

Sys_Price = Estimated price of complete system (including ground support equipment)
(scaled to 0 - 100)

Of these variables, the performance dimensions (*Prop_Mass*, *Prop_Vol*, *Time*) and *Sys_Price* are a function of both the mission AV and the technology chosen. In all cases, the actual values for a given AV are computed for each technology option and the results are scaled from 0 - 100 to eliminate units and allow for normalised comparison between options. *Power*, *Integrat*, *Tech_Risk*, *Logistics* and *Safety_Cost* are assumed to be functions of the technology option alone.

The approach taken in operations research is to combine variables through linear combination. However, in reality each variable does not necessarily have the same importance for a given mission. Therefore, it is necessary to provide some means of weighting each accordingly. Recognising the necessity of consciously trading off the various dimensions, I have elected to derive these dimensional weighting by rank order. Depending on the basic mission environment, as determined during the Mission Definition Phase, the nine dimensions are rank ordered in importance from 8 to 0, with 8 being the most important and 0 implying no importance. For example, a given mission scenario may want to maximise total payload and may not be concerned at all about how long the total manoeuvre takes. Therefore, for this example, mass would be ranked at number 8 and time as 0.

The total cost function is written as follows:

$$\text{Total_Cost} = A \cdot \text{Prop_Mass} + B \cdot \text{Prop_Vol} + C \cdot \text{Time} + D \cdot \text{Power} + E \cdot \text{Logistics} + F \cdot \text{Integrat} + G \cdot \text{Safety_Cost} + H \cdot \text{Tech_Risk} + I \cdot \text{Sys_Price} \quad \text{Eqn. 7-1}$$

where

A-I = Weightings on each dimension (appropriate units to produce a dimensionless final cost)

The next section will apply this figure of merit to three mission scenarios to compare the cost-effectiveness of each option.

7.3. Comparing Total Cost

This section will determine the propulsion cost figures of merit for various mission scenarios and technology options. This method will first be presented, followed by a discussion of each scenario and its corresponding dimensional weightings. The technology options to be considered will then be presented along with values for their multi-dimensional cost.

7.3.1. Approach

Figure 7-4 illustrates the approach used in the cost analysis methodology developed. The approach begins with the selection of a mission scenario. This determines, on the one hand, the mission environment which drives the weightings applied to the nine cost dimensions. On the other hand, the mission scenario determines the total ΔV required which drives the performance dimensions that can be derived for each technology option. These are combined with the other mission costs inherent in each option using the total cost function discussed in the last section. This approach will be applied to various missions to compare the relative costs of each system option and determine the most cost-effective for a given scenario. Results from this analysis will be used to assess the overall utility of the technique.

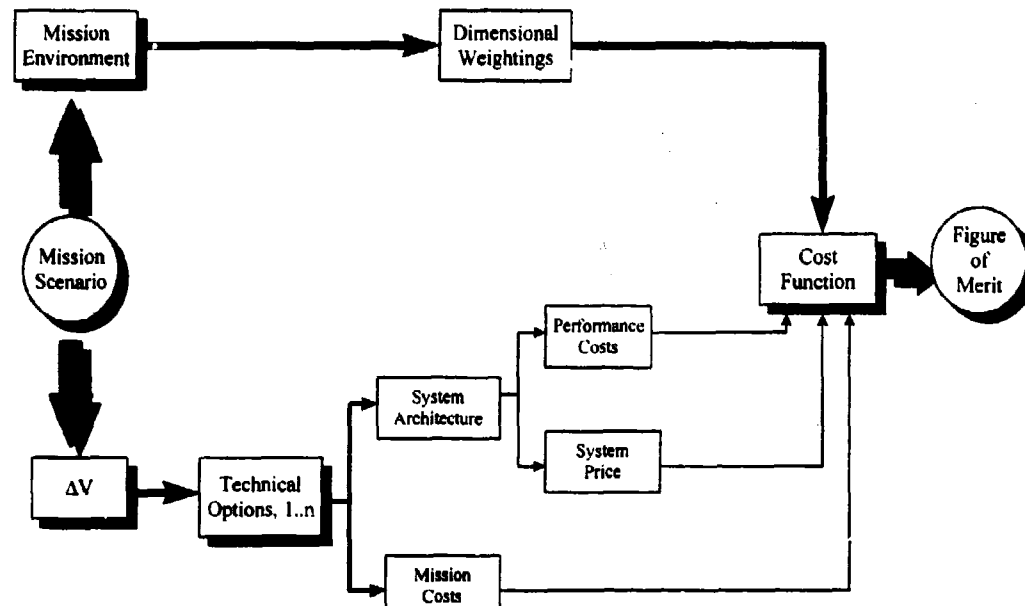


Figure 7-4: Basic approach for applying the total cost figure of merit.

7.3.2. Mission Scenarios

For purposes of comparison, the following three mission scenarios were considered which span the range of typical missions envisioned for UoSAT-class minisatellites:

1. *Commercial Mission*—Commercial minisatellite communications or remote sensing satellite in either LEO or GEO. $\Delta V = 200$ m/s, based on a conservative estimate of the amount needed to provide 3 years of station keeping.
2. *Experimental Mission*—LEO minisatellite mission to demonstrate autonomous on-orbit manoeuvre capability. $\Delta V = 20$ m/s, sufficient to provide ~40 km of semi-major axis change to demonstrate capability and objectively verify performance using ground and onboard measurement techniques. Launch site undefined. System design must be flexible enough to accommodate a variety of launchers and launch sites to take advantage of the lowest cost option either as a primary or secondary payload.
3. *Lunar Orbit Mission*—Minisatellite Lunar mission beginning in GTO. $\Delta V = 1600$ m/s. Launch site undefined. System design must be flexible enough to accommodate a variety of launchers and launch sites to take advantage of the lowest cost option either as a primary or secondary payload.

These scenarios allow us to view three widely different mission environments with correspondingly different weightings applied to the nine cost dimensions. To demonstrate the analysis technique, the first scenario, commercial station keeping, will be examined from two different mission perspectives. The first perspective is a traditional commercial approach which emphasises performance above other cost dimensions. The second approach will be that of an SSTL-type company which strives to attain the lowest price solution and is willing to sacrifice some performance to that end. Once the results of this analysis are presented, the remaining two scenarios will be examined to demonstrate the flexibility of the approach. The dimensional rank orderings for each scenario are shown in Table 7-1. A justification follows.

Rank (weighting)	Traditional Commercial Mission	Non-traditional Commercial Mission	Experimental Mission	Lunar Orbit Mission
8	Mass	Price	Price	Time
7	Volume	Integration	Integration	Price
6	Technical Risk	Safety	Logistics	Safety
5	Integration	Logistics	Safety	Logistics
4	Logistics	Technical Risk	Power	Integration
3	Safety	Mass	Volume	Technical Risk
2	Price	Volume	Technical Risk	Volume
1	Power	Power	Mass	Mass
0	Time	Time	Time	Power

Table 7-1: Dimensional rank orderings for each mission scenario.

A traditional commercial mission places the highest priority on those dimensions that most affect the mission performance of the primary payload—mass, volume, technical risk and integration complexity. Because such missions are directly financed by a paying customer who is most interested in the delivery of clear images or communication channels, lower priority is placed on price, logistics, power and time. This is not to imply, for example, that safety is not important. Rather, the mission is prepared to trade-off the cost of providing safety infrastructure in favour of mass and volume.

In contrast, a non-traditional commercial mission, such as one undertaken by SSTL, would have different priorities. For such a mission, price is the driving cost dimension. As discussed in Chapter 1, there is a critical threshold price level above which the mission cannot proceed. Important price-sensitive dimensions such as integration, safety and logistics also rank highly for such a mission. Integration cost was ranked next highest because of the potential impact on payload operations and the overall desire to keep development cost for the ADCS system low. The logistics cost was ranked third because of the mission environment that intends to retain flexibility on the final launch site selection until late in the mission design phase. This flexibility is needed to take advantage of low-cost launches but means that extensive logistics may be required to support launches from these remote sites. The same is true of safety cost at these sites. Of much lower priority are mass and volume. These higher risk missions are more willing to trade these dimensions in order to get a lower mission price.

For an experimental mission, such as one conducted in a University environment, the top priorities are similar to those of the non-traditional commercial mission. However, the ΔV for this mission is very much lower, allowing us to assess the effect of changing performance requirements on figures of merit. A high-risk lunar orbit mission operates within a mission environment similar to the experimental mission. This mission would take advantage of a secondary payload launch opportunity to geosynchronous transfer orbit (GTO). Commercial communication missions bound for geostationary orbit (GEO) are normally launched first into GTO from which an upper stage performs

the necessary manoeuvre to place it into GEO. The OSCAR P3-D mission, as discussed in Chapter 6, will start from GTO and then manoeuvre to a 16 hour Molniya orbit. Interestingly enough, the ΔV needed to go from GTO to Lunar orbit is approximately the same as that needed to go to GEO. Several researchers have proposed using these GTO opportunities as springboard for low-cost Lunar exploration [Uphoff 92] [Belbruno 87] [Chicarro 94]. UoSAT/SSTL have similar plans to launch a minisatellite to the Moon by the end of the century, probably starting from GTO.

The ΔV to go from GTO to Lunar orbit can be readily approximated using patched conic techniques described in [Sellers 94a]. This value is about 1600 m/s. Cost priorities are effected by the choice of initial orbit. By beginning in GTO, the highest cost priority is time. Spacecraft in GTO travel through the entire depth of the Van Allan belts twice per day, receiving a high total dose of ionising radiation, damaging sensitive electronic components. A Lunar mission as currently envisioned by UoSAT would achieve the lowest cost by relying on the same proven electronic components that have been used on microsatellites in LEO. Unfortunately, this means the lifetime limit in GTO is less than three months [Underwood 95]. The next most important cost dimensions for such a mission are price, safety and logistics. The fate of such a mission, completely funded by in-house funds, would hinge on keeping the total mission price low. Furthermore, with launch intended from a remote, low-cost site such as Svobodny, Russia, mission planners are not in a position to finance required safety equipment and logistics requirements to support certain options, preferring to trade off mass and volume to gain this flexibility. Power is lowest in priority for this mission because no payload operations would begin until after the major mission ΔV has been completed.

The propulsion system options to be considered for each scenario are addressed in the next subsection.

7.3.3. Propulsion System Options

Table 7-2 lists the technology options considered and summarises the basic performance values assumed for this analysis. It should be noted that for operational reasons, the solid option would not be practical for the low ΔV experimental mission or for the station keeping application of the commercial mission. Similarly, due to the very low $disp$ requiring impractically large tanks, the cold-gas option was not considered for the higher ΔV commercial or lunar missions. Finally, because the very low thrust of the PPT requires transfer times that are far too long, it was not considered for the lunar mission.

System	Isp (sec)	Oxidiser/ Propellant specific gravity	Fuel specific gravity	O/F	dIsp	Thrust (N)	Power (W)
Bi-Propellant	290	1.447	0.8788	1.65	337.33	20	2
Hydrazine mono-propellant	225	1.008			226.80	20	1
Hybrid	295	1.36	0.93	8	381.60	500	1
Cold-gas	65	0.23			14.95	0.1	.5
H ₂ O Resistojet	185	1.0			185.00	0.3	500
Solid (STAR 17-A)	286.7	1.661			476.21	16000	0
Hydrazine Resistojet	304	1.008			306.43	0.33	500
PPT	1500	2.16			3240.00	7.0×10^{-4}	20
HTP mono-propellant	150	1.36			204.00	1	1

Table 7-2: Comparisons between propulsion technology options (based on data from in Chapter 3).

As emphasised throughout this thesis, the actual performance for a given technology options depends not only on the inherent efficiency of the technology itself (*Isp*, *dIsp*, etc.) but on the system support architecture as well. The basic architectures for each option are shown in Figure 7-5 through Figure 7-9.

To maximise inherent safety, the bi-propellant system was designed with independent blow-down of each propellant as discussed in Chapter 6. The mono-propellant system options were also designed for blow-down, accepting the minor performance loss for overall simplicity. However, due to the natural O/F shift during long burns, the hybrid system was designed with regulated oxidiser pressurisation. For low cost, the regulation scheme used was a “bang-bang” system as discussed in Chapter 6. Therefore, the potential exists to actually change oxidiser delivery pressure, thus flow rate and O/F, during the mission which would not be possible in blow-down mode. The cold-gas system was also based on this approach. Finally, the need to carefully control very low flow rates for resistojet systems means a regulated pressurisation is needed, again using the “bang-bang” approach. No system architecture is shown for the solid or PPT systems as they requires very little in the way of support infrastructure. The price of each of these options will be the subject of the following subsection.

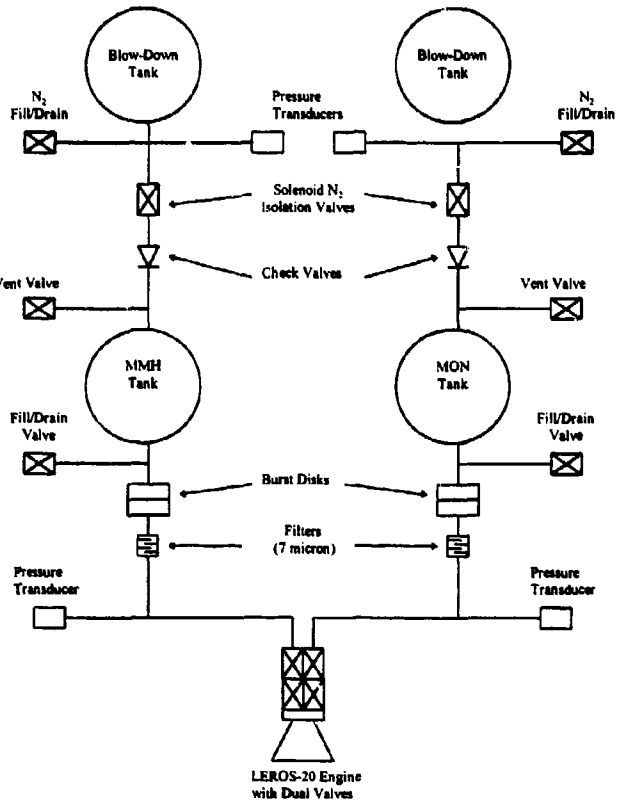


Figure 7-5: Basic system architecture for bi-propellant option.

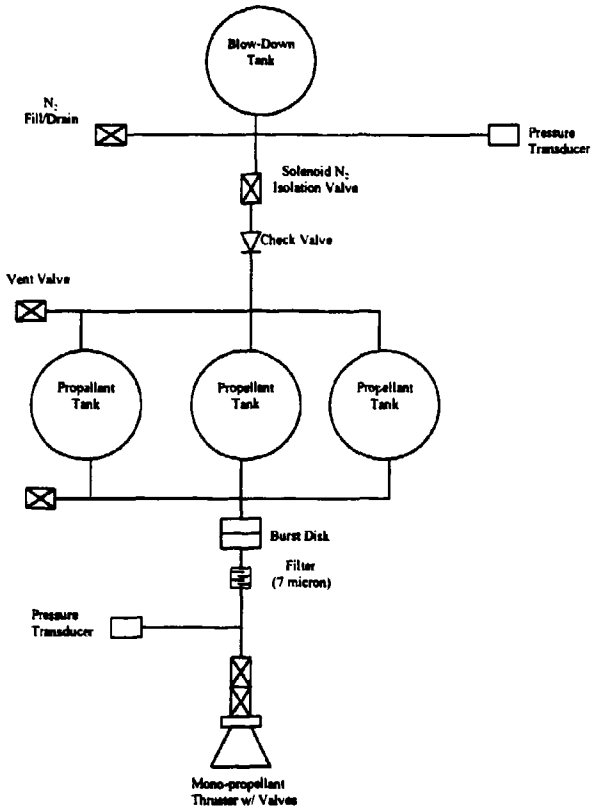


Figure 7-6: Basic system architecture for mono-propellant options.

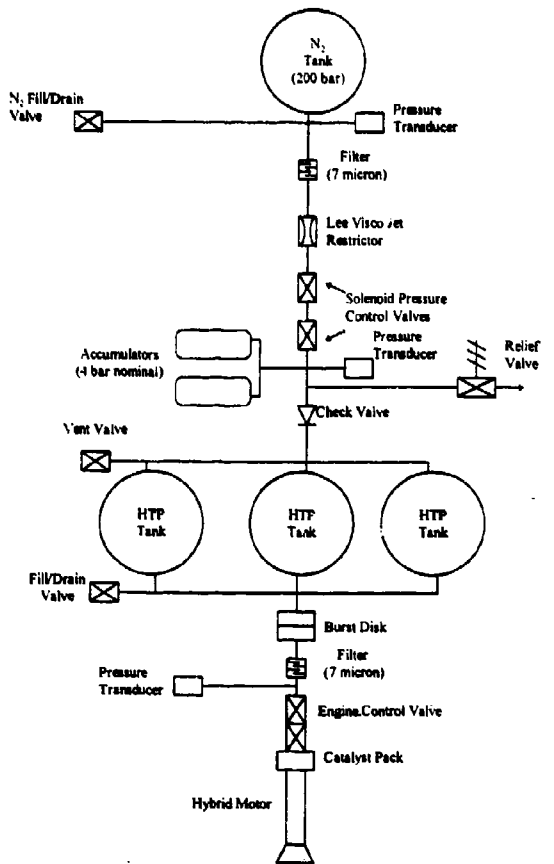


Figure 7-7: Basic system architecture for hybrid option.

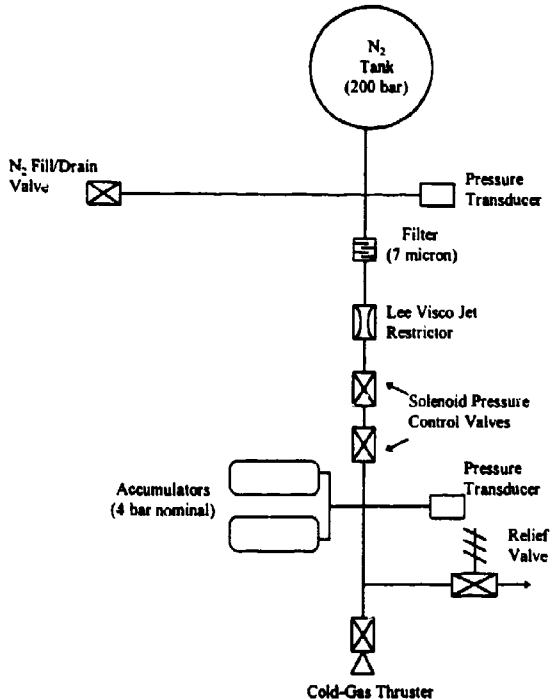


Figure 7-8: Basic system architecture for cold-gas option.

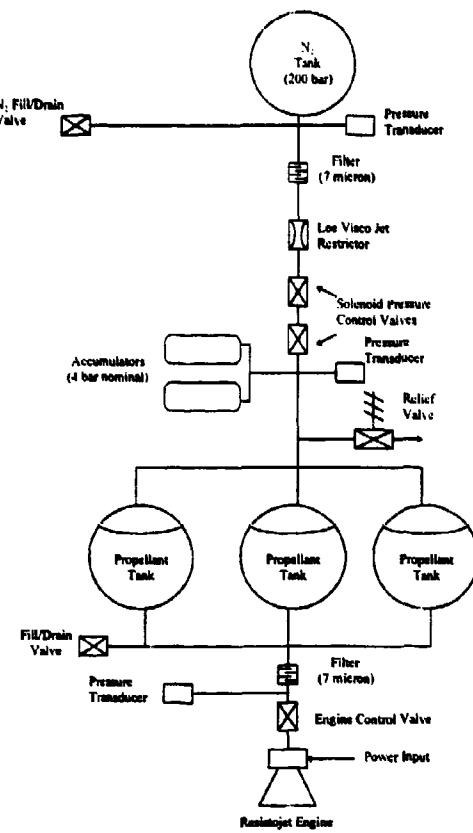


Figure 7-9: Basic system architecture for resistojet options.

7.3.3.1. System Price

As stated earlier, the actual system price for a given mission depends on the final system architecture as presented in the previous subsection. This total system price can be divided into fixed and variable prices. Table 7-3 lists the component breakdown and total fixed price for each system option. Fixed prices were derived based on the system architectures assumed in the previous section and the system price model developed in Chapter 6. The system variable price depends entirely on the number of propellant tanks used. This number was determined by dividing the total propellant volume needed by the tank volume. For simplicity, it was assumed that all propellant tanks are 10 litres. Stated another way, a 20 litre tank is assumed to cost twice as much as a 10 litre tank. This assumption is approximate but gives a final result adequate for purposes of relative system comparison.

System	System Fixed Cost (\$)	Variable Cost
<i>Bi-Propellant</i>	\$151,423	Number of Propellant Tanks
<i>Hydrazine mono-propellant</i>	\$94,378	Number of Propellant Tanks
<i>Hybrid</i>	\$158,919	Number of Propellant Tanks
<i>Cold-gas</i>	\$35,086	Number of Nitrogen Tanks
<i>H₂O Resistojet</i>	\$81,258	Number of Propellant Tanks
<i>Solid (STAR 17-A)</i>	\$710,000	None
<i>Hydrazine Resistojet</i>	\$204,378	Number of Propellant Tanks
<i>PPT</i>	\$0	\$200,000/20,000 Ns impulse
<i>HTP mono-propellant</i>	\$84,378	Number of Propellant Tanks

Table 7-3: Propulsion system fixed and variable monetary costs. Based on thruster cost data presented in Chapter 3 and system cost model data presented in Chapter 6.

7.3.3.2. Mission Cost Factors

As presented in Chapter 3, the technology options differ widely in their inherent mission costs. To enable direct comparison of these qualitative factors, the technology mission costs summarised in Chapter 3 were each assigned a value on a scale of 0 - 100, with 0 being no cost (such as PPT logistics) and 100 being high cost (such as hybrid technical risk). This scaling was based on the analysis presented in Chapter 3 and on my own engineering judgement. These qualitative factors are listed in Table 7-4.

Option	Safety Cost Factor	Technical Risk Factor	Integration Factor	Logistics Factor
<i>Bi-Propellant</i>	100	50	80	100
<i>Hydrazine mono-propellant</i>	90	40	70	90
<i>Hybrid</i>	50	100	100	60
<i>Cold-gas</i>	10	10	10	20
<i>H₂O Resistojet</i>	10	80	20	20
<i>Solid</i>	20	30	100	80
<i>Hydrazine Resistojet</i>	90	40	40	90
<i>PPT</i>	10	80	80	10
<i>HTP mono-propellant</i>	50	80	70	60

Table 7-4: Comparison of qualitative cost dimensions for five propulsion technology options. Scale is 0 - 100 with 100 representing the highest cost. Based on discussion presented in Chapter 3.

In the next section this data will be applied to the total cost function to derive figures of merit for each option and mission scenario.

7.4. Results

7.4.1. Commercial Missions

Applying the cost function developed earlier in the Chapter to the commercial mission scenarios discussed in the previous section produces the results summarised in Table 7-5. The table ranks the system options for each scenario based on the figures of merit. For comparison, total propellant mass and system price are also given. Figure 7-10 and Figure 7-11 plot the figures of merit for visual comparison.

Looking at the results for the traditional commercial mission scenario, the most cost-effective options overall were the electric propulsion systems with the highest *Isp* option, PPT, clearly ahead of the rest. Note that the cheapest overall option, PPT, was actually the most expensive in terms of price alone. These results are to be expected given the traditional focus on the mass and volume dimensions of cost as the primary mission drivers, irrespective of system price. Furthermore, these results justify the research emphasis placed on developing technologies such as PPT or ion thrusters in order to attain the highest possible performance, regardless of the final system price.

With these results alone, the utility of this figure of merit procedure would be questionable. However, applying this process to a non-traditional approach for the same mission reveals some interesting and counter-intuitive results. For this mission, the most cost-effective option is a simple water resistojet thruster, a technology that has received very little attention. Despite its much lower *Isp* (185 vs. 1500 sec), its total cost was determined to be significantly lower than the PPT. Furthermore, another little-used option, the HTP mono-propellant, demonstrated relatively low total cost. For a mission planner of such a non-traditional commercial mission, these results would indicate that by simply "following the pack" and adopting the traditional approach of using a PPT, you exclude the possibility of other options which, when considered from a total cost perspective, may offer a more cost-effective solution over all. More general conclusions from these results will be addressed in the next section.

Mission	System	Propellant Mass (kg)	System Price (\$)	Normalised Total Cost
<i>Traditional Commercial</i>	PPT	3.37	\$500,000	47.4
	Hydrazine Resistojet	16.22	\$229,942	74.3
	H ₂ O Resistojet	26.09	\$119,604	77.7
	Hybrid	16.69	\$171,701	84.3
	Bi-Propellant	16.97	\$176,987	84.9
	Hydrazine mono-propellant	21.66	\$132,724	88.8
	HTP mono-propellant	31.77	\$122,724	100.0
<i>Non-Traditional Commercial</i>	Hydrazine Resistojet	1.67	\$217,160	3.2
	H ₂ O Resistojet	26.09	\$119,604	56.2
	PPT	3.37	\$500,000	76.1
	HTP mono-propellant	31.77	\$122,724	86.3
	Hydrazine Resistojet	16.22	\$229,942	90.0
	Hybrid	16.69	\$171,701	91.7
	Hydrazine mono-propellant	21.66	\$132,724	92.0
	Bi-Propellant	16.97	\$176,987	100.0

Table 7-5: Summary of cost analysis results for traditional vs. non-traditional commercial mission scenarios.

Comparison of Propulsion System Cost Figures of Merit for Traditional Commercial Mission Scenario

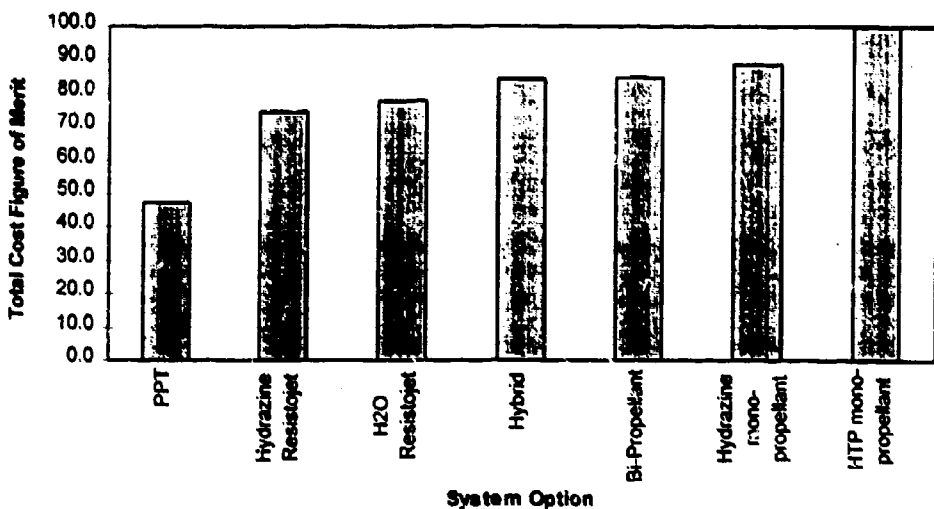


Figure 7-10: Figure of merit results for a traditional commercial mission scenario.

Comparison of Propulsion System Cost Figures of Merit for a non-Traditional, SSTL-type Commercial Mission Scenario

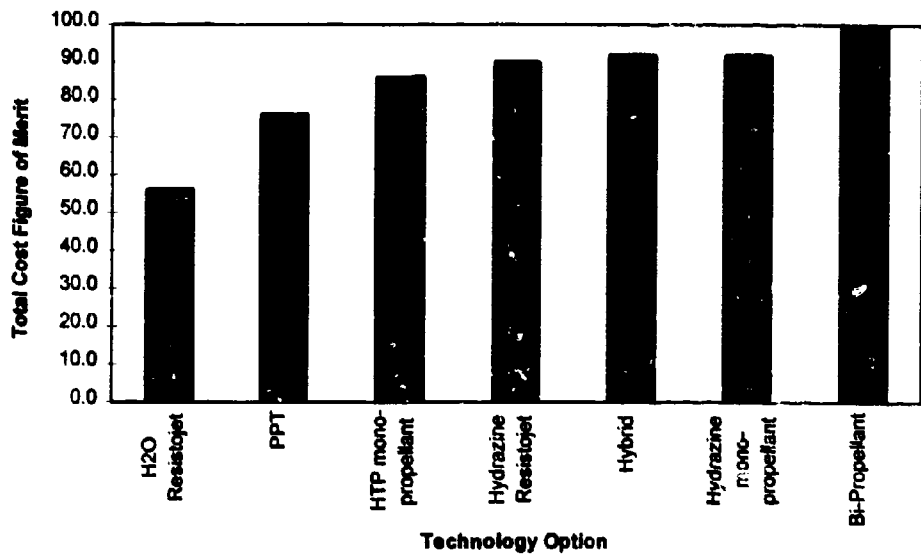


Figure 7-11: Figure of merit results for a non-traditional commercial mission scenario.

7.4.2. Experimental and Lunar Missions

To demonstrate the versatility of the figure of merit process, it was also applied to both the experimental and Lunar orbit missions described earlier. Results for both are summarised in Table 7-6 including mass and price data for comparison. Figure 7-12 plots the figures of merit for the experimental mission and Figure 7-13 for the Lunar orbit mission.

For the experimental mission scenario, the most efficient option in terms of mass is clearly the PPT. However, the least mass efficient option, cold-gas, comes out the overall most cost-effective due to the high weighting put on price, integration and logistics dimensions for this particular mission. Furthermore, as with the non-traditional commercial mission, other little-used options, the H₂O resistojet and HTP mono-propellant, are shown to offer cost-effective advantages over more traditional approaches such as the hydrazine mono-propellant.

The results for the Lunar orbit mission are equally interesting. Traditionally, the clear choice for such a mission would be solid, hydrazine mono-propellant or bi-propellant. However, this total cost analysis reveals that not only are these options more expensive in price and mass terms, they do not offer the most overall cost-effective option. Instead, the hybrid rocket, a technology that has never seen application in space emerged as the clear choice, even when the high technical risk for a first-use mission is considered.

The results for both these missions highlight the flexibility of the total cost figure of merit process. It can easily be applied to widely different missions with varying ΔV cost priorities. More general conclusions will be addressed in the next section.

Mission	System	Propellant Mass (kg)	System Price (\$)	Normalised Total Cost
<i>Experimental</i>	Cold-gas	7.72	\$77,594	30.9
	H ₂ O Resistojet	2.82	\$94,040	46.7
	HTP mono-propellant	3.37	\$97,160	65.4
	PPT	0.34	\$200,000	67.4
	Hydrazine mono-propellant	2.26	\$107,160	79.5
	Hybrid	1.72	\$171,701	89.2
	Hydrazine Resistojet	1.67	\$217,160	97.9
	Bi-Propellant	1.75	\$176,987	100.0
<i>Lunar orbit</i>	Hybrid	106.18	\$248,393	49.0
	HTP mono-propellant	165.72	\$237,762	59.1
	Hydrazine mono-propellant	128.90	\$260,544	59.8
	Bi-Propellant	107.54	\$279,243	64.0
	Solid (2 x STAR 17-A)	108.46	\$1,420,000	68.5
	H ₂ O Resistojet	148.98	\$272,988	69.6
	Hydrazine Resistojet	103.80	\$332,198	100.0

Table 7-6: Summary of Total System Cost analysis results for an experimental mission and a Lunar orbit mission.

**Comparison of Total System Cost Figures of Merit
for Experimental Mission Scenario**

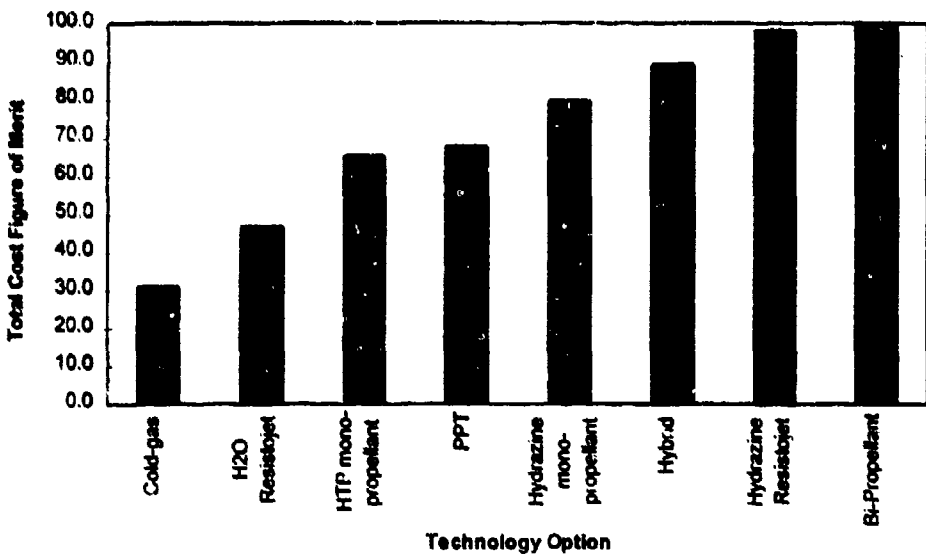


Figure 7-12: Total system cost figure of merit for experimental minisatellite mission scenario.

**Comparison of Total Mission Cost Figures of Merit
for Lunar Orbit Mission Scenario**

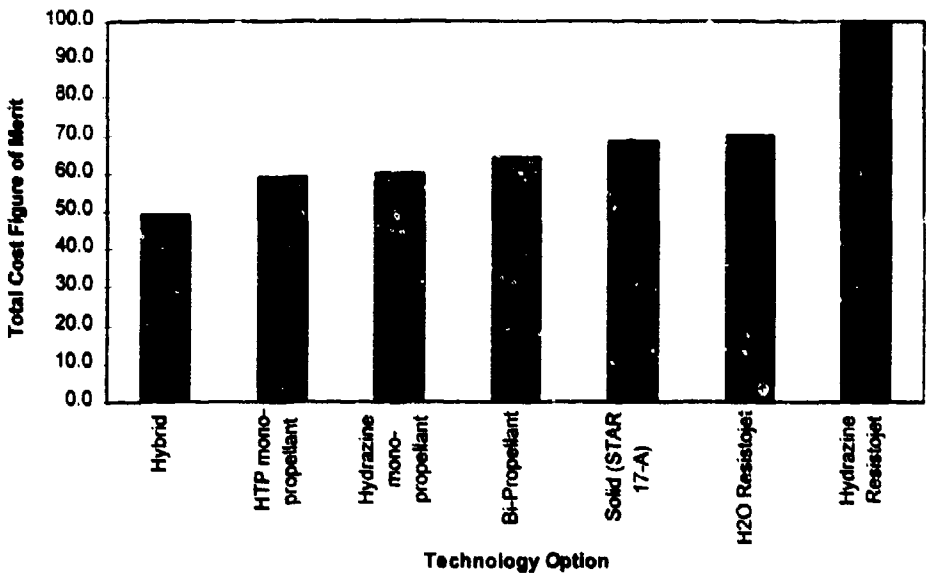


Figure 7-13: Total cost figures of merit for Lunar orbit mission scenario.

7.5. Conclusions

Reviewing the results presented in the last section, some important general conclusions can be drawn about the efficacy of the total cost figure of merit approach developed in this Chapter. In some respects, some of these results could be considered controversial. PPTs, for example, are currently enjoying considerable research support by NASA [Myers 94]. However, for certain applications they did not emerge as the most cost-effective option despite their promise of high performance. Furthermore, solid motors, often preferred for high ΔV missions, such as the Lunar Orbit scenario, appear far too costly compared to other options, especially the hybrid which has struggled to receive support within the aerospace community.

It is important to emphasise that the results presented above are not intended to be the final word. My purpose in developing this process was to produce results from which to start discussion, not iron-clad answers intended to end all debate. For example, different schools of thought may take exception with the exact qualitative values assigned to certain technology options or the weightings applied to various dimensions for a given mission scenario. This is to be expected. The results may differ depending on the actual assumptions made, although, the process used remains the same. Therefore, the more general conclusions about the utility of the process itself are the most important to consider.

To begin with, this unique method for comparing system options provides a versatile tool for mission planners that allows them to quickly quantify and compare all available technologies and assess their relative total mission costs. Thus, for the first time, complex system information can be easily quantified. As pointed out in chapter 1, low-cost satellite engineering at the University of Surrey and elsewhere has epitomised the virtue of applying appropriate technology to a given problem. The appropriateness of a technology is judged by taking a wider view that encompasses more than simply price or performance. Until now, engineers typically relied on completely subjective engineering judgement or "gut feeling" in order take into account such indirect cost factors as integration and safety. The total cost figure of merit process now provides a quantifiable means of making those important engineering decisions.

Furthermore, because the process results in a quantifiable parameter, it can serve as a useful total quality planning tool. By quantifying the starting point for various options, this technique can provide important indications of where best to invest in improvement and enables any incremental improvements to be measured. In this way, the controversial results reported above may help to spark debate and force a re-examination of research priorities for small satellite propulsion. For example, in deciding where best to invest money in a PPT development program, this process (as evidenced by the results above) would indicate that more effort should be aimed at lowering the price and

integration complexity of the thruster rather than on increasing its delivered *Isp*. In doing this, it would clearly offer a better overall cost-effective solutions to competing options.

The most immediate application for this method as a research planning tool is at the University of Surrey. These results indicate that three propulsion technologies offer real benefit for future mission scenarios:

- *Cold-gas*—for near-term experimental missions to develop basic orbit control techniques.
- *H₂O resistojet*—for commercial applications for the minisatellite bus for station keeping requirements in LEO or GEO.
- *Hybrid rockets*—for future high ΔV options such as a Lunar mission. Research into this technology also provides an HTP mono-propellant capability as a necessary spin-off which is a competitive option in its own right for other mission scenarios.

In summary, this chapter has presented the development of a total propulsion system cost analysis tool. Figures of merit for system options can be derived within the context of a specific mission scenario. Preliminary results offer important quantifiable data to direct future research at the University of Surrey. Beyond the university environment, this process provides a valuable planning tool to industry, enabling complex system options to be easily quantified. In application, this tool can empower mission planners and research directors to effectively trade-off the multi-dimensional aspects of propulsion cost to determine how best to invest in future technology.

7.6. References

- [Belbruno 87] Belbruno, E.A., "Lunar Capture Orbits, a Method of Constructing Earth Moon Trajectories and the Lunar Gas Mission," 19th AIAA/DGLR/JSASS International Electric Propulsion Conference, Colorado Springs, Colorado, 11 - 13 May 1987.
- [Burgess 95] Burgess, E.L., Lao, N.Y., Bearden, D.A., "Small-Satellite Cost Estimating Relationships," Presented at the 9th Annual AIAA/Utah State University Conference on Small Satellites, 18-21 September 1995.
- [Chicarro 94] Chicarro, A., "MORO—A European Moon-Orbiting Observatory for Global Lunar Characterisation," *ESA Journal*, Vol. 18, 1994.
- [Christensen 92] Christensen, C.B., Wagenfuehrer, C., "Standard Cost Elements for Technology Programs," published in *Space Economics*, edited by Greenberg, J.S. Hertzfeld, H.R., Progress in Astronautics and Aeronautics, Seebass, A.R. editor-in-chief, Vol. 144, AIAA, 1992.
- [Hillier 86] Hillier, F.S., Leiberman, G.J., *Introduction to Operations Research*, 4th edition. Holden-day, Inc., Oakland, California, 1986.
- [Mandell 92] Mandell, H.C.jr., "Cost-Estimating Relationships for Space Programs," published in *Space Economics*, edited by Greenberg, J.S., Hertzfeld, H.R., Progress in Astronautics and Aeronautics, Seebass, A.R. editor-in-chief, Vol. 144, AIAA, 1992.
- [Myers 94] Myers, R.M., Oleson, S.R., "Small Satellite Propulsion Options," AIAA 94-2997, 30th Joint Propulsion Conference, Indianapolis, Indiana, June 27-29, 1994.
- [Sellers 94a] Sellers, J.J., Astore, W.J., Crumpton, K.S., Elliot, C., Giffen, R.B., Larson, W.J. (ed), *Understanding Space: An Introduction to Astronautics*, McGraw-Hill, New York, N.Y., 1994.
- [Underwood 95] Underwood, C., Radiation Issues for UnSAT Lunar Mission, informal presentation at SSTL, December 1995.
- [Uphoff 92] Uphoff, C., "Practical Aspects of Transfer from GTO to Lunar Orbit," Presented at the Flight Mechanics/Estimation Theory Symposium, Greenbelt, Maryland, 5 - 7 May 1992.

Chapter 8

Conclusions

8.1. RESULTS

8.2. CONCLUSIONS

8.3. ACCOMPLISHMENTS

This final chapter reviews the specific results presented in the thesis. Significant conclusions are highlighted which include:

- Spacecraft hardware cost drivers can be identified and resolved during each phase of a mission—definition, design and acquisition. By focusing on these cost drivers and making quantifiable trade-offs between the various cost dimensions, a truly cost-effective system design results.
- Propulsion system cost includes far more than just *Isp* and price. A new paradigm for understanding the total cost of propulsion systems, one that includes nine dimensions of performance, price and mission costs, was defined and validated through application to individual technology options and complete systems. The total cost figure of merit process derived allows these cost dimensions to be combined into a useful, quantifiable results for mission planning and research management.
- Hybrid rockets offer a safe, high-thrust rocket technology which is a more versatile, cost-effective alternative to solid rocket motors. Furthermore, high test peroxide, HTP, is a safe and effective hybrid oxidiser that can also be used mono-propellant applications.

Recommendations for future work are also included. Notable accomplishments are summarised.

8. Conclusions

8.1. Results

An effective way to summarise the results of this research is to return to the research goals laid out in Chapter 1 and review specific results from each. Table 8-1 lists these four main research goals and enumerates their significant results. These results have been discussed in detail throughout the thesis. The following sections will summarise important conclusions along with recommendations for future applications for these results and potentially fruitful areas for additional research. An overview of significant accomplishment completes the chapter.

Research Objective	Results
1. Determine key cost drivers for spacecraft systems to identify useful cost-effective engineering practices and develop a paradigm for evaluating the total cost of propulsion system options.	<ul style="list-style-type: none"> • Detailed methodology for understanding spacecraft hardware cost drivers during each phase of a mission with specific engineering recommendations for how to address them. • A new paradigm for evaluating the total cost of propulsion systems.
2. Identify candidate propulsion technology options and investigate them to a sufficient level to fully characterise their total cost, performance, and overall potential for small satellite application.	<ul style="list-style-type: none"> • All propulsion technology options with potential for near-term application on small satellites identified and fully characterised with respect to the total cost paradigm. • A significant hybrid research program defined and completed. <ul style="list-style-type: none"> • Concept proven—hybrids were proven to be an accessible technology within reach of the small satellite research environment. Important engineering problems were identified and solved. • Performance characterised—hybrid combustion performance was experimentally modelled allowing realistic mission planning and upper stage design. • Total cost assessed—hybrid monetary and mission costs were completely defined allowing for credible comparison with competing options.
3. Design and evaluate a representative propulsion system architecture for the minisatellite in order to identify and evaluate useful cost-effective engineering practices and fully characterise total system costs.	<ul style="list-style-type: none"> • Propulsion system design case study completed which focused on the total cost paradigm and applied the cost-reduction strategies defined by my research. • Demonstrated the importance of looking at complete systems rather than technology alone. • A useful “generic” system designed and evaluated that can be immediately adapted for a variety of small satellite applications.
4. Develop a useful metric for evaluating the cost-effectiveness of system options by using the results from the previous objectives to derive a total cost figure of merit and demonstrate its utility for future mission planning.	<ul style="list-style-type: none"> • Total system cost figure of merit process derived. • Figures of merit determined for all system options using representative mission scenarios. • Usefulness of the figure of merit technique demonstrated as a mission and research planning tool.

Table 8-1: Summary of results for each research goal.

8.2. Conclusions

This section will summarise fundamental conclusions from the three broad areas of my research:

- Spacecraft hardware costs
- Cost-effective propulsion systems
- Propulsion Technology

Recommendations for future research in each area will also be offered.

8.2.1. Spacecraft Hardware Costs

A coherent strategy for understanding and resolving spacecraft hardware cost drivers during every mission phase can be defined. During the Mission Definition Phase, important aspects of the launch and space environment are established, both of which effect the cost decisions made later on. During the Mission Design Phase, performance requirements and margins are established along with quality requirements and fundamental system architecture. It is during this phase that designers can take full advantage of low-cost engineering practices. As the mission moves into the Hardware Acquisition Phase, an iteration loop can be established with the mission design to allow the selection of low-cost components as part of well-integrated procurement process. All of these issues were documented as part of the system design case study for future reference.

The ultimate proof of these conclusions will be in the applications they see. These results will be published as part of new industry-standard reference edited by Dr. Jim Wertz called *Reducing Space Mission Cost*. With this wide dissemination , it will be possible to revisit these cost issues with the benefit of a greater experience base to refine and expand the model for future use.

8.2.2. Cost-Effective Propulsion Systems

The cost of a propulsion system depends on far more than its specific impulse or thruster price. By expanding the paradigm to include other performance dimensions—along with price and less obvious, but often more important, mission costs—a new perspective on total system cost is obtained. In application, this total cost paradigm allows all available systems to be re-evaluated in a new light. Furthermore, the total cost figure of merit process developed based on this paradigm gives a versatile tool for quantifying and comparing system options within the context of a given mission.

These conclusions will see immediate application at the University of Surrey as this approach is applied to future mission planning. For example, a Lunar mission is envisioned for the turn of the Century for which a cost-effective propulsion system will be a critical issue. Applying these new tools to that problem will enable mission planners to sift through the many options and select the most cost-effective option for that application.

8.2.3. Propulsion Technology

Although the actual propulsion hardware itself may only represent a small portion of the overall system price, the technology on which it is based drives the other cost dimensions. As a result, the conclusions in this area are of particular relevance.

8.2.3.1. Hybrid Rockets

Hybrid rockets offer a simple, safe high-thrust rocket technology that is a more versatile and cost-effective alternative to solid or liquid systems for certain applications. This research has taken this technology to point where it can seriously be considered for in-orbit use. The remaining development issues have been clearly identified. Most importantly, this research has demonstrated the ease with which this hybrid development can be conducted within the under-capitalised context of a University or small-company environment.

Of the many potential hybrid research topics awaiting further attention, the following are essential ones for most rapidly developing the technology for a near-term demonstration mission:

- *Examine combustion characteristics of other fuel options*—The obvious next fuel option to consider is hydroxyl terminated polybutadiene (HTPB or rubber). This is perhaps the most widely used hybrid fuel and is commonly used as the fuel base for solid propellants. Its advantages were discussed in Chapter 5. While preliminary work was done with this fuel, additional work would be needed to fully characterise combustion behaviour.
- *Model and demonstrate multiple restarts*—One of the biggest advantages of hybrid rockets is their ability to be stopped and re-started on demand. While I was able to demonstrate this capability during my research, further investigation is required to measure and model the start-up characteristics during multiple restarts, ideally following the expected manoeuvre schedule for given mission application.
- *Investigate nozzle robustness*—A significant challenge to adapting a hybrid for space use is designing and testing a nozzle capable of withstanding multiple vacuum restarts over widely varying temperature extremes. My research has proven the inherent robustness of a graphite/pyrolytic graphite throat insert. However, more work is needed to determine if this is a viable option for space applications. If it is not, alternative technologies would have to be considered including exotic, refractory metals (which are potentially very expensive) or regenerative cooling (which is more complex).
- *Investigate multi-port injection/combustion*—Because volume is at a premium for satellite applications, multi-port, such as “double-D” or “wagon wheel,” or rod & tube combustion chamber configurations deserve careful consideration. These options can serve to shorten and condense the combustion chamber, making it easier to package within the spacecraft.
- *Investigate start-up characteristics and combustion stability*—My research revealed relatively long start-up times and the potential for unstable combustion. Further research is needed in this area with high speed data recording to better measure and model these phenomena and determine what design steps can be taken to address these issues.

While this list of research topics may seem daunting at first, realise that most of these can be pursued in parallel as part of an overall development program. Another area of applied research which must also be pursued in parallel concerns the use of HTP.

8.2.3.2. Hydrogen Peroxide

HTP is a safe, versatile oxidiser that also be used as a cost-effective mono-propellant. My research indicates that Type-8 catalyst, pure silver gauze, would offer an effective, long-lived and inexpensive option for mono-propellant or hybrid applications.

Figures of merit indicate that a simple HTP mono-propellant thruster offers an attractive option for some applications. Most important, this capability comes as a ready-to-use spin-off from the hybrid development. Thus, in a cost-constrained research environment, unable to pursue multiple propulsion options, the HTP hybrid/mono-propellant combination allows for technology to cover a wide range of mission options.

While special care and attention is needed when handling HTP, it represents a much safer option than hypergolic propellants. The most important integration problem with this oxidiser involves its long term storage onboard a spacecraft. As indicated in Chapter 4, long term orbit storage has been demonstrated, but that was over 25 years ago. Furthermore, while our experience demonstrates the inherent safety of this oxidiser, this conclusion is not universally shared by the aerospace community. Considerable effort may be needed, for example, to convince launch authorities to allow its use on a secondary payload.

Some interesting areas for future research related to HTP applications are:

- *Long-term HTP storage*—While evidence suggests that HTP has been stored on-orbit for years without mishap [HPHB 67] this would need to be verified before undertaking any mission. Two important variables effecting the long-term storability would be the tank material and the passivation method used. Work is already underway with Arde, Inc. who have offered to provide a flight-like tank which can be used for long-term compatibility experiments. To be most effective, these experiments must be conducted over months or even years to return the best data. I recommend that such experiments begin as soon as possible. Fortunately, this experiment is quite passive in nature. Once the HTP is sealed into the tank, only periodic (say once per month) monitoring of temperature, pressure and concentration is required.
- *Catalyst lifetime*—As discussed in Chapter 5, the best catalyst configuration tested was pure silver gauze treated with samarium nitrate. Unlike the silver-plated gauze which has very well-defined wear-out mechanisms, the silver gauze has no readily obvious mechanical means of depletion. As of this writing, the lifetime of this catalyst is unknown. During a full-blown hybrid development program, this catalyst lifetime issue could also be resolved to better predict on-orbit performance and duration.
- *Catalyst performance variables*—During the catalyst pack research, there appeared to be a correlation between HTP temperature, catalyst temperature and performance. Furthermore, evidence presented in Chapter 5 indicates that after long idle periods the catalyst pack needs to be “run-in” again to return it to its original efficiency. Again, these performance variables would need to be observed and understood during a full-scale program.

8.2.3.3. Liquid Systems

Based on the analysis of available liquid systems and on the results from the system design case study, one can conclude that small satellites that plan to use hypergolic propellants can benefit

choosing small thrusters originally designed for attitude control on large satellites. The LEROS-20 bi-propellant engine is an excellent example of a state-of-the art engine designed for low-cost manufacture. These engines are capable providing large total impulse while allowing for more cost-effective integration than larger, 400-N class engines which are the industry standard for large manoeuvre requirements. Furthermore, the analysis of the figures of merit for various mission options indicates that while mono-propellant hydrazine engines do appear more cost-effective than bi-propellant, the difference is not nearly as big as conventional wisdom would expect.

Well-established large satellite builders have a significant investment in the necessary safety and logistics infrastructure needed to use conventional liquid propulsion options. Certainly, these technologies will continue to see wide applications for many years to come. However, for a small satellite builder with no vested interest in these technologies, a frank assessment of their mission costs may dissuade mission planners from committing to their use in favour of less efficient, but logically more versatile options such as hybrid or water resistojets.

Because of the inherent danger of hypergolic propellant handling, there is little or no hands-on research to be recommended for this technology. Actual system application would have to be handled on a mission-by-mission bases.

8.2.3.4. Cold-gas Systems

Cold-gas systems offer a safe and simple option for small satellite attitude control as well as limited station keeping. They can be included as part of a hybrid or liquid system with a modest additional cost and very little additional complexity. However, because of their low thrust, they offer a significant advantage over hybrid or liquid systems in terms of attitude control system integration. As a result, cold-gas thrusters are an ideal technology on which to learn the basics of propulsion system integration and on-orbit navigation and guidance. Analysis indicates they are the lowest cost option for such a technology demonstration mission. I have recommended a complete cold-gas system for the UoSAT-12 mission.

As cold-gas thrusters are a very mature technology, there is very little additional research that can be recommended. It is not clear that a thruster produced in-house would offer significant cost or performance advantages over the ones offered by Arde.

8.2.3.5. Electric Propulsion

The figures of merit for both hydrazine and water resistojets indicate that both could offer cost-effective applications for station keeping missions. While the hydrazine option offers a clear performance advantage over water, it comes with the inherent mission costs of hypergolic propellants. Although the PPT option offers the best performance of any option studied, its exorbitantly high price tag make it much less attractive overall compared to other options.

Future research into a water-based resistojet could have significant long term benefits for small satellite station keeping. The use of water as a propellant offers the ultimate in flexibility for mission that face launch operations from remote sites with little in the way of safety infrastructure. A small scale program with the same basic objectives as the hybrid program could conceivably be undertaken for a modest initial investment.

Another resistojet option to consider is one using HTP. Like the hydrazine option, the decomposing HTP is already at high temperature so less additional power is needed to raise its temperature to high levels. While this option was not considered as part of the systems analysis done in Chapter 7, it is an interesting option worthy of future consideration.

In addition, these results point the way for future development directions for PPT. If this highly efficient, low-power system can be reduced in price, even at the sacrifice of performance, it could revolutionise current approaches to station keeping propulsion.

8.3. Accomplishments

As you can see, this research has made unique contributions to the field of hybrid rocket technology specifically, and to satellite engineering in general. The most notable of these contributions include the first ever:

- Publication of a coherent strategy for understanding and resolving spacecraft hardware cost drivers during each mission phase.
- Complete characterisation of propulsion system options with respect to all relevant cost dimensions.
- Hybrid research program aimed solely at satellite application.
- Documented case study of a small satellite propulsion system design justification process.
- Development of a technique to quantify total propulsion system cost.

Most important, each research goal was met and the primary objective of the research—evaluating cost-effective propulsion system options for small satellites—was achieved. I believe my work has made a significant contribution to astronautics and will be an important basis for continued propulsion work both at the University of Surrey and elsewhere. I hope this research will help to make affordable access to space a more achievable goal.

Bibliography

General Background

- [Allied 95] Allied Signal, Inc., *AlliedSignal Aerospace Capabilities in Satellite Systems*, Corporate Handout, June 1995.
- [Baker 78] Baker, D., *The Rocket: The History and Development of Rocket & Missile Technology*, New Cavendish Books, London, 1978.
- [Curtis 90] Curtis, A.R., *Space Almanac*, Arcsoft Publishers, Maryland, U.S.A., 1990.
- [Eschbach 90] *Eschbach's Handbook of Engineering Fundamentals*, 4th Edition, Tapley, B.D. (ed.), John Wiley & Sons, 1990.
- [Greenway 94] Greenway, A., Private communication, Defense Research Agency, 1994.
- [Larson 92] Larson, W.J., Wertz, J.R. (ed), *Space Mission Analysis and Design*, 2nd edition, Microcosm, Inc. Torrance, California and Kluwer Academic Publishers, Dordrecht, The Netherlands, 1992.
- [Paul 95] Paul, M., Propulsion Systems Engineer, SSTL, Personal communication, 1995.
- [Sellers 94a] Sellers, J.J., Astore, W.J., Crumpton, K.S., Elliot, C., Giffen, R.B., Larson, W.J. (ed), *Understanding Space: An Introduction to Astronautics*, McGraw-Hill, New York, N.Y., 1994.
- [Wertz 96] Wertz, J. (editor), *Reducing Space Mission Costs*, Kluwer Publishing, to be published 1996.
- [White 86] White, F.M., *Fluid Mechanics*, McGraw-Hill, Inc., USA, 1986.

General UoSAT

- [Allery 93] Allery, M.N. and Ward J.W., The potential for store and forward communications using low Earth orbit microsatellites, 3rd European Satellite Communications Conference, Manchester, UK, November 1993.
- [Fouquet 92] Fouquet, M., "The UoSAT-5 Earth Imaging System -- In-Orbit Results," Proceedings of SPIE conference on Small Satellite Technologies and Applications II, Orlando Florida, 21-22 April 1992.
- [Hodgart 92] Hodgart, M.S., *Gravity Gradient and Magnetorquing Attitude Control for Low Cost Low Earth Orbit Satellites --The UoSAT Experience*, PhD Thesis, Department of Electronic and Electrical Engineering, University of Surrey, Guilford, U.K., June 1992.
- [Hodgart 94] Hodgart, M.S., Ong, W.T., "Gravity Gradient and Magnetorquing Attitude Control for Low Earth Orbit Satellites," to be presented at 2nd ESA International Conference on Spacecraft Guidance, Navigation and Control System, Noordwijk, The Netherlands, 12 - 15 April 1994.
- [Leitmann 93] Leitmann, M., Fouquet, M., Rebordao, J.M., & Sepulveda, T., "Attitude and Position Determination Using a Star Mapper on the Small Satellite Platform PoSAT-1," Proceedings of SPIE conference on Small Satellite Technologies and Applications III, Orlando Florida, 14-15 April 1993.
- [Sellers 94b] Sellers, J.J., Sweeting, M., Hodgart, M.S., "UoSAT and Other European Activities in Small Satellite Attitude Control," Presented at the 17th Annual

Bibliography

- AAS Guidance and Control Conference, Keystone, Colorado, February, 1994.
- [Underwood 94] Underwood, C.I., Brock, D.J., Kim, S., Dilao, R., Santos, P.R., Brito, M.C., Dyer, C.S., Sims, A.J., "Radiation Environment measurements with the Cosmic Ray Experiments On-Board the KITSAT-1 and PoSAT-1 Micro-Satellites," To be published in IEEE, 1994.
- [Underwood 95] Underwood, C., Radiation Issues for UoSAT Lunar Mission, Informal presentation at SSTL, December 1995.
- [Unwin 92] Unwin M.J., Hashida Y., "The Application of GPS on a Microsatellite," Presented at the UK Civil Satellite Navigation Group Symposium, Norwich, 14 October, 1992.
- [Unwin 93a] Unwin M.J., "The PoSAT Microsatellite GPS Experiment," Presented at the ION GPS-93 Conference, Salt Lake City, Utah, USA, September, 1993.
- [Unwin 93b] Unwin M.J., Y. Hashida, "Satellite Attitude from a Single GPS Antenna," Poster-board Paper at the ION GPS-93 Conference, Salt Lake City, Utah, USA, September, 1993.
- [Unwin 93c] Unwin M.J., Hashida Y., "Found in Space: Tracking Microsatellites with GPS," GPS World, June, 1993, Vol. 4, No. 6, pp. 32-38.
- [Unwin 94a] Unwin M.J., "Differential GPS Implementation on Microsatellites," Presented at the Differential Satellite Navigation Systems Conference (DSNS 94), Published in proceedings - Paper No. 52. London, April, 1994.
- [Unwin 94b] Unwin M.J. & Sweeting M.N., "Results from the PoSAT GPS Experiment," Presented at the IEEE, Position Location and Navigation Symposium (PLANS 94), Las Vegas, Nevada, USA, April, 1994.
- [Unwin 94c] Unwin M.J. & Sweeting M.N., "First Results from the PoSAT GPS Experiment," Presented at the ION National Technical Meeting, San Diego, CA, USA, Jan, 1994.
- [Ward 90] Ward, Jeffrey W., "Store-and-Forward Message Relay Using Microsatellites: The UoSAT-3 PACSAT Communications Payload," Presented at the 4th annual USU/AIAA Conference on Small Satellites, Logan, Utah, 27-30 September, 1990.
- [Ward 95] Ward, J., "Minisatellite Program Objectives," SSTL internal memo, 1995.

Software

- [Selph 92] Selph, C., *Isp Computer Code*, Personal communication to Dr. Ron Humble, 1992.

General Propulsion

- [AERO 62] Aerojet-General Corp., "Design Guide for Pressurisation System Evaluation Liquid Propulsion Rocket Engines, Vol. I—Use of Design Guide, General Design Data," Report No. 2334, 30 September 1962.
- [Barton 94] Barton, J., Olin Aerospace, phone conversation, 14 November 1994.
- [Berman 60] Berman, K., "The Plug Nozzle: A New Approach to Engine Design," *Astronautics*, April 1960.

Bibliography

- [Casci 68] Casci, C., Gismond, E., Angelino, G., "An Experimental Study of the Application of Plug Nozzles to Solid-Propellant Rockets—2," *Spaceflight*, Vol. 10, 1968.
- [Chang 89a] Chang, I., *Rocket Propulsion Fundamentals*, AA280 Notes, Stanford University, Spring 1989.
- [Chang 89b] Chang, I., Advanced Space Propulsion, AA286 Notes, Stanford University, Spring 1989.
- [Clark 72] Clark, John, *Ignition: An Informal History of Liquid Rocket Propellants*, Rutgers University Press, New Brunswick, N.J. 1972.
- [Ellis 72] Ellis, R.A., "Continuing Evolution of Nozzle Design and Analysis Techniques," AIAA 72-1190, 1972.
- [Fatig ??] Fatig, M., "The SmallSAT Paradigm," Allied Signal Aerospace Company, Lanham, Maryland, no date.
- [DCI] ArianeSpace, *Dossier de Contrôle des Interfaces (Interface Control Document)*, UoSAT-F, DCI 10/392 01, Issue 2, Rev. 0, March 1991.
- [WRR] WRR 127-1, *Range Safety Requirements*, 30th Space Wing, United States Air Force, 30 June 1993.
- [MS 1522A] MIL-STD-1522A Standard General Requirements for Safe Design and Operation of Pressurized Missile and Space Systems, United States Air Force, 28 May 1984.
- [Furstenau ??] Furstenau, R.P., McCay, T.D., Mann, D.M., "US Air Force Approach to Plume Contamination," Air Force Rocket Propulsion Laboratory, Plume Technology Office, Edwards AFB, California, no date.
- [Gray 64] Gray, P.D., "Effects of the Space Environment on Liquid Rocket Systems," *Chemical Engineering Progress Series*, No. 52, Vol. 60, 1964.
- [Hopkins 68] Hopkins, D.F., Hill, D.E., "Transonic Flow in Unconventional Nozzles," *AIAA Journal*, Vol. 6, No. 5, May 1968.
- [Humble 95] Humble, R., Henry, G.N., Larson, W.J., *Space Propulsion Analysis and Design*, McGraw-Hill, Inc., College Custom Series, 1995.
- [Purohit 92] Purohit, G.P., Nordeng, H.O., Ellison, J.R., "Loading Operations for Spacecraft Propulsion Subsystems," AIAA 92-3065, AIAA/SAE/ASME/ASEE 28th Joint Propulsion Conference, Nashville, Tennessee, 6-8 July 1992.
- [Randall 52] Randall, L.N., "Rocket Applications of the Cavitating Venturi," *American Rocket Society Journal*, January-February 1952.
- [Rao 61] Rao, G.V.R., "Recent Developments in Rocket Nozzle Configurations," *American Rocket Society Journal*, November 1961.
- [Sutherland 66] Sutherland, G.S., Maes, M.E., "A Review of Microrocket Technology: 10-6 to 1 lbf Thrust," *Journal of Spacecraft and Rockets*, Vol. 3, No. 8, August 1966.
- [Sutton 52] Sutton, G.P., "Rocket Propulsion Progress: A Literature Review," *ARS Journal*, Jan-Feb 1952.
- [Sutton 92] Sutton, G.P., *Rocket Propulsion Elements*, 6th Edition, John Wiley & Sons, Inc., 1992.

Bibliography

- [Southerland 66] Southerland, G.S., Maes, M.E., "A Review of Microrocket Technology: 10-6 to 1 lbf Thrust," *Journal of Spacecraft and Rockets*, Vol. 3, No. 8, August 1966.
- [Sule 73] Sule, W.P., Mueller, T.J., "Annular Truncated Plug Nozzle Flowfield and Base Pressure Characteristics," *Journal of Spacecraft*, Vol. 10, No. 11, November 1973.

Bi-Propellant

- [Gray 90] Gray, C., "Development of a 110lbf Dual Mode Liquid Apogee Engine," AIAA 90-2424, AIAA/SAE/ASME/ASEE 26th Joint Propulsion Conference, Orlando, Florida, 16-18 July 1990.
- [MBB 81] MBB, Proposal for 10-N Thrust Engine for AMSA III-B, TN RT351-2 1981.
- [Meinzer 95] Meinzer, K., Personal communication, May 1995.
- [RO 94] Royal Ordnance, personal communication Ref: PDC/JE/313, 30 November, 1994.
- [Wood 90] Wood, R.S., "Development of a Low Cost 22N Bi-propellant Thruster," AIAA 90-2056, AIAA/SAE/ASME/ASEE 26th Joint Propulsion Conference, Orlando, Florida, 16-18 July 1990.
- [Wood 95] Wood, R.S., Royal Ordnance Rocket Motors Division, Westcott, Personal communications during system design effort, 1995.

Electric Propulsion

- [Bender 62] Bender, R.W., "A Chemical Arc-jet Rocket Feasibility Study," Presented at the ARS Electrical Propulsion Conference, Berkeley, California, 14-16 March 1962.
- [Clauss 95] Clauss, C.W., Tilley, D.L., Barnhart, D.A., "Benefits of Low-Power Stationary Plasma Thruster Propulsions for Small Satellites," Presented at 9th AIAA/Utah State University Conference on Small Satellites, 1995.
- [Fearn 94] Fearn, D.G., Martin, A.R., "The Promise of Electric Propulsion for Low-Cost Planetary Missions," IAA Conference on Low-Cost Planetary Missions, Johns Hopkins University, Laurel, Maryland, 12-15 April 1994.
- [Gray 94] Gray, H., Smith, P., Fearn, D.G., "UK-ION Propulsion System Development," CNES/ESA International Conference on Spacecraft Propulsion, 1994.
- [Greco 72] Greco, R.V. et al, "Resistojet and Plasma Propulsion System Technology," AIAA-72-1124, AIAA/SAE 8th Joint Propulsion Specialist Conference, New Orleans, Louisiana, November 29 - December 1, 1972.
- [Hoskins 95] Hoskins, A., "Electric Propulsion," *Aerospace America*, Vol. 33, No. 12, p. 47, December 1995.
- [Kaufman 72] Kaufman, H.R., Reader, P.D., "Electrostatic Thrusters," AIAA-72-1123, AIAA/SAE 8th Joint Propulsion Specialist Conference, New Orleans, Louisiana, November 29 - December 1, 1972.

Bibliography

- [Malyshev ??] Malyshev, G., Popov, G., Kulkov, V., "New Space Technologies, New Stage of Aerospace," Moscow Aviation Institute, Research Institute of Applied Mechanics and Electrodynamics, Presented at ??
- [Manzella 89] Manzella, D.H., Carney, L.M., "Investigation of a Liquid-Fed Water Resistojet Plume," NASA Technical Memorandum 102310, AIAA-89-2840, Prepared for the 25th Joint Propulsion Conference, Monterey, California, July 10-12, 1989.
- [Morren 88] Morren, W.E., Stone, J.R., "Development of a Liquid-Fed Water Resistojet," AIAA-88-3288, AIAA/ASME/SAE/ASEE 24th Joint Propulsion Conference, Boston, Massachusetts, 11 - 13 July 1988.
- [Morren 93a] Morren, W.E., "Gravity Sensitivity of a Resistojet Water Vaporiser," NASA Technical Memorandum 106220, AIAA-93-2402, 29th Joint Propulsion Conference, Monterey, California, June 28-30, 1993.
- [Morren 93b] Morren, W.E., MacRae, G.S., "Preliminary Endurance Tests of Water Vaporizers for Resistojet Applications," AIAA-93-2403, 29th Joint Propulsion Conference, Monterey, California, June 28-30, 1993.
- [Myers 95] Myers, R., NASA Lewis Research Center, Private communication, November 1995.
- [NASA 93] NASA, "Ultra-Low-Power >Arcjet Thruster Performance", NASA TM 106400, Nov 93.
- [Olin 96b] Olin Aerospace Company, MR-510 Electrothermal Hydrazine Thruster, ROM cost and performance data, FAXed personal communication from Mr. J.J. Galbreath, 6 February 1996.
- [Zube 95] Zube, D., Messerschmid, E.W., Dittmann, A., "Project ATOS—Ammonia Arcjet Lifetime Qualification and System Component Test," AIAA 95-2508, 31st AIAA/ASME/SEA/ASEE Joint Propulsion Conference and Exhibit, 10-12 July 1995.

Costs

- [Arde 96] Arde, Inc., UoSAT Minisatellite Propulsion System Phase-1 Contract Deliverable, component price quotations, SSTL Proprietary Information, 1996.
- [AstroTech 96] AstroTech, Inc., Cape Canaveral Florida, personal communication, Mr. Dwight Light, 8 January 96:
- [Burgess 95] Burgess, E.L., Lao, N.Y., Bearden, D.A., "Small-Satellite Cost Estimating Relationships," Presented at the 9th Annual AIAA/Utah State University Conference on Small Satellites, 18-21 September 1995.
- [Christensen 92] Christensen, C.B., Wagenfuehrer, C., "Standard Cost Elements for Technology Programs," published in *Space Economics*, edited by Greenberg, J.S., Hertzfeld, H.R., Progress in Astronautics and Aeronautics, Seebass, A.R. editor-in-chief, Vol. 144, AIAA, 1992.
- [Dean 90] Dean, E., "The Design-To-Cost Manifold," Presented at the International Academy of Astronautics Space Systems Cost Estimation Methodologies and Applications, San Diego, California, 10-11 May 1990.

Bibliography

- [Dean 91] Dean, E., Unal, R., "Designing for Cost," *Transactions of the American Association of Cost Engineers*, pp. D.4.1 - D.4.6, Seattle, Washington, 23-26 June, 1991.
- [Engine 92] *Operational Integrated Modular Engine, Final Report Inputs, Prepared by Engine Analysis (600-105)*, Advanced Programs, EA92-018, 1992.
- [Fad 88] Fad, B.E., Summers, R.M., "Parametric Estimating for New Business Ventures," *Engineering Cost and Production Economics*, vol. 14(2), 1988.
- [Hillier 86] Hillier, F.S., Leiberman, G.J., *Introduction to Operations Research*, 4th edition, Holden-day, Inc., Oakland, California, 1986.
- [ITT 88] ITT Statistical Programs Group, *Taguchi Methods—SPC Case Studies*, 1988.
- [Mandell 92] Mandell, H.C.jr., "Cost-Estimating Relationships for Space Programs," published in *Space Economics*, edited by Greenberg, J.S., Hertzfeld, H.R., Progress in Astronautics and Aeronautics, Seebass, A.R. editor-in-chief, Vol. 144, AIAA, 1992.
- [Noble 89] Noble, J.S., Tanchoco, J.M.A., "Cost Modelling for Design Justification," *Cost Analysis Applications of Economics and Operations Research*, Gulledge, T.R., jr, Litteral, L.A. (eds). Proceedings, Washington, DC, Springer-Verlag, New York, NY, 1989.
- [Phadke 89] Phadke, M.S., *Quality Engineering Using Robust Design*, Prentice-Hall, Inc., 1989.
- [ref] Taguchi Methods
- [RMD 94] British Aerospace Rocket Motors Division, "Baikonur Launch Site Visit," Internal Report 200 972-TR/1/E000, August 1994.
- [Sellers 95] Sellers, J.J., Meerman, M., Paul, M., Sweeting, M., "A Low-Cost Propulsion Option for Small Satellites," *Journal of the British Interplanetary Society*, Vol. 48, pp. 129-138, March, 1995.
- [Sjovold 89] Sjovold, A.R., Morrison, D.C., "Rocket Propulsion Cost Modelling," *Cost Analysis Applications of Economics and Operations Research*, Proceedings, Gulledge, T.R.jr, Litteral, L.A., (eds), Springer-Verlag, New York, N.Y., 1989.
- [Smith 84] Smith, P., Horton, M.A., "Advanced Propulsion Systems for Geostationary Spacecraft—Study Results," The Marconi Company, AIAA-84-1230, 1984.
- [Valentine 94] Valentine, A., "Kazakhstan: Radiation and Chemical Hazard Conditions/Precautions General Health Precautions," Prepared by The Delphi Groupe, Inc., Austin, Texas, for Motorola, Inc., Phoenix, Arizona, August 1994.
- [Wertz 96] Wertz, J., *Reducing Space Mission Costs*, Kluwer Publishing, to be published 1996.

Small Satellite Propulsion

- [AMSAT 95] The Phase 3D Design Team, "Phase 3D, A New Era For Amateur Satellites," *The AMSAT Journal*, March/April 1995.
- [ARSENE 92] "ARSENE Satellite," Publicity handout prepared by CNES, 1992.

Bibliography

- [Clark 80] Clark, T., Kasser, J., "Ariane Launch Vehicle Malfunctions, Phase IIIA Spacecraft Lost!" *Orbit*, June/July 1980.
- [Daniels 95] Daniels, R., FAXed personal communication on OSCAR P-3 propulsion systems, 12 December 1995.
- [Dudzinski 95] Dudzinski, L.A., Myers, R.M., "Advanced Propulsion Benefits to New Millennium Class Missions, Presented at the 9th Annual AIAA/Utah State Conference on Small Satellites, 1995.
- [Grahn 93] Grahn, S., "The FREJA Magnetospheric Research Satellite Design and Flight Operations," Presented at the 7th Annual AIAA/USU Conference on Small Satellites, 13 - 16 September 1993, Logan, Utah.
- [Llareus 94] Llareus, M., ENSAE, Phone conversation with author, 5 January 1994.
- [Lorenz 88] Lorenz, R.D., "UoGAS—A Get Away Special Satellite With Orbit-Raising Capability," Presented at the 2nd Annual AIAA/USU Small Satellite Conference, Logan, Utah, 18-21 September 1988.
- [Meinzer 94] Meinzer, K., AMSAT-DL, Phone conversation with author, 27 January 1994.
- [Myers 94] Myers, R.M., Oleson, S.R., "Small Satellite Propulsion Options," AIAA 94-2997, 30th Joint Propulsion Conference, Indianapolis, Indiana, June 27-29, 1994.
- [OSCAR 93] "ARSENE, The End?" *OSCAR NEWS*, AMSAT-UK, October 1993, Number 103.
- [Pidoux 92] Pidoux, B., "The Mission of the Amateur Radio Satellite ARSENE," Proceedings of the 7th AMSAT-UK Colloquium, University of Surrey, July 1992.

Satellite Missions

- [Daniels 87] Daniels, R.L., "The Propulsion Systems of the Phase-III Series Satellites," Presented at 1st Utah State Conference on Small Satellites, 7 October 1987.
- [Greenway 94] Greenway, A., Private communication, Defence Research Agency, 1994.
- [Grahn 93] Grahn, Sven "The FREJA Magnetospheric Research Satellite Design and Operations," presented at the 7th AIAA/USU Conference on Small Satellites, Utah State University, September 11 - 16, 1993.
- [Murphy 63] Murphy, C. G., "A Syncrom Satellite Program," AIAA Summer Meeting, LA California, June 17-20, 1963.

General HTP

- [AL 94] Air Liquide, Specification sheet for hydrogen peroxide, electronic grade, July 1994.
- [AL 95] Air Liquide, HTP density as a function of percentage, FAXed information, 11 July 1995.
- [Andrews 90] Andrews, David "The Advantages of Hydrogen Peroxide as a Rocket Oxidant," *Journal of the British Interplanetary Society*, Vol. 43, No. 7 July 1990

Bibliography

- [Andrews 94] Andrews, D., Personal Communication, 15 June 1994.
- [Andrews 95] Andrews, D., Personal Communication, 6 March 1995.
- [Barclay 68] Barclay, L.P., "Hydrogen Peroxide Evaluation," Technical Report No. AFRPL-TR-68-208, Air Force Rocket Propulsion Laboratory, Edwards AFB, CA, November 1968.
- [Baumgartner 63a] Baumgartner, H.J., et al, "Decomposition of Concentrated Hydrogen Peroxide on Silver I. Low Temperature Reaction and Kinetics," *Journal of Catalysts*, 2, 405-414, 1963.
- [Baumgartner 63b] Baumgartner, H.J., et al, "Decomposition of Concentrated Hydrogen Peroxide on Silver II. High Temperature Decomposition," *Journal of Catalysts*, 2, 415-420, 1963.
- [Bloom 57] Bloom, R.Jr., Brunsvoold, N.J., "Anhydrous Hydrogen Peroxide as a Propellant," *Chemical Engineering Progress*, Vo. 53, No. 11, November 1957.
- [Bofors 94] Bofors Underwater Systems, Personal Communication from M. Tremblot, Air Liquide on a catalyst system for submarines, 28 September 1994.
- [Cambridge 91] Cambridge Encyclopaedia, Cambridge University, Cambridge, 1991.
- [Coltron 67] "Coltron Introduces Hot Shave Cream," Detergent Age, November 1967.
- [CPIA 84] Chemical Propulsion Information Agency Publication 394, Vol. III, Hazards of Chemical Rockets and Propellants, Johns Hopkins University, Applied Physics Laboratory, Laurel, Maryland, September 1984.
- [Davis 52] Davis, N.S., Keefe, J.H., "Equipment for Use with High-Strength Hydrogen Peroxide," *Journal of the American Rocket Society*, Vol. 22, No. 2, March-April 1952.
- [Davis 60] Davis, N.S., jr., McCormick, J.C., "Design of Catalyst Packs for the Decomposition of Hydrogen Peroxide," Liquid Rockets and Propellants, Bollinger, L.E., Goldsmith, M., & Lemmon, A.W., jr, (eds.), A Symposium of the American Rocket Society, Ohio State University, Columbus, Ohio, 18-19 July, 1960.
- [Gould 91] Gould, R.D., Harlow, J., "Black Arrow—The First British Satellite Launcher," IAA91-689, 42nd Congress of the International Astronautical Federation, Montral, Canada, 5 - 11 October 1991.
- [Gray 64] Gray, P.D., "Effects of the Space Environment on Liquid Rocket Systems," *Chemical Engineering Progress Symposium Series*, No. 52, Vol. 60., 1964.
- [HPHB 67] Hydrogen Peroxide Handbook. Chemical and Material Sciences Department, Research Division, Rocketdyne—a division of North American Aviation, Inc., Canoga Park, California, Technical Report AFRPL-TR-67-144, July 1967.
- [Kross 95] Kross, J., "These Are Not Your Father's Rocketships Anymore," Ad Astra, pp. 22-29, March/April 1995.
- [LaTona 94] LaTona, A., Valcor, Inc., private communication, 7 September 1994.
- [McCormick 63] McCormick, J.C., "For All-Around Performance: 98% H₂O₂," *Space/Aeronautics*, 15 July 1963.

Bibliography

- [Meade 95] Meade, A., Royal Ordnance, HTP decomposition thermochemistry data, FAXed personal communication, 26 June 1995.
- [Runckel 63] Runckel, J.F., Willis, C.M., Salters, L.B.jr, "Investigation of Catalyst Beds for 98-Percent-Concentration Hydrogen Peroxide," NASA Technical Note D-1808, June 1963.
- [Rusek 95] Rusek, J.J., "Cation Variance Effects in Hydrogen Peroxide Decomposition," AIAA 95-3087, 31st AIAA/ASME/SEA/ASEE Joint Propulsion Conference and Exhibit, 10-12 July 1995.
- [Saunders 95] Saunders, D.J., Personal communication, June 1995.
- [Tremblot 96] Tremblot, A., Air Liquide, private communications, February/March 1996.
- [Willis 60] Willis, C. M., "The Effect of Catalyst-Bed Arrangement on Thrust Buildup and Decay Time for a 90 Percent Hydrogen Peroxide Control Rocket," Langley Research Centre, Langley Field, Va., NASA Technical Note D-516, September 1960.
- [Zubrin 95] Zubrin, R.M., Clapp, M.B., "Black Horse: Winging it to Orbit," *Ad Astra*, pp. 40-43, March/April 1995.

RO References

- [Maggs 54] Maggs, F.T., Avery, M.J., "A Preliminary Investigation of the Loss of Efficiency of an HTP Decomposer During Use," Technical Memo No. RPD 53, RAE, Farnborough, June 1954.
- [Maggs 56] Maggs, F.T., Sutton, D., "HTP for Decomposers Using Silver Catalyst," Technical Memo No. RPD 115, RAE, Westcott, October 1956.
- [Maggs 63] Maggs, F.T., Sutton, D., Southern, G.R., "Some Aspects of the Catalytic Decomposition of Hydrogen Peroxide by Silver: Part IX, Tests with Decomposers," RPE Report No. 42, RPE, Westcott, June 1963.
- [Shufflebothom 57] Shufflebotham, N., Walder, H., "Decomposition Tests of Non-Stabilised HTP on Silver Catalyst," Technical Memo No. RPD 134, RAE, Farnborough, June 1957.
- [Southern 67] Southern, G.R., Sutton, D., "Some Aspects of the Catalytic Decomposition of Hydrogen Peroxide by Silver: Part X. Decomposer Tests Using HTP at Concentrations up to 98% w/w," RPE Technical Report No. 67/9, RPE, Westcott, August 1967.
- [Sutton 55] Sutton, D., "The Surface Areas of Silver Gauze Catalysts as a Measure of their Reactivity Toward Hydrogen Peroxide," Technical Memo No. RPD 78, RAE, Farnborough, May 1955.
- [Sutton 55] Sutton, D., Walder, H., "The Analysis of Silver Catalyst Decomposer Packs After Use," Technical Memo No. RPD 90, RAE, Farnborough, December 1955.
- [Sutton 60] Sutton, D., "Some Aspects of the Catalytic Decomposition of Hydrogen Peroxide by Silver," RPE Technical Note No. 197, Rocket Propulsion Establishment, Westcott, December 1960.
- [Sutton 62a] Sutton, D., "Some Comments on the Efficiency and Life of the Silver Catalyst Pack for the Decomposition of HTP," Technical Memo No. 248, RPE, Wesctott, February 1962.

Bibliography

[Sutton 62b] Sutton, D., Bennett, C.R., "Some Aspects of the Catalytic Decomposition of Hydrogen Peroxide by Silver: Part VIII. The Effects of Additives," RPE Technical Note No. 211, RPE, Westcott, February 1962.

[Walder 55] Walder, H., Spalding, E.G., "Influence of HTP stabiliser (sodium stannate) on the silver catalyst," Technical Memorandum No. RPD 68, Rocket Propulsion Department, Westcott, January, 1955.

Hybrid Upper Stage

[Jansen 88] Jansen, D.P.L.F., Kletzkine, P., "Preliminary Design for a 3 kN Hybrid Propellant Engine," ESA Journal, Vol. 12, 1988.

[McMillen 89] McMillen, D., Krabbe, K.P., "The SPINSAT Bus: New and Old in a Small Package," Presented at 3rd Annual AIAA/Utah State University Conference on Small Satellites, Logan, Utah, 26-28 September 1989.

[AMROC 94] AMROC, "Aquila Launch Vehicle Family," American Rocket Company, Ventura, California, June 1994.

[Witinghill 94] Witinghill, G., AMROC, Personal Communication, 26 July 1994.

General Hybrid

[Adams 68] Adams, M.B., Bialla, P.H., Michaelis, R.H., "Hybrid Development Planning Manual," NASA CR-66698, March 1968.

[Ankarsward 79] Ankarsward, B., Magnusson, U., "Presentation of the Hybrid Rocket Engine HR 4," Svenska Flygmotor Aktiebolaget, Trollhattan, Sweden, 7 December 1979.

[Ballal 92] Ballal, D.R., "Propellants and Combustion," *Aerospace America*, December 1992.

[Boyer 95] Boyer, W., "Lack of Financing Cripples AMROC," *Space News*, 10-16 July 1995.

[Cook 92] Cook, J.R., et al, "Hybrid Rockets: Combining the Best of Liquids and Solids," *Aerospace America*, July 1992.

[Cruttenden 67] Cruttenden, A.J., "Some Aspects of Hybrid Rocket Combustion," Technical Memo. No. 423, Rocket Propulsion Establishment, Westcott, January 1967.

[Davis 94] David, L. "U.S. Defence Conversion Effort Buys Amroc Hybrid Fuel Work," *Space News*, 7-13 February, 1994.

[Dasch 95] Dasch, P., Kross, J., "Amroc Sinks in Sea of Red Ink," *Ad Astra*, November/December 1995.

[Dembo 93] Dembo, P., et al, ASPIRE II—Initial Design and Progress Report of the Second UDSEDS Rocket Project, UKSEDS, 1993.

[Dijkstra 95] Dijkstra, F., "An Engineering Model To Assess Hybrid Propulsion Based Rocket Systems," AIAA 95-2394, 31st AIAA/ASME/SEA/ASEE Joint Propulsion Conference and Exhibit, 10-12 July 1995.

[Estey 92a] Estey, P.N., "Hybrid Rockets," *Aerospace America*, December 1992.

Bibliography

- [Estey 92b] Estey, P.N., Whittinghill, G.R., "Hybrid Rocket Motor Propellant Selection Alternatives," AIAA 92-3592, AIAA/SAE/ASME/ASEE 28th Joint Propulsion Conference, Nashville, Tennessee, 6-8 July 1992.
- [Purohit 92] Purohit, G.P., Nordeng, H.O., Ellison, J.R., "Loading Operations for Spacecraft Propulsion Subsystems," AIAA 92-3065, AIAA/SAE/ASME/ASEE 28th Joint Propulsion Conference, Nashville, Tennessee, 6-8 July 1992.
- [Green 63] Green, L. jr, "Introductory Considerations on Hybrid Rocket Combustion," *Heterogeneous Combustion*, edited by Wolfhard, H.G., Glassman, I., and Green, L.jr., based on papers at *Heterogeneous Combustion Conference*, Palm Beach, Florida, December 11-13, 1963.
- [Goldberg 91] Goldberg, B.E., Wiley, D.R., "Hybrids: Best of Both Worlds," *Aerospace America*, June 1991.
- [Greiner 92] Greiner, B., Frederick, R.A.jr, "Results of Labscale Hybrid Rocket Motor Investigation," Propulsion Research Centre, University of Alabama, AIAA 92-3301, 1992.
- [Greiner 93] Greiner, B., Frederick, R.A.jr, "Hybrid Rocket Instability," AIAA 93-2553, 29th AIAA/ASME/SAE/ASEE Joint Propulsion Conference, Monterey, California, 28 - 30 June 1993.
- [Grigorian 94] Grigorian, V., "Propellant Characterisation and Design of a Hybrid Rocket Engine," 45th Congress of the International Astronautical Federation, Jerusalem, Israel, 9-14 October 1994.
- [Holzman 84] Holzman, A. L., *Constant Thrust Hybrid Rocket Motor*, United States Patent No. 4,424,679, 10 January 1984.
- [Jain 85] Jain, S.R., Rajendran, G., "Performance Parameters of Some New Hybrid Hypergols," *Journal of Propulsion*, Vol. 1, No. 6, November/December 1985.
- [Karabeyoglu 95] Karabeyoglu, M.A., Altman, D., Bershad, D., "Transient Combustion in Hybrid Rockets," AIAA 95-2691, 31st AIAA/ASME/SEA/ASEE Joint Propulsion Conference and Exhibit, 10-12 July 1995.
- [Kilby 96] Kilby, B., "The Great Hybrid Flyoff," *High Power Rocketry*, January 1996.
- [Holzman 94] Holzman, A. L., "Hybrid Rocket Propulsion," United Technologies Chemical Systems, Presentation by the Hybrid Propulsion Industry Action Group, Received as part of a private communication, 1994.
- [Jenkins 95] Jenkins, R.M., Cook, J.R., "A Preliminary Analysis of Low Frequency Pressure Oscillations in Hybrid Rocket Motors," AIAA 95-2690, 31st AIAA/ASME/SAE/ASEE Joint Propulsion Conference, San Diego, California, 10 - 12 July 1995.
- [Kuentzmann 91] Kuentzmann, P., Sternfeld, H.J., "What Future for Hybrid Rocket Propulsion?," Proceedings from the Symposium on Launcher Propulsion Toward the Year 2010, Bordeaux, France, 11-12 June 1991.
- [Lydon 93] Lydon, M., et al, "Hybrid Sounding Rocket Development at the United States Air Force Academy," AIAA Paper 93-2264, 29th Joint Propulsion Conference Monterey, CA, June 1993.
- [Marshall 95] Marshall Star, "Hybrid Motor Development Accelerates at Marshall," NASA, Vol. 36, No. 7, 18 October 95.

Bibliography

- [Murthy 87] Murthy, K.N., Jain, S.R., "Studies of Some Novel Hypergolic Hybrid Systems," IAF 87-271, 38th Congress of the International Astronautical Federation, Brighton, England, 10-17 October 1987.
- [Nagappa 91] Nagappa, R., Deepak, D., "Hybrid Propulsion—Capabilities and Potentials," *Journal of the Aeronautical Society of India*, Vol. 43, 1991.
- [Netzer 72] Netzer, D.W., "Hybrid Rocket Internal Ballistics," Naval Postgraduate School, Prepared by CPIA, January 1972.
- [Ordah 65] Ordah., D.D., Rains, W.A., "Recent Developments and Current Status of Hybrid Propulsion," *Journal of Spacecraft*, Vol. 2, No. 6, Nov-Dec 1965.
- [Schmucker 78] Schumucker, R.H., et al, "Hybrid Propulsion Systems: Technology and Applications," ESA-TT-448; DLR-IB-456-76/11, February 1978.
- [SpaceNews 95] Space News, "Hybrid Rocket Draws Attention," 13-26 November 1995.
- [Tucci 94] Tucci, L., "Hybrid Rocket Tests Impress NASA Skeptics," *Space News*, 20-26 July 1994.
- [Vincent 95] Vincent, B., "Hybrid Rockets," *Aerospace America*, Vol. 33, No. 12, December 1995.
- [Wagnner ??] Wagner, W., "Fireflies and Other UAVs," Midland Publishing, Ltd., ISBN 1-85780-005-2, Data ??.
- [Waidmann 88] Waidmann, W., "Thrust Modulation in Hybrid Rocket Engines," *Journal of Propulsion*, Vol. 4, No. 5, September/October 1988.
- [Williams 66] Williams, F. A., "Grain Design and Throttling of Hybrid Rocket Motors," *Chemical Engineering Progress Symposium Series*, No. 61, Vol. 62, 1966.

HTP Hybrids

- [Brown 96] Brown, R. Project Machinery, private communication, 15 February 1996.
- [Hercules 70] Hercules, Inc., "Feasibility of High Performance Fluid Controlled Solid Propellant," Final Technical Report, NAS 7-745, Bacchus Works, Magna, Utah, Document No. H250-12-1-3, July, 1970.
- [Moore 56] Moore, G. E., Berman, K., "A Solid-Liquid Rocket Propellant System," *Jet Propulsion*, November, 1956.
- [Pugibet 70] Pugibet, M., Moutet, H. "On the Use of Hydrogen Peroxide as Oxidiser in Hybrid Systems," NASA Technical Translation, NASA TT F-13034, May 1970.
- [Ventura 93] Ventura, M., Heister, S., "Hydrogen Peroxide as an Alternate Oxidiser for a Hybrid Strap-on Booster," AIAA/SAE/ASME/ASEE 29th Joint Propulsion Conference and Exhibit, Monterey, California, June 28-30, 1993.
- [Wernimont 94] Wernimont, E.J., Meyer, S.E., "Hydrogen Peroxide Hybrid Rocket Engine Performance Investigation," AIAA 94-3147, 30th Joint Propulsion Conference, Indianapolis, IN, June 1994.
- [Wernimont 95] Wernimont, E.J., Heister, S.D., "Performance Characterisation of Hybrid Rockets Using Hydrogen Peroxide Oxidiser," AIAA-95-3084, 31st AIAA/ASME/S AE/ASEE Joint Propulsion Conference and Exhibit, San Diego, California, 10-12 July 1995.

Bibliography

Lunar Missions

- [Uphoff 92] Uphoff, C., "Practical Aspects of Transfer from GTO to Lunar Orbit," Presented at the Flight Mechanics/Estimation Theory Symposium, Greenbelt, Maryland, 5 - 7 May 1992.
- [Belbruno 87] Belbruno, E.A., "Lunar Capture Orbits, a Method of Constructing Earth Moon Trajectories and the Lunar Gas Mission," 19th AIAA/DGLR/JSASS International Electric Propulsion Conference, Colorado Springs, Colorado, 11 - 13 May 1987.
- [Chicarro 94] Chicarro, A., "MORO—A European Moon-Orbiting Observatory for Global Lunar Characterisation," *ESA Journal*, Vol. 18, 1994.
- [Warren 93] Warren, P.A., Loucks, M.E., "Small Spacecraft Conceptual Design for a Lunar Polar Mapping/Educational Spacecraft," Presented at 7th Annual AIAA/Utah State University Small Satellite Conference, Logan, Utah, 1993.
- [Kluever 94] Kluever, C.A., Pierson, B.L., "Optimal Low-Thrust Earth-Moon Transfers with Switching Functions," *The Journal of Astronautical Sciences*, The American Astronautical Society, Vol. 42, No. 3, July-September 1994.
- [Kerr 94] Kerr, R.A., "Scaling Down Planetary Science," *Science*, Vol. 264, 27 May 1994.
- [Butler 88] Butler, P., Stein, A., "Deep Space Missions for Small Satellites," Presented at 2nd Annual AIAA/Utah State Conference on Small Satellites, 18-21 September, 1988.
- [Redd 92] Redd, F., Anderson, S.D., "Copernicus—Lunar Surface Mapper," Presented at 6th Annual AIAA/Utah State University Conference on Small Satellites, 1992.

Hydrazine

- [Bunker 90] Bunker, R.L., Baker, D.L., Lee, J.H.S., "Explosive Decomposition of Hydrazine by Rapid Compression of a Gas Volume," American Institute of Aeronautics and Astronautics, 1990.
- [Olin 94] Olin Aerospace Inc., Mr. Jim Barton, phone conversation, 15 November 1994.
- [Olin 95a] Olin Aerospace Company, Cost information on MR-106E Hydrazine Thruster, Mr. Jim Bartron, personal communication, 11 October 1995.
- [Olin 95b] Olin Aerospace Company, Information on MR-106E Hydrazine Thruster, Mr. Jim Bartron, FAXed personal communication, 12 October 1995.
- [Olin 96a] Olin Aerospace Company, email personal communication on pulsed plasma thruster (PPT) performance and cost, 10 January 1996.
- [Priles 85] Priles, O., Hagemann, D., Benz, F.J., Farkas, T., "Explosive Decomposition of Hydrazine Due to Rapid Gas Compression," In 1985 JANAF Propulsion Meeting, K.L. Strange (ed.), Johns Hopkins University, Laurel, Maryland: Chemical Propulsion Information Agency, April 1985.

Bibliography

Hypergolic

- [GSC 87] Guiana Space Centre, Safety Training, S3B Facility, Arianespace, CNES, 1987.
- [CPIA 70] Chemical Propulsion Information Agency, Chemical Rocket/ Propellant Hazards, Vol. III, Liquid Propellant Handling, Storage and Transportation, JANNAF Propulsion Committee, The JANNAF Hazards Working Group, May 1970.

Solids

- [Thiokol 93] Thiokol Corporation, *Space Motor Catalog*, Tactical Operations, Elkton Division, 1993.
- [Thiokol 96] Thiokol Corporation, Personal Communication, EP612-96 (PO29), ROM Prices for Small STAR Motors, W. Lloyd McMillan, 1 March 1996.

Space Systems

- [AWST 95] Aviation Week & Space Technology, "NOAA-14 To Restore Forecasting Capability," 9 January 1995.
- [Campbell 93] Campbell, W.A. jr., Scialdone, J.J., *Outgassing Data for Selected Spacecraft Materials*, NASA Reference Publication 1124, Revision 3, September 1993.
- [Iida 93] Iida, T., et al, "Application of Car Electronic Parts to Small Satellites," Japan-U.S. Cooperation in Space Project Workshop, Maui, Hawaii, 12-14 November, 1993.
- [Lee 84] Lee Company, *Technical Hydraulic Handbook*, Westbrook, Connecticut, USA, 1984.
- [Jersa 85] Jersa, A.S. (editor), *Handbook of Geophysics and the Space Environment*, Air Force Geophysics Laboratory, Air Force Systems Command, United States Air Force, 1985.
- [Jollet 86] Jollet, P., Outgassing and Thermo-Optical Data for Spacecraft Materials, MATLAB 001, Materials Section, European Space and Technology Centre, Noordwijk, The Netherlands, October 1986.
- [Kitfield 94] Kitfield, James, "The End of the Line for MilSPEC?", *Air Force Magazine*, October 1994, pp. 43-45.
- [Smith 95] Smith, B.A., "Pyrovalves Suspect in Satellite Failures," *Aviation Week and Space Technology*, 9 January 1995.
- [TSS 94] *Technology for Small Spacecraft*, Panel on Small Spacecraft Technology, Committee on Advanced Space Technology, Aeronautics and Space Engineering Board, Commission on Engineering and Technical Systems, National Research Council, National Academy Press, Washington, D.C., 1994.
- [Underwood 96] Underwood, C. *Commercial Microelectronic Devices in the Space Radiation Environment*, Ph.D. Thesis, University of Surrey, to be published 1996.

Bibliography

Dynamics & Orbital Mechanics

- [Greenwood 88] Greenwood, D.T., *Principles of Dynamics*, Prentice-Hall, Inc., Englewood Cliffs, NJ, 1988.
- [USAFA 92] Department of Astronautics, U.S. Air Force Academy, Course Readings, A422, 1992.
- [Kozai 59] Kozai, Y., "The Motion of a Close Earth Satellite," *Astronautics Journal*, Vol. 64, 367-377, November, 1959.
- [Brower 59] Brower, D., "Solution of the Problem of Artificial Satellite Theory Without Drag," *Astronautics Journal*, Vol. 64, 378-397, November, 1959.
- [Burton 92] Burton, R.L., Wassgren, C., "Time-Critical Low-Thrust Orbit Transfer Optimisation," *Journal of Spacecraft*, Vol. 29, No. 2., Engineering Notes, March/April 1992.
- [Smith 62] Smith, D.E., "The Perturbation of Satellite Orbits by Extra-Terrestrial Gravitation," *Planetary and Space Science*, Vol. 9, 659, 1962.
- [Cook 62] Cook, G.E., "Luni-Solar Perturbations of the Orbit of an Earth Satellite," *Geophysical Journal*, Vol. 6, 271, 1962.
- [King 81] King-Hele, D.G., "Lifetime Prediction for Satellites in Low-Inclination Transfer Orbits," Technical Report 81119, Royal Aircraft Establishment, October, 1981.
- [Tauber 90] Tauber, M.E., "Atmospheric Trajectories," Notes from AA213, Stanford University, 1990.
- [Harris 62] Harris, I., Priester, W. "Theoretical Models for the Solar Cycle Variation of the Upper Atmosphere," Goddard Space Flight Center Report, NASA-TN-D-144, August 1962.
- [Jacchia 71] Jacchia, L.G. "Revised Static Models of the Thermosphere and Exosphere with Empirical Temperature Profiles," Smithsonian Astrophysical Observatory Special Report No. 332, Cambridge, Mass., May 1971.
- [King 87] King-Hele, D.G., Walker, D.M.C., "The Prediction of Satellite Lifetime," Technical Report 87030, Royal Aircraft Establishment, May, 1987.
- [Frazier 89] Frazier, William E., Culp, Robert, D., Rosborough, George, "Absolute Accuracy Limits of a Transfer Orbit Propagator," AIAA 89-0453, Presented at the 27th Aerospace Sciences Meeting, Reno, Nevada, January 9-12, 1989.
- [USAF 80] NORAD, *Project Space Track: Models For Propagation of NORAD Element Sets*, North American Aerospace Defence Command, U.S. Air Force, December 1980.
- [Houchin 90a] Houchin, P.P., "STRV-1 Perigee Height Variations," Working Paper SP (90) WP8, Royal Aerospace Establishment, Space Department, February, 1990.
- [Houchin 90b] Houchin, P.P., "Evolution of Apogee and Perigee Height in Geostationary Transfer Orbit for STRV-1 Using the SAPRE Orbit Prediction Model," Working Paper SP-91-WP-17, Royal Aerospace Establishment, Space Department, September, 1990.

Appendix A

Rocket Propulsion Fundamentals

A.1. BACKGROUND

A.2. BASIC ROCKET SCIENCE

A.3. REFERENCES

The purpose of this appendix is to provide a general overview of the rocket propulsion concepts most relevant to my thesis. For a more detailed background on these topics the reader is referred to the general references listed in the bibliography. This appendix begins with a summary of significant developments in rocket history. Basic rocket science concepts and relationships are then reviewed including dynamics, thermodynamics, thermochemistry and performance.

A.1. Background

Several good references [Baker 78] [Sellers 94] [Humble 95] [Clark 72] can provide the reader with details of rocket development throughout history beginning with the invention of gun powder sometime during the Han Dynasty in China, around 200 B.C. Table A-1 summarise the major developments which have influenced the current state-of-the art.

Given this perspective on rocket development, the next section present additional background in the form of an overview of the fundamental principles of rocket science are discussed. This discussion will firmly lay the foundation for the detailed analysis of rocket propulsion technology options that follows.

A.2. Basic Rocket Science

For a complete introduction to the fundamentals of rocket science and propulsion systems the reader is referred to *Understanding Space: An Introduction to Astronautics* by Sellers, et al [Sellers 94]. Humble, et al, in *Space Propulsion Analysis and Design* [Humble 95] and Sutton in *Rocket Propulsion Elements* [Sutton 92] offer a more detailed treatment of these topics. This section presents a brief overview of the basic concepts and parameter which were particularly relevant to my research.

A.2.1. Dynamics

The basic principle of rocket thrust derives from Newton's Third Law, "for every action there is an equal and opposite reaction." Mass is expelled from one end of a rocket at high velocity producing a equal but opposite reaction in the other direction. A rocket has three basic part—a combustion chamber, throat and nozzle (the discussion here will focus on conventional, chemical rockets, more exotic types i.e. ion, solar sails, etc. rely on slightly different principles of operation). Within the combustion chamber, propellant is burned producing hot gasses. The throat is designed to restrict the outflow of these gases, causing pressure in the chamber to increase. At the throat, the flow becomes choked, meaning the exhaust products are flowing at the speed of sound, achieving the maximum possible flow rate. The exhaust products are then expanded through the nozzle which directs their flow in the desired direction. Expanding a fluid already at sonic conditions causes the velocity to increase to supersonic. Thus we have hot gasses (mass) moving out the back end of a rocket with very high velocity.

Appendix A: Rocket Propulsion Fundamentals

Date	Significant Rocket Event
1232	<ul style="list-style-type: none"> Chin Tartars defend Kai-feng-fu in China by firing rockets at the attacking Mongols
1806	<ul style="list-style-type: none"> British army fires over 200 rockets developed by Sir William Congreve (1772-1828) in less than 30 minutes against the French at Boulogne. They are also used against Copenhagen in 1807 to prevent the French from seizing the Danish fleet. Although Britain created a rocket corps as an adjunct to the Royal Artillery in 1815, their utility in battle is soon supplanted by more accurate and longer ranged conventional artillery.
1880s	<ul style="list-style-type: none"> Konstantin Tsiolkovsky (1857-1935) calculates the "rocket equation." He made the first serious analysis of the problems of space flight.
1926	<ul style="list-style-type: none"> Robert Goddard (1882-1945) launches first liquid fuelled rocket.
1927	<ul style="list-style-type: none"> Society for Space Travel founded in Germany.
1930	<ul style="list-style-type: none"> Italian researcher Luigi Crocco fires first rocket using nitrogen tetroxide (N_2O_4) as oxidiser.
1937	<ul style="list-style-type: none"> British Interplanetary Society prepares a detailed study of a lunar landing spaceship.
1936 - 1945	<ul style="list-style-type: none"> During World War II, German rocket scientists at Peenemuende develop the V-2. Its liquid engine burned alcohol (actually 70-30 alcohol/water) and liquid oxygen (hydrogen peroxide, "T-Stoff" was used to drive the fuel turbopumps).
1940	<ul style="list-style-type: none"> Helmut von Zborowski and Heinz Mueller at BMW discover that certain fuels ignite spontaneously on contact with nitric acid (oxidiser). Zborowski's code name for nitric acid was "Ignol" and for his fuel "Ergol." Out of this grew the term still in use today, in German, English and French, "hypergol" or the adjective "hypergolic" which describes this ignition process.
1946-1957	<ul style="list-style-type: none"> During the post-War era, American rocket development efforts focused on Intercontinental Ballistic Missile (ICBM) systems such as the Thor and Atlas. These liquid systems would later form the core of America's expendable launch vehicles.
July 1957	<ul style="list-style-type: none"> Responding to requirements for storability and rapid response, the U.S. Air Force begins to pursue a solid propellant ICBM which would later be called "Minuteman."
October 1957	<ul style="list-style-type: none"> Soviets shock the world with the launch of Sputnik 1. The rocket engines used liquid oxygen and kerosene.
1961	<ul style="list-style-type: none"> Yuri Gagarin becomes the first human to orbit the Earth. His rocket is not significantly different than the one used to launch Sputnik 1. President Kennedy sets goal of landing men on the Moon before the end of the decade.
1962	<ul style="list-style-type: none"> John Glenn becomes the first American to orbit the Earth on 20 February (5 days before the authors birth!).
1969	<ul style="list-style-type: none"> Apollo 11 mission fulfils Kennedy's goal by delivering Neil Armstrong and Buzz Aldrin to the Moon. The massive Saturn V booster used both LOX/kerosene and LOX/H₂ engines. The Lunar Excursion Module engines used Aerozine-50 (50-50 mixture of hydrazine and UDMH) and NTO. First test of the NERVA-XE nuclear rocket engine demonstrating an efficiency more than double that of chemical engines.
1971	<ul style="list-style-type: none"> First and only launch of Britain's Black Arrow launcher. First, second and third stage engines used hydrogen peroxide/kerosene. Fourth stage was a solid motor.
1972	<ul style="list-style-type: none"> First in-space use of an ion thruster aboard the SERT II spacecraft.
1981	<ul style="list-style-type: none"> First launch of the Space Shuttle and first-ever use of solid rocket boosters on a manned vehicle. UoSAT-1 launched on a NASA Delta-II booster.
1986	<ul style="list-style-type: none"> Challenger accident and Titan 34/D explosion, both linked to solid rocket booster burn-throughs.
1994	<ul style="list-style-type: none"> First successful test of the University of Surrey hybrid rocket motor.

Table A-1: Summary of significant events in the history of rocketry.

Where does the thrust come from? Newton defined linear moment as

$$\vec{p} = m\vec{V}$$

Eqn. A-1

where

Appendix A: Rocket Propulsion Fundamentals

$\dot{\vec{p}}$ = linear momentum (kg m/s)

m = mass (kg)

\vec{V} = velocity (m/s)

The exhaust gasses depart a rocket with significant linear momentum. Momentum is a vector quantity and because total momentum is conserved, the moment gained in one direction by the exhaust gasses must be matched in the other direction by a gain in moment of the rocket.

$$\dot{\vec{p}}_{rocket} = -\dot{\vec{p}}_{exhaust} \quad \text{Eqn. A-2}$$

or

$$\dot{\vec{p}}_{rocket} = -\dot{m}\vec{V}_{exit} \quad \text{Eqn. A-3}$$

where

$\dot{\vec{p}}_{rocket}$ = time rate of change of momentum of the rocket (N)

\dot{m} = mass flow rate of exhaust products (kg/s)

\vec{V}_{exit} = exit velocity of exhaust products (m/s)

Notice that the momentum change of the rocket has the same units as force. This is equivalent to thrust, which in this case, is defined as the moment thrust of the rocket (dropping vector notation).

$$F_{momentum_thrust} = \dot{m}V_{exit} \quad \text{Eqn. A-4}$$

But momentum thrust isn't the only consideration when determining the thrust on a rocket. Consider the control volume around a rocket. Acting on the boundaries of this control volume, everywhere but the exit, is atmospheric pressure. At the exit we have P_{exit} . Due to symmetry, $P_{atmosphere}$ cancels everywhere but in the direction parallel to momentum thrust.

This pressure thrust is therefore defined as

$$F_{pressure} = A_{exit}(P_{exit} - P_{atmosphere}) \quad \text{Eqn. A-5}$$

The total thrust on a rocket can then be expressed as

$$F_{thrust} = \dot{m}V_{exit} + A_{exit}(P_{exit} - P_{atmosphere}) \quad \text{Eqn. A-6}$$

Typically, we define the *effective exhaust velocity*, c , to be

$$c = V_{exit} + \frac{A_{exit}}{\dot{m}}(P_{exit} - P_{atmosphere}) \quad \text{Eqn. A-7}$$

Total thrust can then be expressed as

$$F_{thrust} = \dot{m}c \quad \text{Eqn. A-8}$$

Appendix A: Rocket Propulsion Fundamentals

This makes intuitive sense. The greater the velocity of the mass ejected (higher c) or the higher the rate of mass ejection (higher \dot{m}) the more thrust is produced. From Newton's First Law we also know

$$F = \frac{dp}{dt} \quad \text{Eqn. A-9}$$

Setting this equal to Eqn. A-8 we can then solve for the famous rocket equation (the complete rigorous derivation can be found in [Sellers 94])

$$\Delta V = c \ln\left(\frac{m_{initial}}{m_{final}}\right) \quad \text{Eqn. A-10}$$

where

ΔV = velocity change imparted to a rocket (m/s)

c = effective exhaust velocity (m/s)

$m_{initial}$ = initial rocket mass (kg)

m_{final} = final rocket mass (kg)

From a mission planning standpoint, this is perhaps the single most useful equation in all of rocket science. It allows us to easily compute the amount of propellant required to move a satellite from one orbit to another for a given engine.

Applying thrust to a spacecraft for a given amount of time imparts a *total impulse*, I , defined by

$$I = Fdt = dp \quad \text{Eqn. A-11}$$

where

I = total impulse (Ns)

This concept is important because it means the same total impulse can be achieved by applying a large thrust for a short time or a small thrust for a long time. Unfortunately, while total impulse is useful for describing what eventually happens to a spacecraft as a rocket is fired, it does not address efficiency. For this reason, rocket scientist long ago defined a concept called *specific impulse*, I_{sp} , defined as

$$I_{sp} = \frac{I}{dW} \quad \text{Eqn. A-12}$$

where

I_{sp} = specific impulse (sec)

I = total impulse (Ns)

dW = weight change (N)

Note that the non-intuitive units on I_{sp} are the result of using the weight rather than the mass change of the rocket. Unfortunately, this is the long-established convention. I_{sp} can be thought of "miles per gallon" as it tells us the amount of impulse imparted to a rocket by expelling a unit of mass. The higher the I_{sp} the more efficient. I_{sp} can be related to the effective exhaust velocity, c , by

Appendix A: Rocket Propulsion Fundamentals

$$Isp := \frac{c}{g_0}$$

Eqn. A-13

where

g_0 = gravitational acceleration at sea level ($= 9.81 \text{ m/s}^2$)

Armed with these basic rocket equations from simple Newtonian dynamics, we can now examine the thermochemistry within a rocket engine to see where all the energy comes from.

A.2.2. Thermodynamics and Thermochemistry

An understanding of the thermodynamics and thermochemistry actions within a rocket allows the amount of energy liberated by burning a propellant as well as how much thrust it will produce to be determine. We begin by defining some basic concepts.

A.2.2.1. Perfect Gasses

From kinetic theory, a perfect gas satisfies at least two conditions:

1. The spin energy of the particles are negligible.
2. The molecules are widely enough spaced that molecular force fields are not significant.

The perfect gas law can be expressed as

$$P = \rho RT$$

Eqn. A-14

where

P = pressure ($\text{N/m}^2 = \text{Pa}$)

ρ = density (kg/m^3)

R = specific gas constant (J/kgK)

T = temperature (K)

This can also be expressed as

$$P = \frac{\rho R_{univ} T}{M}$$

Eqn. A-15

where

R_{univ} = Universal gas constant ($= 8314.14 \text{ J/kmolK}$)

M = molecular mass of gas (kg/kmol)

The concept of specific heat allows us to determine the amount of heat energy a system gains or losses as a function of temperature change. This quantity is defined as (NOTE: I am using conventional notation. Here specific heat, c , should not be confused with effective exhaust velocity, c).

$$c = \frac{\delta q}{dT} / \text{kg}$$

Eqn. A-16

where

c = specific heat (J/kgK)

(δ indicates path dependence)

q = heat transferred to system (J) T = temperature (K)

A.2.2.2. Specific Heat

The path dependence of the heat transfer requires we consider two types of specific heat. The first, specific heat of constant volume, is defined as

$$c_v = \left(\frac{\partial u}{\partial T} \right)_v \quad \text{Eqn. A-17}$$

where

 c_v = specific heat of constant volume (J/kgK) u = specific internal energy of gas (J/kg)

Similarly, the specific heat of constant pressure is defined as

$$c_p = \left(\frac{\partial h}{\partial T} \right)_p \quad \text{Eqn. A-18}$$

where

 c_p = specific heat of constant pressure (J/kgK) h = specific enthalpy (J/kg)

The two types of specific heat can be related by

$$c_p = c_v + R \quad \text{Eqn. A-19}$$

The ratio of these two values is one of the most useful thermodynamic relationships in rocket performance analysis. This is defined as

$$\gamma = \frac{c_p}{c_v} \quad \text{Eqn. A-20}$$

where

 γ = ratio of specific heats (dimensionless)

A.2.2.3. Assumptions

In practice, the computational fluid dynamics would be required to completely model the flow of superheated gas in a rocket engine. Fortunately, we can make several basic assumptions that will simplify this analysis and deliver reasonable predictions of rocket behaviour within 1% - 5% [Sutton 92].

1. *Isentropic flow*—this means that after combustion, the flow of products from the chamber to the nozzle is reversible and adiabatic. Adiabatic implies that heat transfer does not dissipate energy from the flow.
2. *One dimensional flow*—for most nozzles this assumption is good to within 5%.
3. *Exhaust products obey the perfect gas law*.
4. *Frozen flow*—exhaust products do not change once they leave the combustion chamber.
5. *Steady flow*—this implies mass, momentum and energy are constant.

From these assumptions we can develop several useful relationships. To begin with, the speed of sound, a (the velocity of the exhaust products in the throat) can be found from

$$a = \sqrt{\gamma RT}$$

Eqn. A-21

where

 a = speed of sound (m/s)The mach number, $Mach$, is defined by

$$Mach = \frac{V}{a}$$

Eqn. A-22

where

 $Mach$ = mach number V = flow velocity (m/s)

Because the velocity of flow within the combustion chamber is relatively low (typically $Mach < 0.3$) we can apply stagnation conditions which allows us to develop a useful relationship between expansion conditions between the throat and the nozzle exit, the ratio of specific heats of the exhaust products, and the exhaust velocity.

$$\epsilon = \frac{A_e}{A_t} = \frac{1}{Mach_{exit}} \sqrt{\left\{ \frac{2}{\gamma + 1} \left(1 + \frac{\gamma - 1}{2} Mach_{exit}^2 \right) \right\}^{\frac{(\gamma + 1)}{(\gamma - 1)}}}$$

Eqn. A-23

where

 ϵ = expansion ratio A_e = nozzle exit area (m^2) A_t = nozzle throat area (m^2) $Mach_{exit}$ = mach number of exhaust products at nozzle exit

A.2.2.4. Thrust

Another useful definition is the coefficient of thrust which allows us to analyse the nozzle independent of the rest of the rocket.

$$c_F = \frac{F}{A_t P_c}$$

Eqn. A-24

where

 c_F = thrust coefficient (dimensionless) F = thrust (N) P_c = chamber pressure ($Pa = N/m^2$)

From continuity we know mass flow rate in the throat is given by

$$\dot{m} = \rho A_t V_t$$

Eqn. A-25

Applying this to sonic relationships within the throat the following expression for thrust can be developed

$$F = A_t P_c \gamma \left\{ \frac{2}{\gamma - 1} \left(\frac{2}{\gamma + 1} \right)^{\frac{\gamma+1}{\gamma-1}} \left[1 - \left(\frac{P_{exit}}{P_c} \right)^{\frac{\gamma-1}{\gamma}} \right] \right\}^{\frac{1}{2}} + (P_{exit} - P_{ambient}) A_e \quad \text{Eqn. A-26}$$

and for c_F

$$c_F = \left\{ \frac{2\gamma^2}{\gamma - 1} \left(\frac{2}{\gamma + 1} \right)^{\frac{\gamma+1}{\gamma-1}} \left[1 - \left(\frac{P_{exit}}{P_c} \right)^{\frac{\gamma-1}{\gamma}} \right] \right\}^{\frac{1}{2}} + \frac{(P_{exit} - P_{ambient}) A_e}{P_c A_t} \quad \text{Eqn. A-27}$$

A.2.2.5. Characteristic Exhaust Velocity

Finally, another useful concept, *characteristic exhaust velocity*, C^* , allows us to focus on propellant and chamber performance independent of nozzle. Applying the continuity equation above to the sonic conditions in the throat along with the perfect gas assumption we arrive at an express for mass flow rate.

$$\dot{m} = \frac{A_t P_c}{\sqrt{\gamma RT}} \left\{ \gamma \left(\frac{2}{\gamma + 1} \right)^{\frac{\gamma+1}{2(\gamma-1)}} \right\} \quad \text{Eqn. A-28}$$

Characteristic exhaust velocity is then defined as

$$C^* = \frac{P_c A_t}{\dot{m}} \quad \text{Eqn. A-29}$$

where

C^* = characteristic exhaust velocity (m/sec)

Notice that C^* is only a function of γ , and T which are the gas properties in the combustion chamber. Because these are solely determined by the thermodynamic reaction within the chamber, C^* allows us to analyse the combustion efficiency independent of the nozzle. As we will see in chapters 4 and 5, C^* is the single most important parameter for analysing experimental combustion data. In practice, the measured value of C^* is, at best, around 96% to 98% of the theoretical value (to account for deviations from our original assumptions).

A.2.2.6. Real Nozzles

As mentioned earlier, our assumption of one-dimensional flow is not exactly true for real nozzles. To compensate for this slight non-linearity we apply a performance correction factor based on the divergence half-cone angle of the nozzle, α .

$$\lambda = \frac{\text{actual thrust}}{\text{ideal thrust}} = \frac{1}{2} (1 + \cos \alpha) \quad \text{Eqn. A-30}$$

where

λ = thrust correction factor

α = nozzle half-cone angle ($^{\circ}$ or rad)

The optimum half-cone angle is between 12° and 18° [Sutton 92]. A much smaller half-cone angle requires the nozzle be too long to be practical. A much larger angle leads to too great of thrust loss.

A.2.2.7. Thermochemistry

A brief discussion of thermochemistry is useful in order to understand how we solve two basic problems:

1. Determining the chemical reaction products for a given set of propellants and combustion chamber conditions (temperature and pressure).
2. Determining the combustion temperature given the chemical reaction products.

As you can see, this appears to be an unsolvable problem. Fortunately, there are computer codes available which iterate to achieve valid solutions to both problems. There are three basic approaches these codes take to determine the chemical species of combustion:

1. *Frozen flow assumption*—chemical species do not change from the combustion chamber to the nozzle exit (i.e. no reactions outside of the chamber).
2. *Shifting equilibrium assumption*—accepts that reactions do take place outside of the chamber and re-computes a new equilibrium condition at every point.
3. *Kinetics assumption*—somewhere between the frozen and equilibrium assumptions, this approach recognises that a flow field is a chemically reactive gas mixture in which true equilibrium may not actually be achieved.

Because the kinetics assumption is the most realistic, it produces the most accurate results. Unfortunately, its dependence on chemical rate data makes this method very difficult to implement in practice. However, for most applications, the losses due to reacting flow fields accounts for less than 10% of the results obtained by the more simple frozen flow approach [Humble 95] with the equilibrium method falling somewhere in between. Therefore, I chose to use the equilibrium method which is built into a computer code called *Isp* developed by Curt Selph for the U.S. Air Force.

Quoting from the programme description:

"The *Isp* code is based on a standard physical model, whose major assumptions are that the chamber products are completely mixed, at chemical equilibrium, and are equal in enthalpy (adiabatic) to the injected propellants. The flow down the nozzle is assumed to be one dimensional and isentropic and that infinite chemical rates are available to shift the concentrations so as to maintain chemical equilibrium...The solution technique is a variation of the minimisation of free energy method. The free energy is computed for an assumed concentration, and the behaviour of the free energy surface around the initial point is approximated by a second order Taylor series. The derivatives with respect to concentrations are computed and set equal to zero to approximate the stationary or equilibrium point, yielding a set of linear equations, conveniently solvable by standard techniques. The output is a better estimate of composition, which is submitted as the input to a new iteration. The process is repeated until results from additional iterations are unchanged" (converged solution). [Selph 92]

The minimisation of free energy technique used in the *Isp* programme is used to determine the chemical species present at a given temperature. This technique is based on the Second Law of

Appendix A: Rocket Propulsion Fundamentals

Thermodynamics which states that for any spontaneous process, the total entropy of the universe increases. Entropy is a measure of the randomness or disorder in a system. This can be expressed as

$$\Delta S_{univ} = \Delta S_{sys} + \Delta S_{surr} \quad \text{Eqn. A-31}$$

where

ΔS_{univ} = change in total energy of the universe

ΔS_{sys} = change in entropy of the thermodynamic system

ΔS_{surr} = change in entropy of the surroundings

At constant pressure, the change in entropy of the surroundings is based on the heat transferred into or out of the system as expressed by the change in enthalpy, ΔH_{sys} .

$$\Delta S_{surr} = \Delta H_{sys} / T \quad \text{Eqn. A-32}$$

We then define the free energy, or Gibbs free energy, G , as

$$G = H - TS \quad \text{Eqn. A-33}$$

where

G = Gibbs free energy

H = total enthalpy

T = temperature

S = total entropy

or

$$\Delta G = -T\Delta S_{univ} \quad \text{Eqn. A-34}$$

From a rocket combustion stand-point, we are most interested in the case when $\Delta G = 0$ as this implies an equilibrium condition. Thus, the "minimisation of free energy" technique iterates to solve for the chemical equilibrium point using this concept. As described in [Humble 95], "the big advantage of the free energy approach is that a computer program can converge very rapidly on a solution by iterative methods...[and it] can handle a mixture of condensed (solid and liquid) and gaseous species. Today, the minimisation of free energy is the preferred approach."

Once the equilibrium concentration of chemical species is determined, the flame temperature can then be calculated using the available heat method. This too requires iteration as described in the following process:

1. Assume a combustion temperature, $T_c = T_c'$
2. Determine the equilibrium concentration of combustion gases at T_c' and the given chamber pressure, P_c using the minimisation of free energy approach.
3. Determine available heat, $Q_{available}$.
4. Calculate heat absorbed by the products, $Q_{required}$, to take them from standard temperature (298K) to T_c' .

Appendix A: Rocket Propulsion Fundamentals

5. Compare to $Q_{available}$. If the available heat is less than the required heat then the assumed temperature, T_c' , is too low and visa versa. If so, go back to step one and pick a new T_c' . Iterate until convergence.

Fortunately, all this tedious math and reference to standard enthalpy tables for chemical species is built into the *Isp* programme. Chapters 4 and 5 will show how the performance estimates from *Isp* were used in the hybrid rocket motor design process.

A.2.3. Performance

It is now useful to review how these basic rocket science concepts can be used to determine the important performance dimensions of cost listed in Chapter 2. Recall, these are

- Propellant mass
- Propellant volume
- Total elapse thrust time (to complete desired ΔV)
- Power required

Calculations of the first three of these dimensional values depends on the actual mission ΔV , deployed spacecraft mass and the following technical specification of the propulsion technology used.

- Specific impulse, *Isp* (sec)
- Propellant density (kg/m^3)
- Oxidiser/fuel ratio (O/F) (for two-propellant systems)
- Thrust (N)

Propellant mass consumed is found by rearranging the rocket equation.

$$m_{prop} = m_{deployed} - m_{deployed} e^{\left(\frac{-\Delta V}{Isp g_0} \right)} \quad \text{Eqn. A-35}$$

Knowing the mass of propellant, the total propellant volume is found from the propellant densities and O/F ratio.

$$\begin{aligned} m_{ox} &= \frac{O/F}{O/F + 1} m_{prop} \\ m_{fuel} &= \frac{1}{O/F + 1} m_{prop} \end{aligned} \quad \text{Eqn. A-36}$$

$$\begin{aligned} Vol_{ox} &= \frac{m_{ox}}{\rho_{ox}} \\ Vol_{fuel} &= \frac{m_{fuel}}{\rho_{fuel}} \end{aligned} \quad \text{Eqn. A-37}$$

Total elapse thrust time is solved by integrating thrust over the velocity change. This can be closely approximated using the following relationships [FSSR]:

Appendix A: Rocket Propulsion Fundamentals

$$a = \frac{F}{m}$$

Eqn. A-38

$$Vratio = \frac{\Delta V}{6I_{sp}g_0}$$

Eqn. A-39

$$TGO = \frac{\Delta V}{a(1 + 3Vratio + 3Vratio^2)}$$

Eqn. A-40

where

a = Spacecraft acceleration (m/s^2)

$Vratio$ = Dummy variable

g_0 = 9.81 m/s^2

TGO = Time to Go, thrust time (sec)

A.3. References

- [Baker 78] Baker, D., *The Rocket: The History and Development of Rocket & Missile Technology*, New Cavendish Books, London, 1978.
- [FSSR] Functional Subsystem Software Requirements, Guidance Navigation and Control, Space Shuttle Software, NASA, 1995.
- [Humble 95] Humble, R., et al, *Propulsion System Analysis and Design*, To be published, Fall 1995.
- [Sellers 94a] Sellers, J.J., Astore, W.J., Crumpton, K.S., Elliot, C., Giffen, R.B., Larson, W.J. (ed), *Understanding Space: An Introduction to Astronautics*, McGraw-Hill, New York, N.Y., 1994.
- [Selph 92] Selph, C., *Isp Computer Code*, Personal communication to Dr. Ron Humble, 1992.
- [Sutton 92] Sutton, G.P., *Rocket Propulsion Elements*, 6th Edition, John Wiley & Sons, Inc., 1992.